

Technical Report HL-96-1
February 1996

**US Army Corps
of Engineers**
Waterways Experiment
Station

System Simulation of Tidal Hydrodynamic Phenomena in Galveston Bay, Texas

by Bernard B. Hsieh

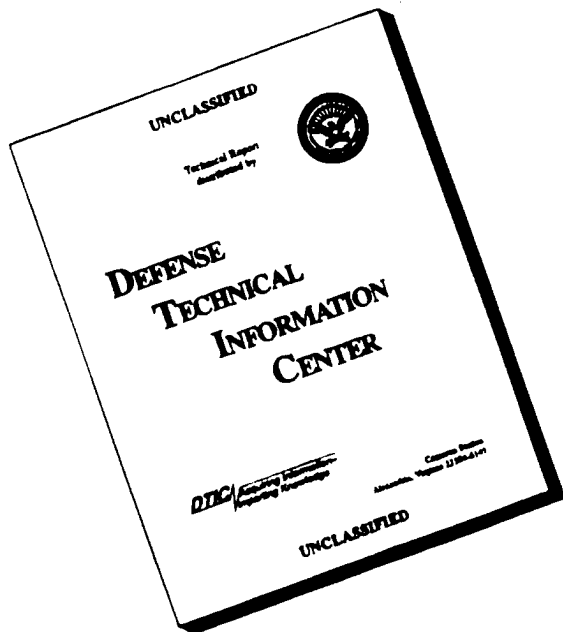
19960305 051

Approved For Public Release; Distribution Is Unlimited

DTIC QUALITY INSPECTED 1

Prepared for U.S. Army Engineer District, Galveston

DISCLAIMER NOTICE



**THIS DOCUMENT IS BEST
QUALITY AVAILABLE. THE
COPY FURNISHED TO DTIC
CONTAINED A SIGNIFICANT
NUMBER OF PAGES WHICH DO
NOT REPRODUCE LEGIBLY.**

The contents of this report are not to be used for advertising, publication, or promotional purposes. Citation of trade names does not constitute an official endorsement or approval of the use of such commercial products.

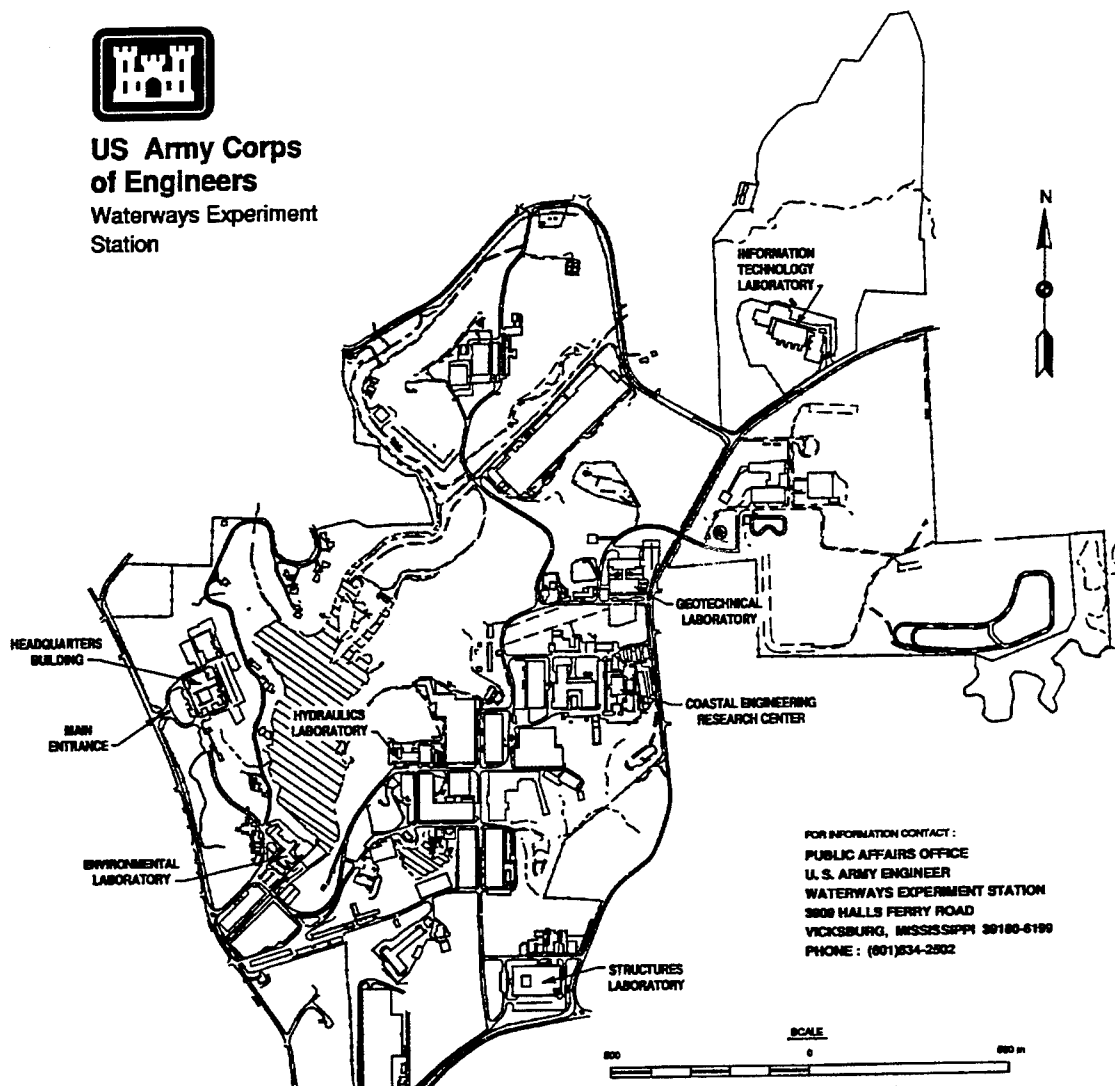


PRINTED ON RECYCLED PAPER



**US Army Corps
of Engineers**

Waterways Experiment
Station



Waterways Experiment Station Cataloging-in-Publication Data

Hsieh, Bernard Bor-Nian.

System simulation of tidal hydrodynamic phenomena in Galveston Bay, Texas / by Bernard B. Hsieh ; prepared for U.S. Army Engineer District, Galveston.

158 p. : ill. ; 28 cm. — (Technical report ; HL-96-1)

Includes bibliographical references.

1. Galveston Bay (Tex.)
 2. Hydrodynamics — Computer programs.
 3. Tides — Texas — Galveston Bay.
 4. Fourier transformations — Computer programs.
- I. United States. Army. Corps of Engineers. Galveston District. II. U.S. Army Engineer Waterways Experiment Station.
- III. Hydraulics Laboratory (U.S. Army Engineer Waterways Experiment Station) IV. Title. V. Series: Technical report (U.S. Army Engineer Waterways Experiment Station) ; HL-96-1.

TA7 W34 no.HL-96-1

Contents

Preface	iv
1—Introduction	1
Background	1
Objective	2
2—System Design and Modeling Considerations	4
Physical Considerations	4
System Simulation	4
Moving Response with Fixed Input Design	5
Group Time Delays and Nonlinearity	5
3—System Model Development Mathematical Description	9
4—System Model Construction	16
Define Input/Output Series	16
Trend Removal	16
System Structure Design	16
Model Verification	17
System Simulation	17
5—Galveston Bay Application	18
6—Conclusions	21
References	22
Plates 1-130	
SF 298	

Preface

This study was conducted as part of the Houston-Galveston Navigation Channels, Texas Project. The three-dimensional hydrodynamic and salinity study presented herein was conducted by the Hydraulics Laboratory (HL), U.S. Army Engineer Waterways Experiment Station (WES). The study was authorized by the U.S. Army Engineer District, Galveston, in conjunction with the study cost-sharing partner, the Port of Houston, Texas, on 3 April 1990.

The study was conducted by HL personnel under the general direction of Messrs. Frank A. Herrmann, Jr., Director, HL; Richard A. Sager, Assistant Director, HL; William H. McAnally, Jr., Chief, Estuaries Division, HL; and David R. Richards, Chief, Estuarine Simulation Branch, Estuaries Division. Mr. William D. Martin, Chief, Estuarine Engineering Branch, Estuaries Division, was the Program Manager. Principal investigator and author of this report was Dr. Bernard B. Hsieh, Estuarine Simulation Branch. Dr. Robert T. McAdory, Estuarine Engineering Branch, provided three-dimensional hydrodynamic simulation results.

At the time of publication of this report, Director of WES was Dr. Robert W. Whalin. Commander was COL Bruce K. Howard, EN.

The contents of this report are not to be used for advertising, publication, or promotional purposes. Mention of trade names does not constitute an official endorsement, approval or recommendation of such commercial products.

1 Introduction

Background

Galveston Bay, the largest estuary on the Texas coast, located in south-eastern Texas along the Gulf of Mexico, is a biologically productive and economically important estuary. The important commercial and recreational fisheries include oyster, shrimp, crab, and various finfish.

The study of circulation and salinities in the Galveston Bay system is complex. A number of physical processes operate in the bay, and their relative importance can vary both spatially and temporally. Bathymetry and geometry of the bay, astronomical tide-induced currents, wind-induced circulation, density variations and resulting gravitational-induced currents, and freshwater inflow are major factors determining bay-wide circulation and salinity patterns. In addition, the proposed deepening and widening of the Galveston Entrance Channel and the Houston Ship Channel could affect both circulation and salinities throughout the bay system.

Houston Ship Channel, the major navigation channel in Galveston Bay, transects the bay from Bolivar Roads at the entrance to Galveston Bay northward to Morgans Point. The channel then continues up to the Main Turning Basin near the city of Houston. The Galveston Channel is much shorter in length and bifurcates from the Houston Ship Channel in the Bolivar Roads area. The channel reach from the inlet to the Gulf of Mexico is known as the Galveston Entrance Channel. At present the width of the Houston Ship Channel is 122 m and the depth of 12 m (40 ft) at mean low tide is maintained along most of the route.

The U.S. Army Engineer Waterways Experiment Station Hydraulics Laboratory is responsible for numerical model testing and long- and short-term field data collection to assess the potential effects of the channel enlargement on the hydrodynamics and transport of the system. Berger et al. (in preparation), Fagerburg et al. (1994), and Lin (1992) discuss other aspects of this project.

With recent advances in computer technology, long-term (1-year) simulation of complicated estuaries with large-scale multidimensional numerical

models has become possible. However, these numerical solutions still require the use of substantial supercomputer central processing unit time. An alternative method, capable of analyzing changes at individual points in an estuary, as opposed to the global solutions generated by the numerical models, is desirable. This alternative method must also be able to be run in a short period of time. A system response approach using the input/output relationships from a numerical model to describe the dynamic behavior of tidal hydrodynamic phenomena can be used to play this role. The system response functions from a numerical model verified for a particular location can be used to simulate the resulting output function, such as change in salinity, when input forcing functions, such as tidal variation and freshwater inflow, change.

This approach was used to address the salinity response due to freshwater inflow changes for 16 selected locations in Galveston Bay, Texas (Figure 1). The system model base was constructed by selecting node points from three-dimensional (3-D) numerical hydrodynamic model results. The annual numerical simulation of both base geometry (12-m-deep (40-ft-deep) channel) and project conditions (13.7-m-deep (45-ft-deep) channel) for 1990 medium-flow conditions was used to construct the system response function. Three major tributaries (Trinity River, San Jacinto River, and Buffalo Bayou) were considered as primary freshwater inflow points.

Objective

The objective of this work was to use the capability of system simulation techniques to evaluate salinity changes at 16 selected points in the bay for conditions projected for medium freshwater inflow conditions in 1999.

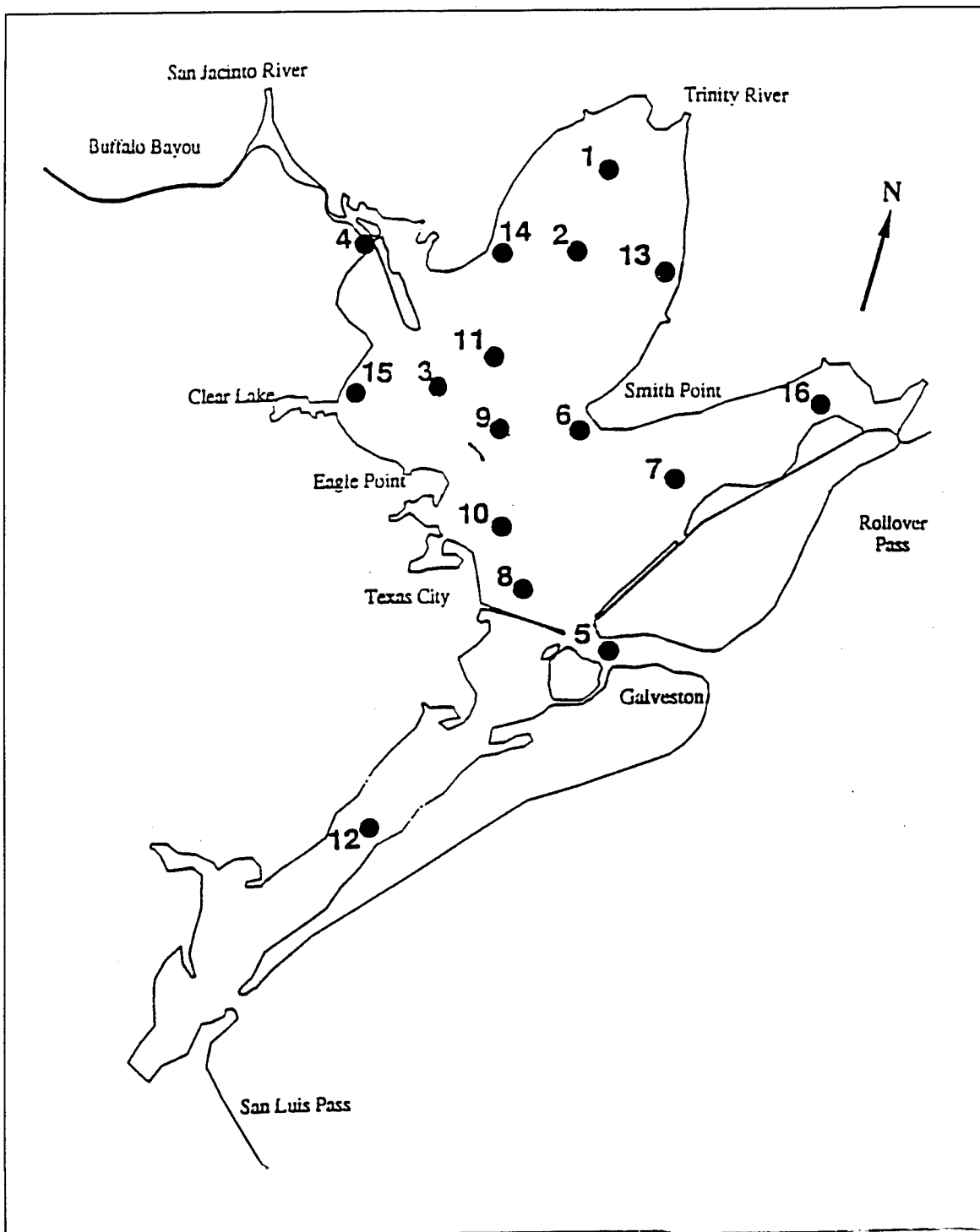


Figure 1. Location of time series points

2 System Design and Modeling Considerations

Physical Considerations

Motion in an estuary is composed of physical processes that occur over a range of frequencies. In the past, researchers have decomposed time-dependent velocities, tides, etc. into the frequency domain and derived linear transfer functions to fill in missing data. However, interactions among a large number of forcing functions (e.g., tides, winds, and freshwater inflows) are sometimes highly nonlinear. Therefore, transfer functions based on nonlinear theory with multiple inputs are required.

Physically, the offshore tide becomes strongly distorted as it propagates into a shallow area system. This is the result of finite amplitude effects caused by friction, nonlinear advection, and interactions with channel geometry as the tide oscillates within the estuary. These tidal asymmetries cause falling and rising tides to be unequal in duration, resulting in tidal curves and salinity variation within the tidal cycle. This distortion can be represented as the nonlinear growth of the astronomical constituents. In addition, the variation in freshwater inflow changes the amplitude and phase of tidal fluctuations.

Since tidal energy distribution is concentrated in several very narrow frequency bands, the frequency domain approach can capture characteristics which the time domain approach could miss. For instance, using a 1-hr time interval in the tidal-induced environment, semidiurnal components only appear in the wavelength with periods of 12 and 13 hr. The major M2 component, with a period of 12.42 hr will not be significantly accounted for in the variation.

System Simulation

The governing equations of estuary flow and transport are usually solved by numerical methods. Before these numerical models can be used to address

real-world problems, they must be verified. This requires that field data taken at interior points agree with the computational results from the model. The system parameters then are saved for addressing the management issues such as salinity changes at points within the estuary. This process is well known as simulation via numerical modeling.

For simulation via the system model, system identification is based on the known input and output series. During this identification process, the frequency response function (FRF) links the relationships between input series and output functions. The FRF is obtained by solving a system matrix after converting all input/output series from the time domain to the frequency domain via the FFT. This FRF usually covers the frequency band over the entire simulation period. For example, a discrete one-sided spectrum normally covers the frequencies from 0.000115 to 0.5 for a year-long record of data taken at hourly intervals. The predicted output then is produced in the frequency domain and converted by taking this FRF via the inverse FFT back to the time domain. The system model verification process consists of adjusting the band width and other system parameters, such as maximum lag, integration of frequency range, and memory lengths of response function. These parameters are related to simulation accuracy during the FFT integration processes. The system simulation is performed by taking the best fit FRF of the system through the proposed input series of management concern. Processes for comparing these two simulations are shown in Figure 2.

Moving Response with Fixed Input Design

For an estuary system, the salinity level (output) at one particular location of a computational domain is approximately a function of surface elevation at the tidal boundary, freshwater discharge at the river boundary, and wind forcing (inputs) on the water surface. Therefore, this system can be classified as a multiple input system. In order to incorporate the system model with the numerical model input/output structure, a moving response function with fixed inputs designed for the model was proposed as shown in Figure 3. Thus each system output corresponds to one computational node from the numerical model. The advantage of this design is that the location of the output cell of interest can change but the input functions remain the same. This provides a relative index to examine the response "strength" through the computational domain due to the node chosen.

Group Time Delays and Nonlinearity

In considering the travel time between the input and output series, the phase difference is called the time delay. Time delays are dependent on forcing distance and physical structure. For solving a multiple input system, a group of time delays are involved. This produces very large bias errors when

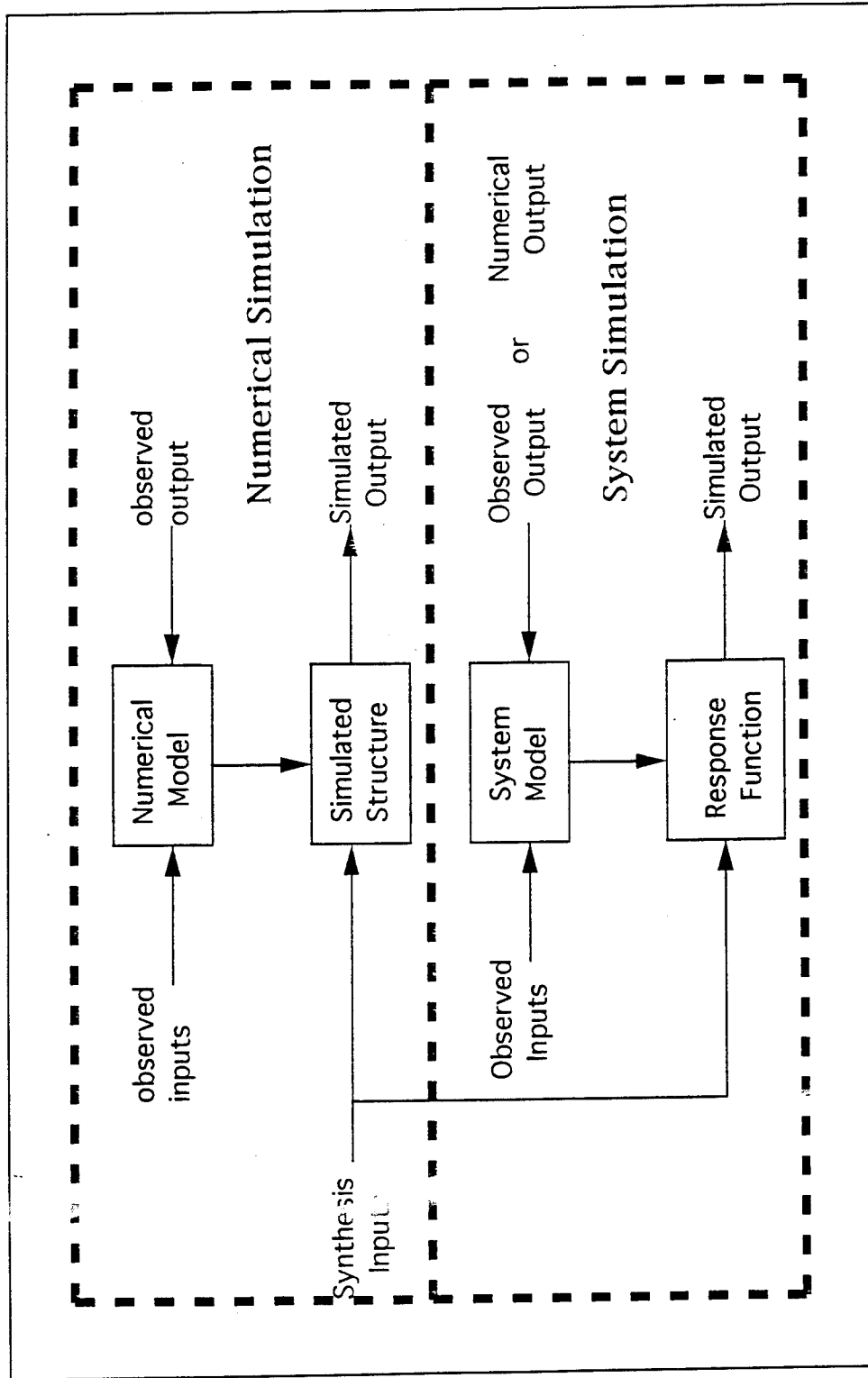


Figure 2. Numerical simulation versus system simulation

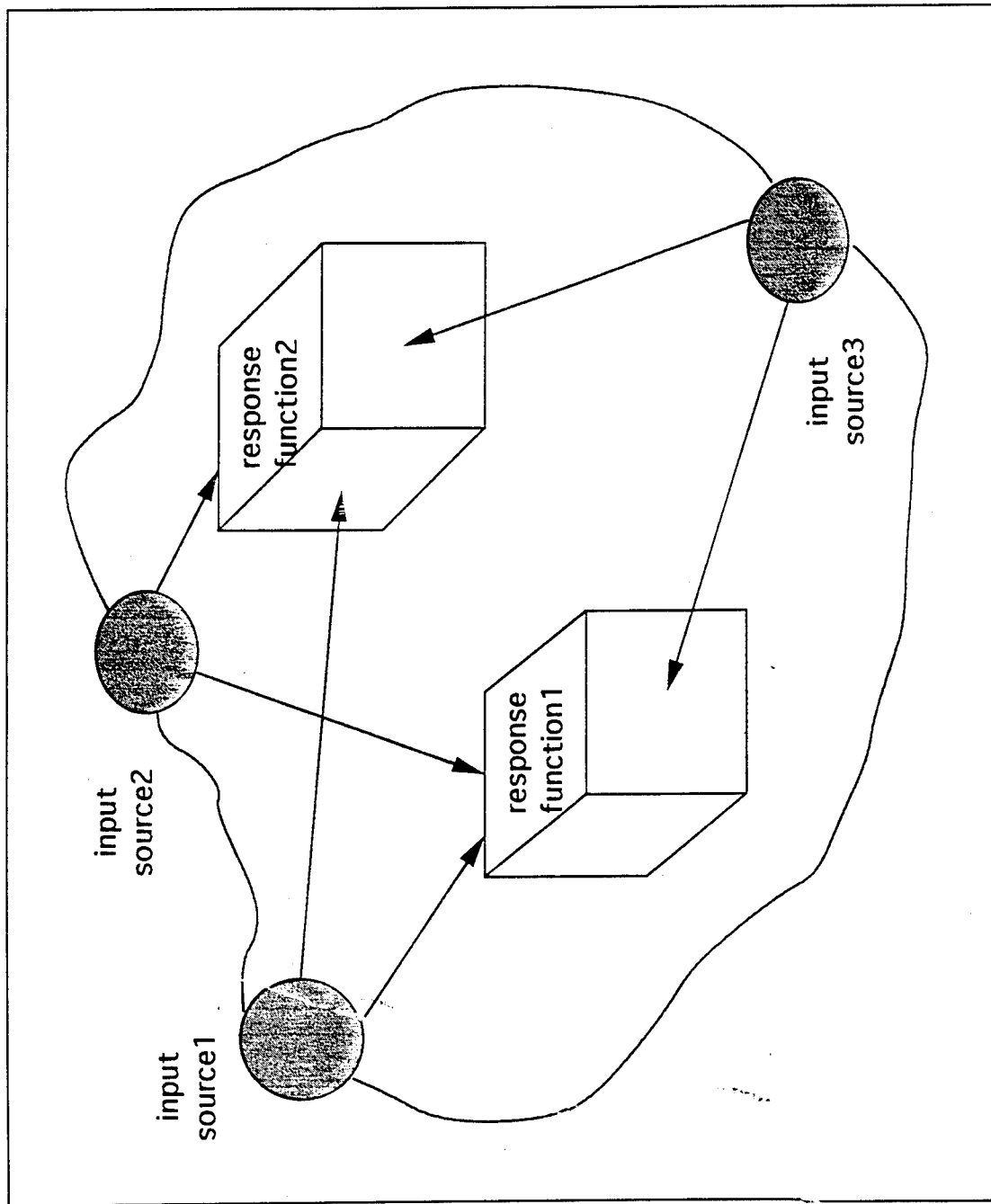


Figure 3. Moving response function with fixed input structure

performing cross-spectral estimates and inverse FFT. A special treatment other than simply reducing the width of the frequency band or conducting multiple time-shifting processes is required. As described before, nonlinearity in the system renders the traditional assumption of multiple linear systems invalid. Solution of these technical difficulties is briefly summarized as follows: (a) the difficulties due to group time delays and nonlinearity are eliminated by decomposing the input and output series into a series of parallel subsystem paths with equivalent computational schemes, (b) a finite-memory nonlinear system is inserted between the input series and subtransfer function. It implies that the multiple frequency response function (MFRF) is the summation of each subfrequency response function, (c) any time delay of each subsystem can be corrected individually.

3 System Model Development, Mathematical Description

Generally, in an estuary system, measurable real input data, such as boundary forcings, are transformed into measurable or computed output data. As a rule, such a system is a multiple one, with several inputs and several outputs. In general, all the input/output series are assumed as stationary series. In the present case, a system with several inputs and one output is considered a so-called multiple input/single output system. By way of the mathematical system model, measured input data are transformed into fictitious, computed output data. Under the conditions of an approximately time-invariant system, the mathematical operation which can simulate the salt transport within an estuary can be represented in the form of the convolution integral. The output $y(t)$ (salinity level at one particular node of the numerical finite-element hydrodynamic model) is, therefore,

$$y(t) = \sum_{I=1}^N \int h_I(\tau) x_I(t-\tau) d\tau + e(t) \quad (1)$$

The $x_I(t-\tau)$ represents the input series I at time level t . The $h_I(\tau)$ are called partial impulse response functions, which describe the estuary system unambiguously and completely. The function $e(t)$ is an uncorrelated noise term which arises because the input and output variables may not be well-controlled. If this error term is neglected, the impulse response functions can be estimated from the values of $x_I(t)$ and $y(t)$ assuming that the data series are realizations of stationary stochastic processes.

For determining the impulse response functions from the design system in the frequency domain, it is necessary to transform the input and output functions from the time domain into the frequency domain. To simplify the mathematical representation, a system with one input and one output may be considered:

$$y(t) = \int h(\tau) x(t-\tau) d\tau + e(t) \quad (2)$$

Neglecting $e(t)$, and using

$$X(f) = \int x(t) e^{-i2\pi ft} dt \quad (3)$$

$$Y(f) = \int y(t) e^{-i2\pi ft} dt \quad (4)$$

and

$$H(f) = \int h(t) e^{-i2\pi ft} dt \quad (5)$$

as FFT of $x(t)$, $y(t)$, and $h(t)$, respectively, with $i = \sqrt{-1}$, the following relation can be developed:

$$Y(f) = H(f) \cdot X(f) \quad (6)$$

Equation 6 replaces the convolution integral (1) by a simple algebraic equation. The FFT $H(f)$ of the impulse response function $h(t)$ is called the frequency response function. Inverse Fourier transformation of $H(f)$ again results in the impulse response function

$$h(t) = \int H(f) e^{i2\pi ft} dt \quad (7)$$

It is noted that Equations 5 and 7 are a transformation pair. It is concluded that a linear time-invariant system consists of an input series, output series and response function if either $H(f)$ or $h(t)$ is given. It can be shown that the frequency response function may be estimated with the aid of the cross spectrum (or cross-spectral density function) between input and output and the power spectrum of the input (auto-spectral density function):

$$H(f) = \frac{G_{xy}(f)}{G_{xx}(f)} \quad (8)$$

where $G_{xy}(f)$ and $G_{xx}(f)$ are the Fourier transforms of the estimate of the crossvariance function $r_{xy}(t)$ and of the autocovariance function $r_{xx}(t)$, respectively. For discrete data series with a finite length, the estimate of the true spectrum at discrete frequencies can be computed according to selected methods such as covariance function and Fast Fourier Transform (FFT). The associated ordinary coherence function estimate is

$$r^2_{xy}(f) = \frac{IG_{xy}(f)I^2}{G_{xx}(f) \cdot G_{yy}(f)} \quad (9)$$

where $G_{yy}(f)$ is a smooth estimate of the output cross-spectrum function. The range of the coherence function is between 0 and 1. For an ideal transfer function, the coherence function is unity over the entire frequency band.

The smoothed value of the true cross-spectrum is a complex-valued quantity defined by the co-spectrum component C_{xy} and quad-spectrum component Q_{xy} as:

$$G_{xy}(f) = C_{xy}(f) - i Q_{xy}(f) \quad (10)$$

The one-sided cross spectrum may be presented in complex polar notation as

$$G_{xy}(f) = I G_{xy}(f) I e^{-iQ_{xy}(f)} \quad (11)$$

where the absolute value and phase angle are determined by

$$IG_{xy}(f)I = \text{SQRT} (C^2_{xy}(f) + Q^2_{xy}(f)) \quad (12)$$

$$P_{xy}(f) = \tan^{-1}(Q_{xy}(f)/C_{xy}(f)) \quad (13)$$

The absolute value $IG_{xy}(f)I$ is called the gain factor and the associated phase angle $P_{xy}(f)$ is called the phase factor. In these terms, the frequency response function takes on a direct physical interpretation and gives an insight into the behavior of the underlying system. Especially, the phase factor gives a useful measure for the time delay through input-output series at any given

frequency f . Similarly, the relationships between Equations 10 and 13 can be combined with Equation 8 (since $G_{xx}(x)$ is the auto spectrum and the real number) to estimate the system gain factor and system phase factor of frequency response function $H(f)$.

According to Equation 1, it is necessary to transform the frequency response function back into the time domain. For a simple single-input and single-output (SISO) system, the discrete expression of Equation 1 can be represented by taking the inverse Fourier transform from the estimate of Equation 9.

$$y(t) = \sum_{k=-p}^u (h(k) \cdot x(t-k)) \quad (14)$$

for

$$u+1 \leq t \leq n-p$$

The output estimate $y(t)$ is the system response estimation due to input series $x(t)$. The procedures for computing Equations 3 through 14 constitute the simplest linear system estimate of output function $y(t)$ via frequency domain approach. The important outputs from these computations are the frequency response function, the system gain factor, the system phase factor, the coherence function, and the output estimate.

For modeling a real physical condition, a more complicated system is considered. Usually, a nonlinear system with multiple inputs is used to describe the system behavior. A model of a linear system responding to N inputs is developed by extending the SISO relationship as

$$y(f) = \sum_{j=1}^N y_j(f) = \sum_{j=1}^N (H_j(f) X_j(f)) \quad (15)$$

The system of linear equations can be written in matrix notation

$$G_{xy}(f) + G_{xx}(f) \cdot H(f) \quad (16)$$

where

$$H(f) = [H_1(f), \dots, H_N(f)]^T \quad (17)$$

$$G_{xy}(f) = [G_{1y}(f), \dots, G_{Ny}(f)]^T \quad (18)$$

$$G_{xx}(f) = \begin{bmatrix} G_{11}(f) & G_{12}(f) & \cdots & G_{1N}(f) \\ \vdots & \vdots & \ddots & \vdots \\ G_{N1}(f) & G_{N2}(f) & \cdots & G_{NN}(f) \end{bmatrix} \quad (19)$$

where

$H(f)$ = N-dimensional vector of the frequency response functions for one frequency f

$G_{xy}(f)$ = N-dimensional vector of the cross spectrum of all inputs with the output, for one frequency f (output spectrum matrix)

$G_{xx}(f)$ = NxN matrix of the cross and auto spectrum of all inputs with each other, for one frequency f (input spectrum matrix)

The multiple frequency response function $H(f)$ is solved by

$$H(f) = G_{xx}^{-1}(f) \cdot G_{xy}(f) \quad (20)$$

For solving a multiple linear system, two solution options exist; namely, the direct inverse matrix computation method, or the parallel SISO linear system decomposition method. While the first method involves more complicated techniques for solving the inverse matrix, such as partitioning the complex variable, the second method offers an easier approach to the computations but it requires removal of the dependency among inputs. Usually, additional transformation is required to convert correlated inputs to uncorrelated inputs. Under the second approach, a new multiple linear system is formed by the multiple frequency response function $L(f)$, and the matrices of $Guu(f)$ and $Guy(f)$.

$$L(f) = [L1(f), L2(f), \dots, Ln(f)]^T \quad (21)$$

$$Guy(f) = [G_{uly}(f), \dots, G_{uNy}(f)]^T \quad (22)$$

$$G_{uu}(f) = \begin{bmatrix} G_{u1u1}(f) & G_{u1u2}(f) & \cdots & G_{u1uN}(f) \\ \vdots & \vdots & \ddots & \vdots \\ G_{uNu1}(f) & G_{uNu2}(f) & \cdots & G_{uNuN}(f) \end{bmatrix} \quad (23)$$

To solve this new linear system, extensive computation is required to fill both the output spectrum matrix and the input spectrum matrix. However, one alternative is to solve this transform matrix $Lxx(f)$ and use computed $Gxx(f)$ and $Gxy(f)$ to estimate the solution $L(f)$ via linear combination technique.

$$U(f) = [U1(f), U2(f), \dots, Un(f)]^T \quad (24)$$

where

$$Uj(f) = Xj(f) - \sum_{i=1}^{j-1} (Lij U_i(f)) \quad j = 1, \dots, N \quad (25)$$

$$L(f) = \sum_{i=1}^N (Lij H_j(f)) \quad j = 1, \dots, N \quad (26)$$

where $Lii=1$ for any i and $Lij = 0$ if $j < i$

$$Lxx(f) = \begin{bmatrix} L_{11}(f) & L_{12}(f) & \cdots & L_{1N}(f) \\ \vdots & \vdots & \ddots & \vdots \\ L_{N1}(f) & L_{N2}(f) & \cdots & L_{NN}(f) \end{bmatrix} \quad (27)$$

$$Lij = G_{ij} \cdot 12\dots(N-1)/G_{ii} \cdot 1.2\dots(N-1) \quad (28)$$

$i=1, \dots, N, \quad J=i, (i+1), \dots, N$

$$G_{i_k,1 \dots j} = \frac{G_{jj,1 \dots (j-1)} \cdot G_{ik} - G_{ij,1 \dots (j-1)} \cdot G_{jk} \cdot 1 \dots (j-1) / G_{jj,1 \dots (j-1)}}{G_{jj,1 \dots (j-1)}} \quad (29)$$

$i=(j+1), \dots, (N-1), j=1, \dots, N, k=1, \dots, N$

$$L(f) = L_{xx}(f) \cdot H(f) = L_{xx}(f) \cdot G_{xx}^{-1}(f) \cdot G_{xy}(f) \quad (30)$$

The multiple coherence function estimate for this system is

$$\begin{aligned} r_{yu^2} &= [L_1(f) \cdot G_{yu1}(f) + \dots + L_N(f) \cdot G_{yuN}(f)] / G_{yy}(f) \\ &= L(f)^T \cdot G_{yu}(f) / G_{yy}(f) \end{aligned} \quad (31)$$

where

$$G_{yi} = G_{yi} - L_j(f) \cdot G_{yji} \quad i=1, \dots, N \quad (32)$$

The multiple coherence function estimates represent the fraction of output power at frequency f which can be attributed to linear relationships in the system.

For a multiple nonlinear system, a decomposition procedure must be conducted. Bendat (1990) has proven that a combination of a finite-memory nonlinear system with a parallel linear system is equivalent to a multiple nonlinear system. A finite-memory nonlinear system could be as simple as the second order of polynomial function between one of the input series and output function. The mathematical detail can be found in Bendat (1990).

4 System Model Construction

Define Input/Output Series

Using physical realization to define the input/output series is the first step to construct the system model. The energy driving sources usually are used to represent the input series and the resulting physical parameters are used to prescribe the output series. The actual number of input series may need to be identified by computing the cross spectrum or correlation coefficients for each pair of input/output series. This allows the model structure to remain simple but include all significant components. For a strong cyclic relationship, harmonic analysis can aid in understanding the significant components. It is suggested that the better representation is to keep the model structure as simple as possible.

Trend Removal

Unlike general numerical model construction, the system model is assumed to be stationary over the entire time horizon. It implies that the trend removal process is applied to both input and output series. Trends that have been removed are added back during the simulation stage. The most common technique for trend removal is to fit a low-order polynomial to the data using the least squares estimation method. Although more complex trends can be removed by higher-order polynomial fits, trend removal using an order of magnitude greater than three is generally not suggested. Sometimes, the filtering of data prior to more detailed analyses may be desired for various reasons, including either the isolation or elimination of periodic components.

System Structure Design

The structure of the system needs to be identified by the order of input significance, the distribution of the energy spectrum, nonlinear effect, and the speed of reaction between input and output series. Several candidates are necessary in the initial stage of modeling. The nonlinear transformation and parallel signal paths (Bendat 1990) need to be defined.

Model Verification

The system model is tested by determining the bandwidth of the frequency domain, maximum lag number, integration frequency range, lag weight coefficients, and memory lengths of the response function. The model is, therefore, tuned until an acceptable error criterion is achieved. The multiple coherence functions or the time series of output residuals are the measure of modeling performance.

System Simulation

Once the system model has been verified, the system coefficients are saved and used to perform system simulation. These system coefficients, especially the multiple frequency response function, remain in the system and combine with desired new input to generate the simulated output. It needs to be mentioned that the driving mechanisms of system modeling are variations over time. Less variation in the input series will receive less response, which will show less impact on the output function. This consideration should be included prior to construction of the model.

5 Galveston Bay Application

Galveston Bay, as most estuary systems, receives boundary forcings from tidal propagation, freshwater inflows from major tributaries, and wind stress on the water surface. The 3-D hydrodynamic numerical model was constructed to simulate present and future salinity conditions due to channel deepening alternatives, wind stress, and freshwater inflow conditions. The system model used numerical results of annual hourly salinity from 16 selected nodes from the computational mesh of the 3-D numerical model as output (Figure 4). The system model uses the same types of forcing functions including the source tide on the boundary, x-component and y-component wind forcing and three major tributaries; namely, Trinity River, San Jacinto River, and Buffalo Bayou to build a six-input/single-output (salinity) nonlinear system. All numerical results for the top layer and bottom layer at these 16 locations (Figure 4, except point 12, with only one layer) were used to construct their individual transfer function models for both base and project conditions. This made 62 dynamic system models under the 1990 and 1999 medium-flow conditions. The system simulation runs were performed after these 62 models were verified.

The first step of the analysis was to normalize the input/output series into the same scale of variation. The wind components and flow data were multiplied by factors of 1000.0 and 0.001, respectively. Increasing the freshwater inflows causes decreasing salinity concentrations, which is not consistent with the fact that increasing the surface elevation at the open (Gulf) boundary causes increasing salinity values. Therefore, a transformation taking reciprocal values of flow was performed. This was the simplest nonlinear transformation among a group of candidates. This also assumed that the system was zero-memory nonlinear through each input/output series.

A long-term time series can be decomposed into three major components to describe its dynamic behavior; namely, the trend component, cyclic or periodic component, and stochastic component. Since the relationships among the input and output series were constructed under a stationary process, the trend had to be removed first. After several tests, a slight linear trend component was removed from all series. The frequency domain approach can simulate each cyclic component through the prescribed techniques. Therefore, the residuals (white noise) can be estimated after determining both the trend and the periodic components through the system.

Harmonic analysis was used to identify the rank of input significance and the distribution of the energy spectrum. It was found that the diurnal tidal components contribute the most high-frequency variation but the subtidal component and neap-spring tidal component dominate the lower frequency band. The final order of input significance was surface elevation, freshwater inflows, and wind components. A strong relationship was found between surface elevation and wind components. Similar results also can be obtained by using cross spectrum calculations with Parzen weights. The input significance order is very important when using the correlated input decomposition method. Although the developed computer code has that option, the final verification process used the full matrix solver.

In order to conduct the model verification, several system coefficients were determined after considering the nature of the data. The bandwidth was the most sensitive parameter. This selection was based on the density of the overall spectrum and the accuracy criteria of the model. The final system parameters were:

Bandwidth = 0.00125 cycles⁻¹

Maximum lag number = 100

Integration frequency range = -0.5 to 0.5 cycles⁻¹

Lag weight coefficients = 1.0

Memory lengths of response function = -100 to 100 hr

The MFRF which represent the overall variation of salinity due to input fluctuations for each point were generated after verifying the model. The multiple impulse response function (MIRF) was obtained when the inverse Fourier transform of the multiple frequency response function was conducted. The simulated salinity was generated by multiplying the MIRF by input series over memory lengths. Plate 1 is a time series comparison of the RMA-10 run (solid line) and the S run (dashed line). A 350-hr low-pass filter was used to smooth the computed results. Agreement between these two runs was very good, especially the low-frequency variation. Plate 2 plots the corresponding residual series. The maximum computation error was about 0.25 ppt. The final verification results are shown as the following four groups:

Group 1 : 1990 medium-flow base top layer (Plates 3-18).

Group 2 : 1990 medium-flow base bottom layer (Plates 19-34).

Group 3 : 1990 medium-flow phase I top layer (Plates 35-50).

Group 4 : 1990 medium-flow phase I bottom layer (Plates 51-66).

The corresponding system simulations were summarized as another four groups of figures (Plates 67-82, Plates 83-98, Plates 99-114, Plates 115-130). The maximum variation of salinity regime during the system simulations due to the flow condition was about 2.0 ppt. No significant cyclic variation was found in these plots. This might be primarily attributed to using the monthly mean input flow to represent hourly flow. This needs further investigation with highly fluctuating flow inputs. However, the advantage of system simulation was time efficiency. The averaged 1-year hourly simulation for

each point of interest only takes 10 sec of Cray Y-MP super-computer central processing unit time.

6 Conclusions

The system modeling technique was used to simulate the hydrodynamic phenomenon of salinity intrusion in the Galveston Bay system. The modeling design used numerical model results as the output and the same boundary forcing as the numerical model for the input to generate response functions. While this technique is limited to a single point of simulation, it offers great time-saving advantages and an easier model verification process. The Galveston application showed very good model verification, but the cyclic variation due to flow condition change was not significant. The success of conducting the simulation using the system model seems to be highly correlated to the degree of dynamic changes for both the input and output series. Further research is needed to identify the minimum sampling interval or input/output series for the general approach.

References

- Bendat, J. S. (1990). *Nonlinear system analysis and identification from random data*. Wiley-Interscience Publication, John Wiley and Sons, New York.
- Berger, R. C., McAdory, R. T., Martin, W. D., and Schmidt, J. H. "Houston-Galveston Navigation Channels, Texas Project; Report 3, Three-dimensional hydrodynamic model verification," in preparation, Technical Report HL-92-7, U.S. Army Engineer Waterways Experiment Station, Vicksburg, MS.
- Berger, R. C., McAdory, R. T., Martin, W. D., Schmidt, J. H., and Hauck, L. H. "Houston-Galveston Navigation Channels, Texas Project; Report 4, Three-dimensional numerical modeling of hydrodynamics and salinity," in preparation, Technical Report HL-92-7, U.S. Army Engineer Waterways Experiment Station, Vicksburg, MS.
- Fagerburg, T. L., Fisackerly, G. M., Parman, J. W., and Coleman, C. J. (1994). "Houston-Galveston Navigation Channels, Texas Project; Report 1, Galveston Bay field investigation," Technical Report HL-92-7, U.S. Army Engineer Waterways Experiment Station, Vicksburg, MS.
- Lin, H-C. J. (1992). "Houston-Galveston Navigation Channels, Texas Project; Report 2, Two-dimensional numerical modeling of hydrodynamics," Technical Report HL-92-7, U.S. Army Engineer Waterways Experiment Station, Vicksburg, MS.

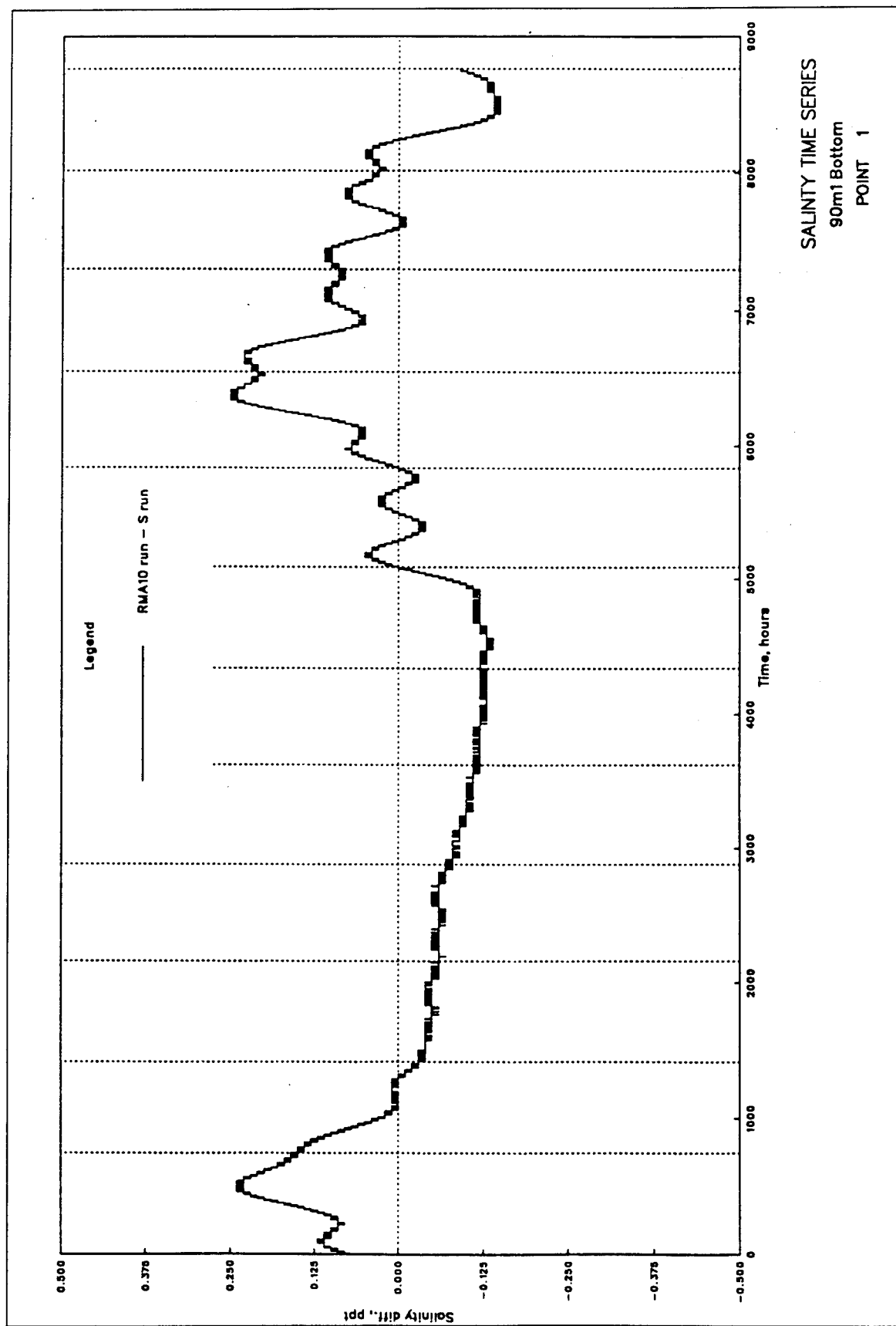


Plate 1

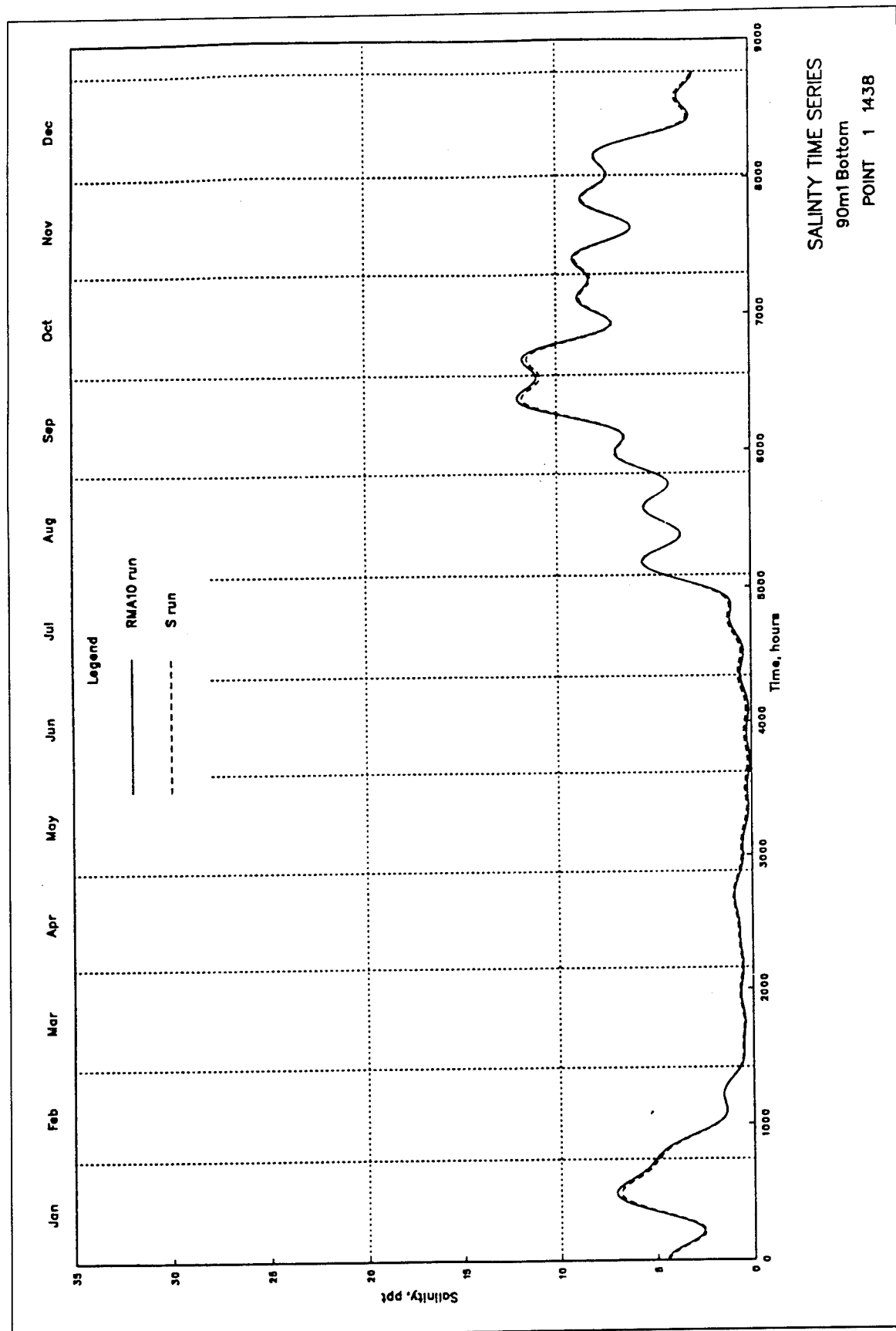
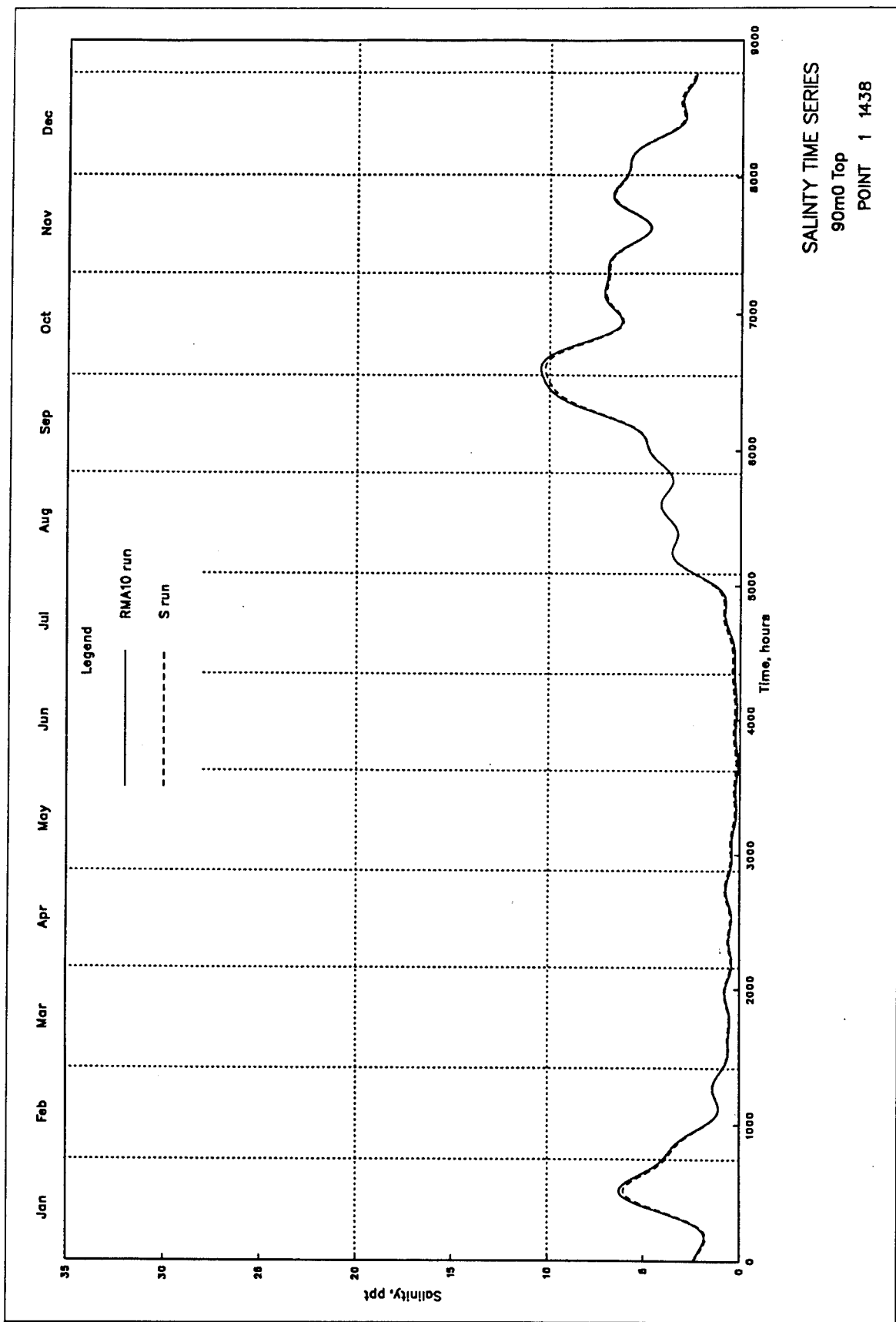


Plate 2



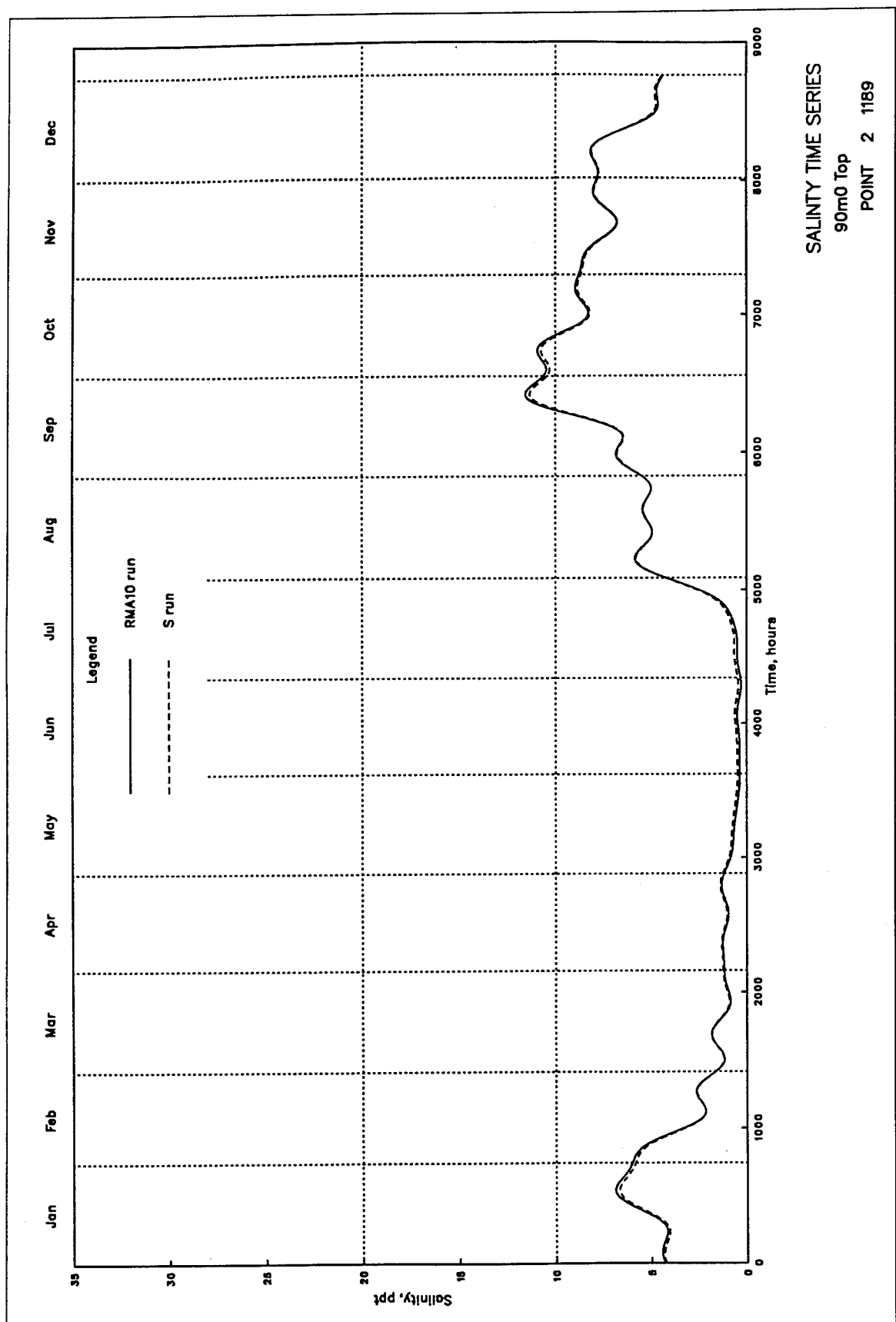
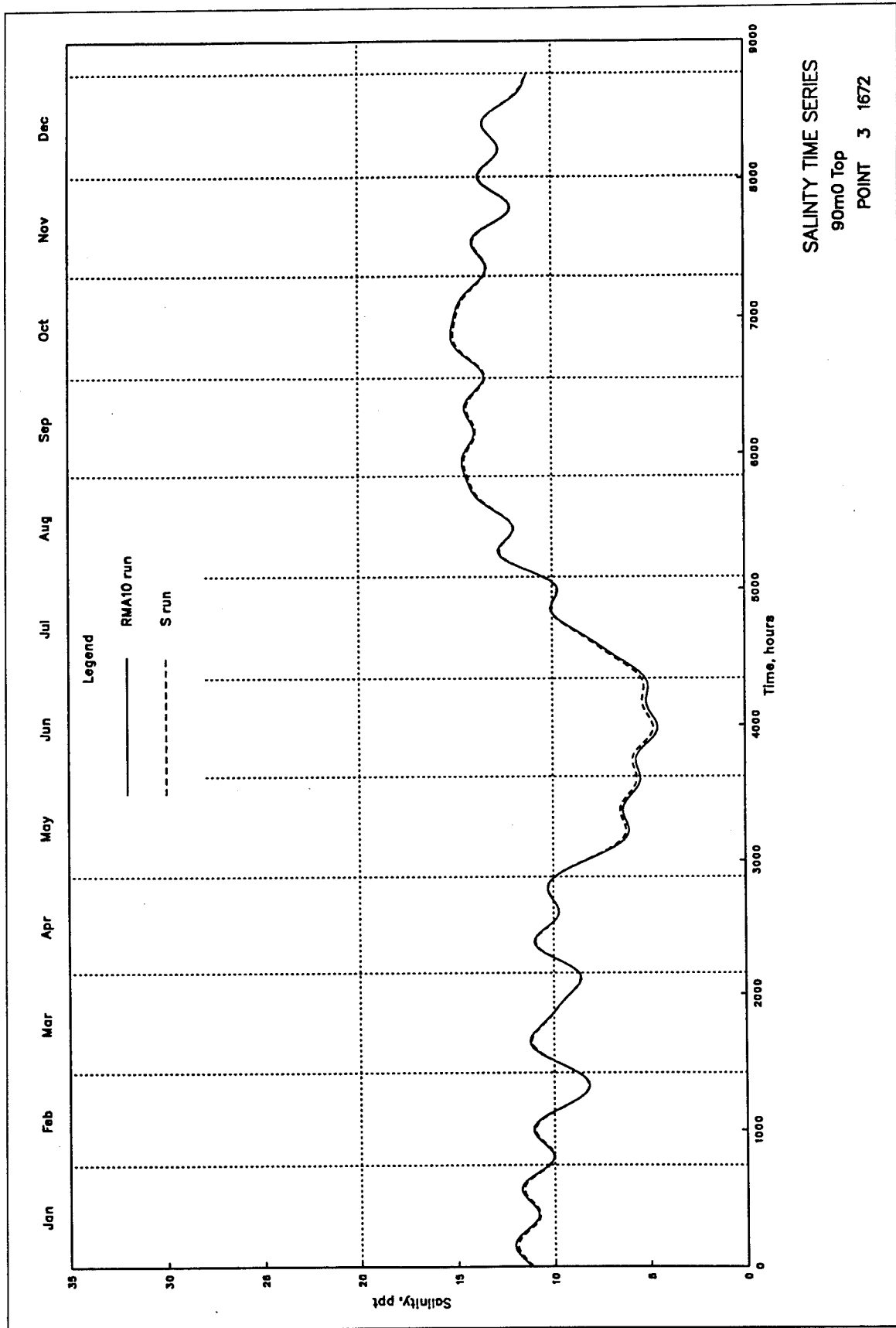


Plate 4



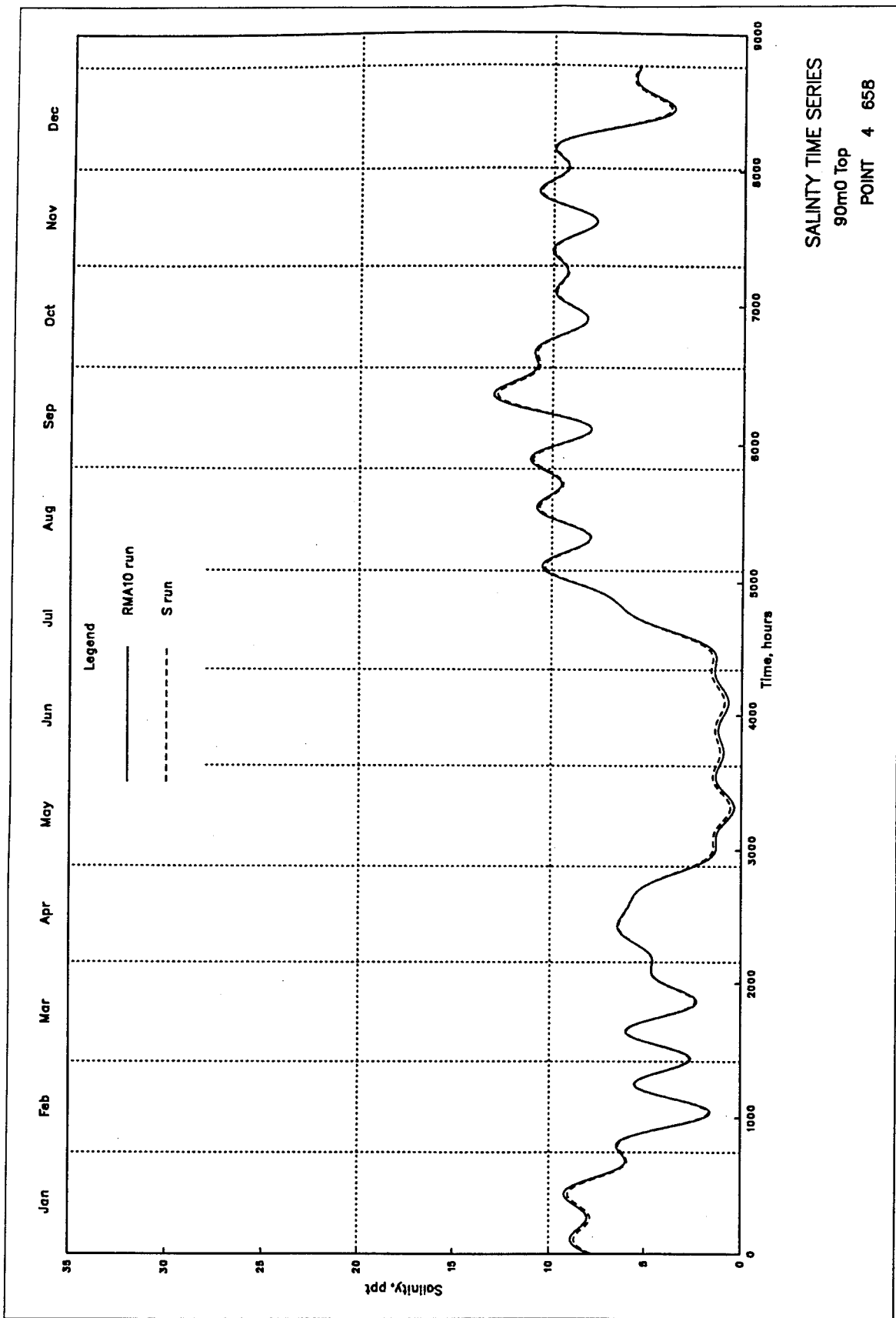


Plate 6

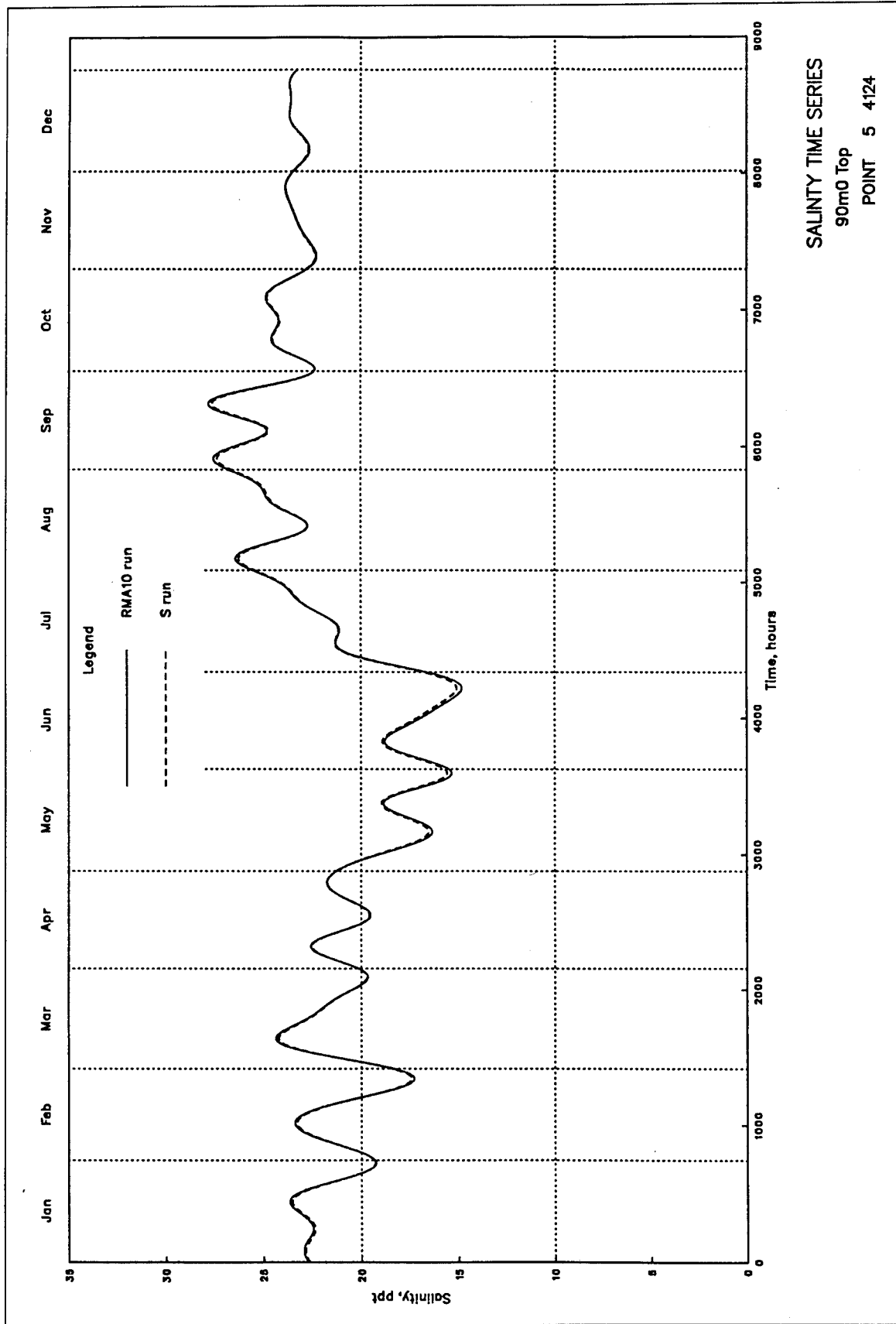


Plate 7

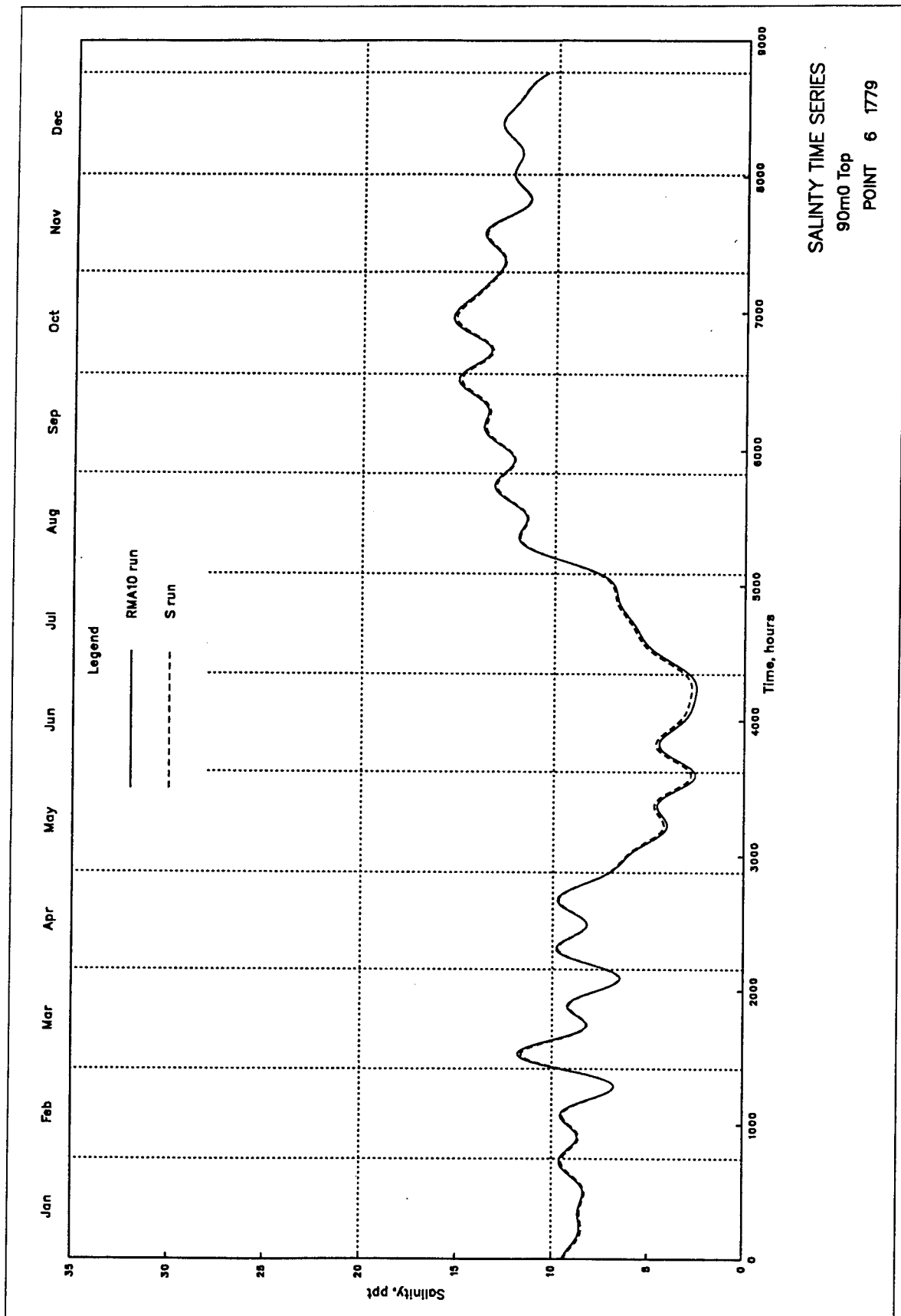
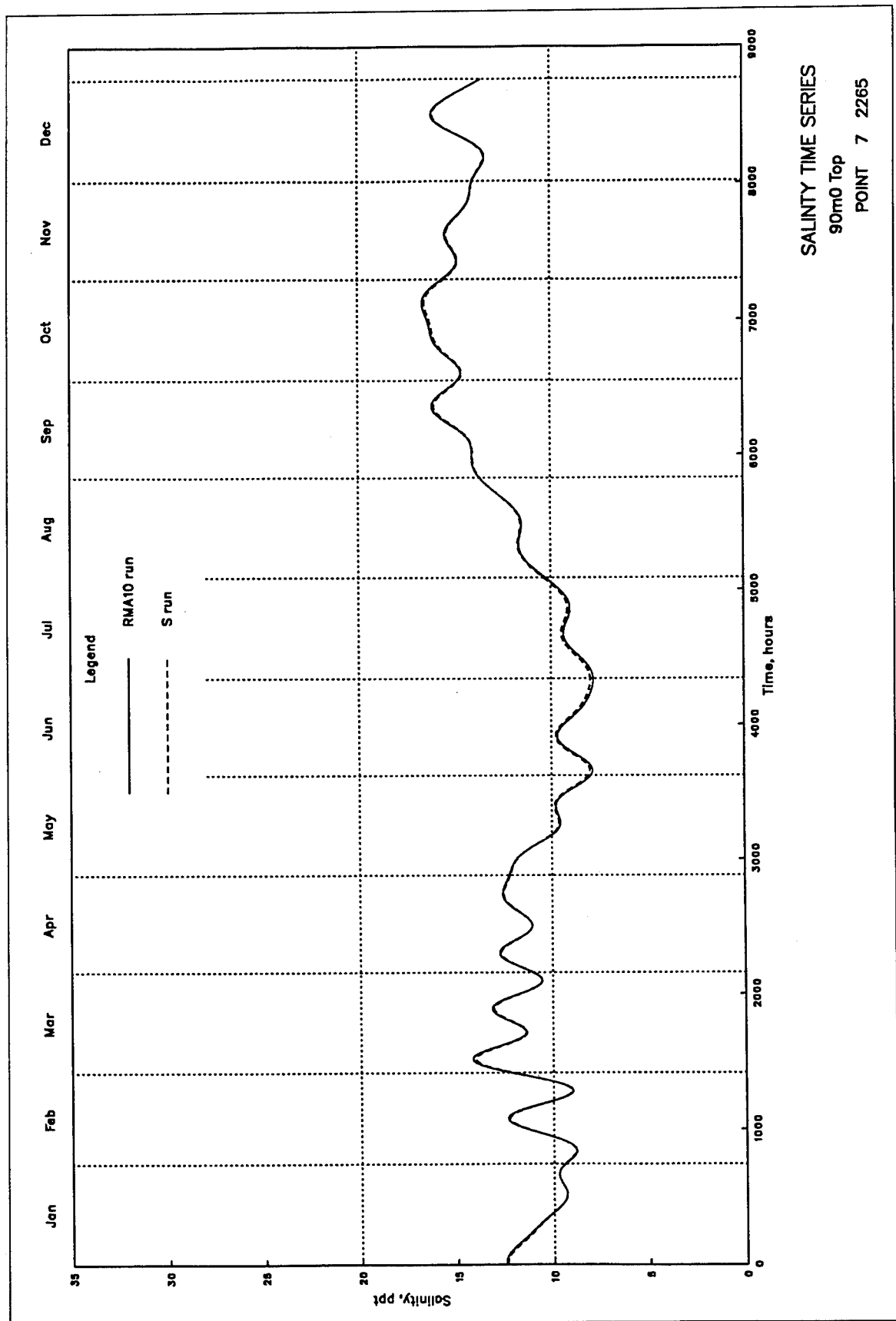


Plate 8



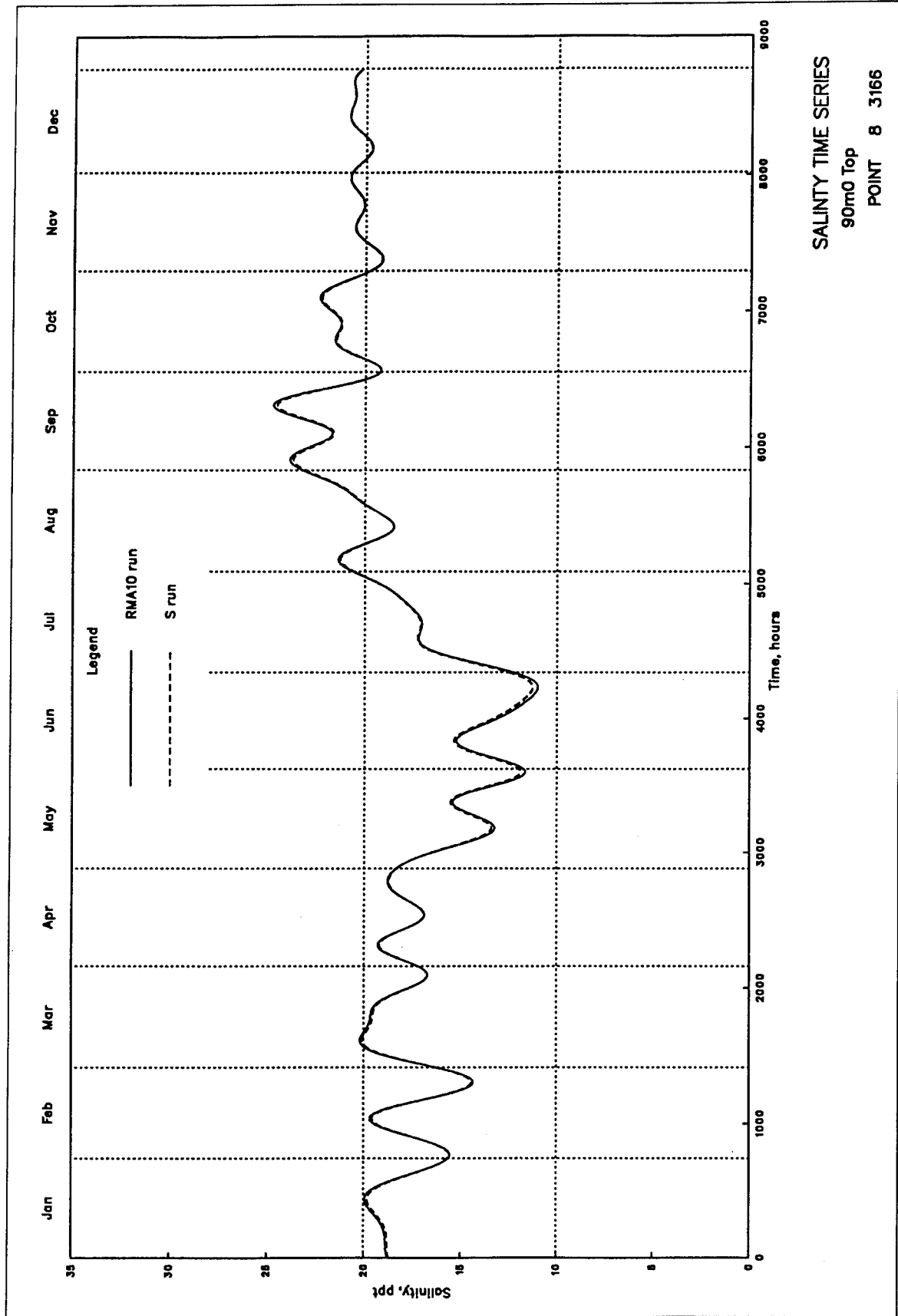
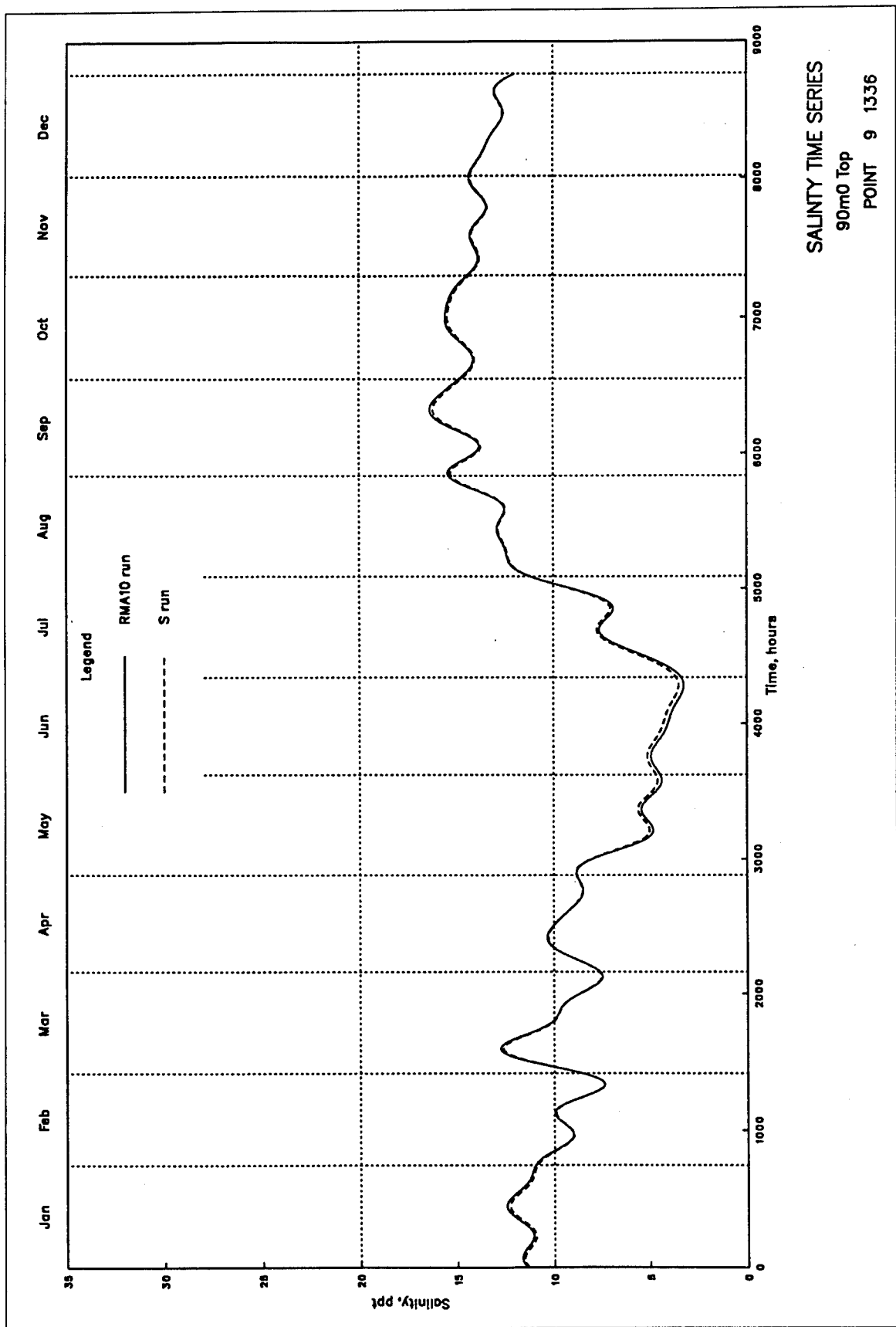


Plate 10



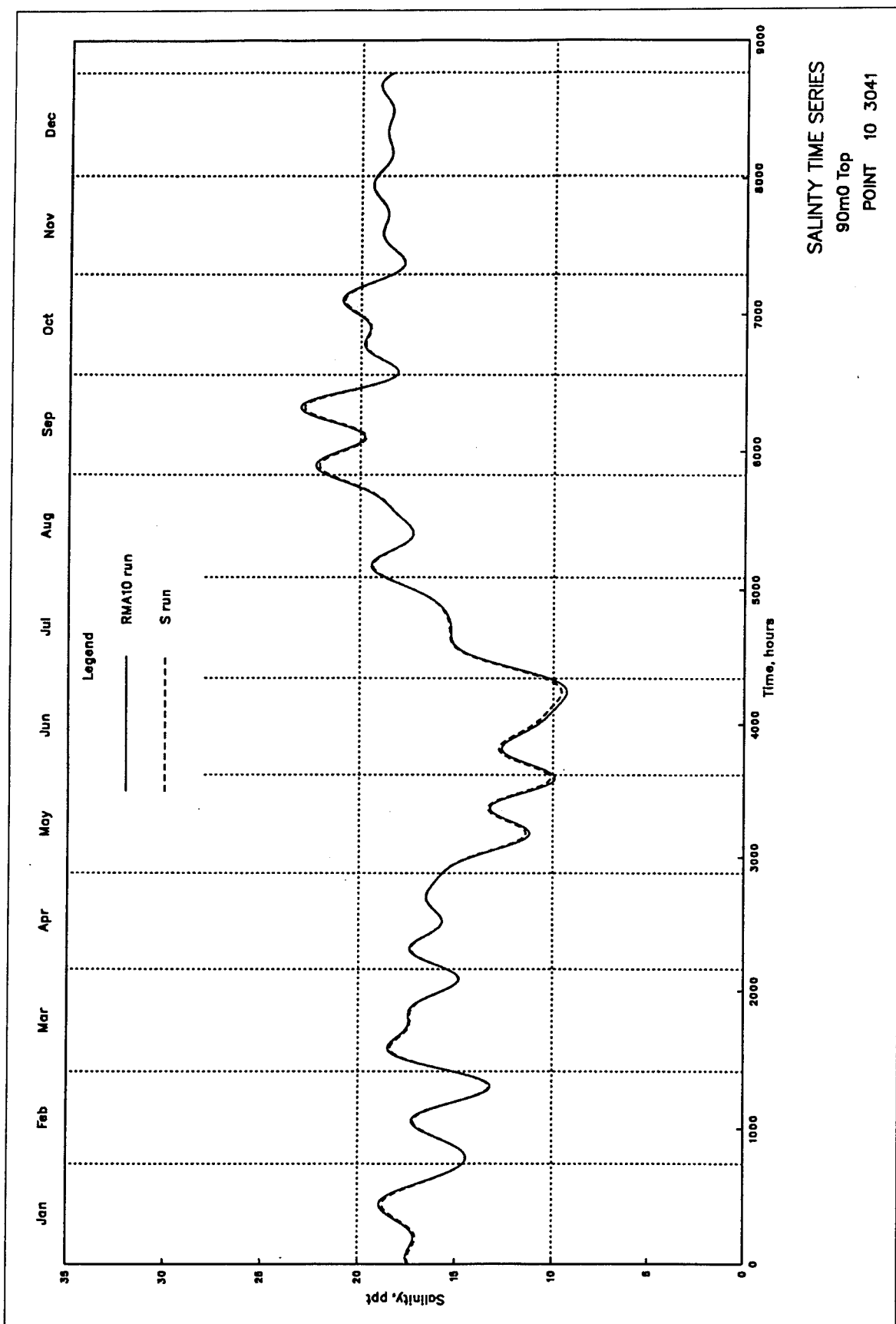
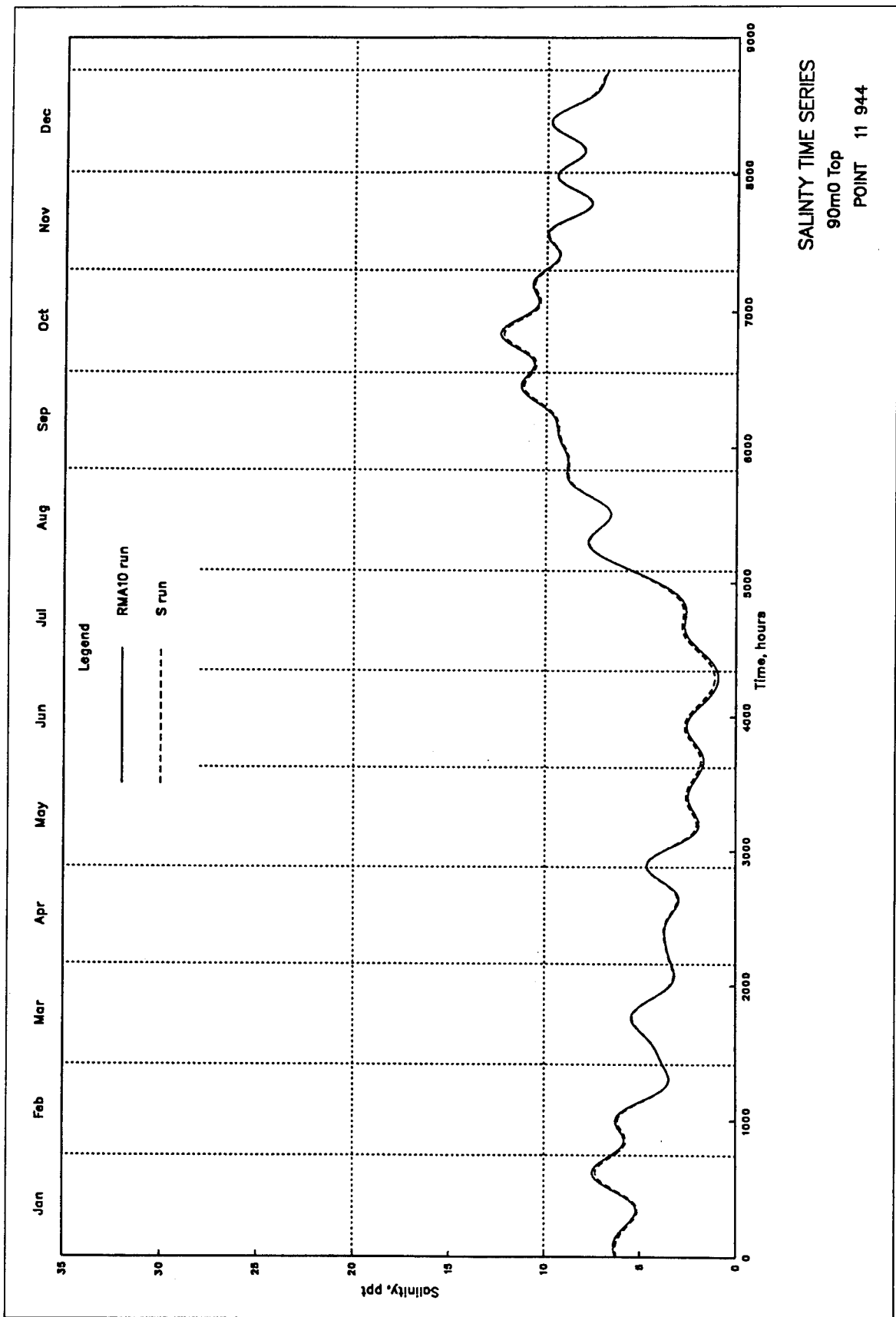


Plate 12



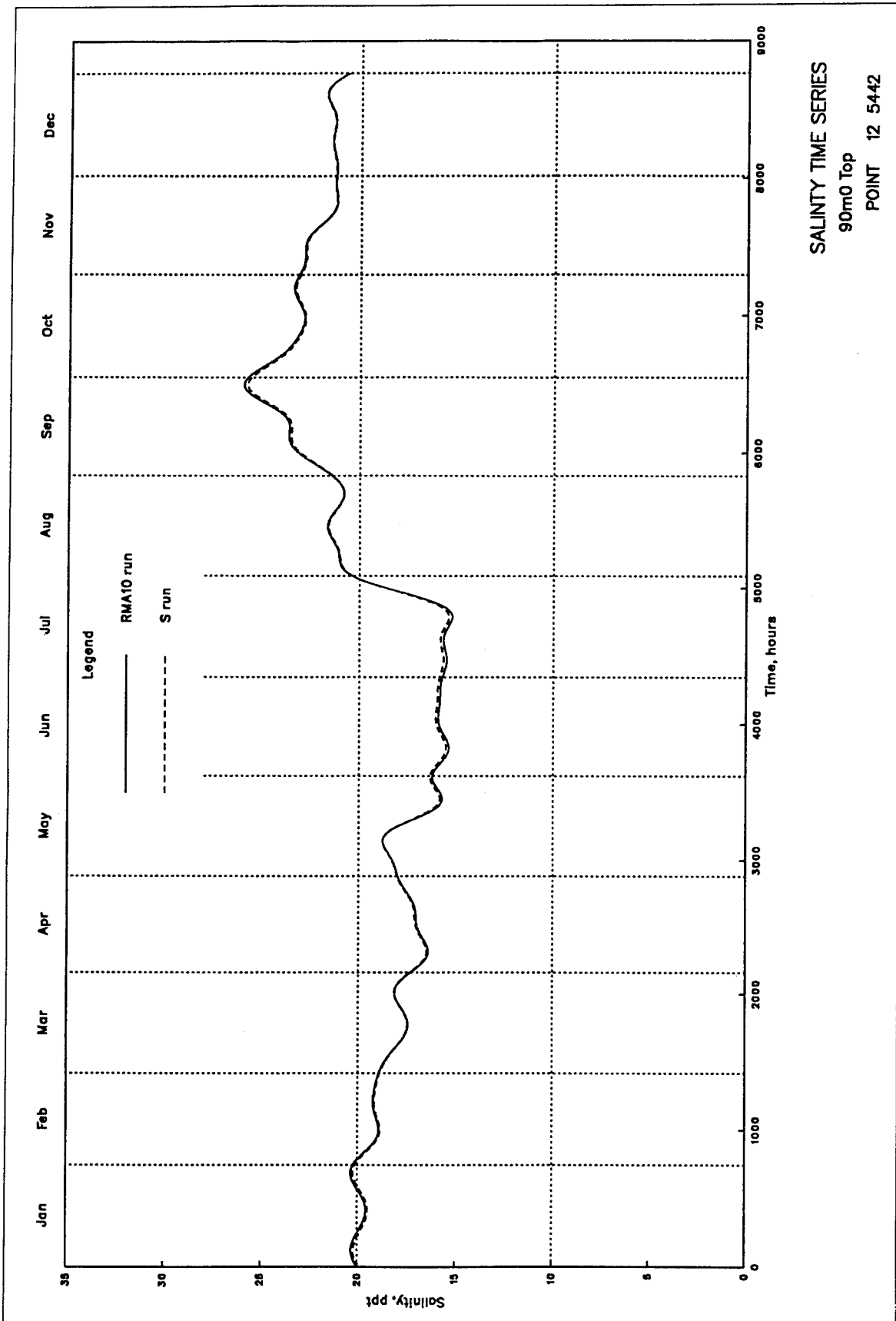
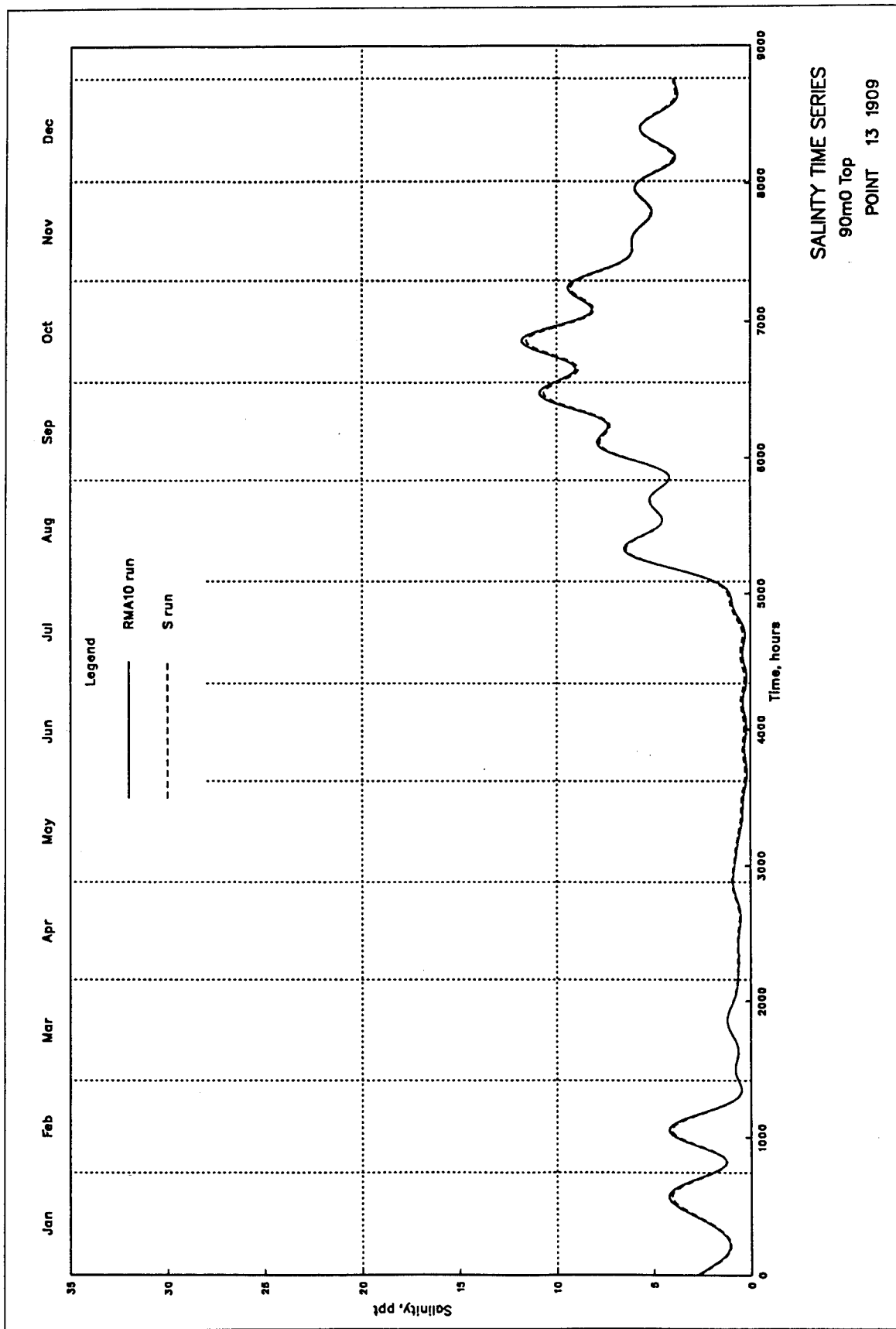


Plate 14



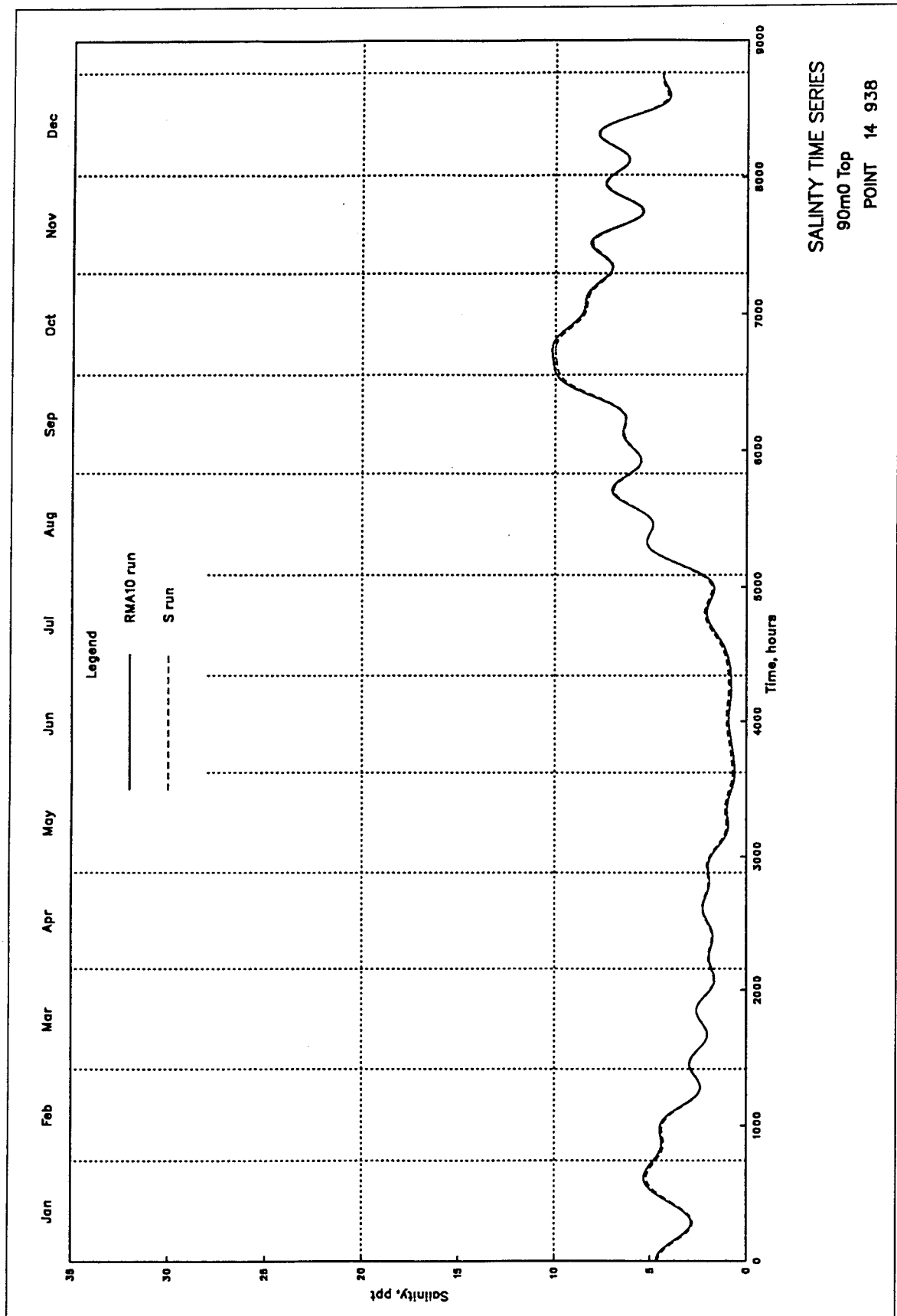
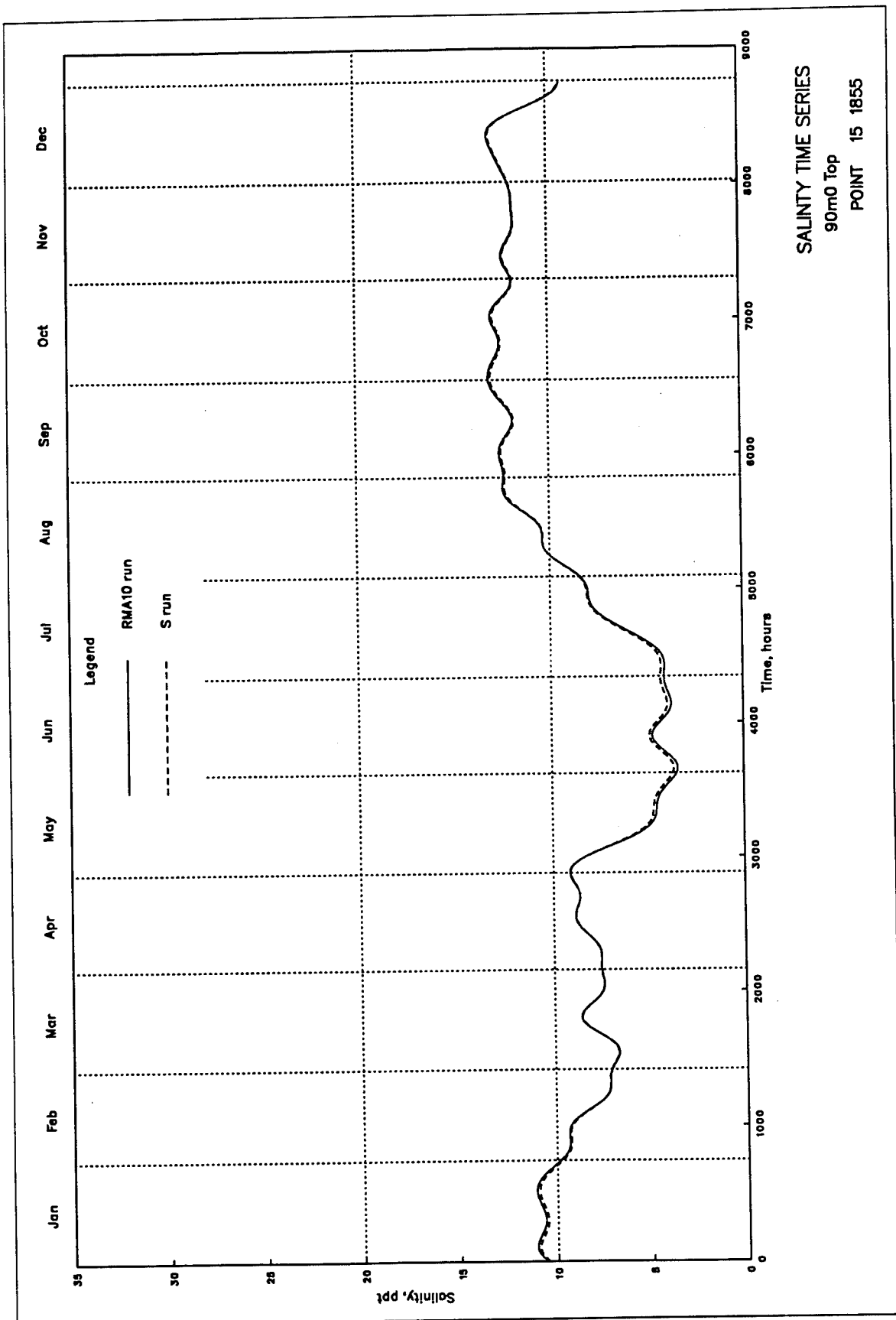


Plate 16



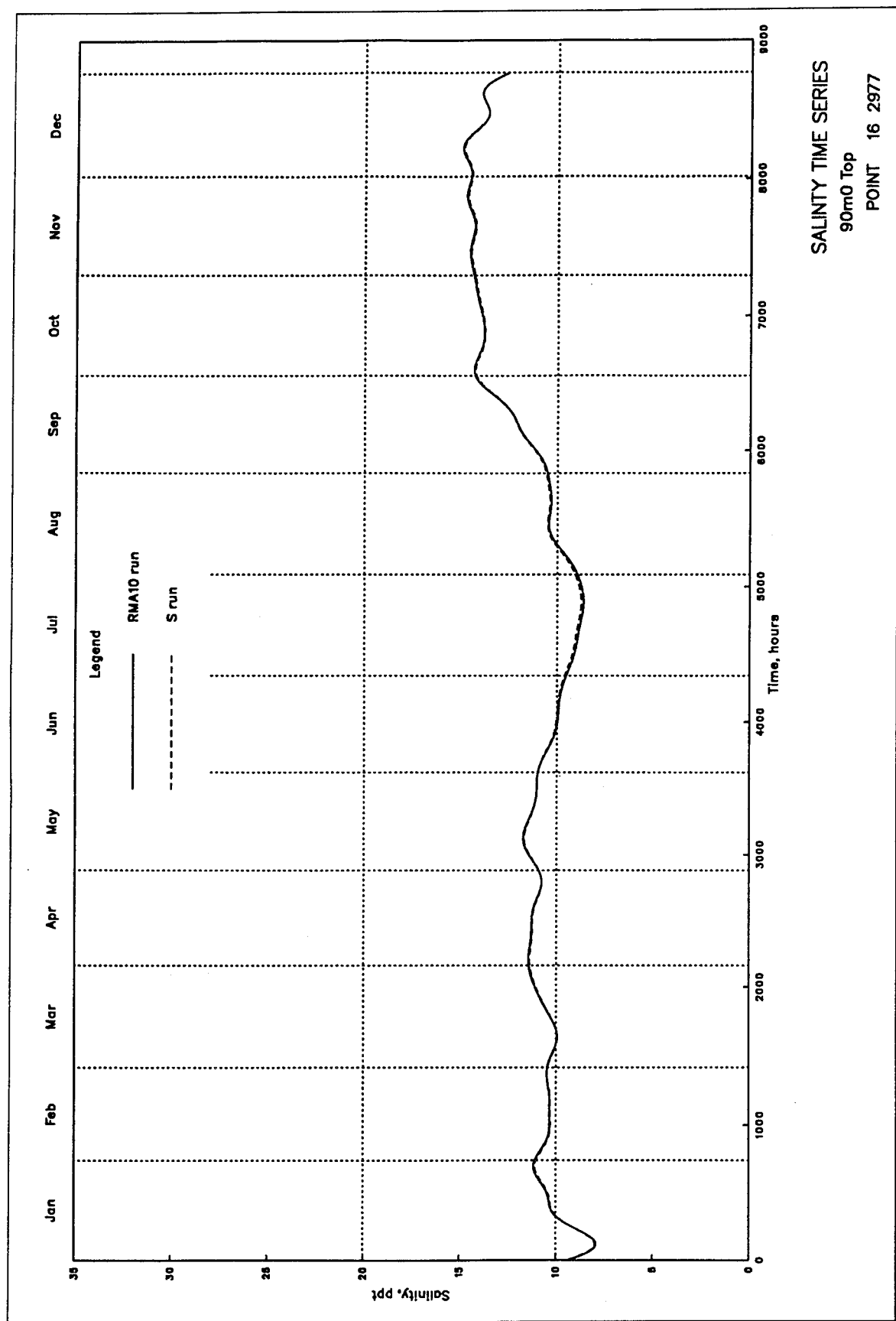
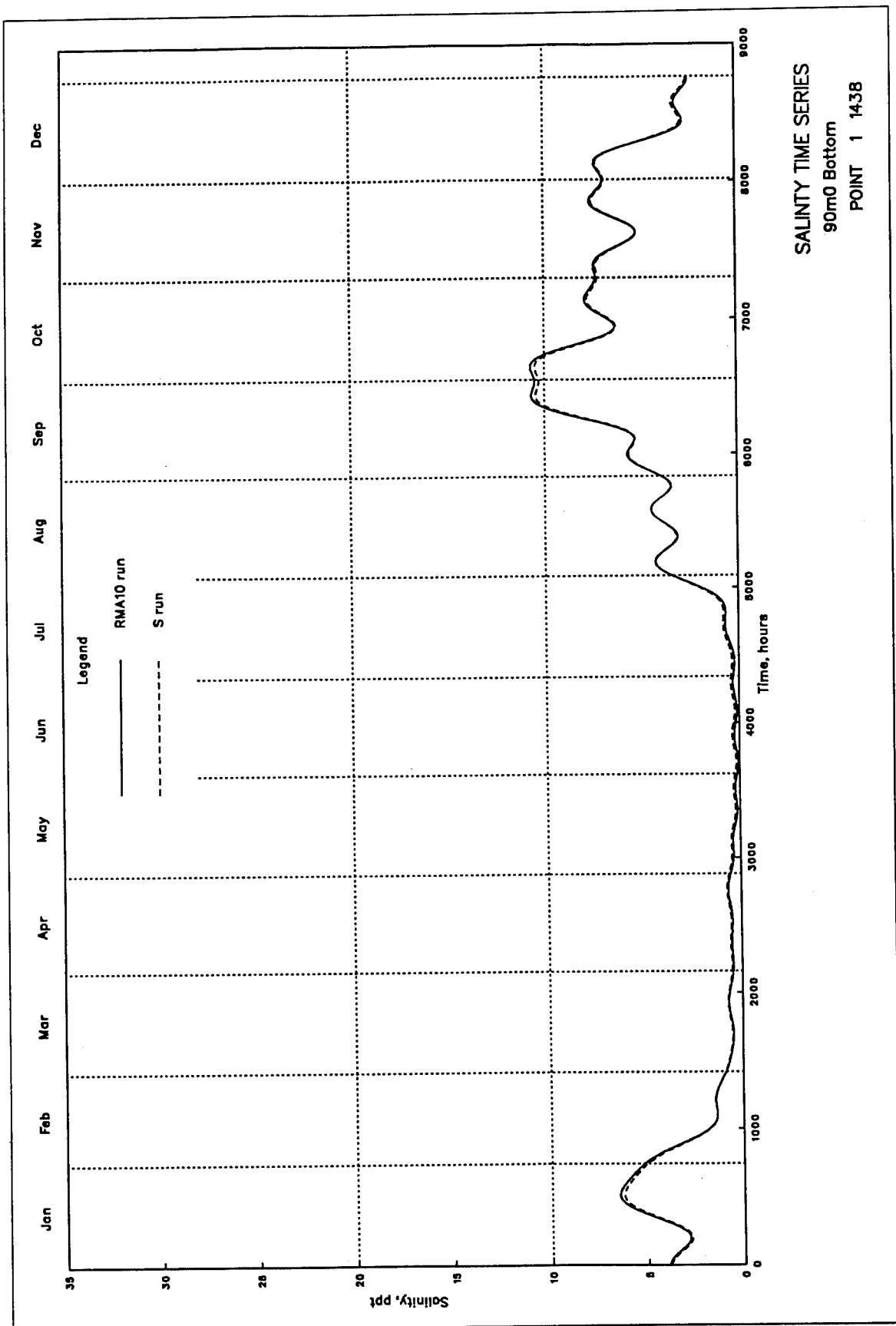


Plate 18



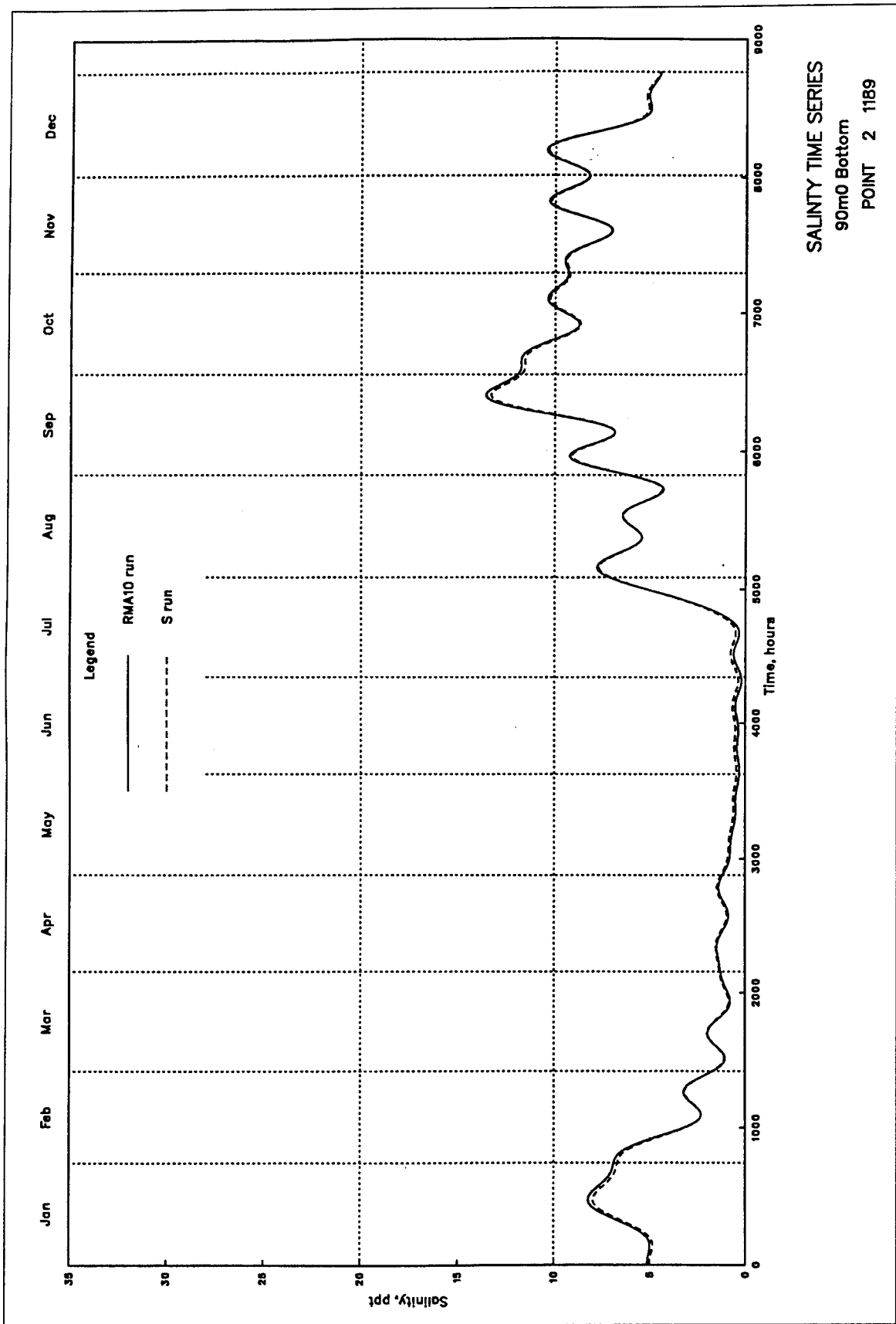
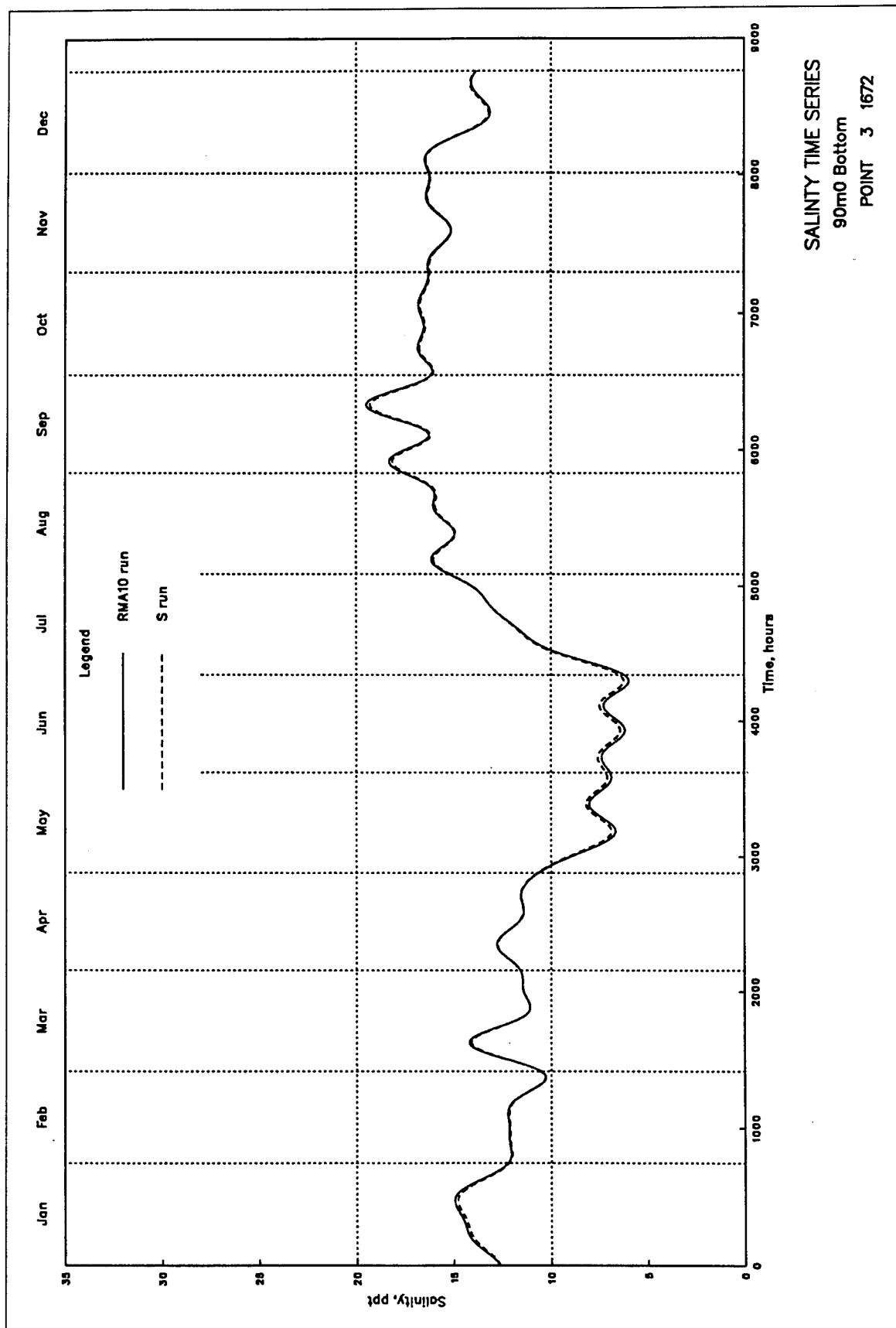


Plate 20



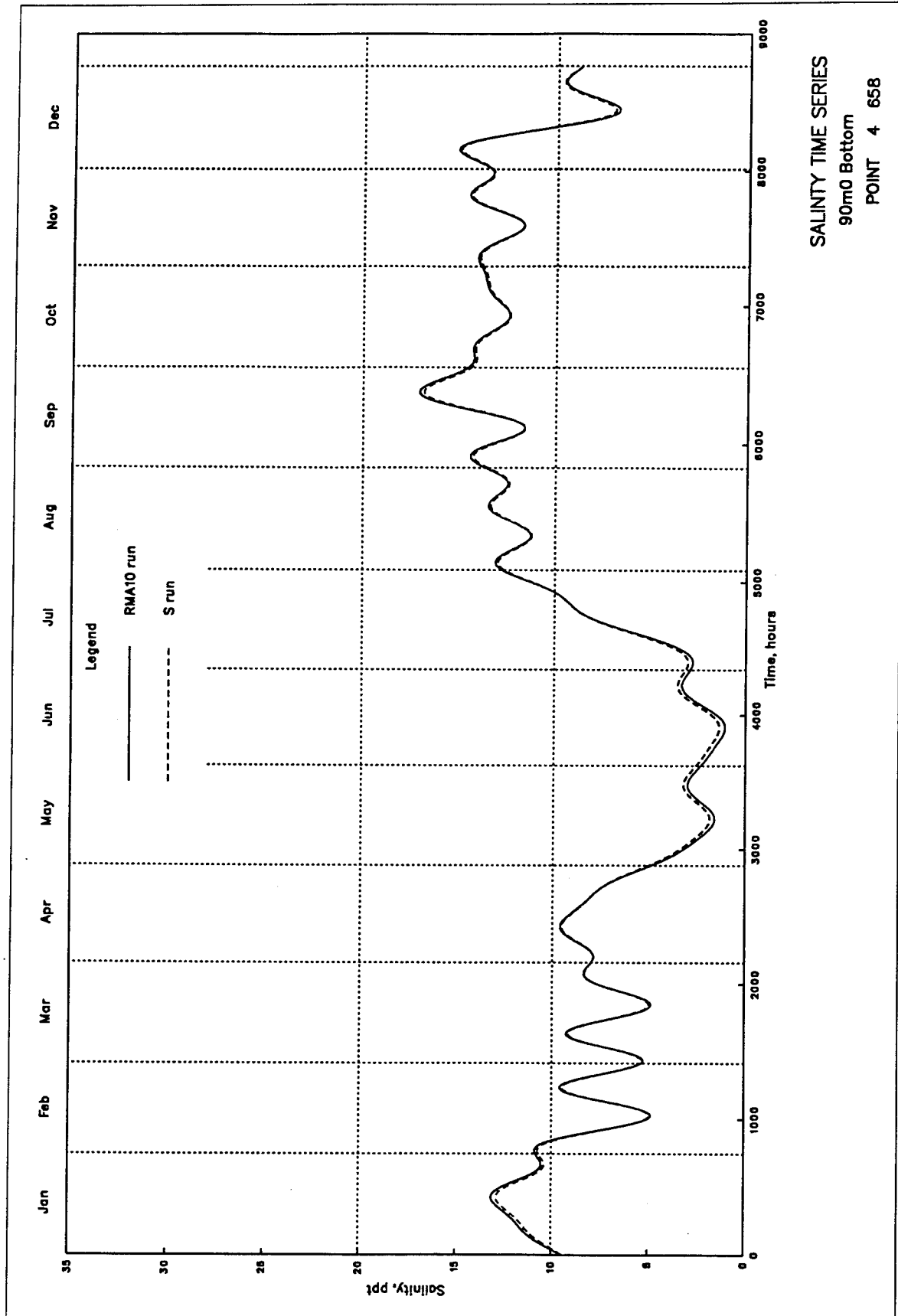
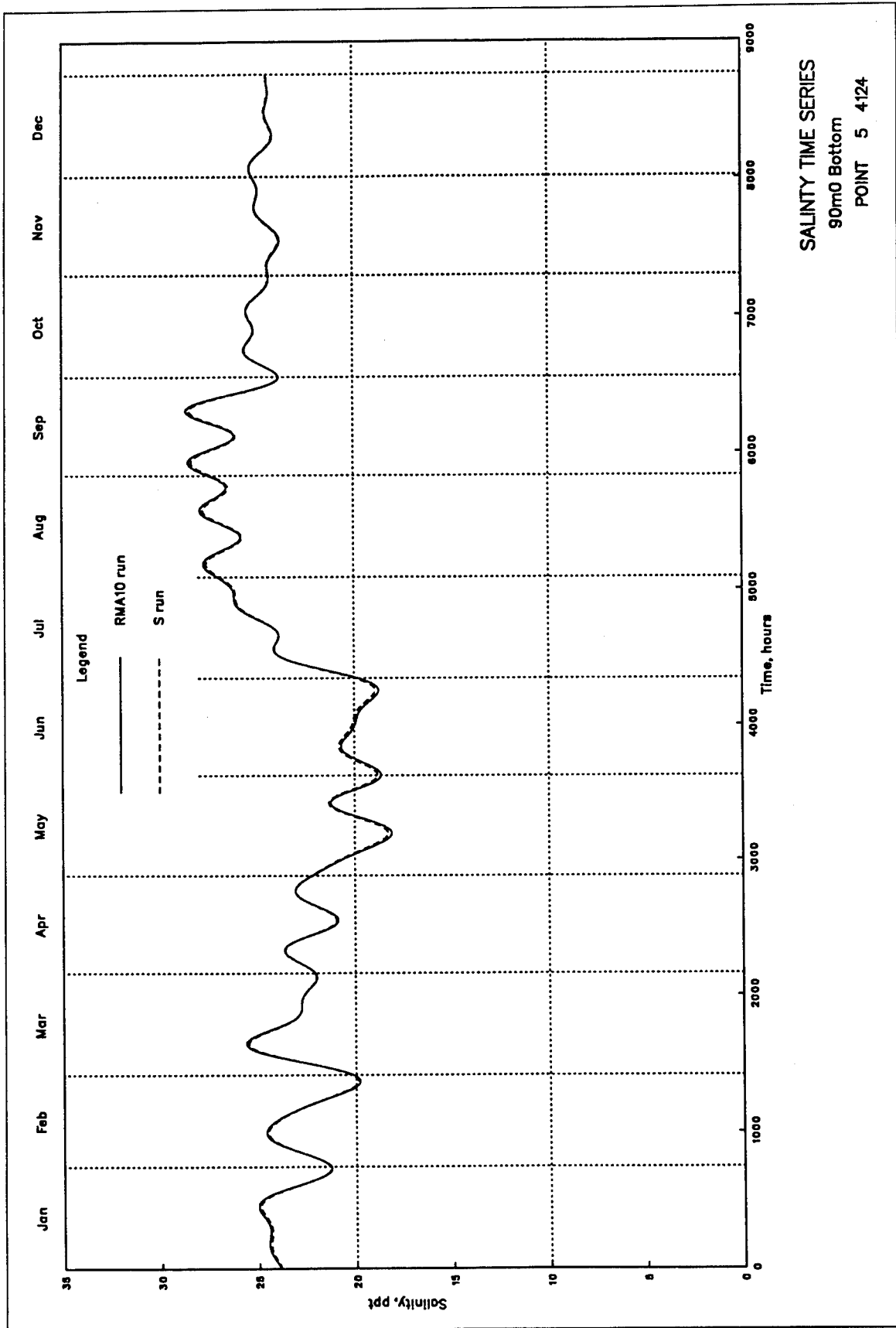


Plate 22



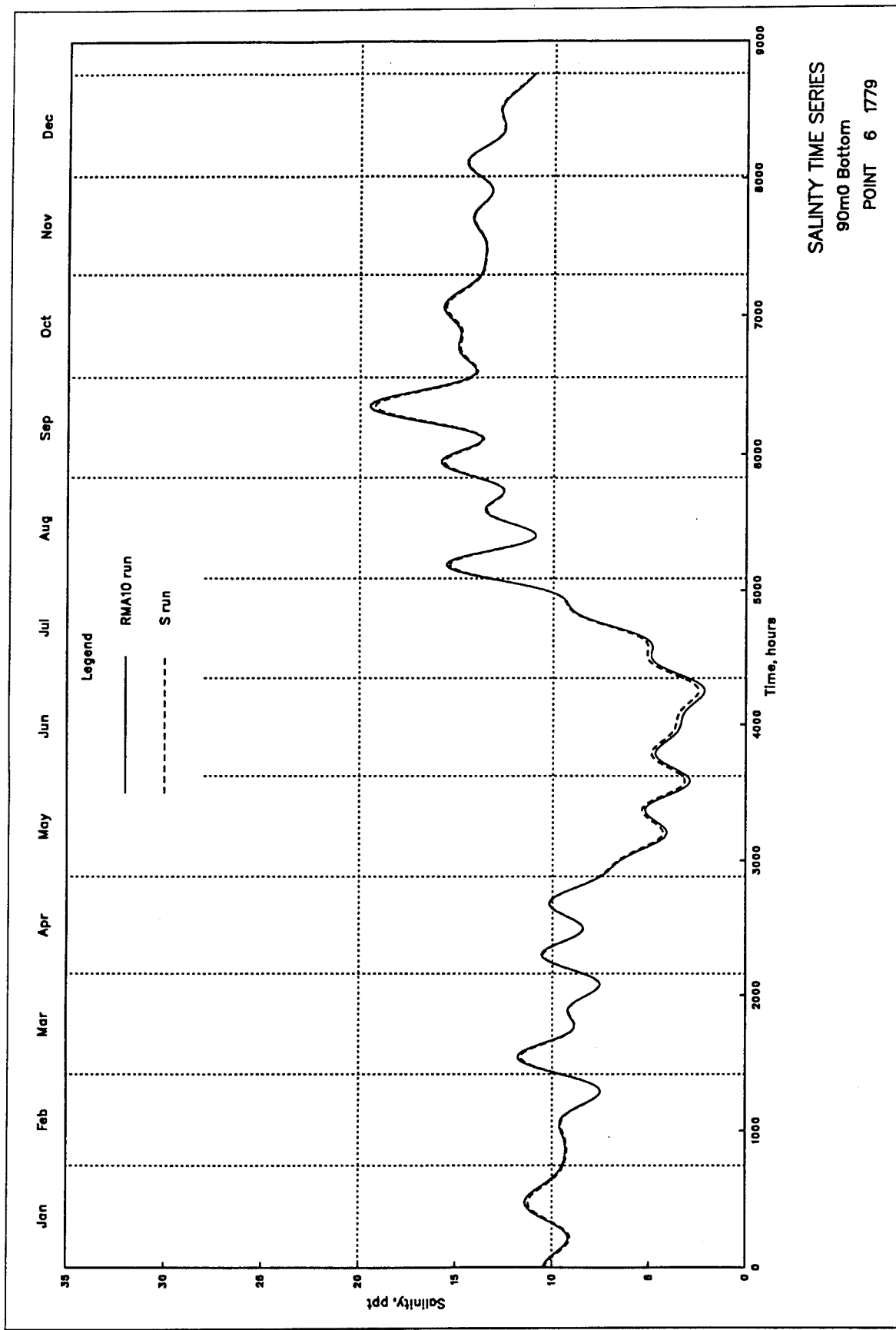
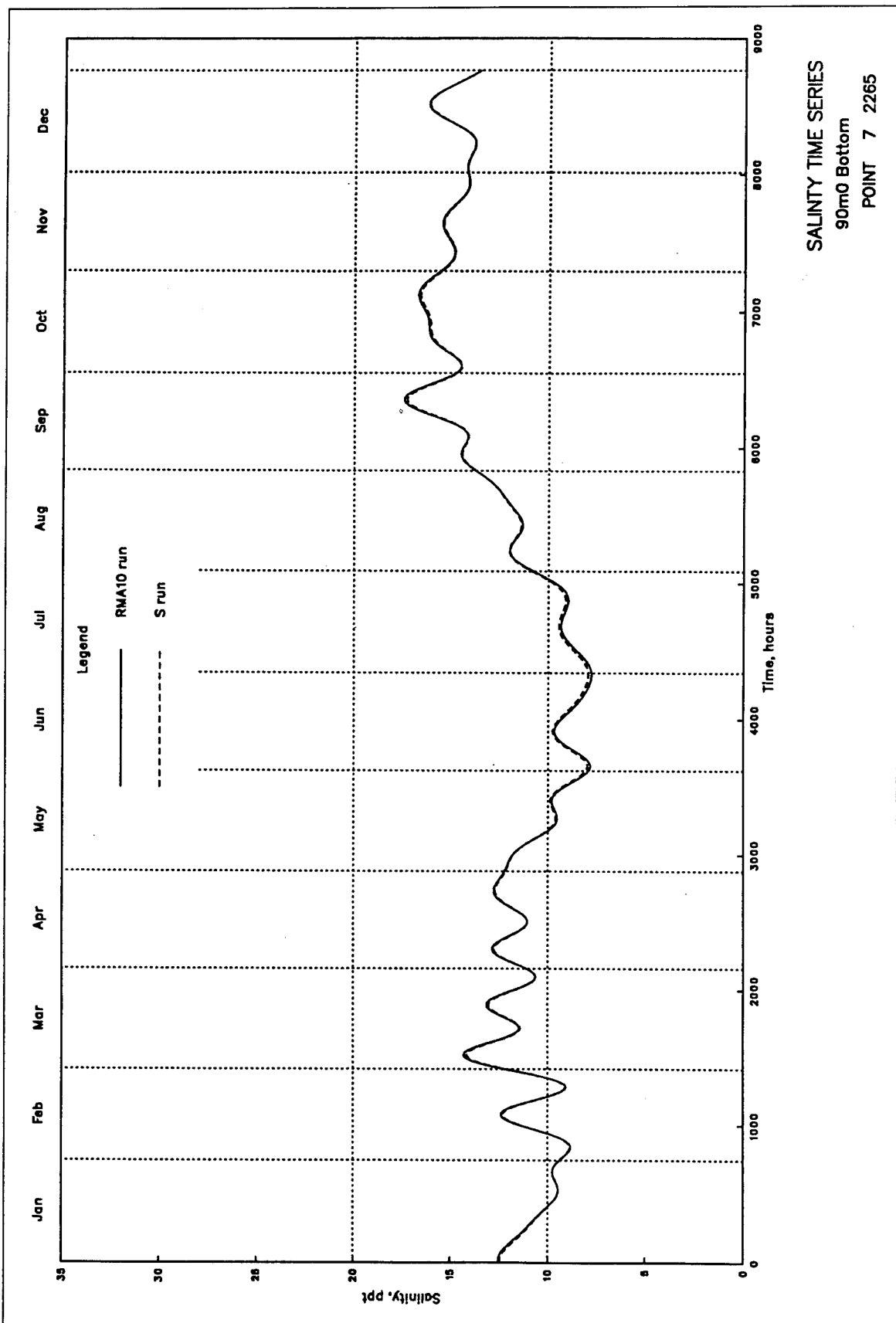


Plate 24



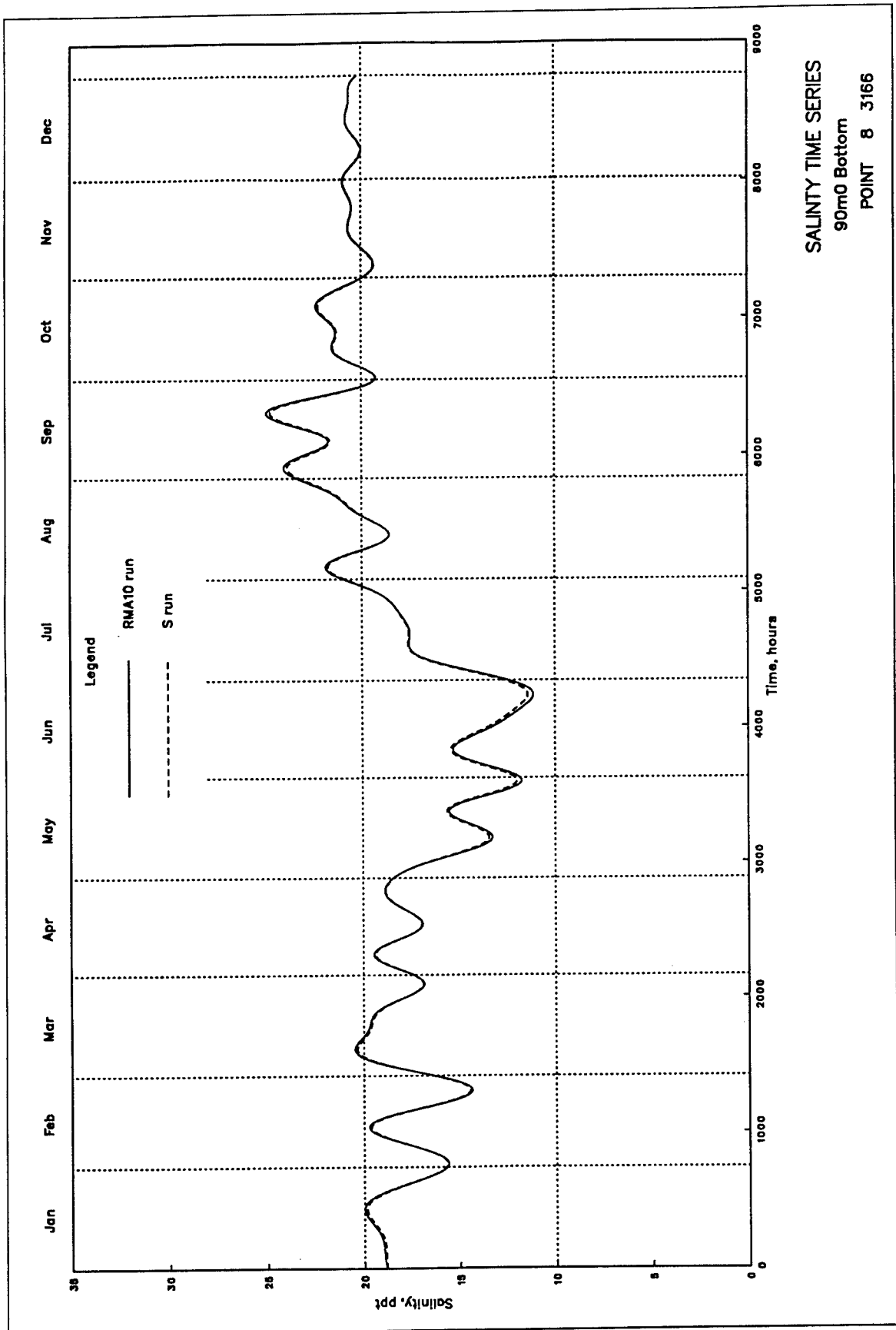
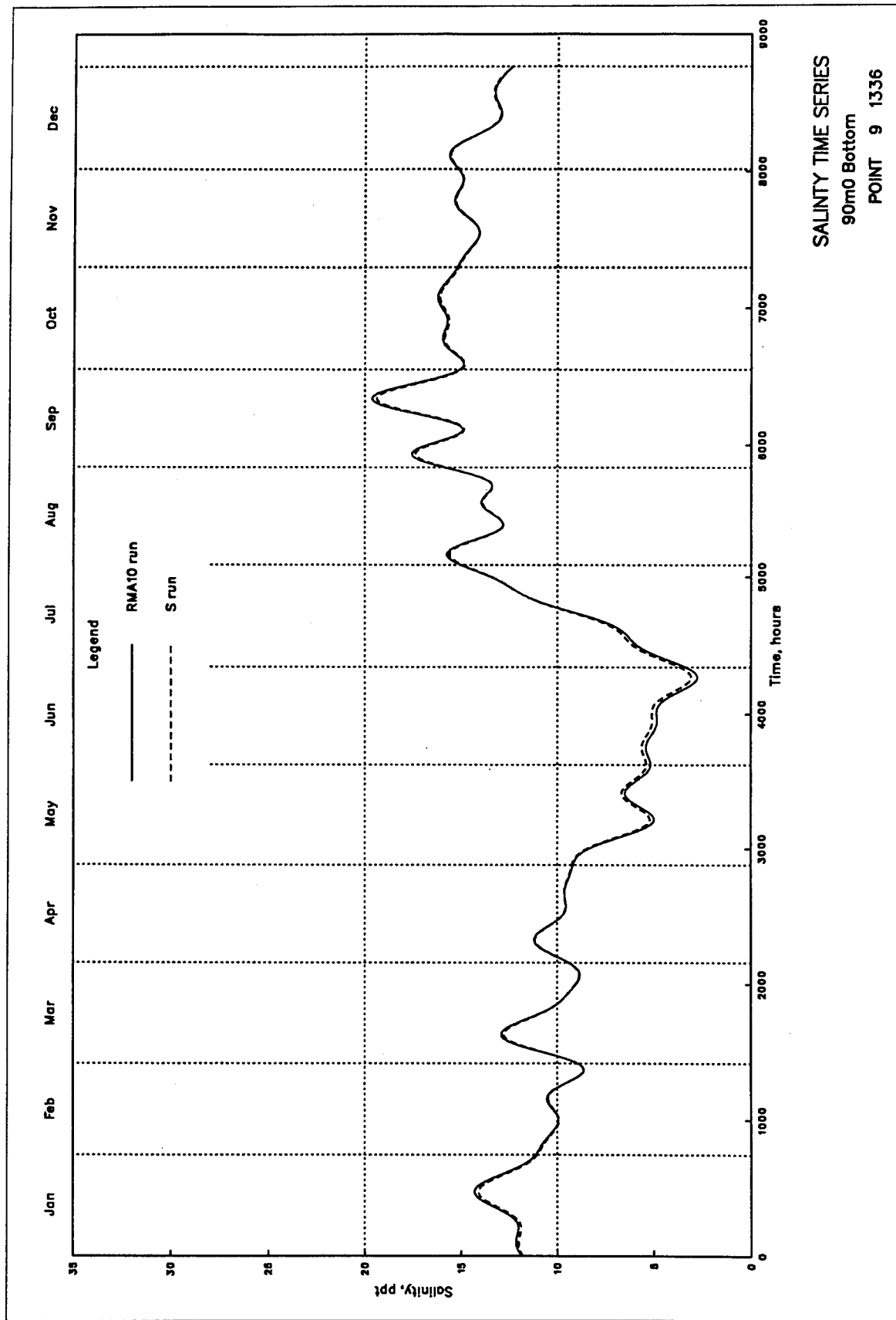


Plate 26



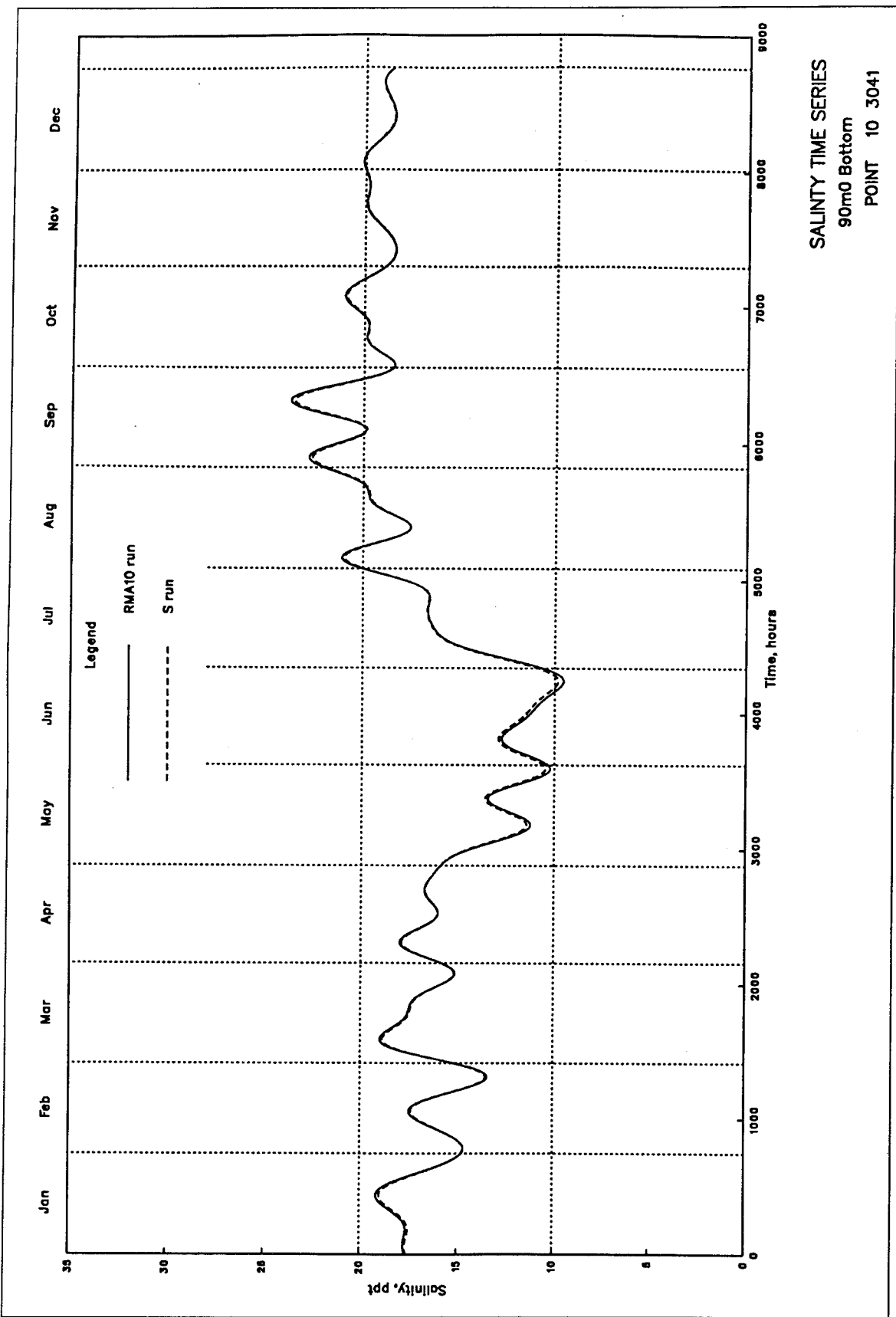
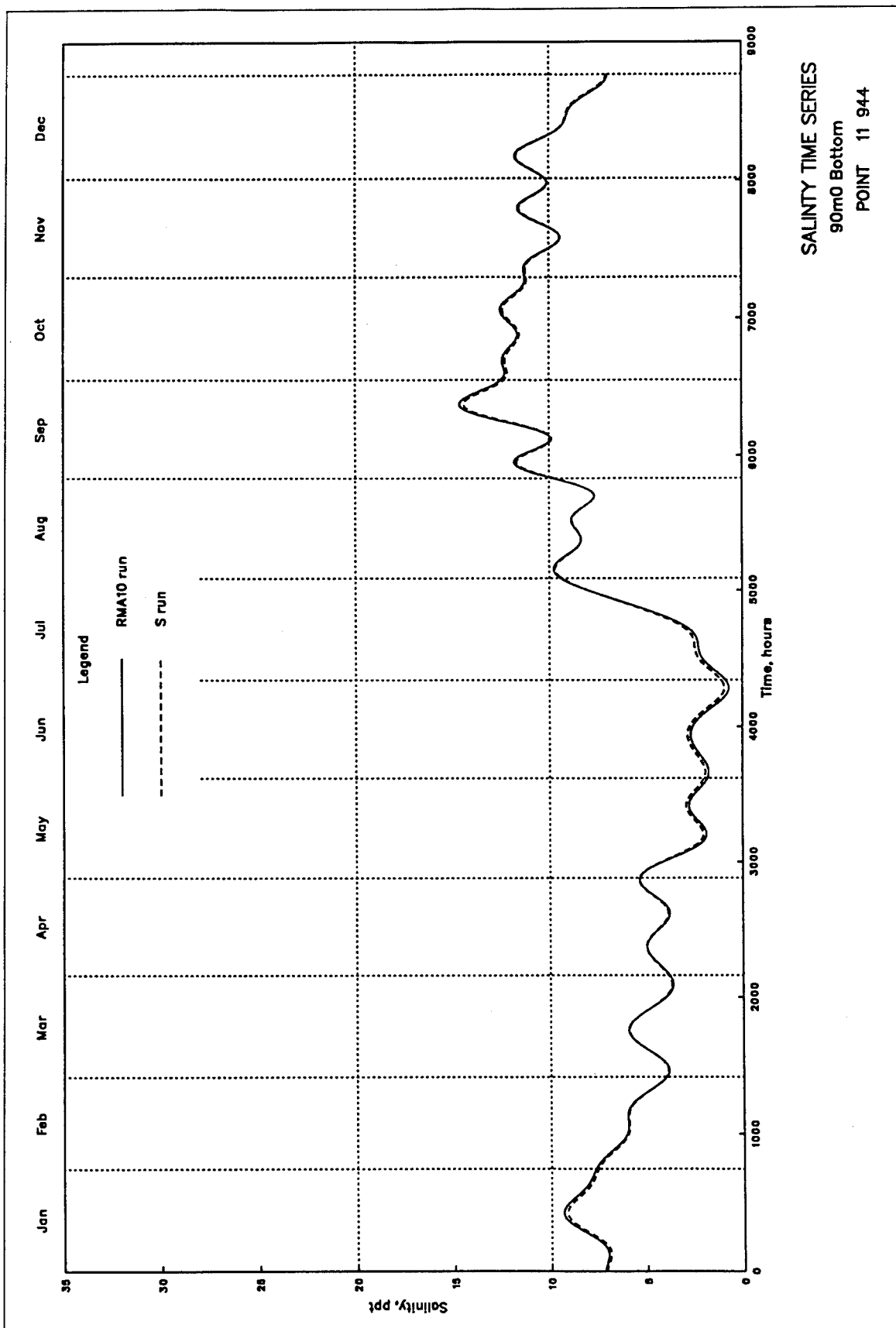


Plate 28



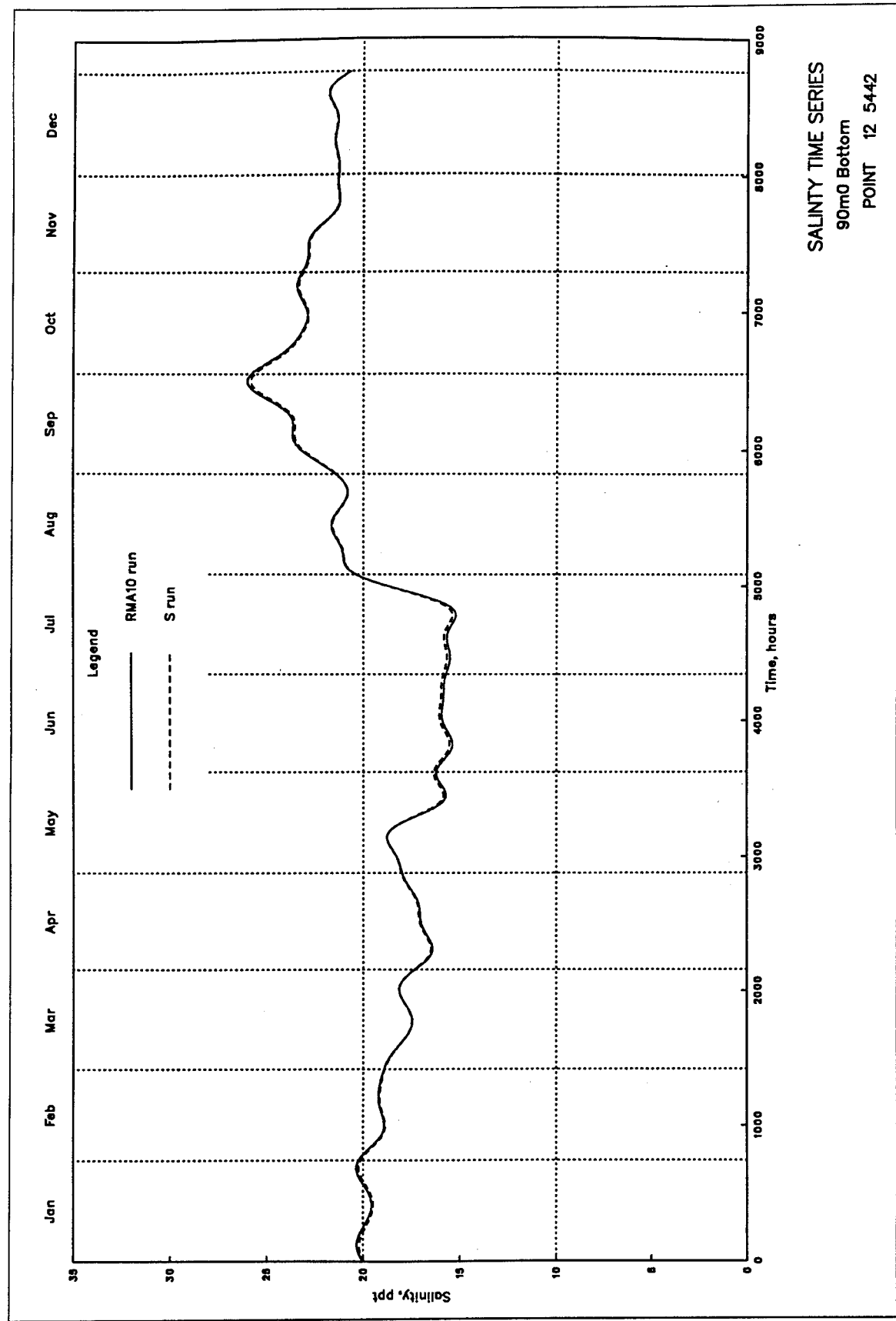
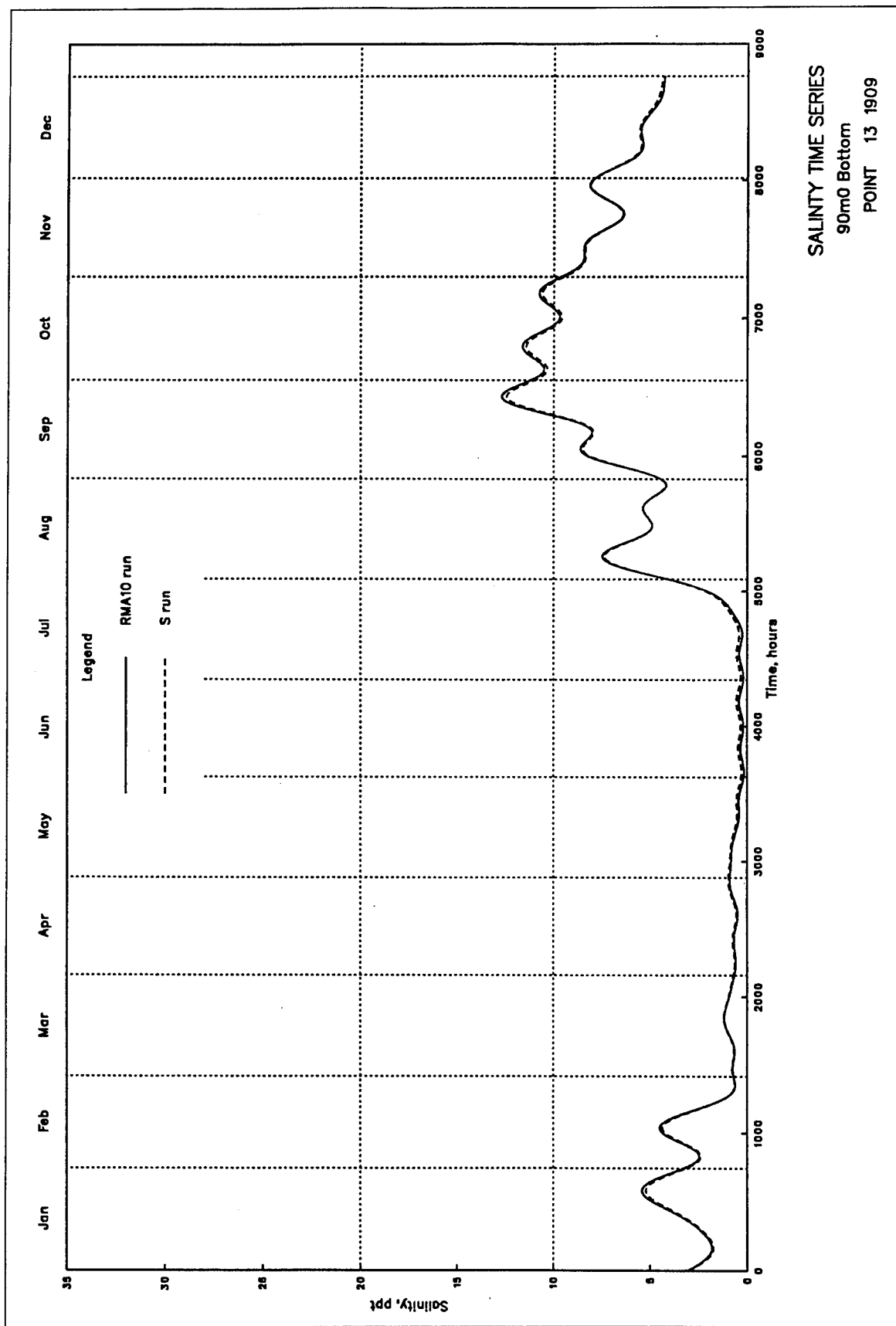


Plate 30



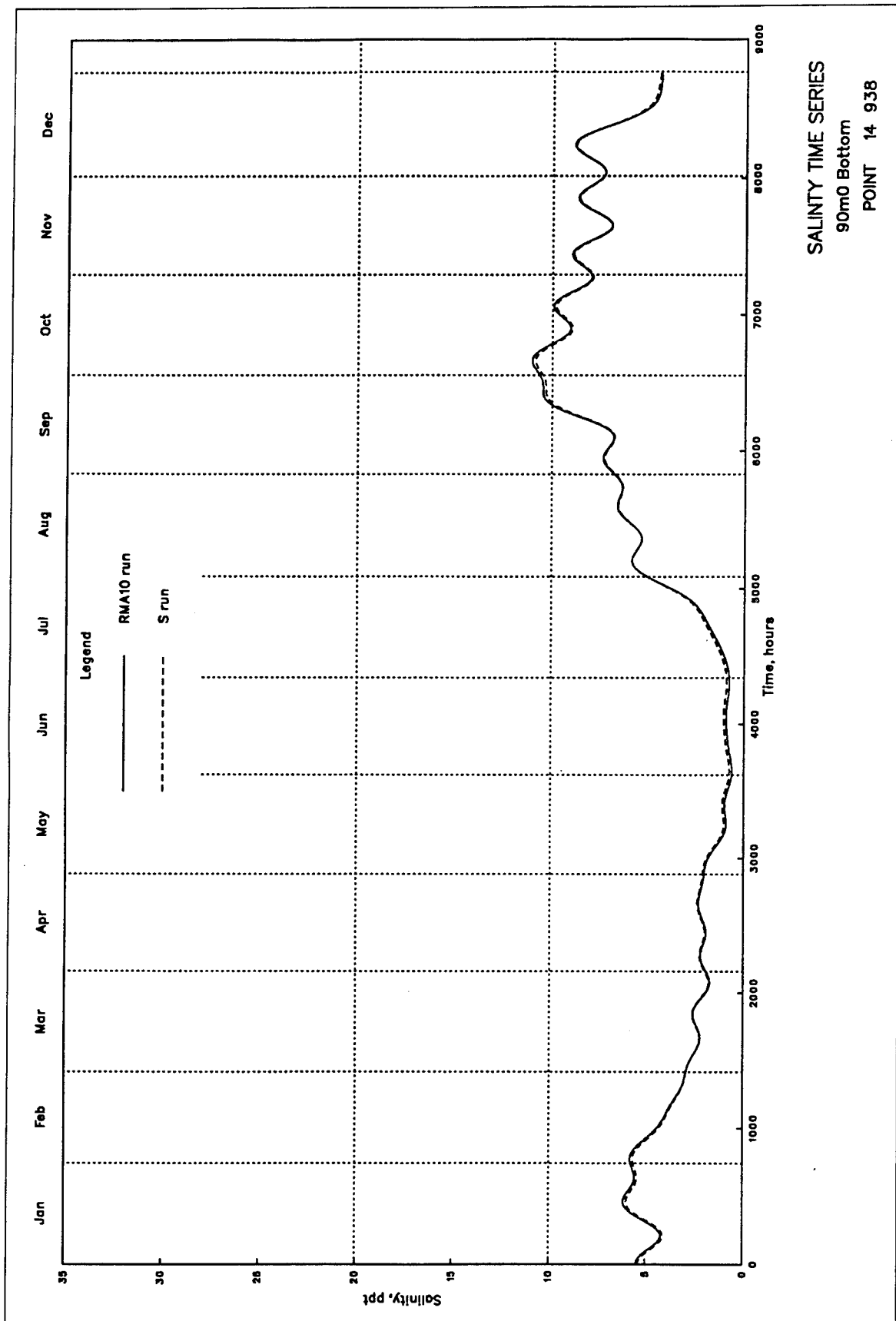
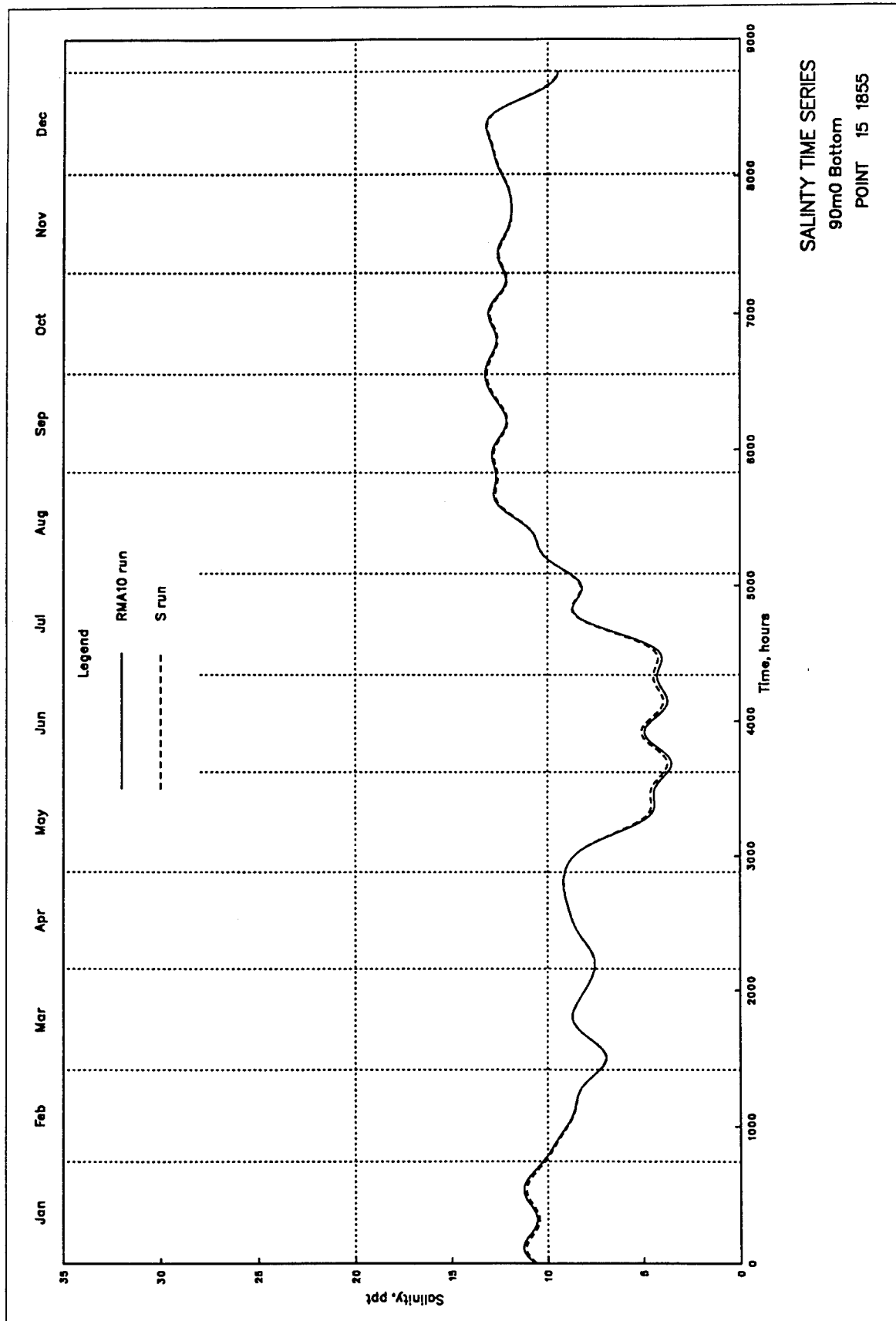


Plate 32



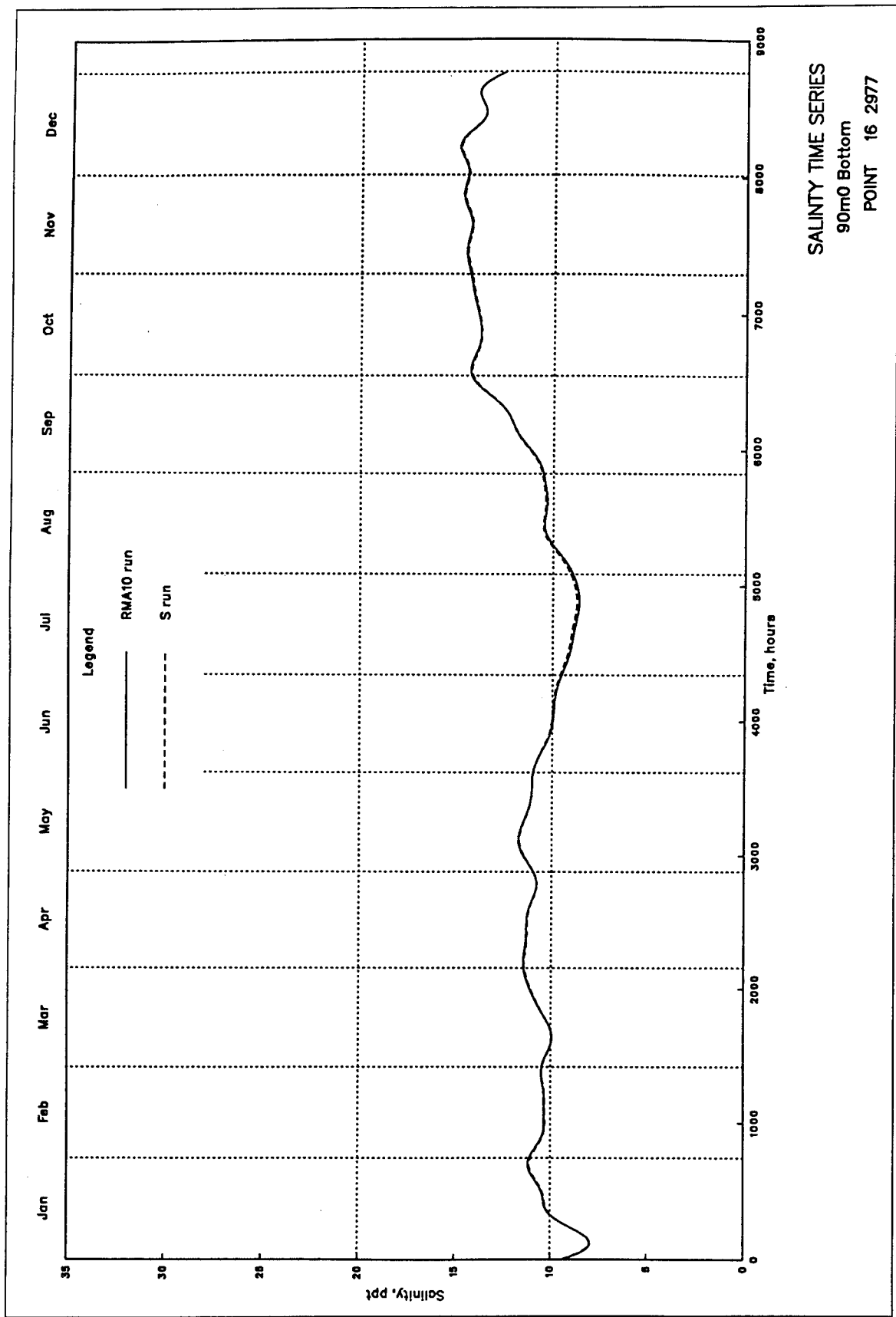
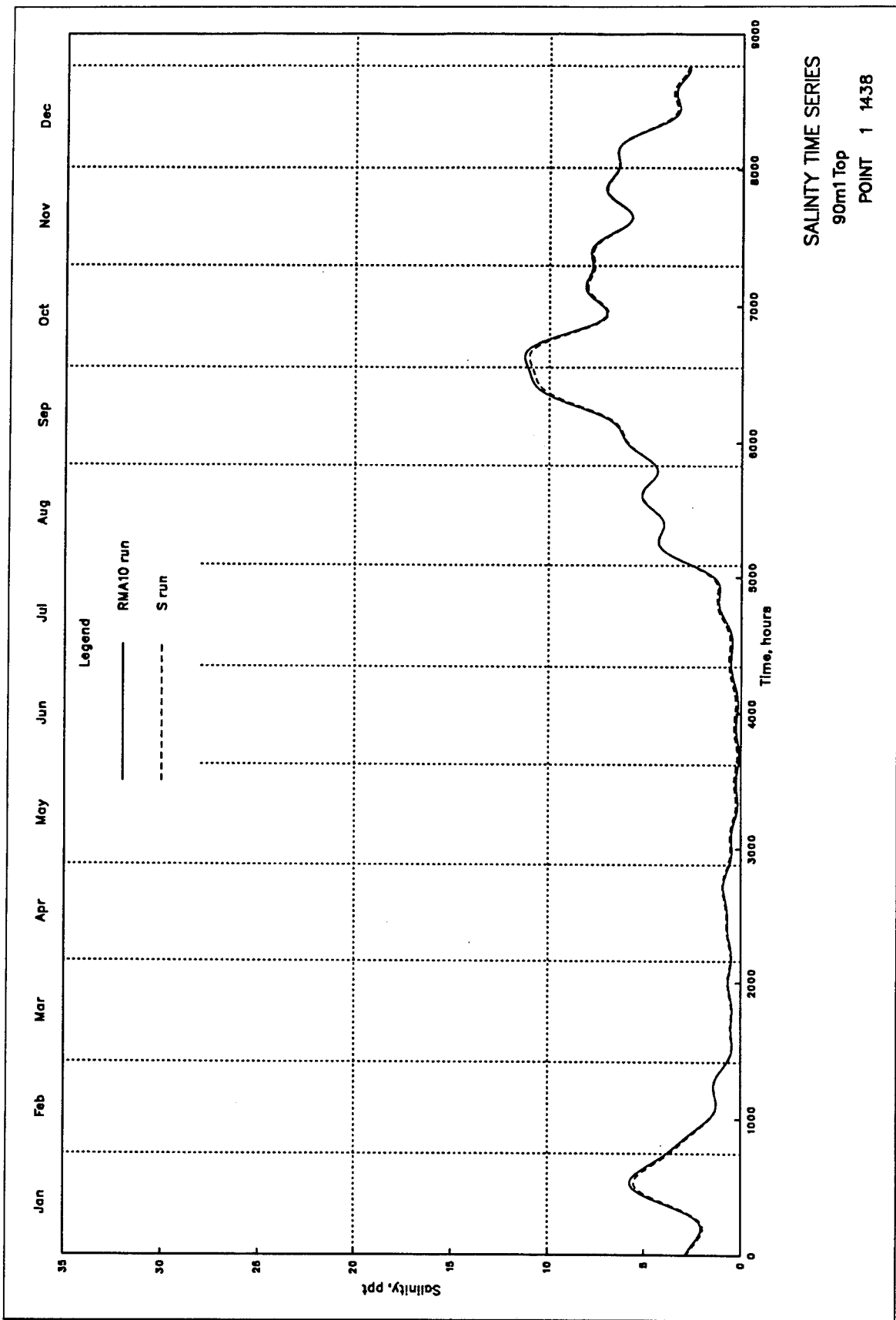


Plate 34



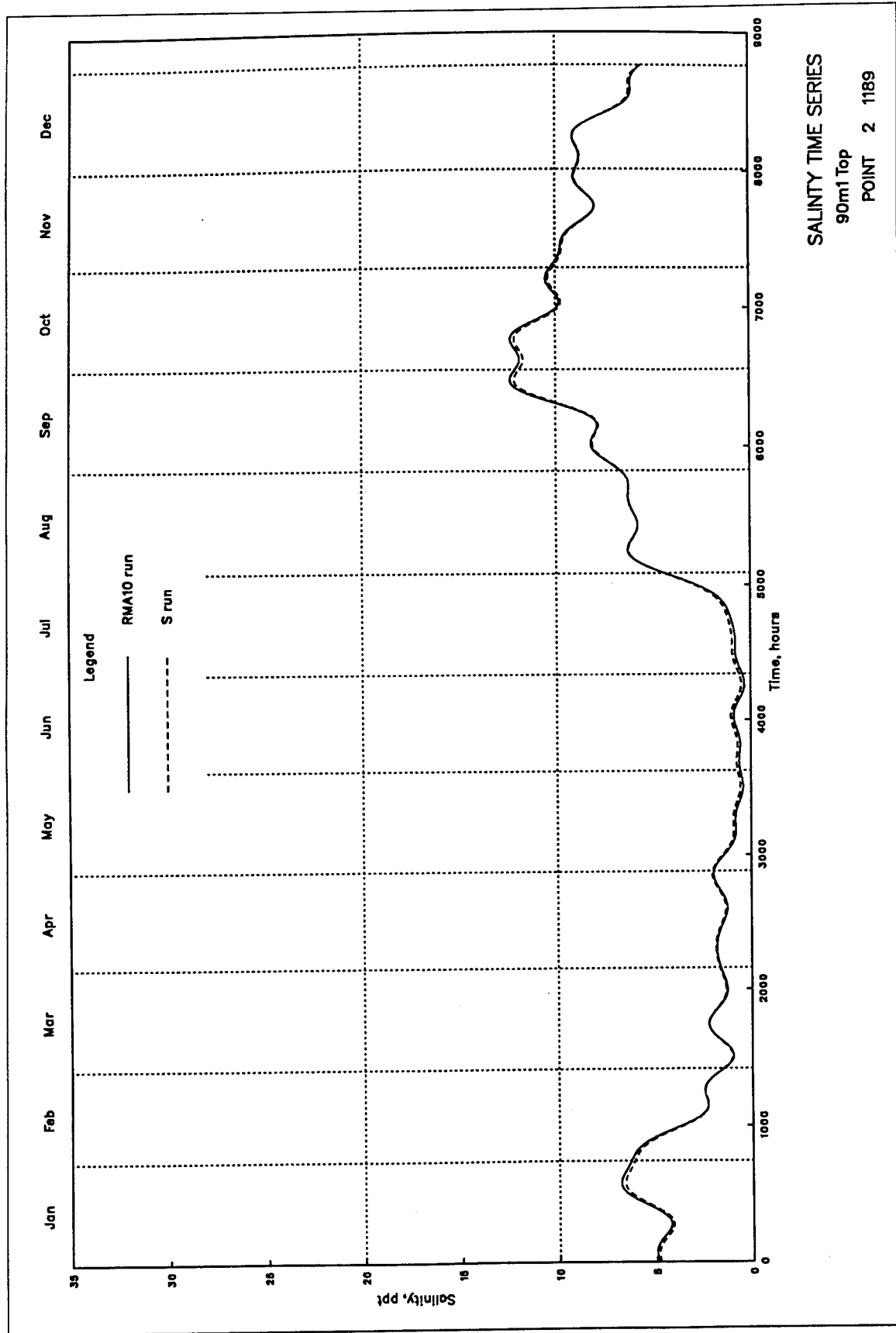
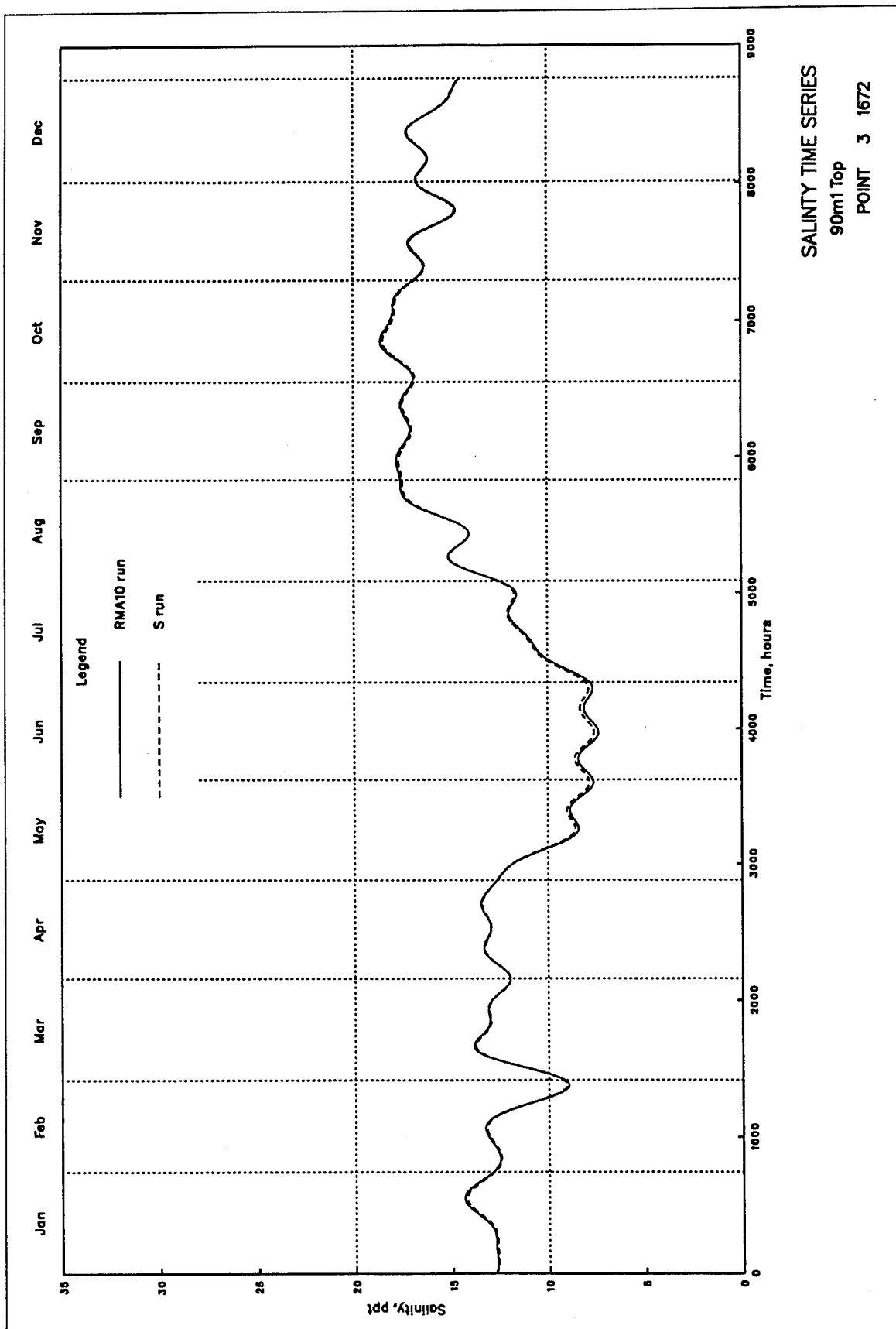


Plate 36



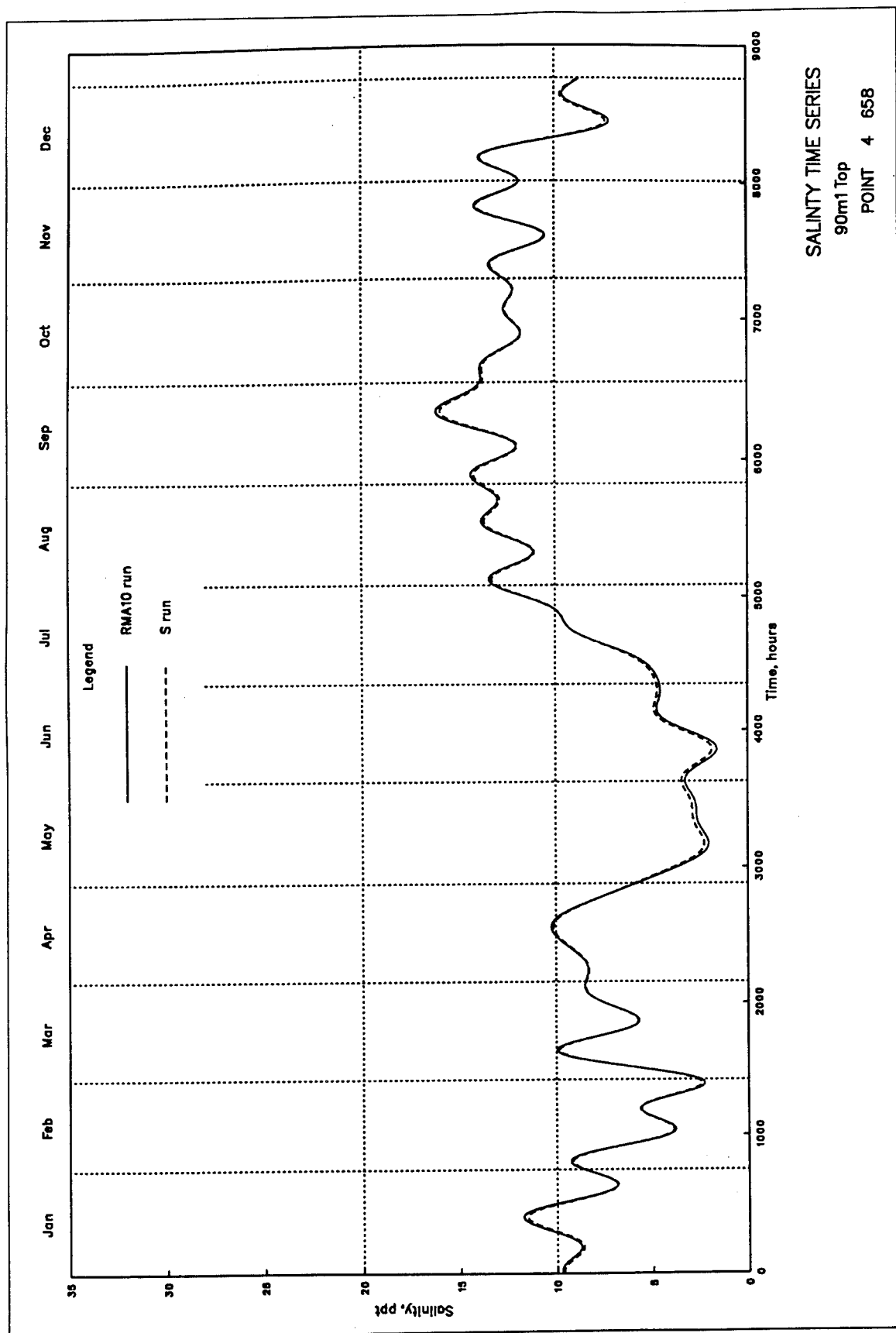
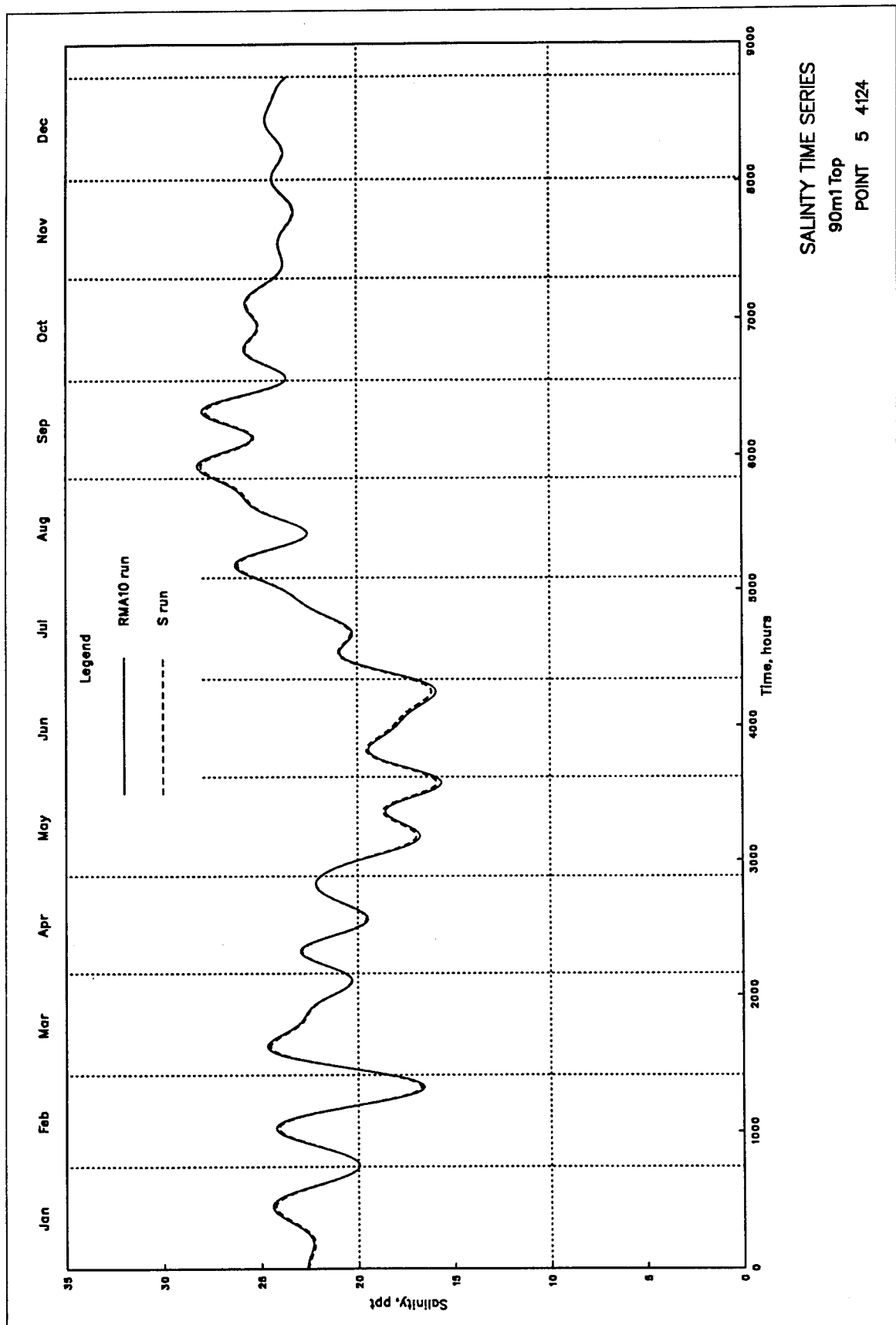


Plate 38



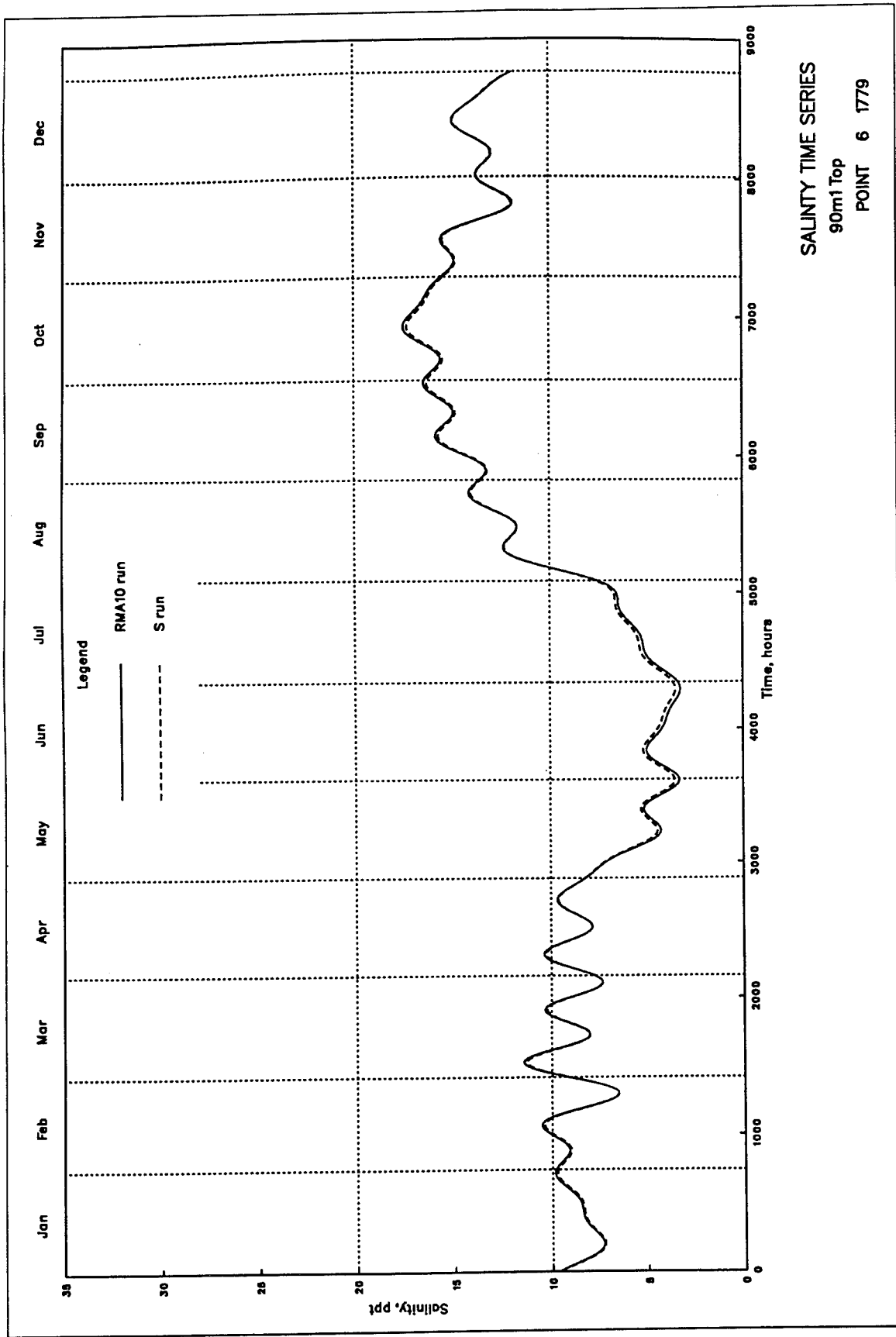
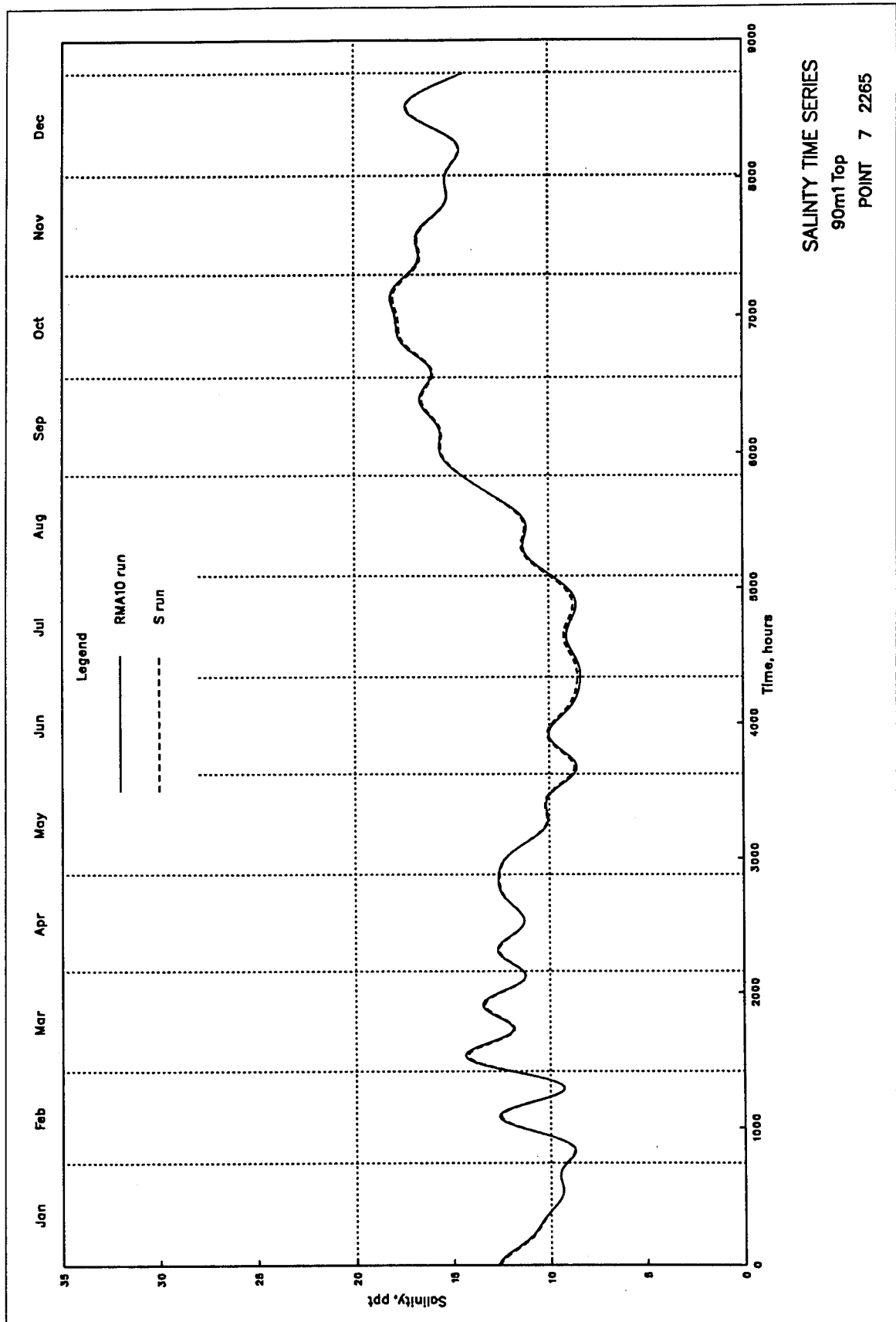


Plate 40



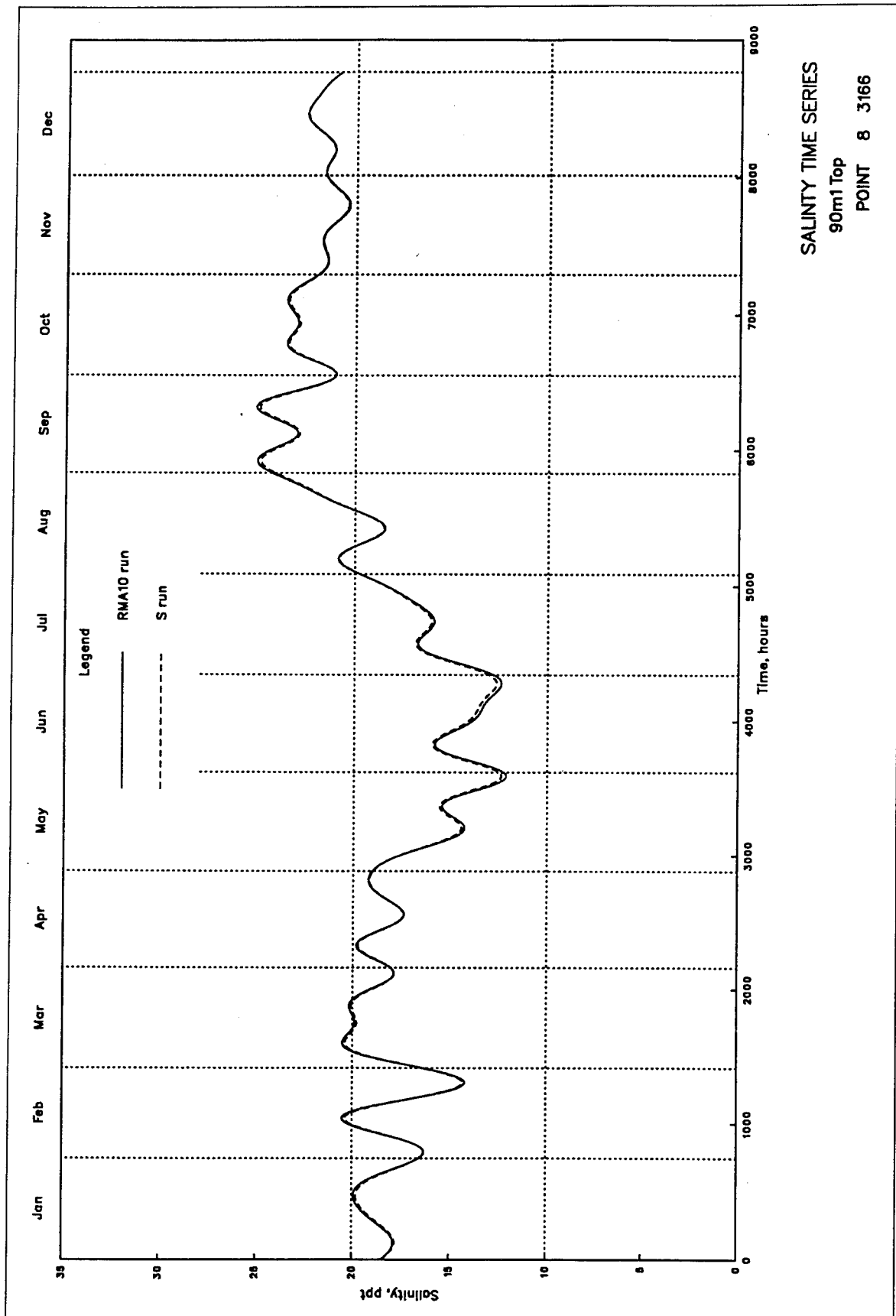
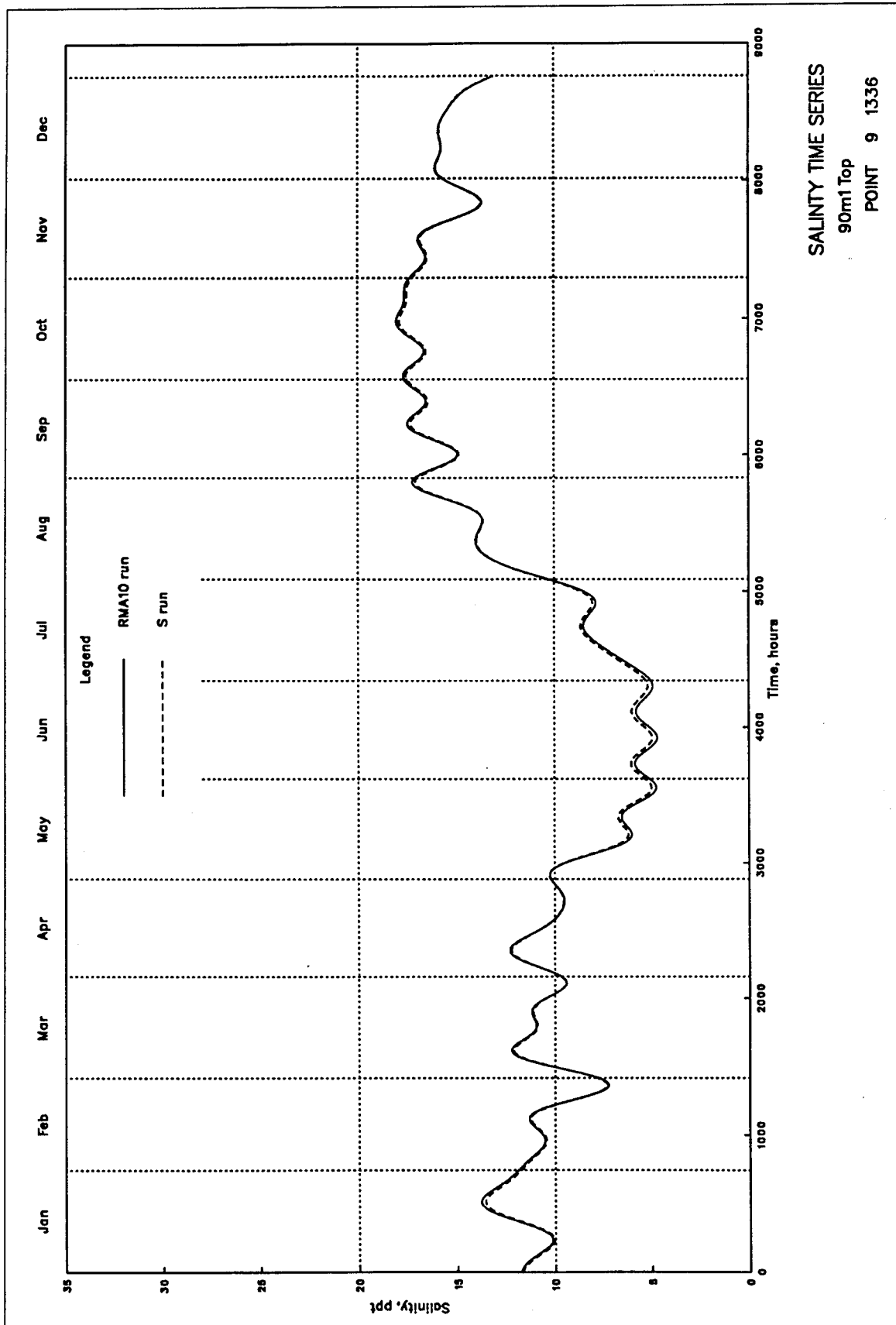


Plate 42



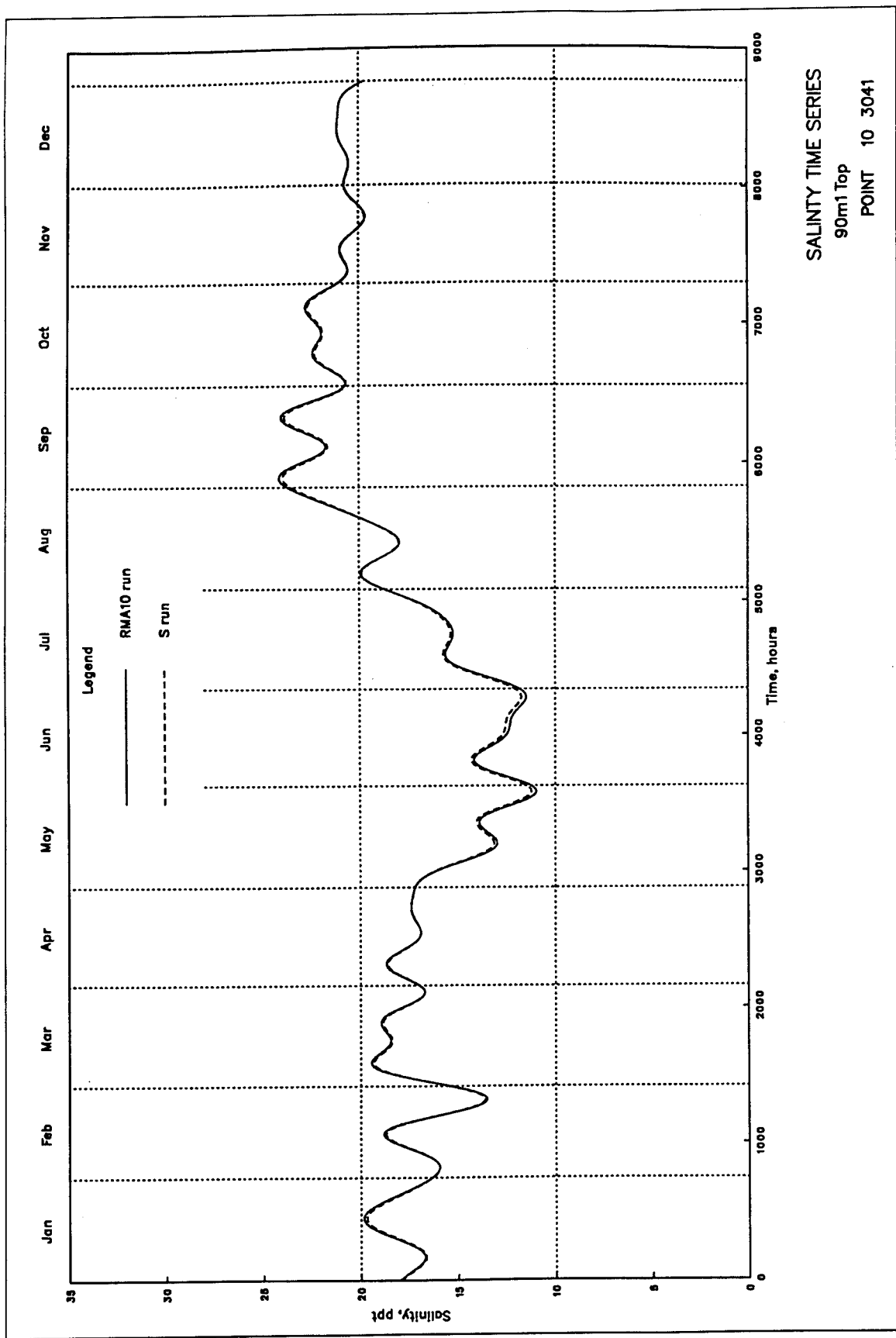
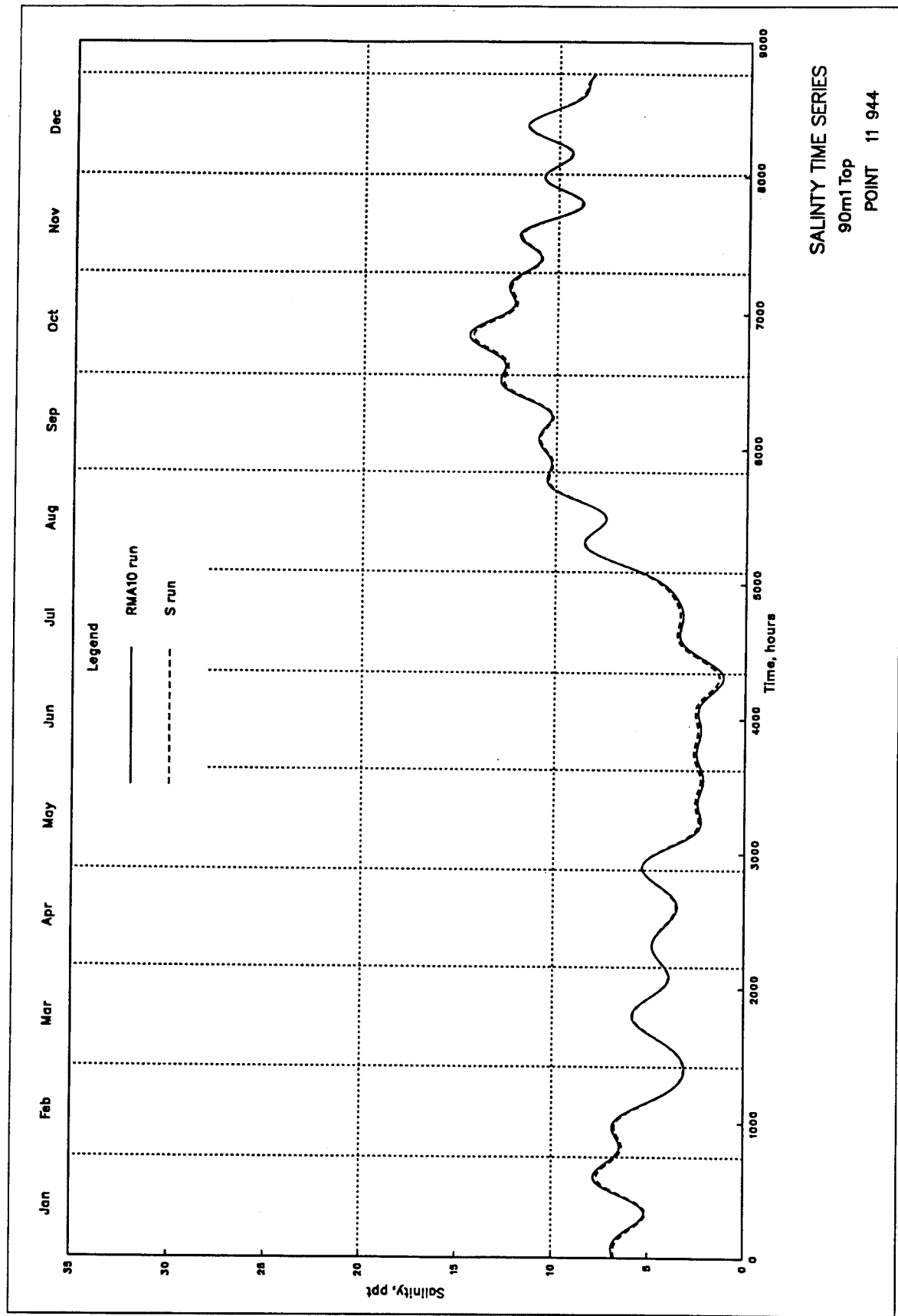


Plate 44



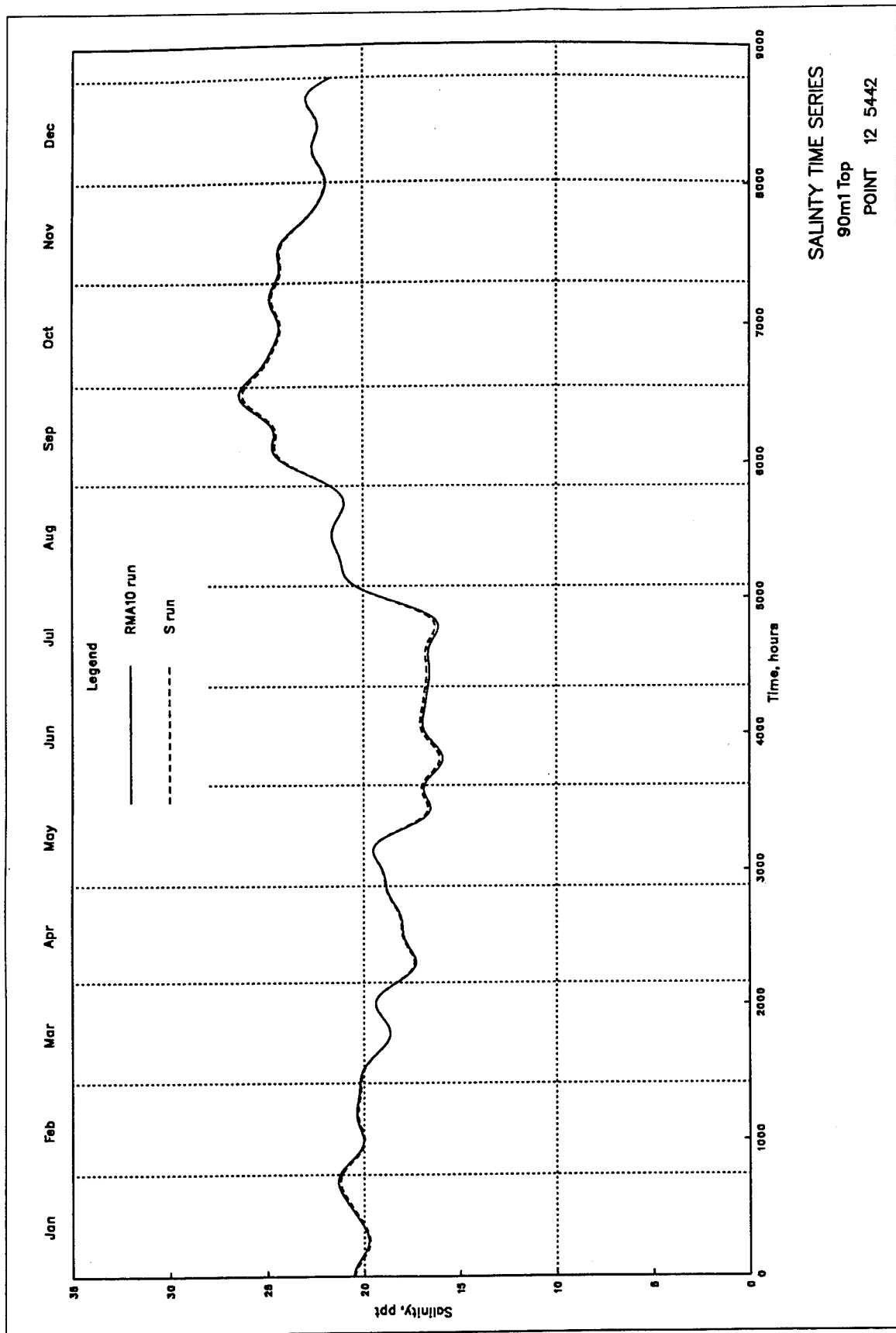
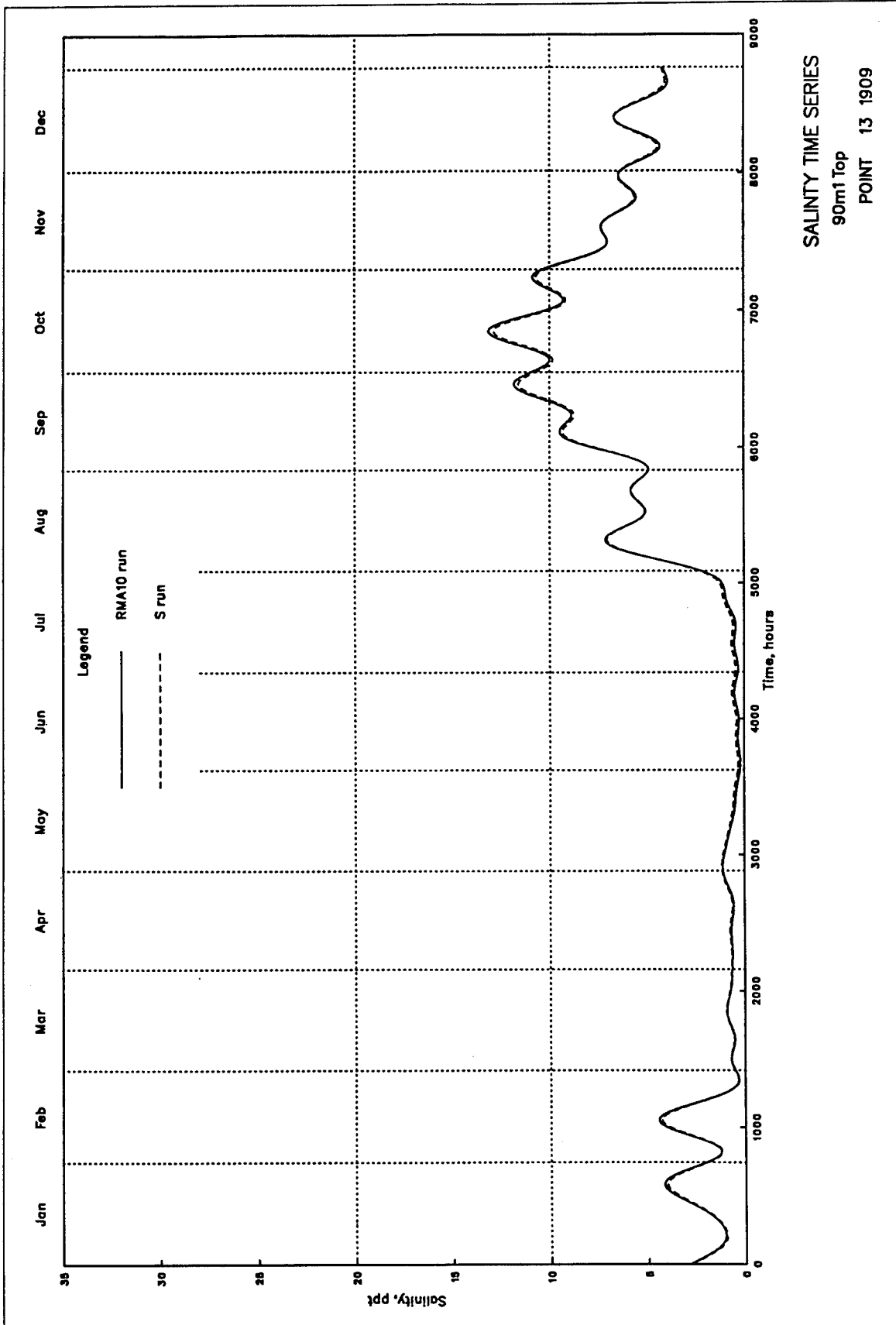


Plate 46



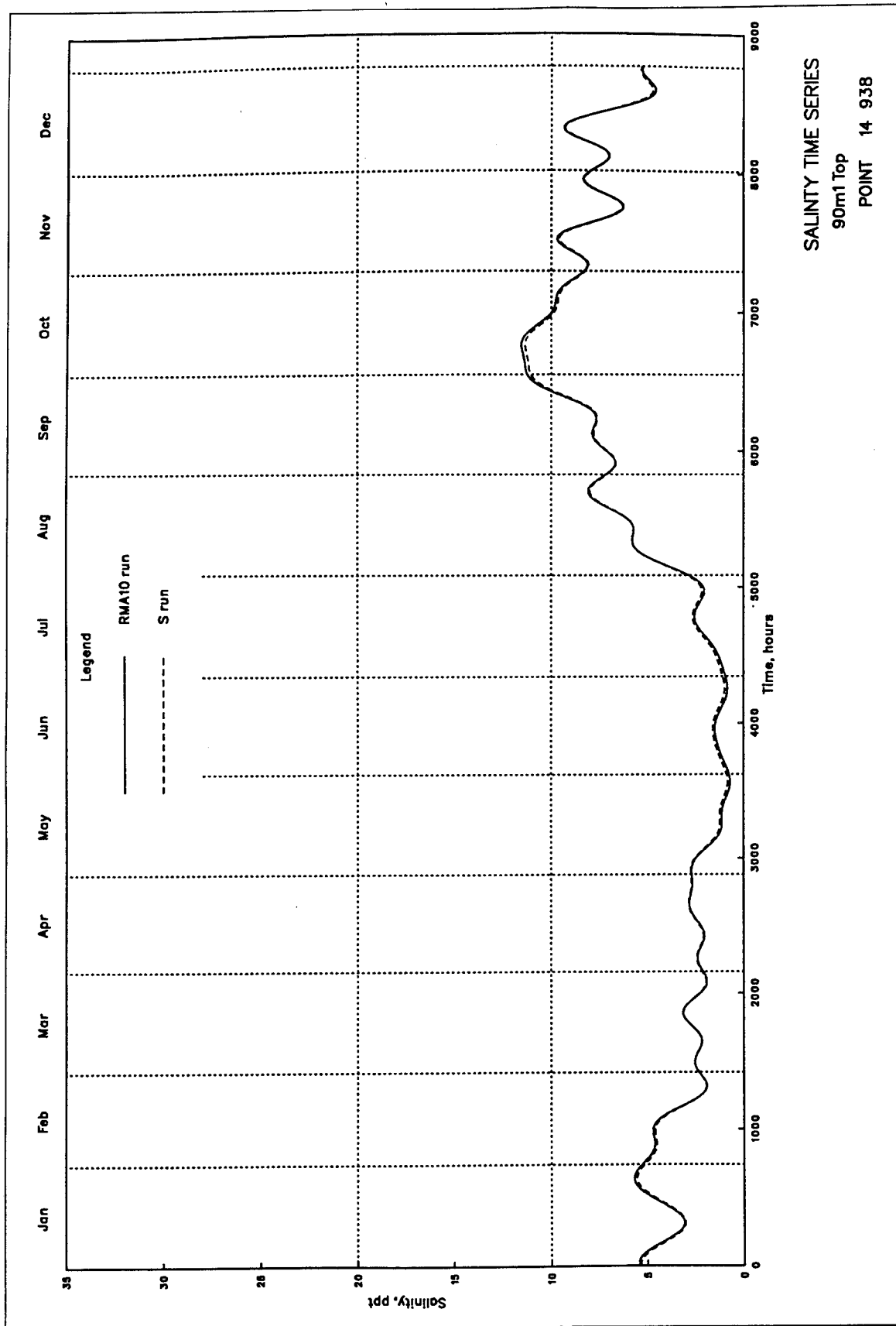
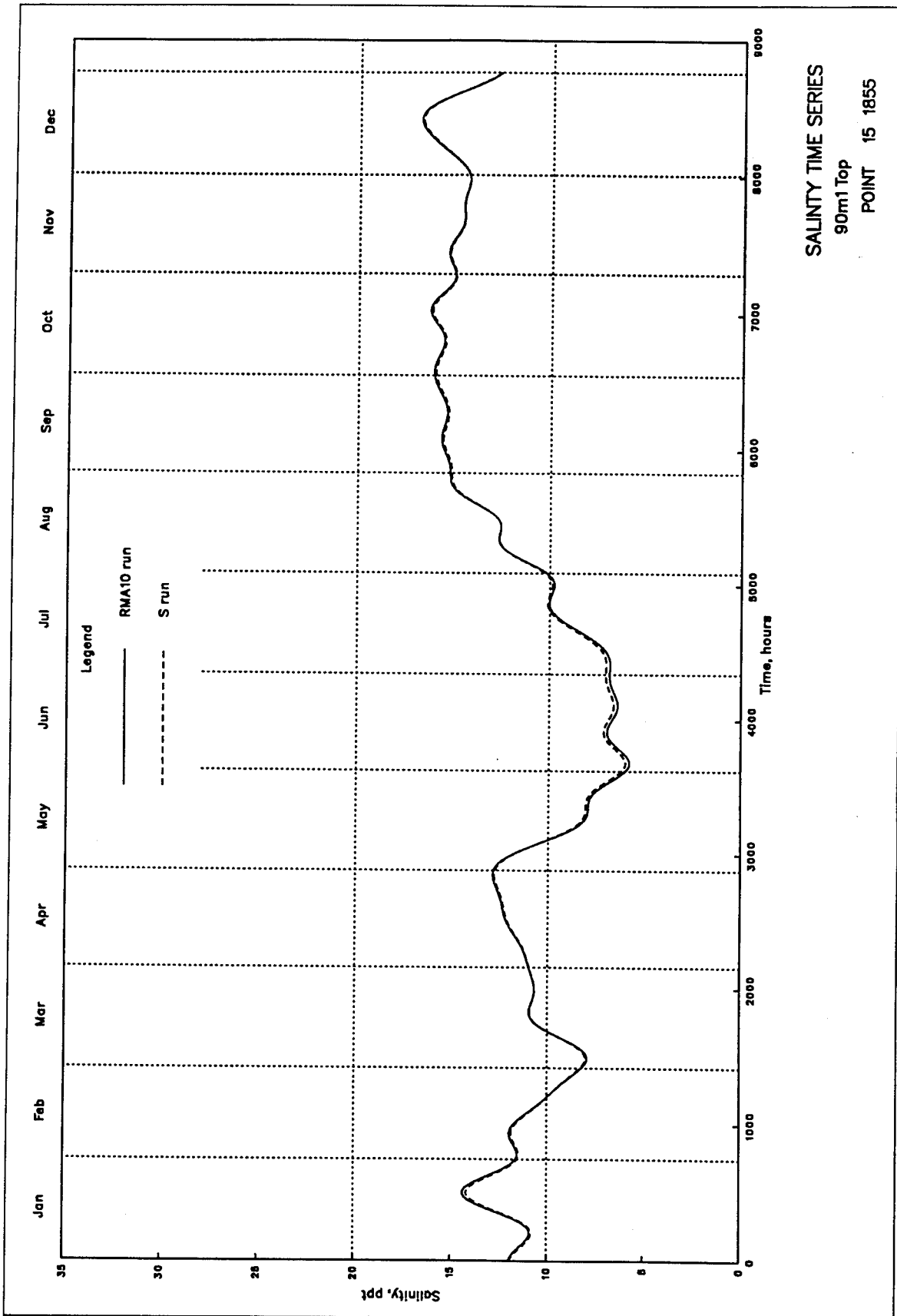


Plate 48



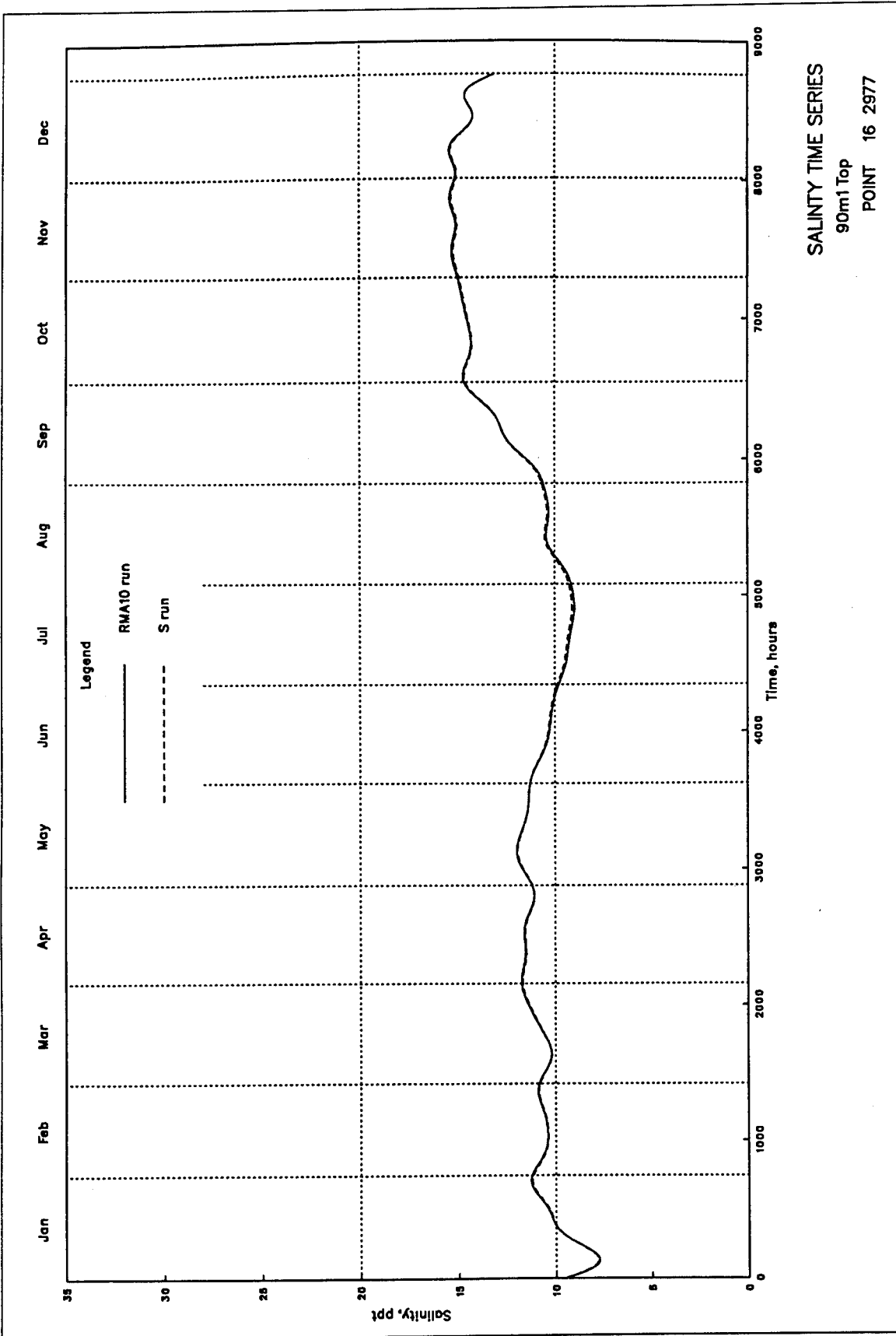
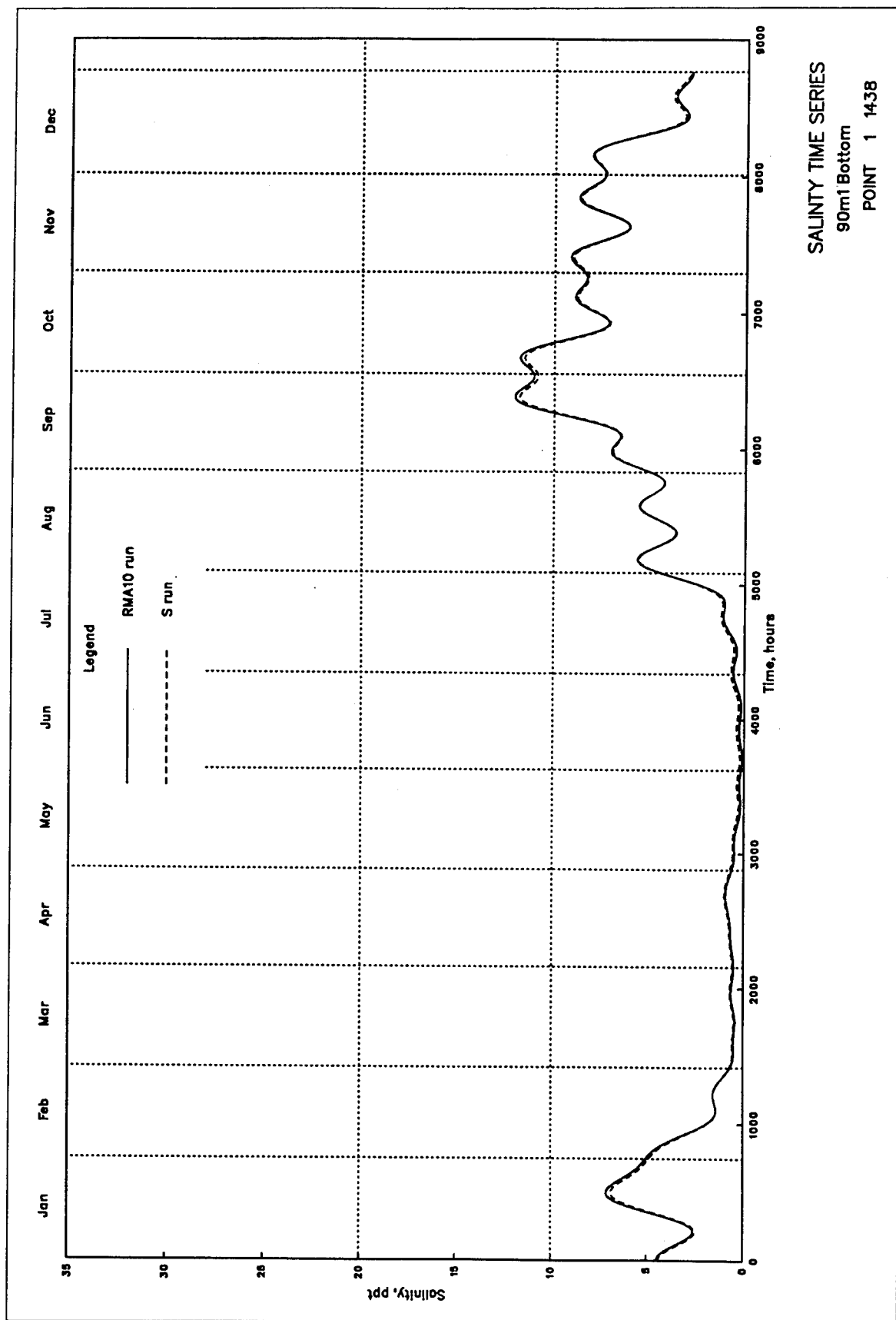


Plate 50



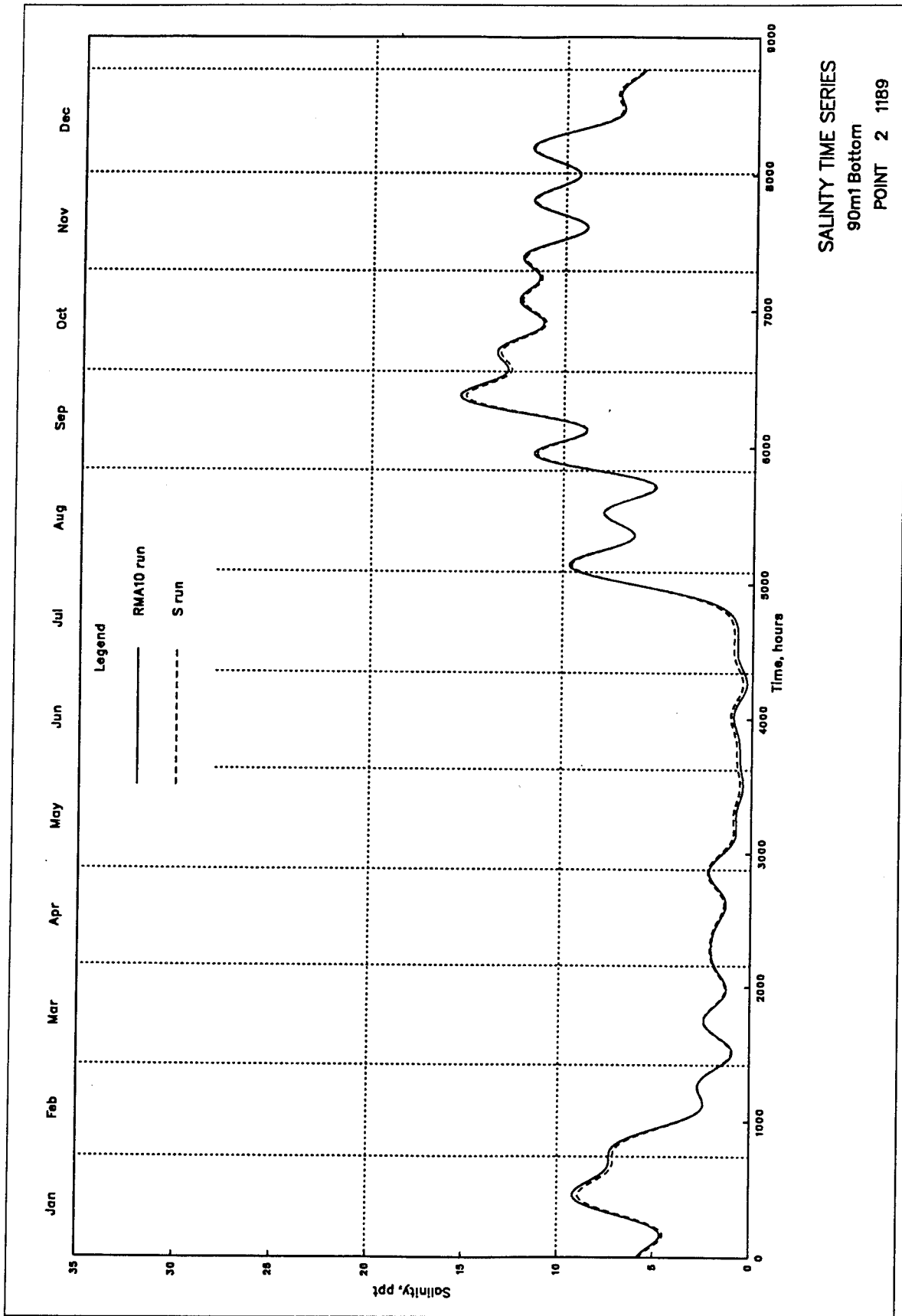
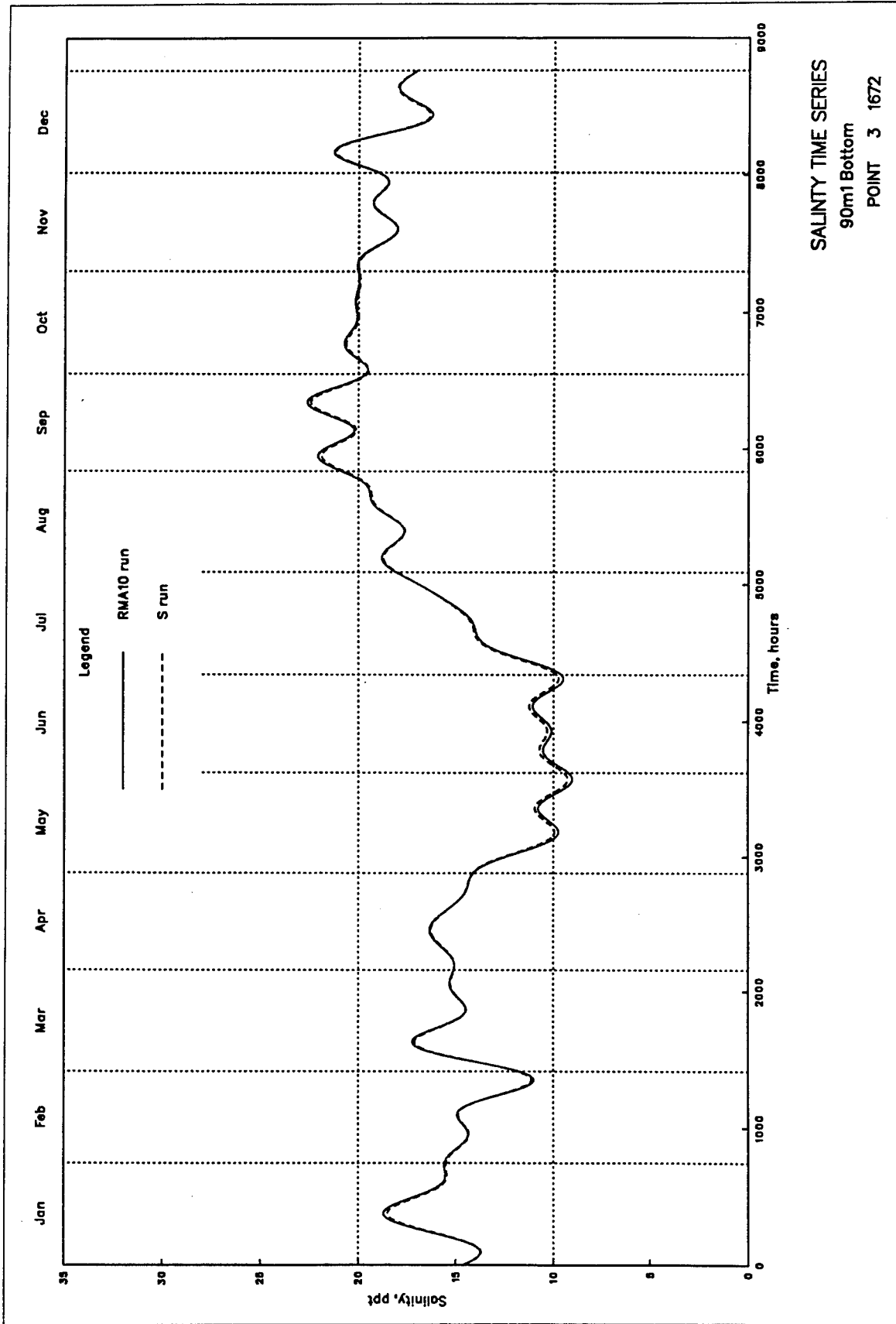


Plate 52



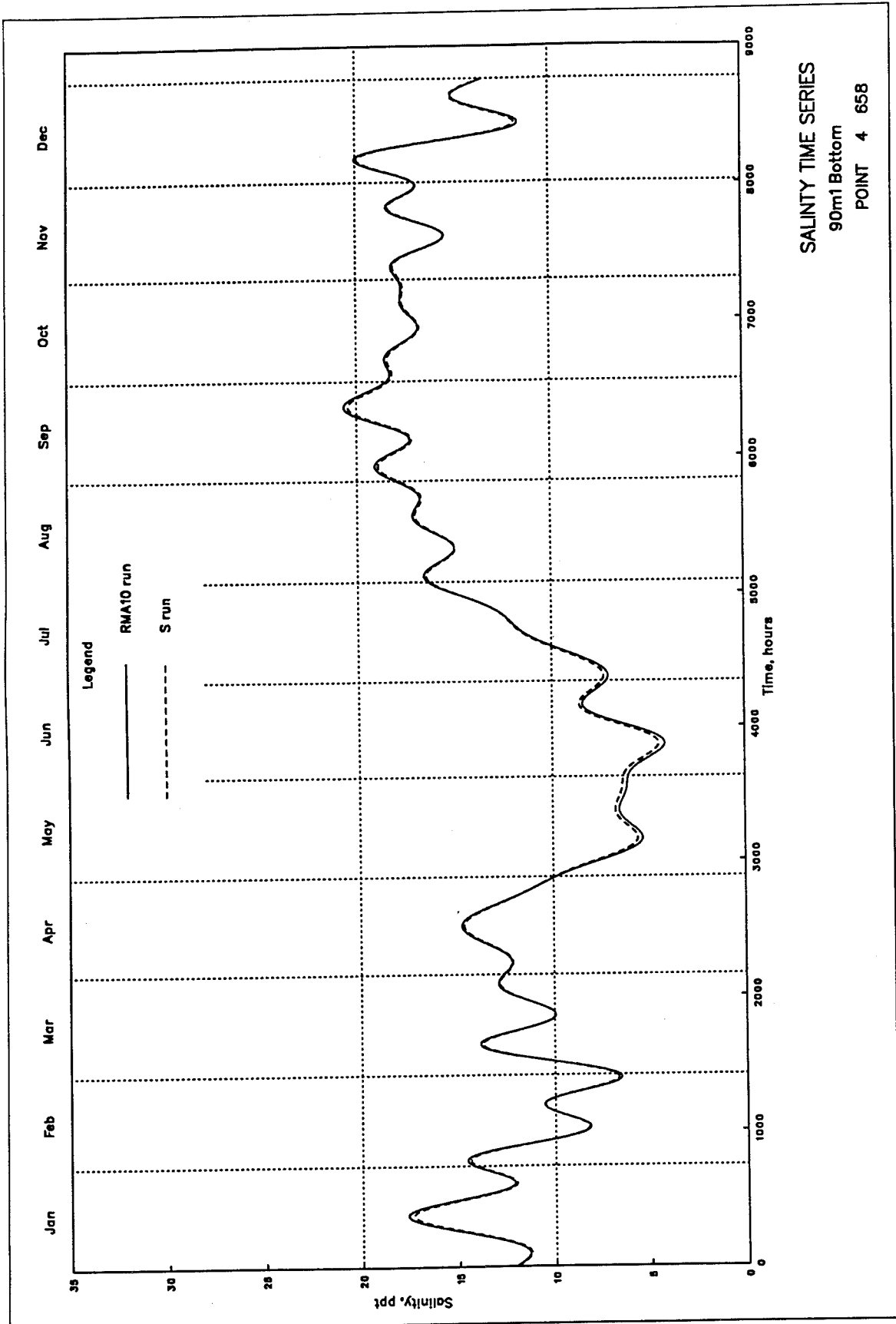


Plate 54

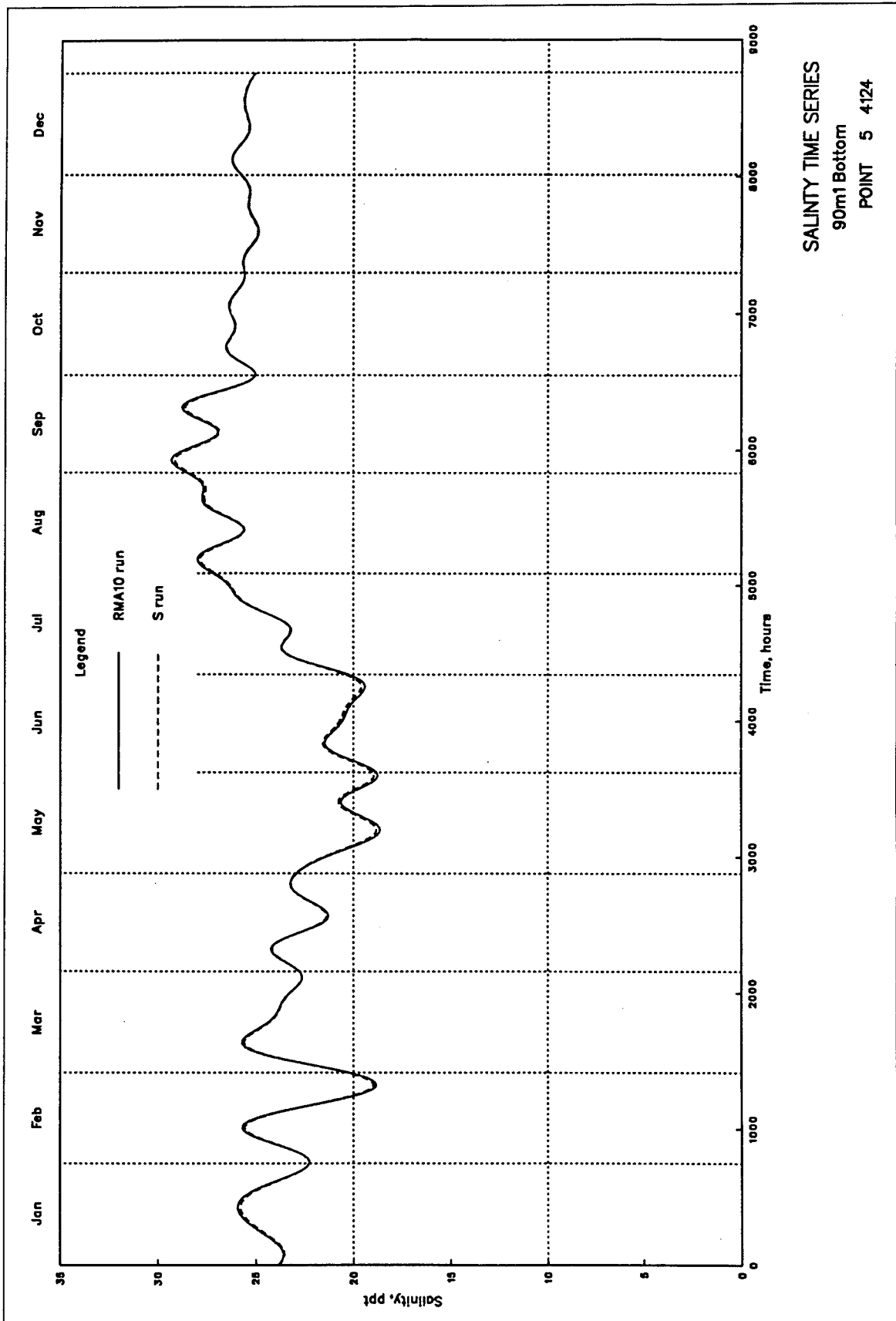


Plate 55

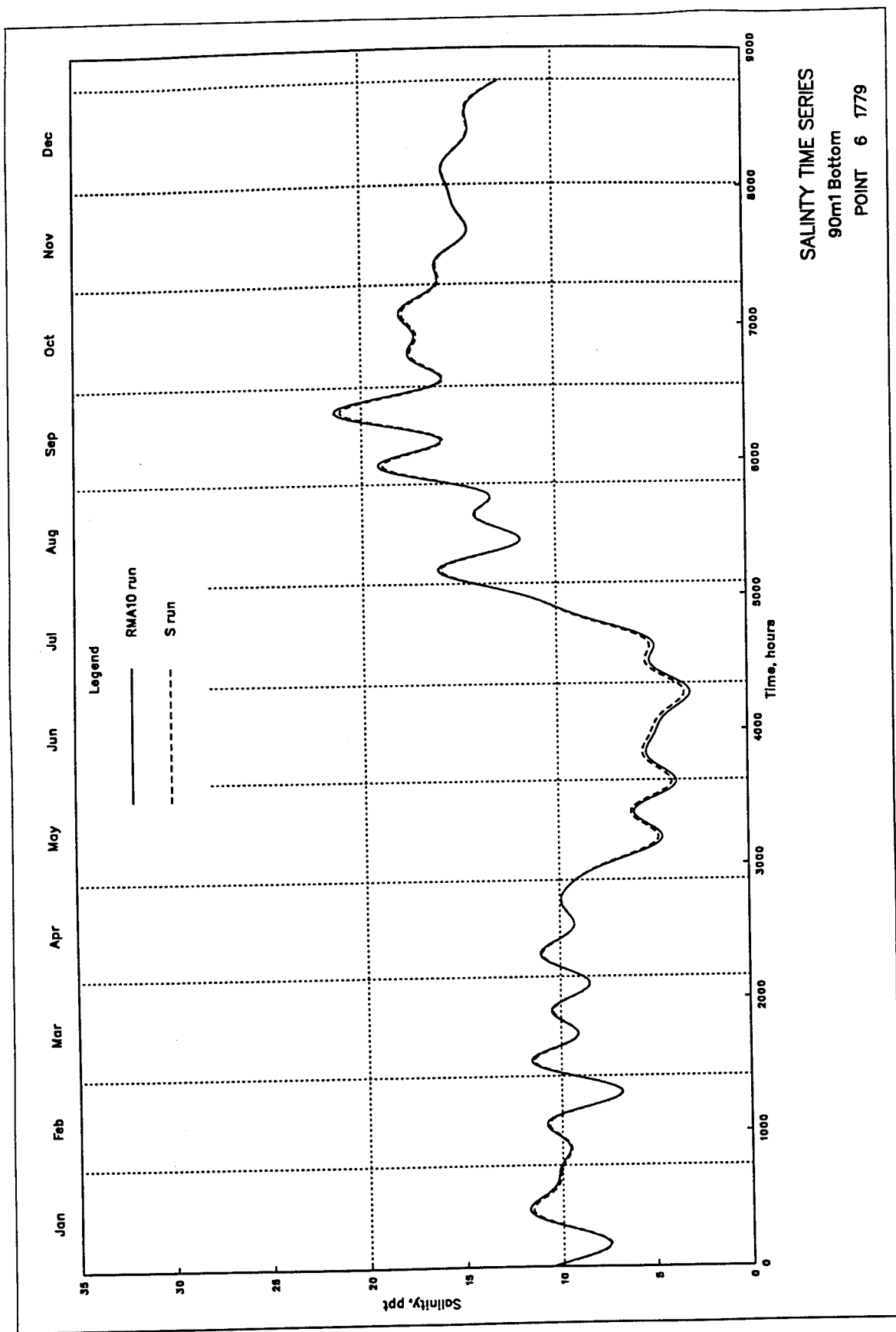
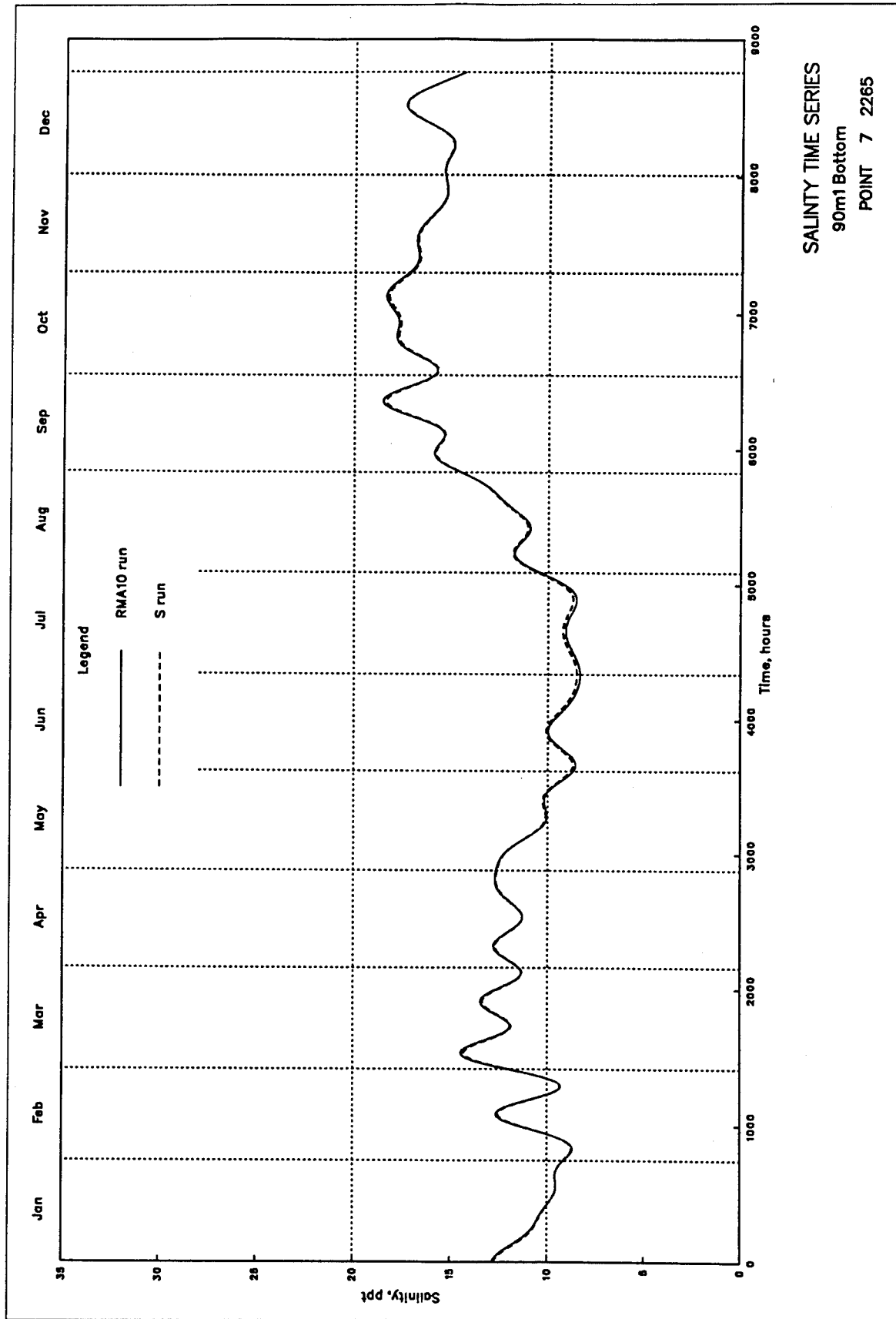


Plate 56



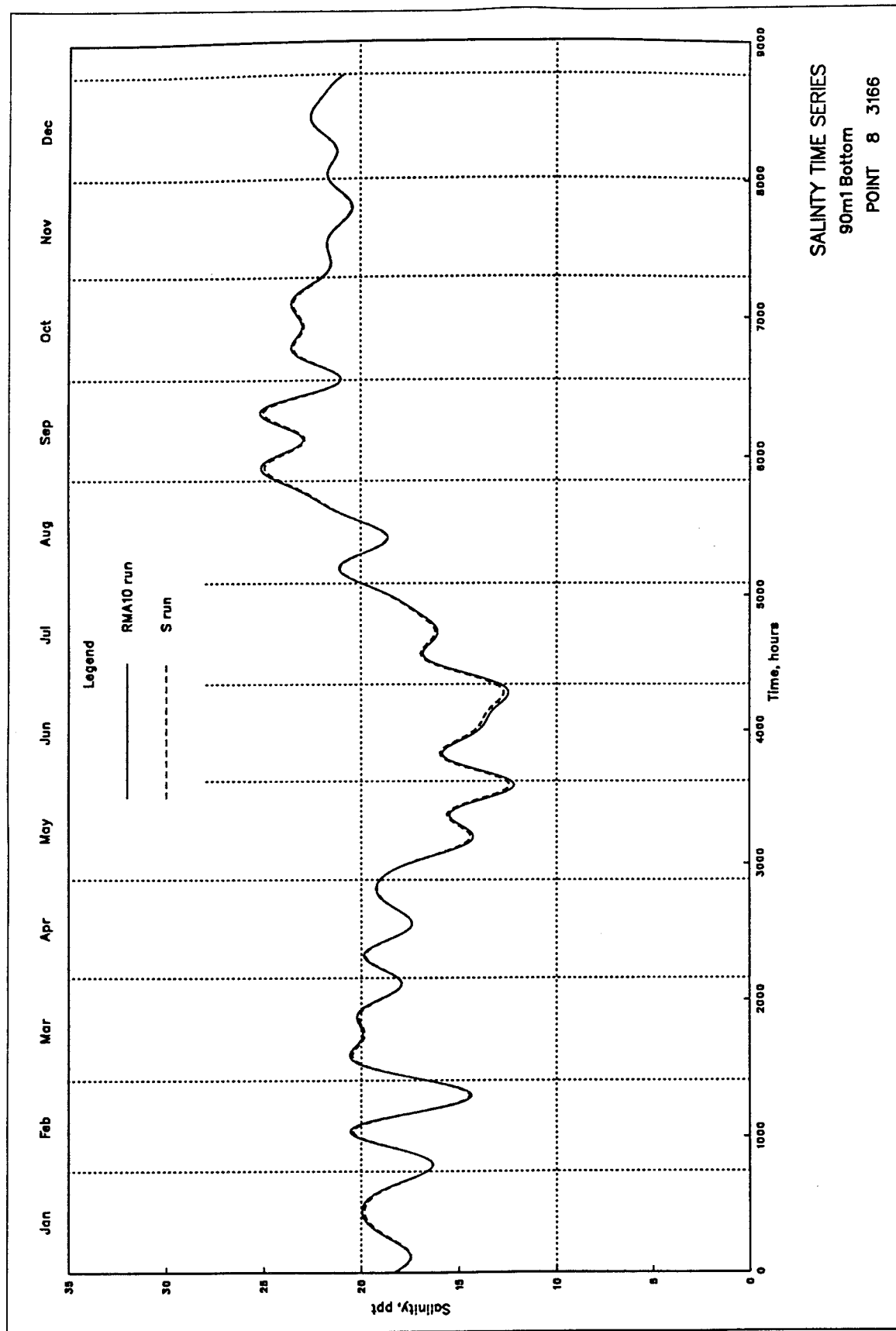
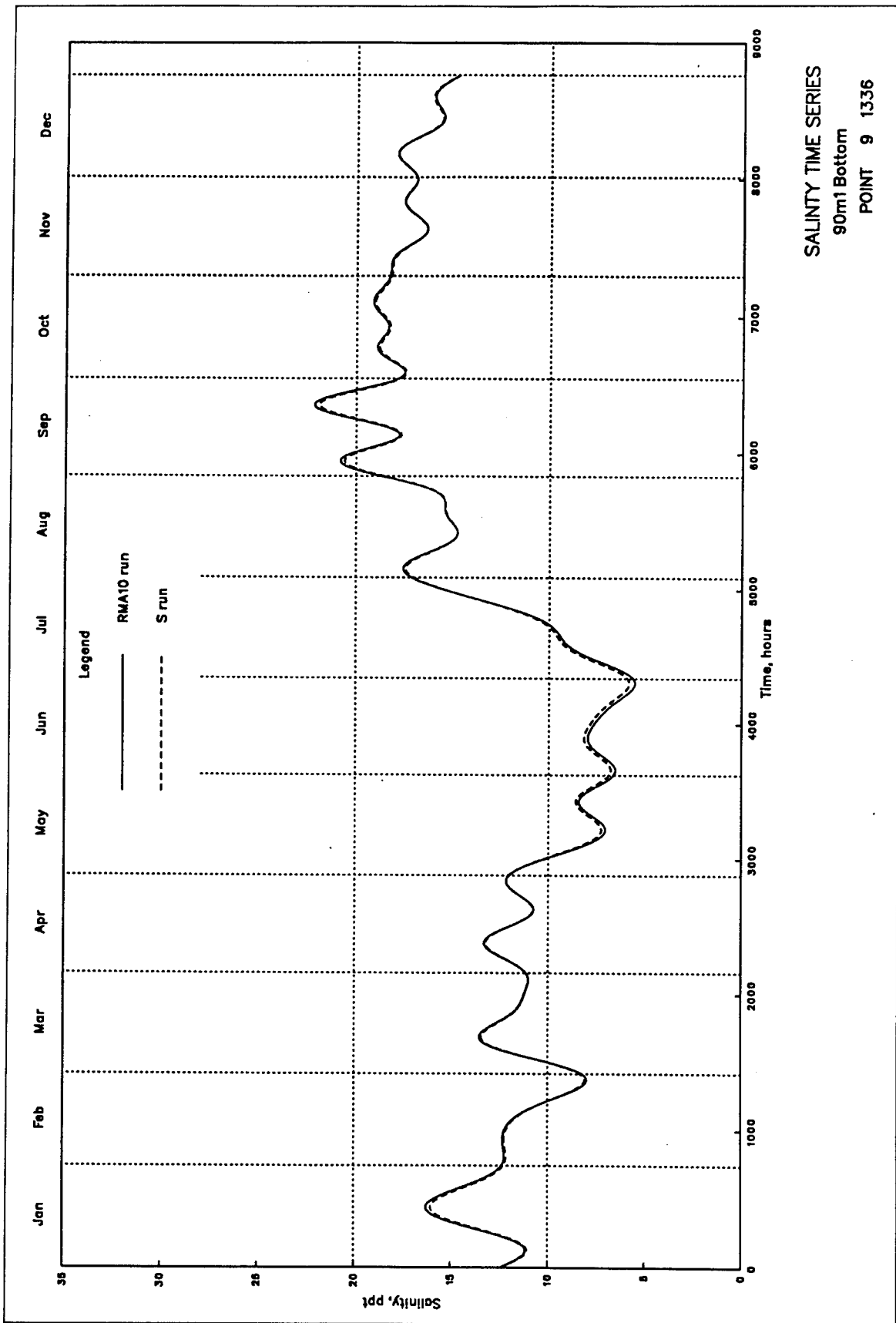


Plate 58



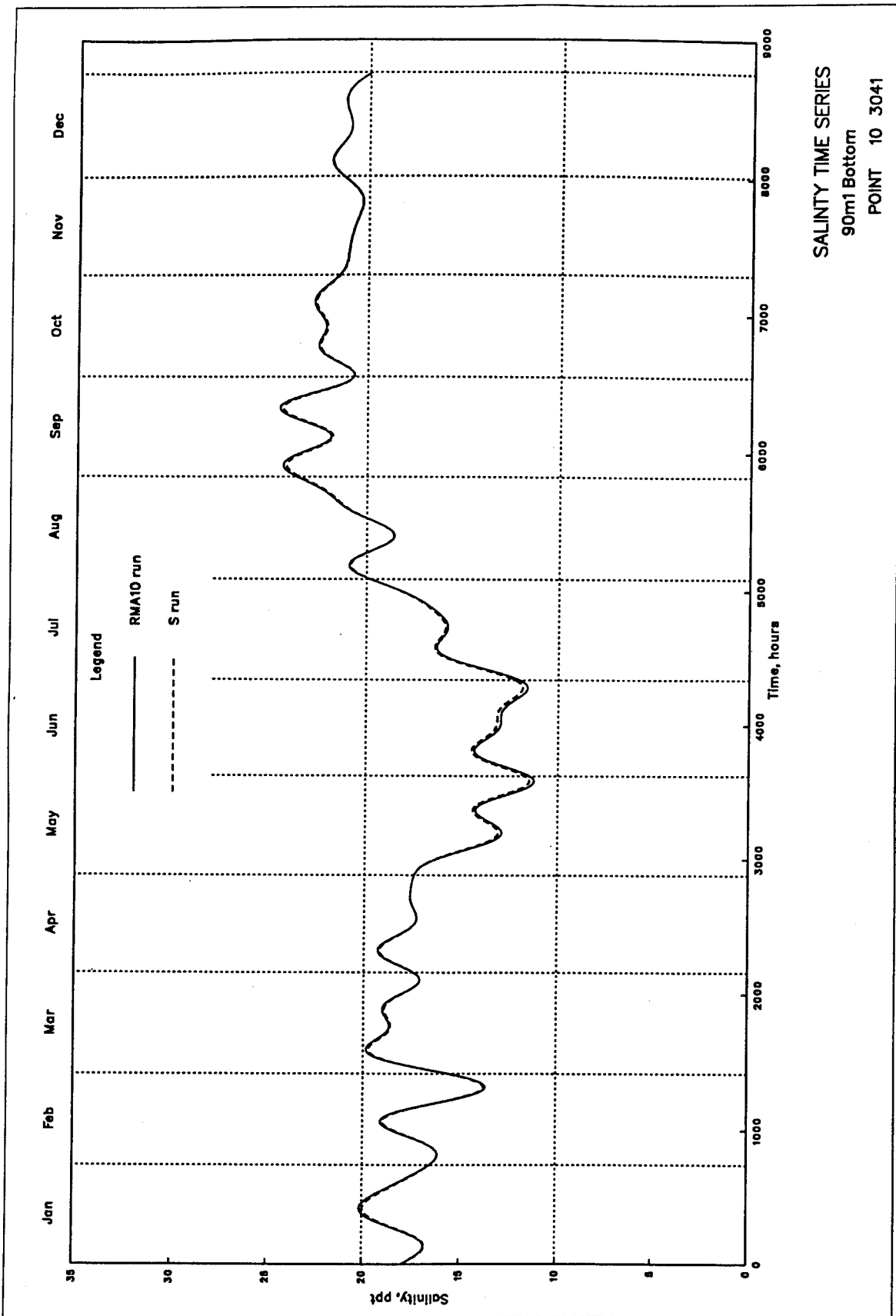
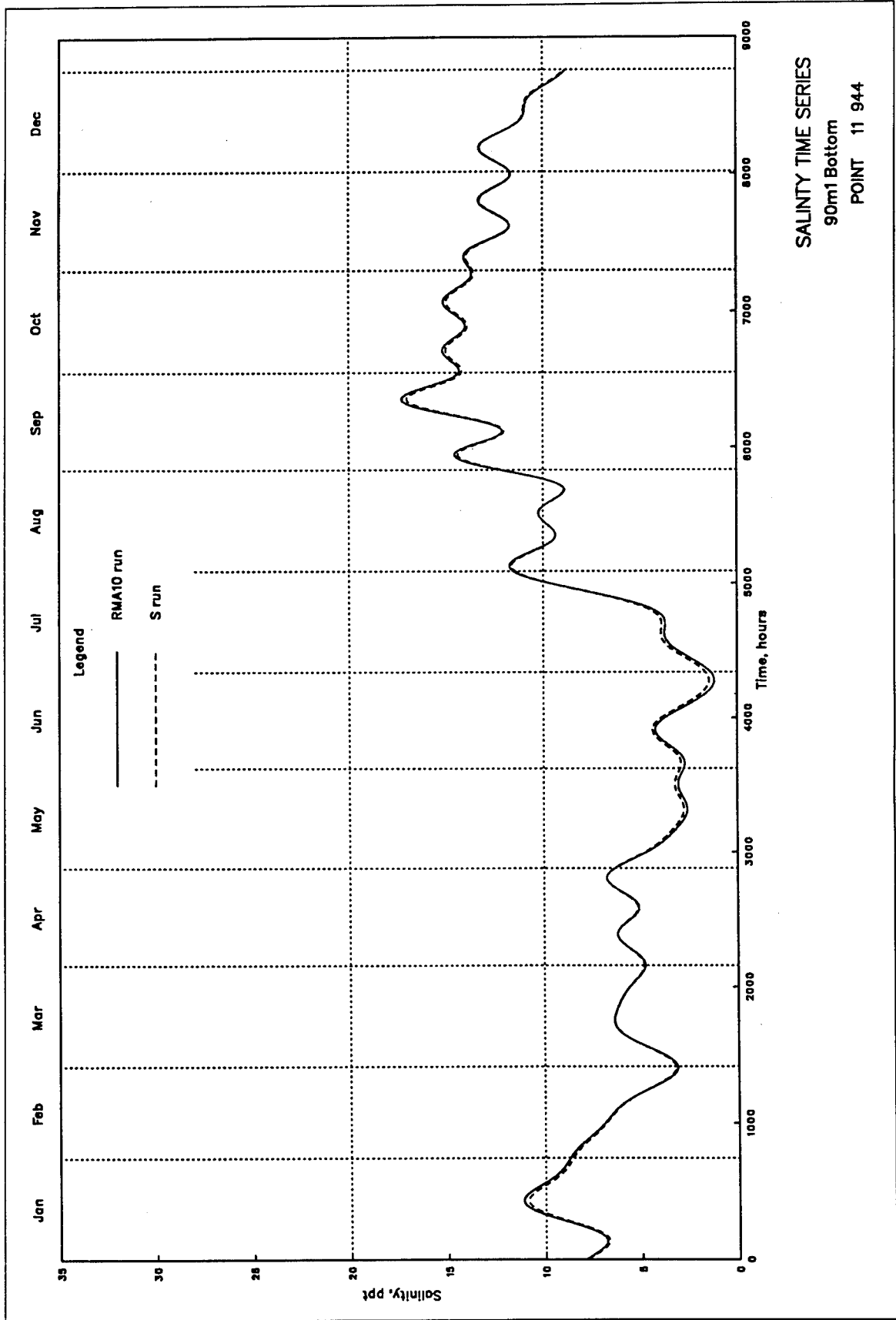


Plate 60



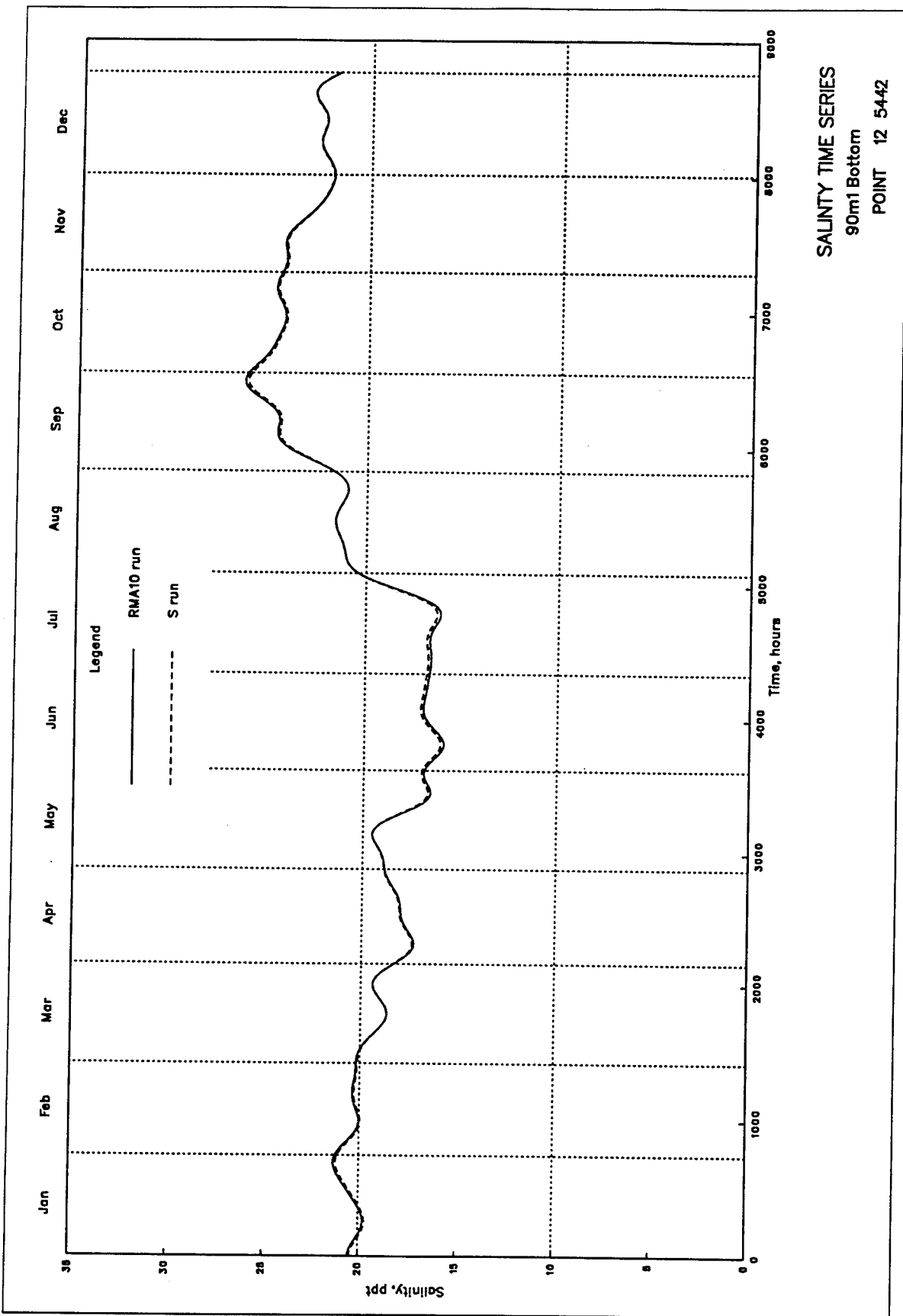
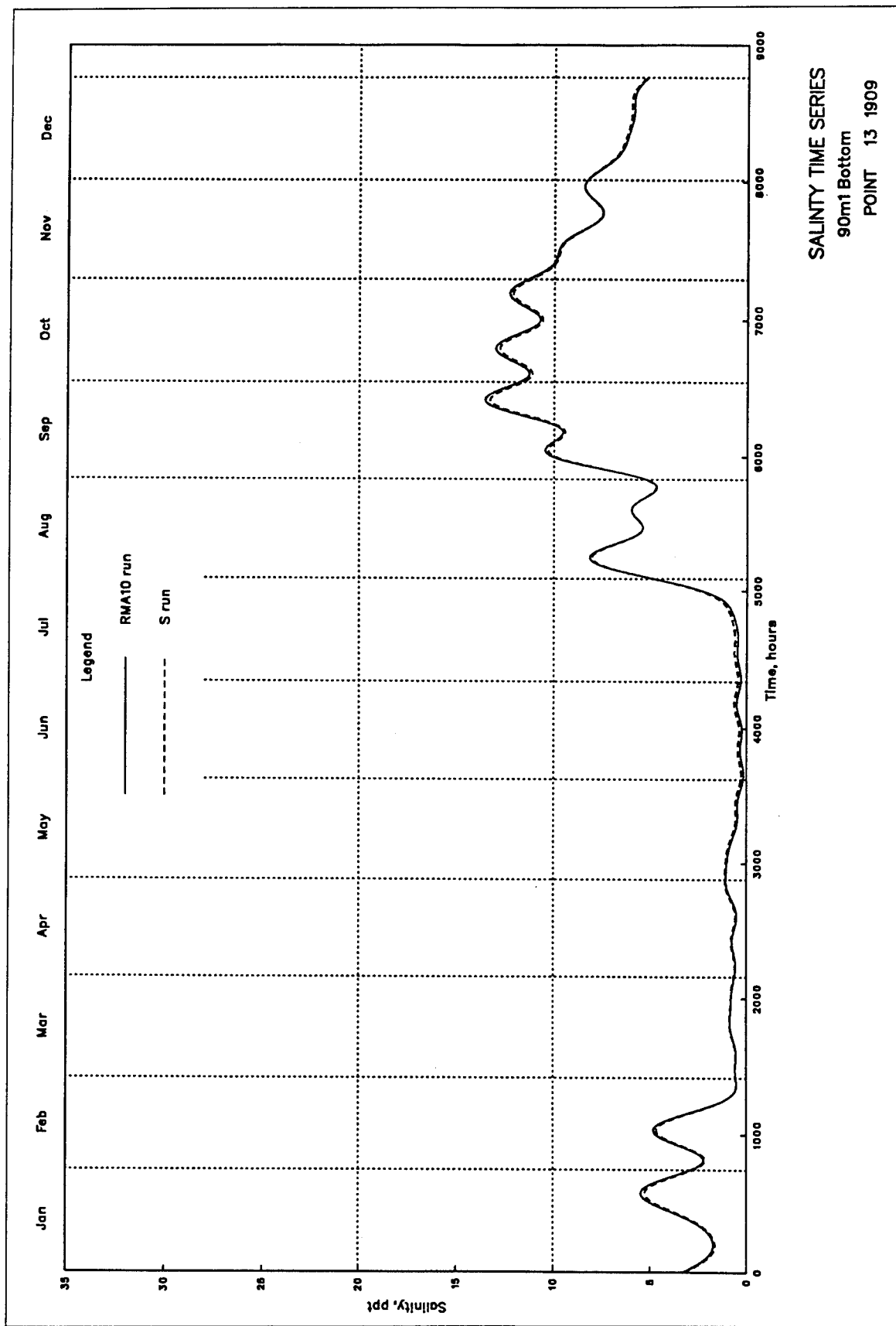


Plate 62



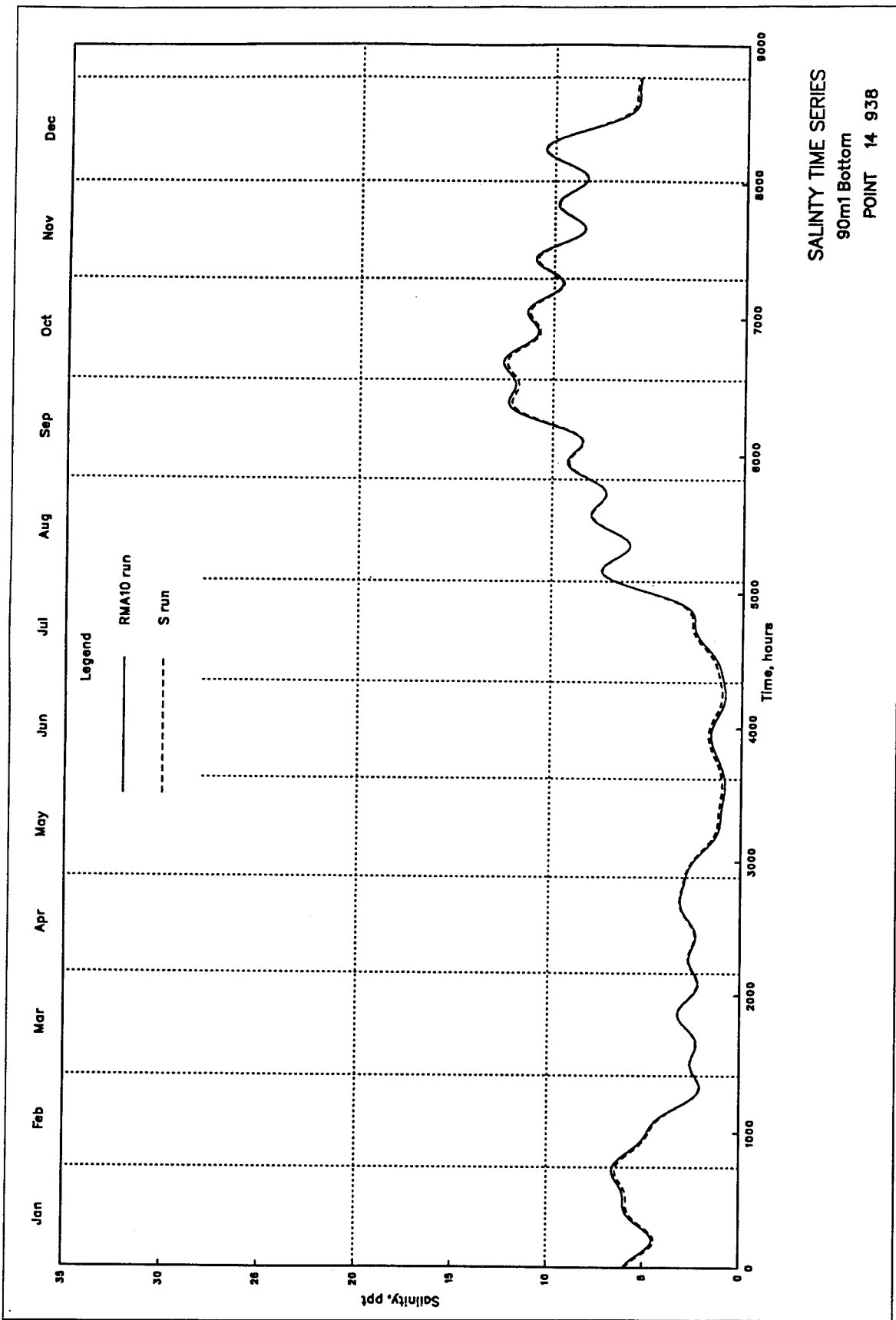
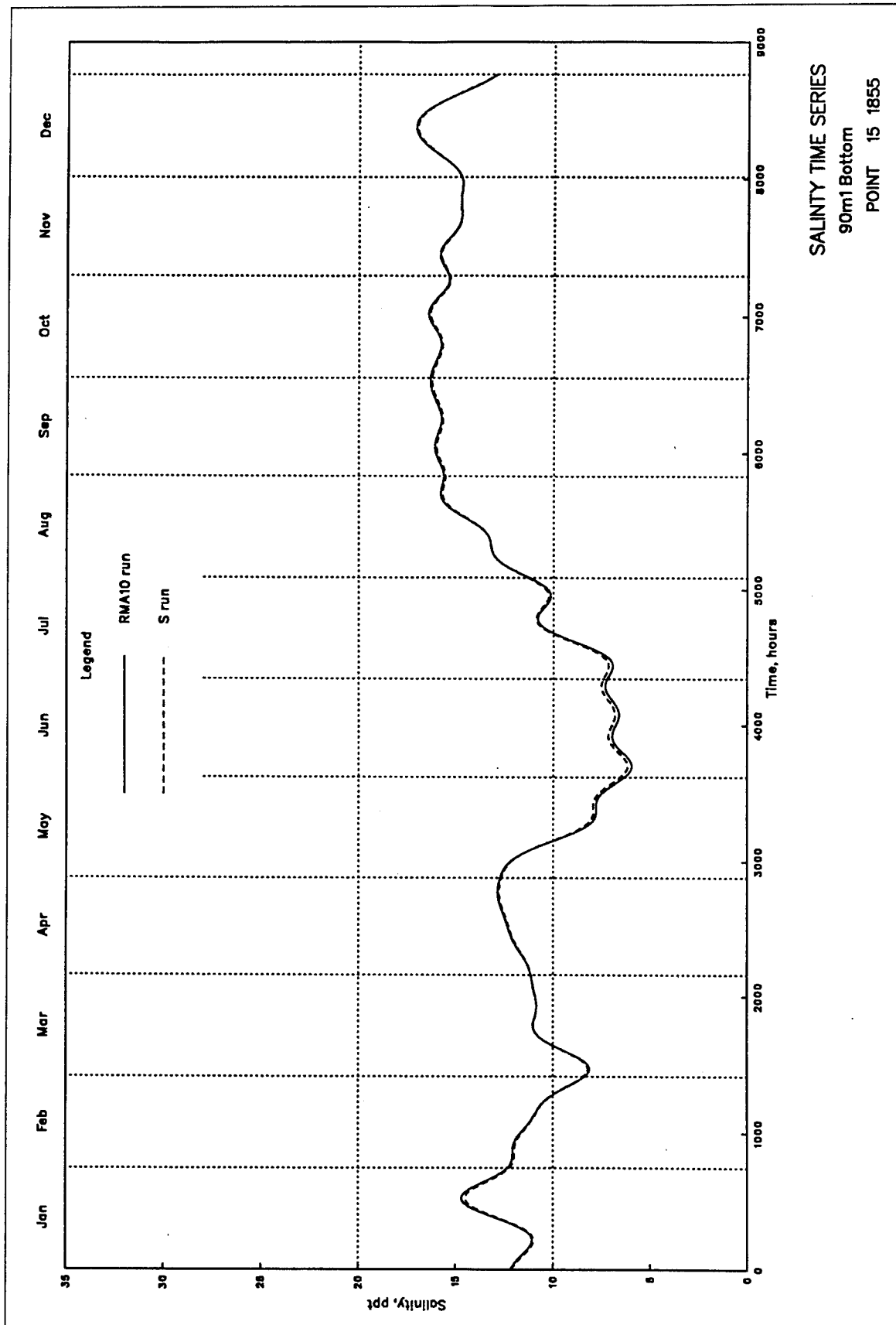


Plate 64



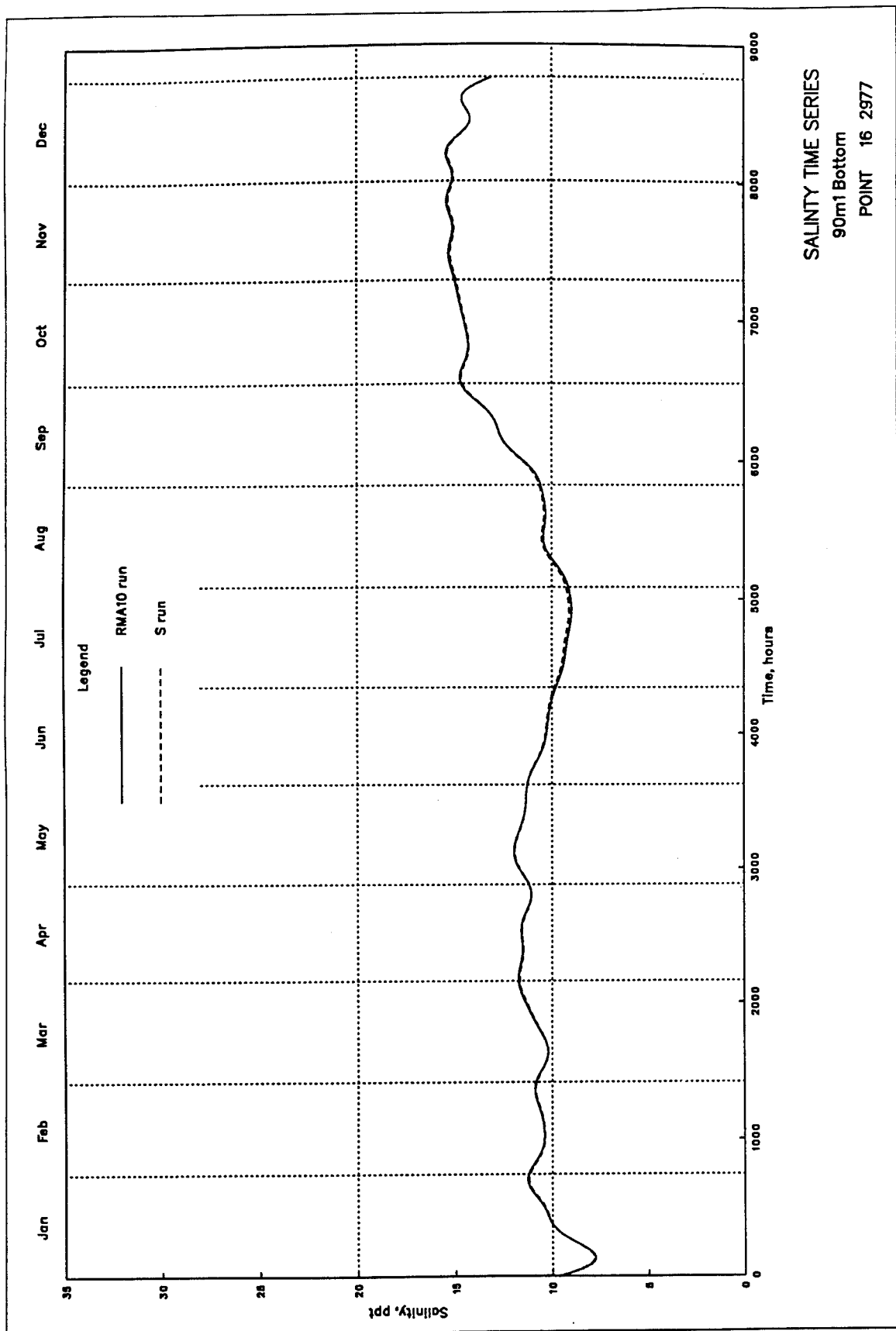
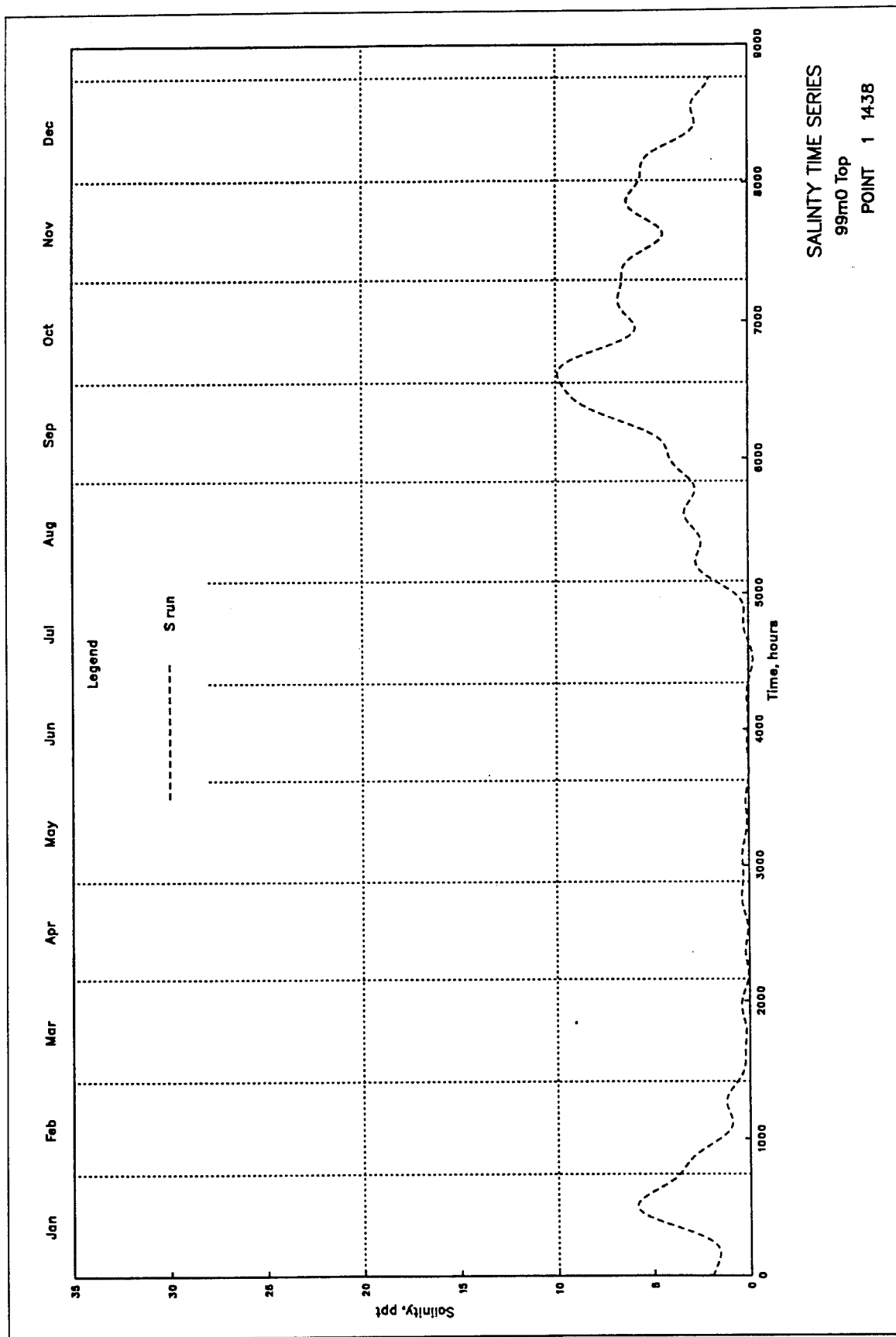


Plate 66



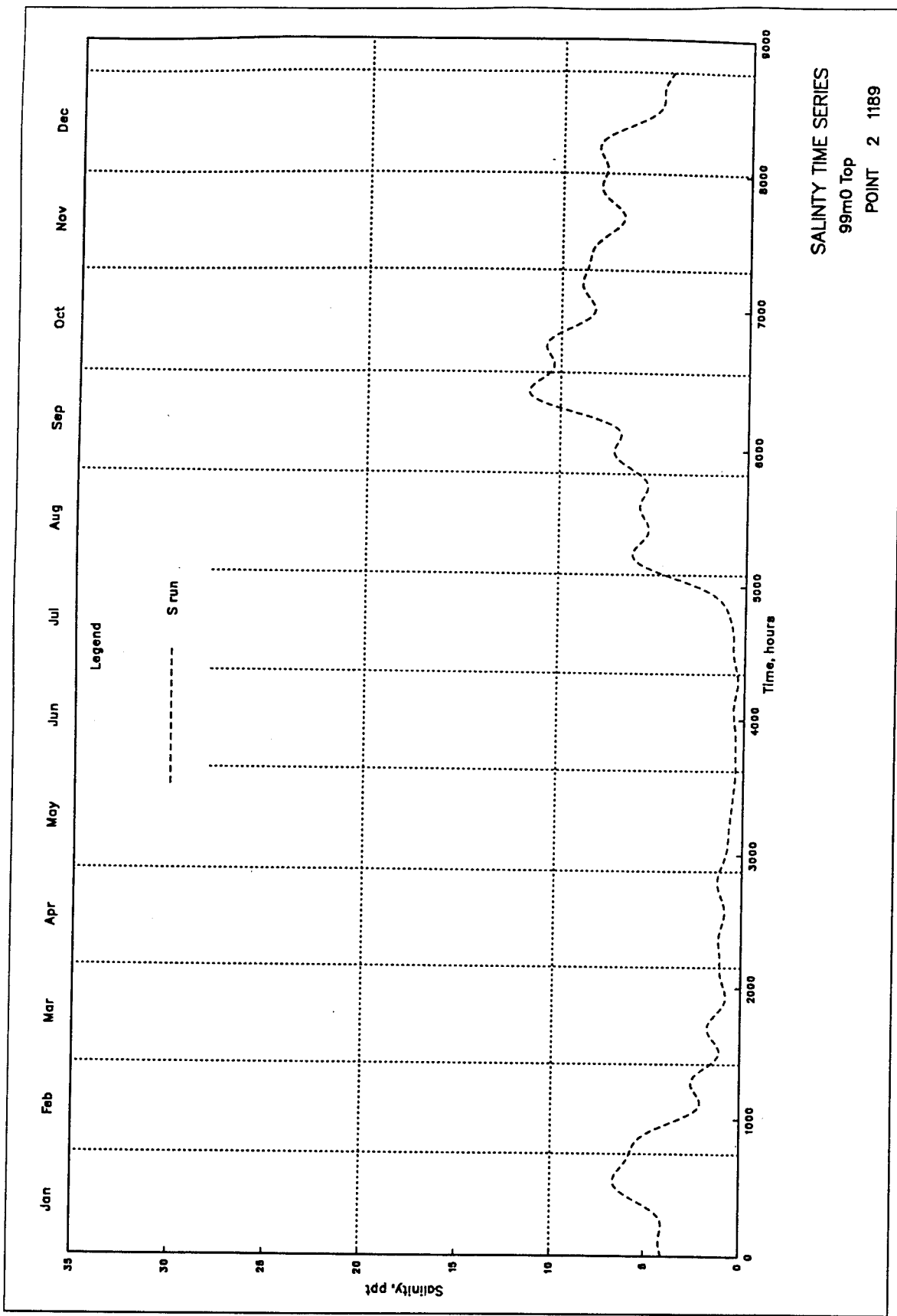
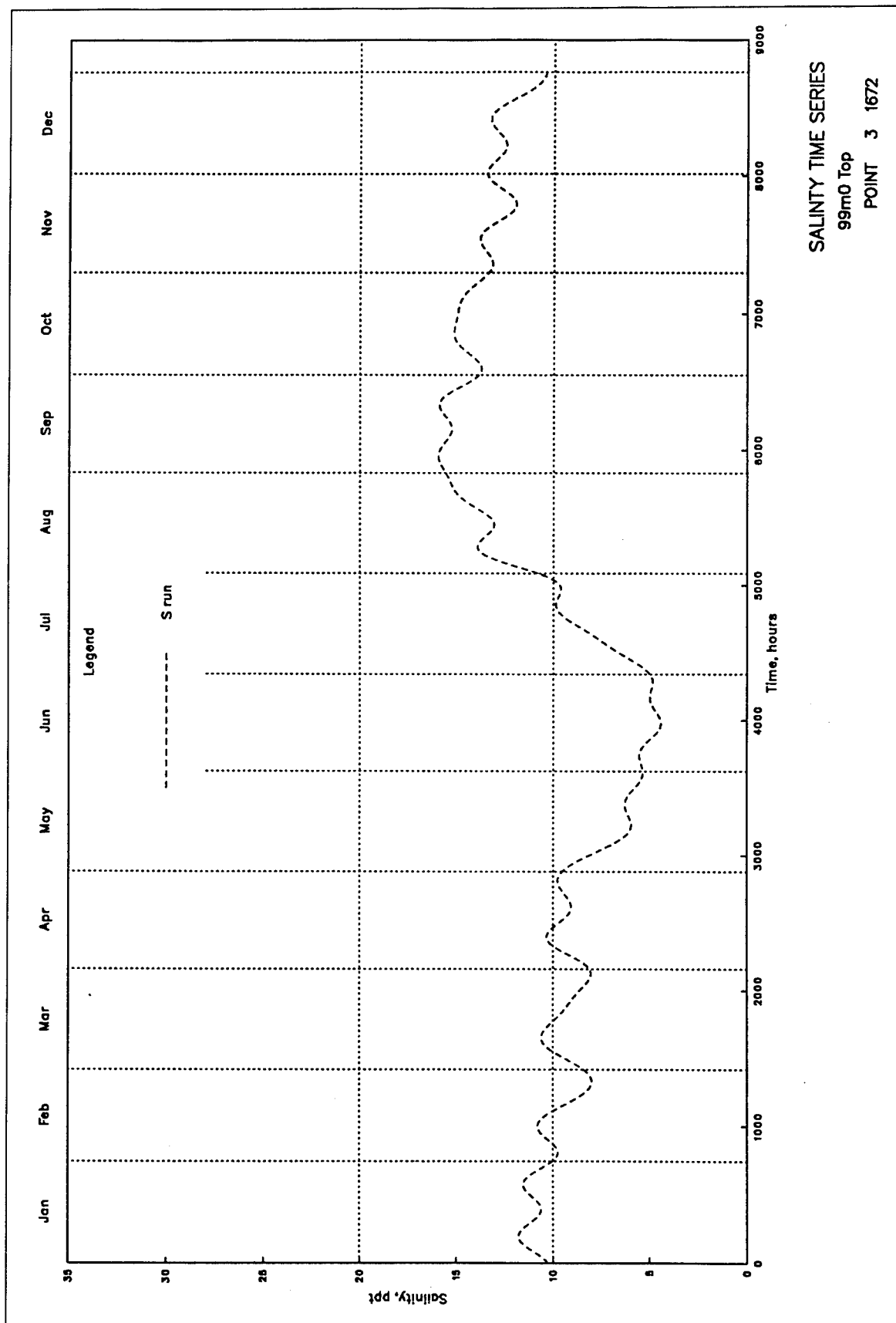


Plate 68



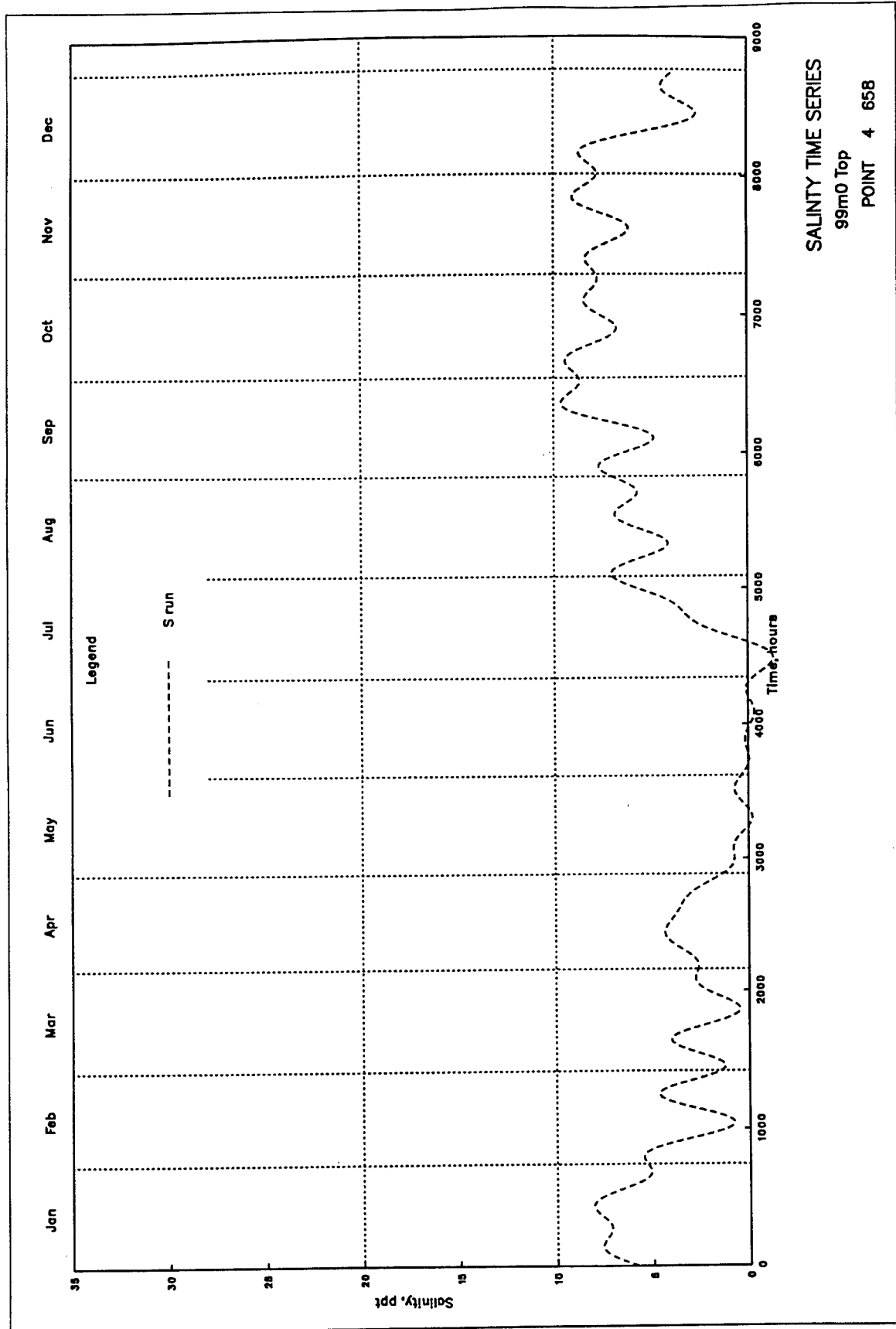
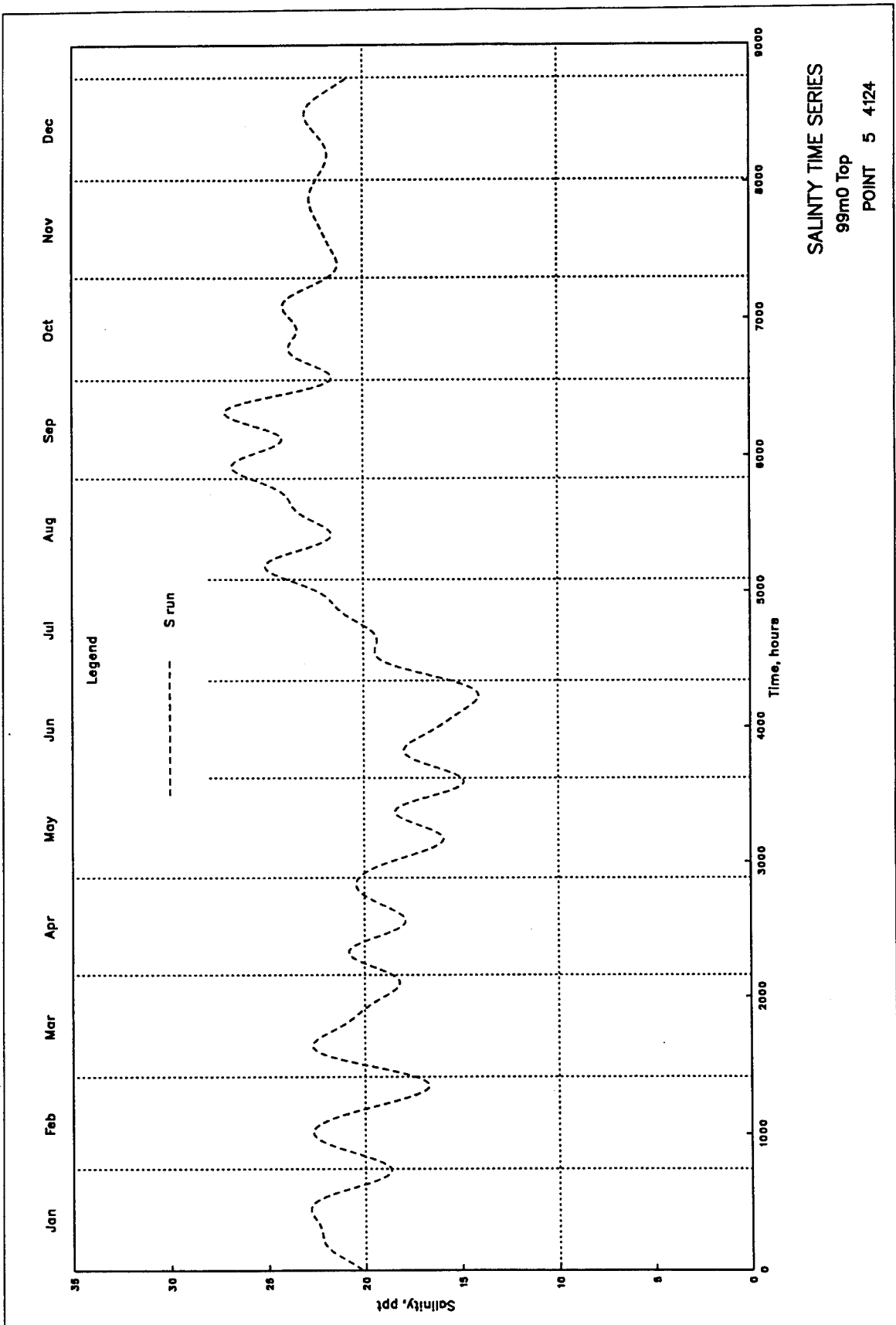


Plate 70



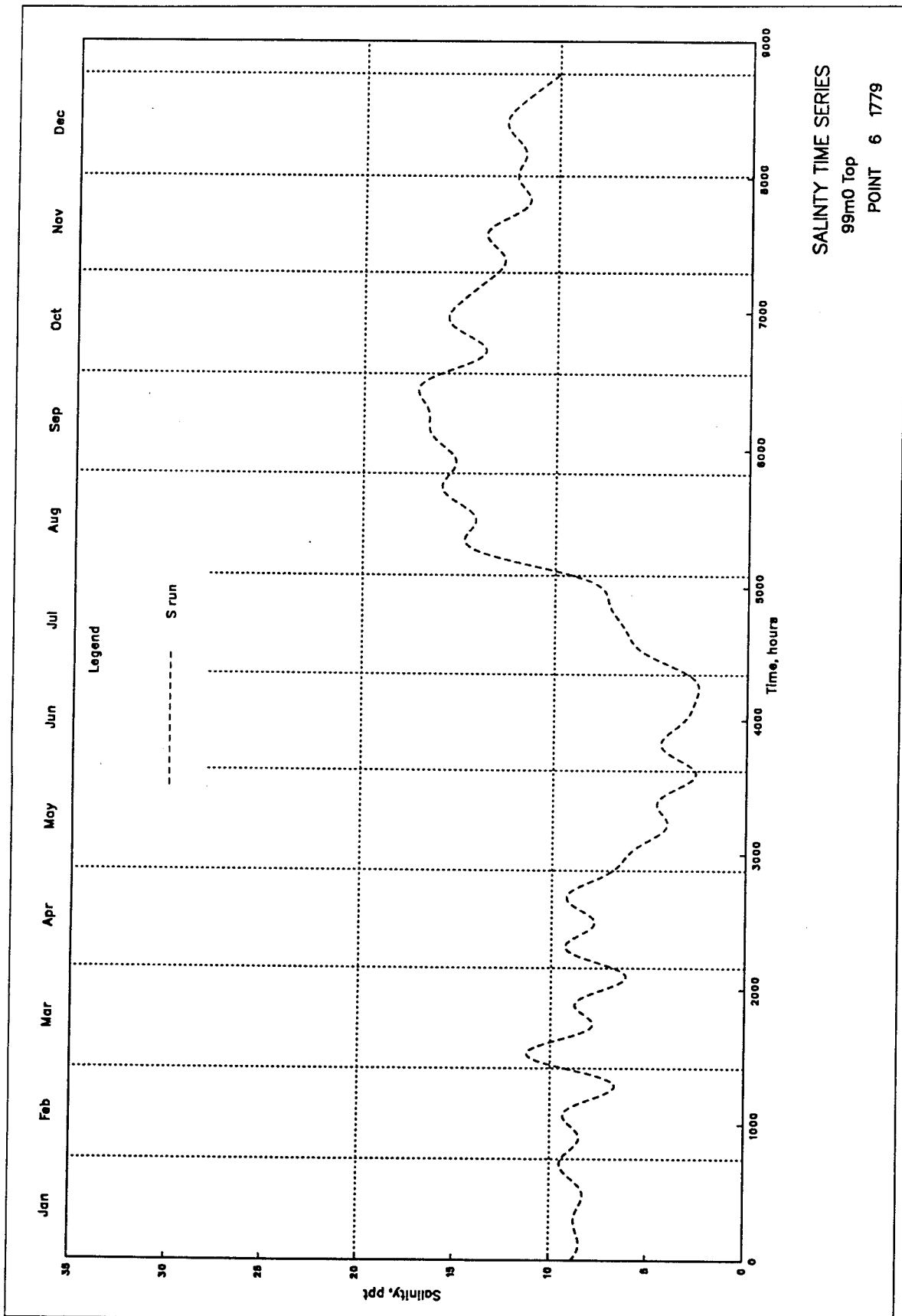


Plate 72

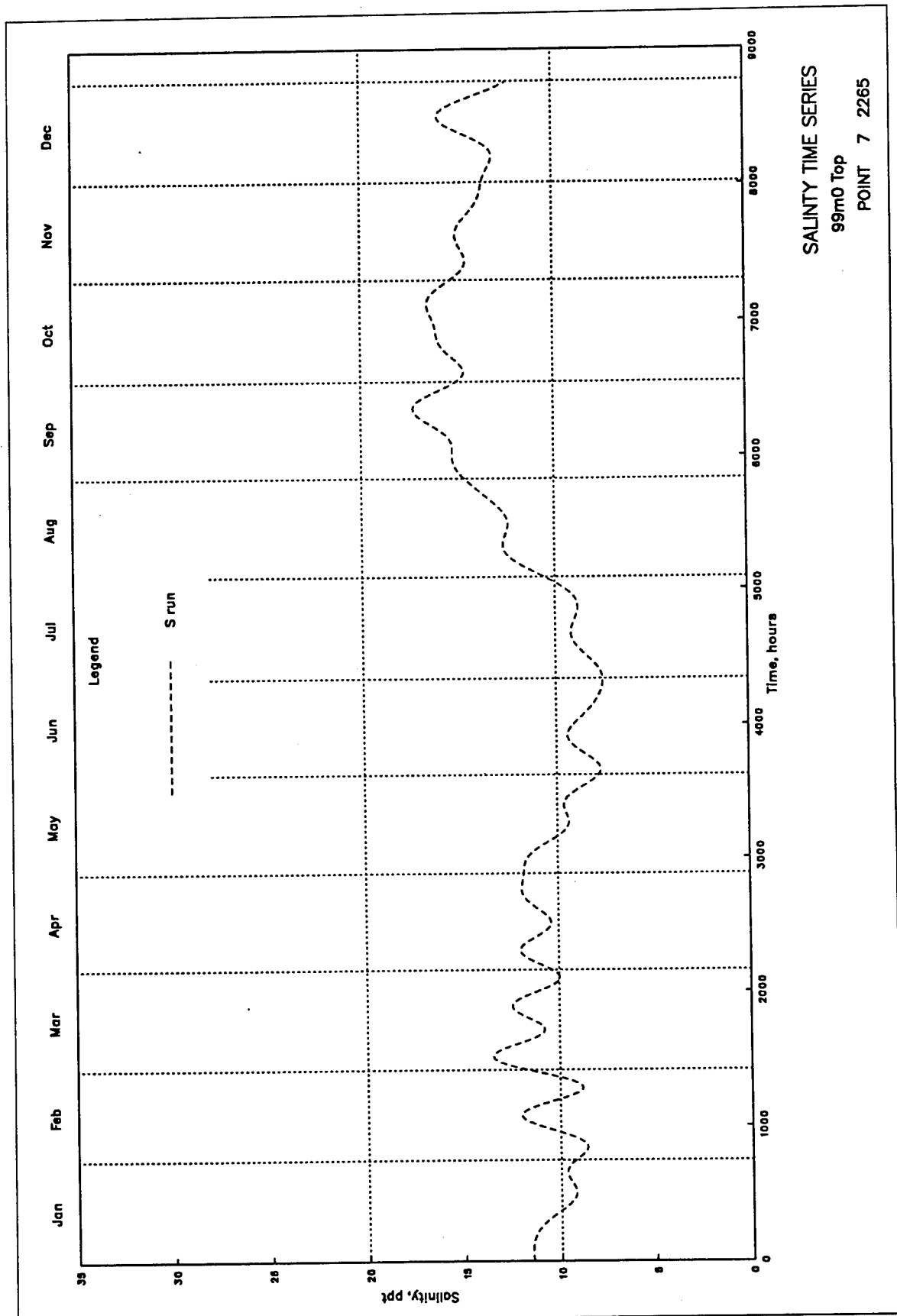


Plate 73

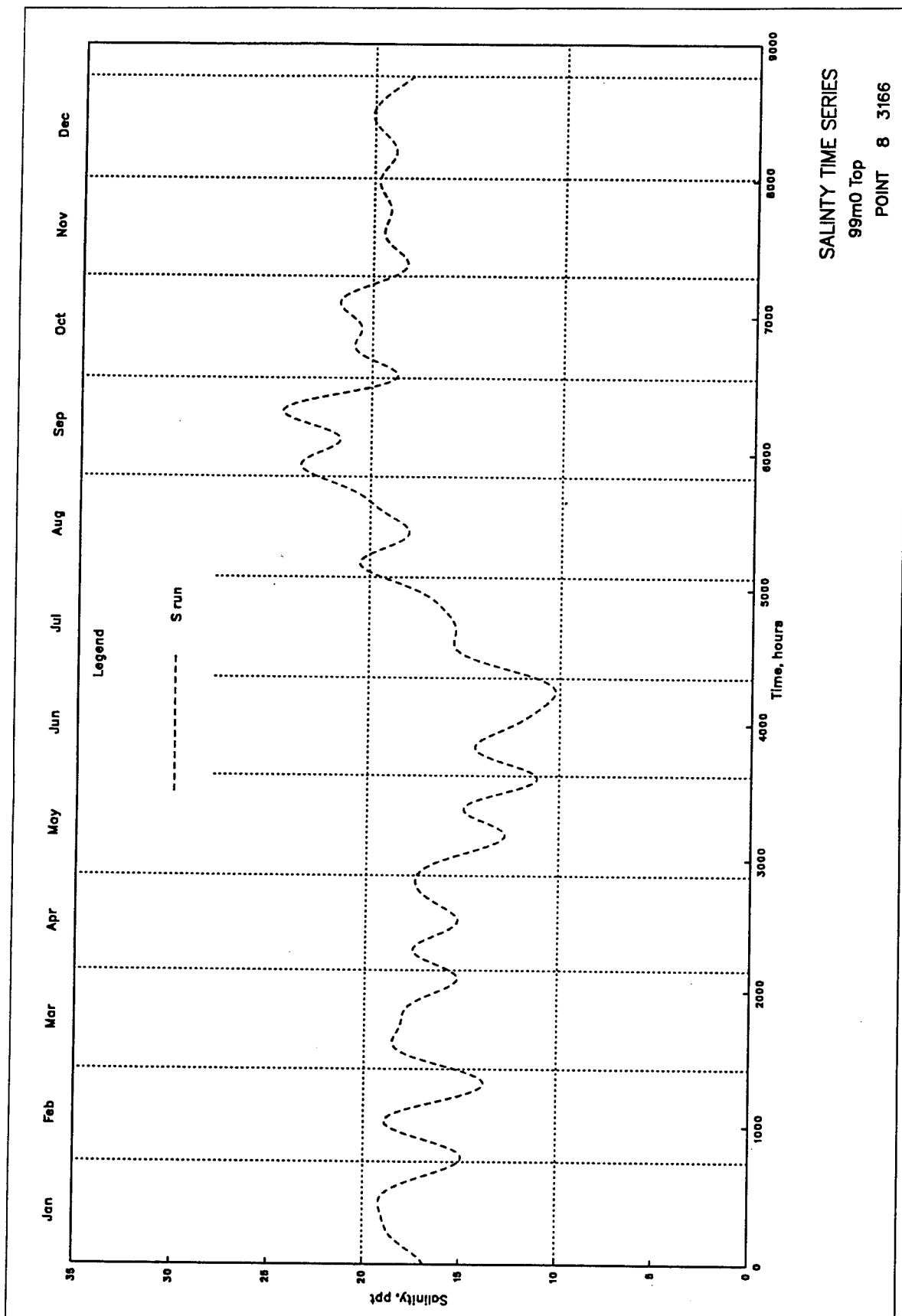
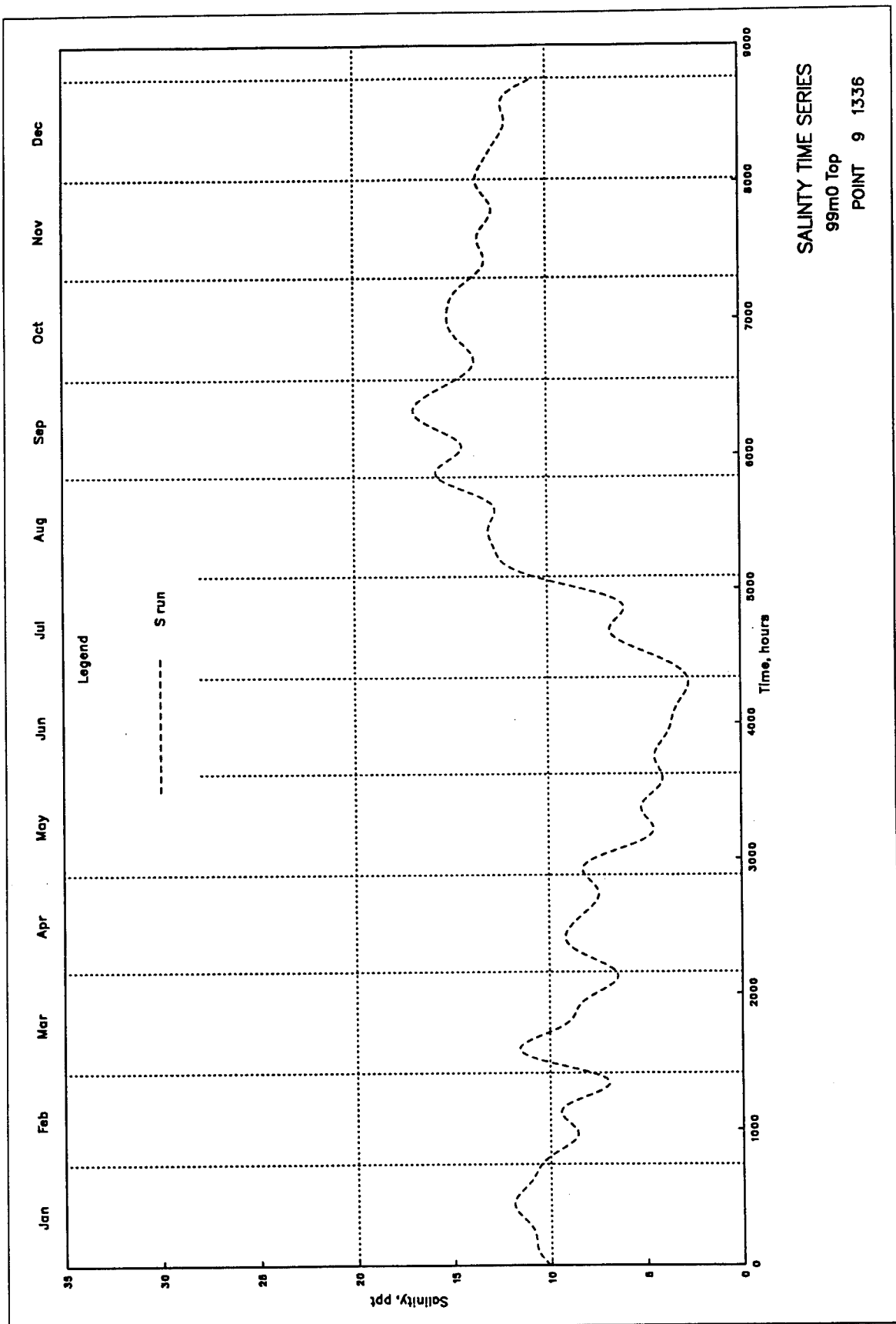


Plate 74



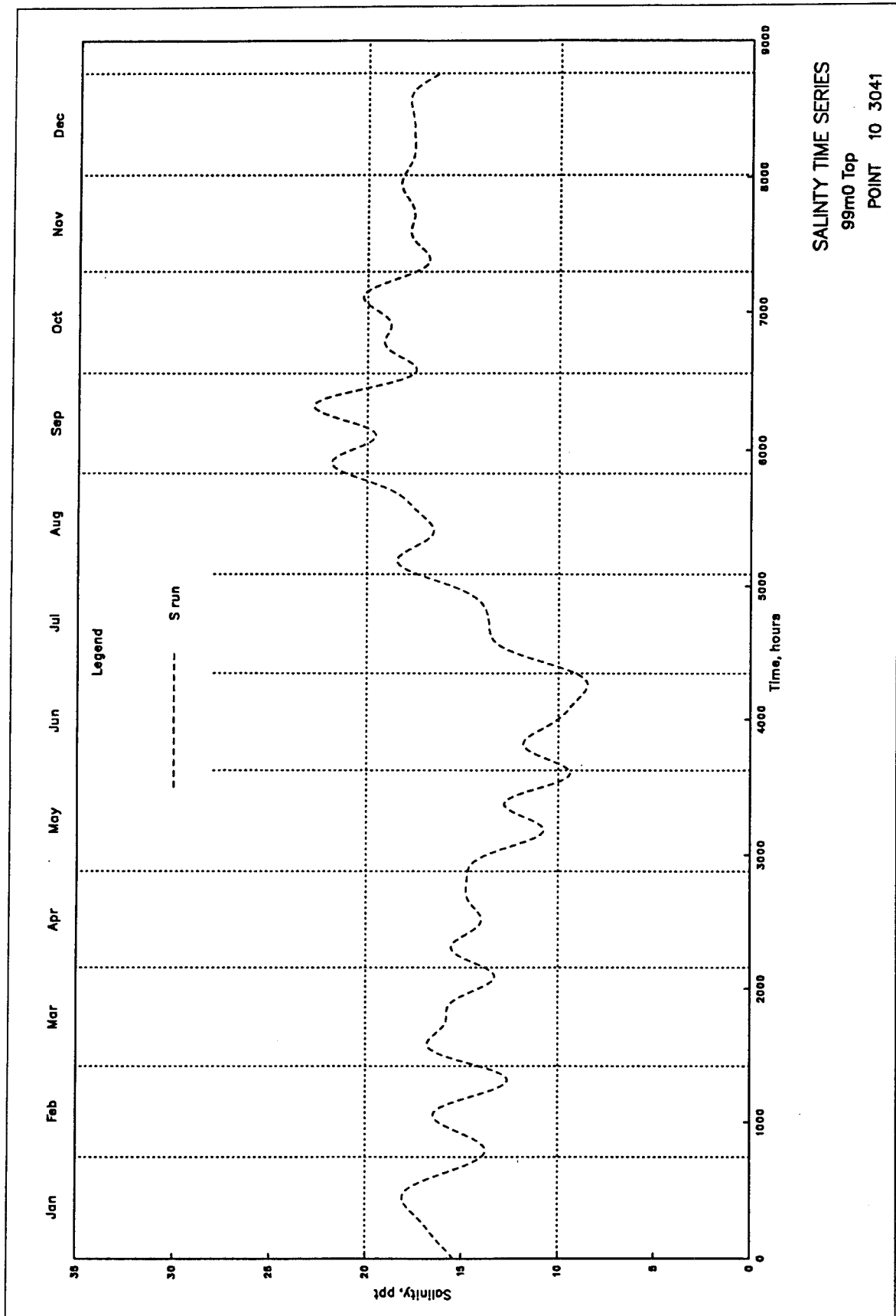
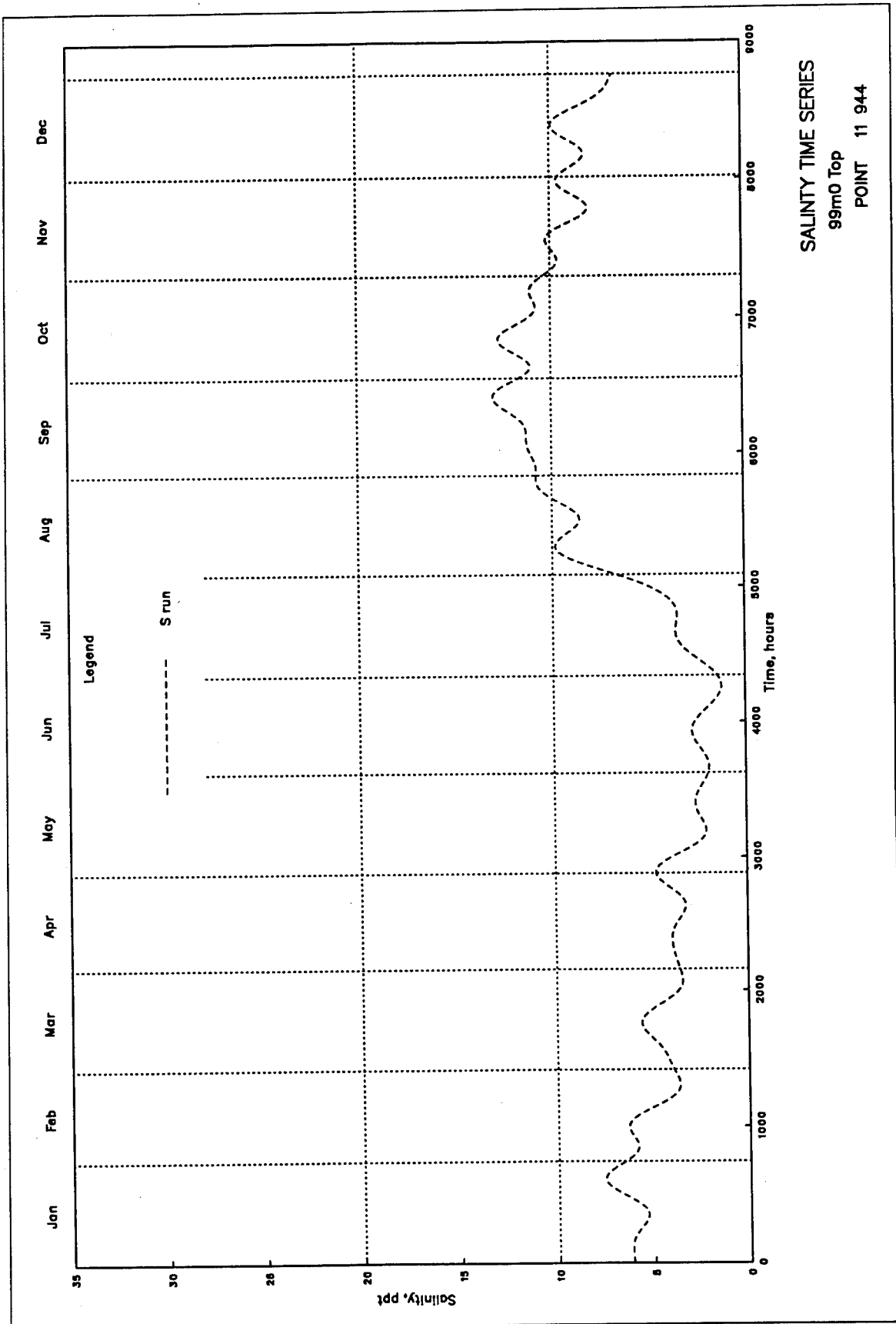


Plate 76



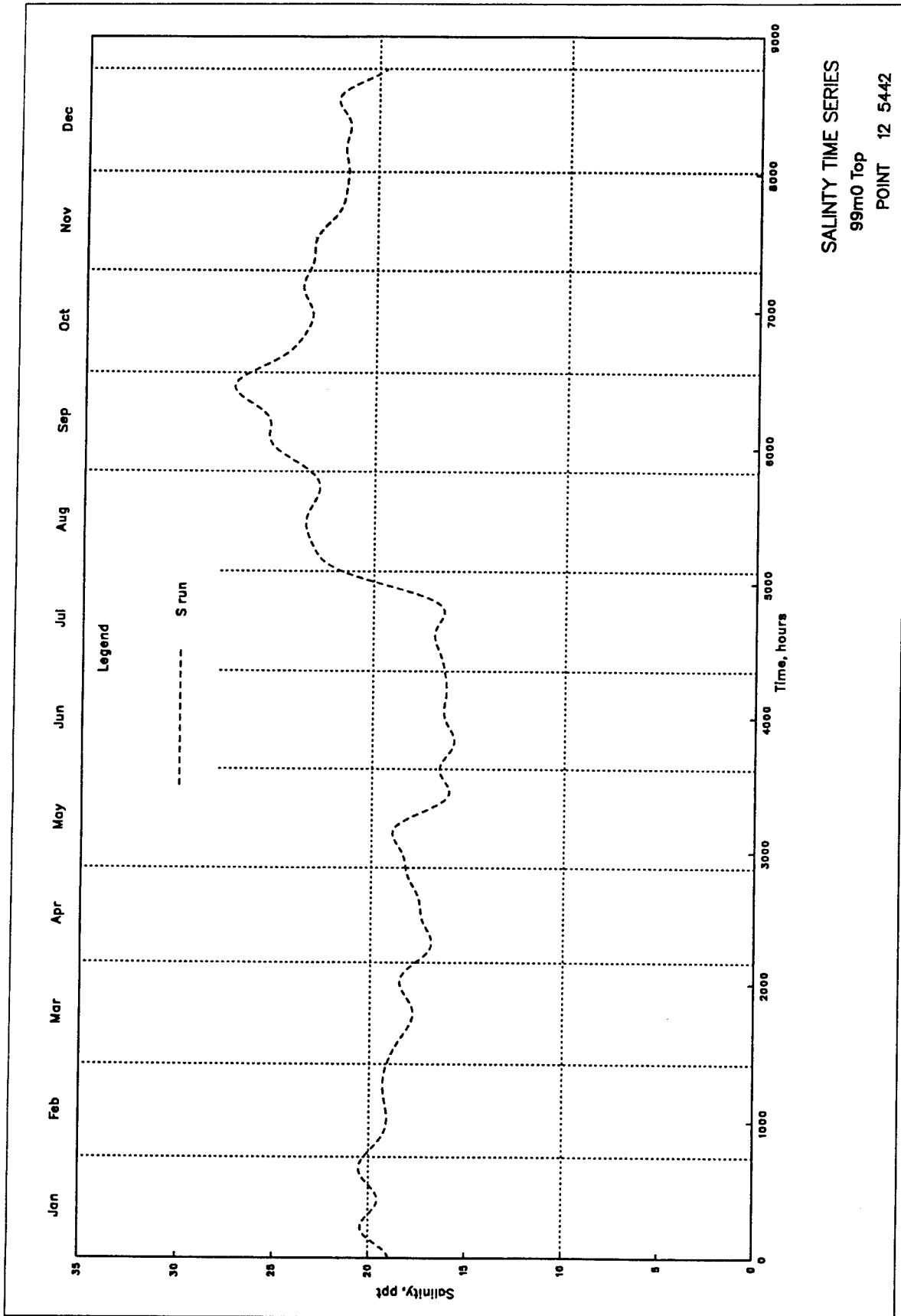
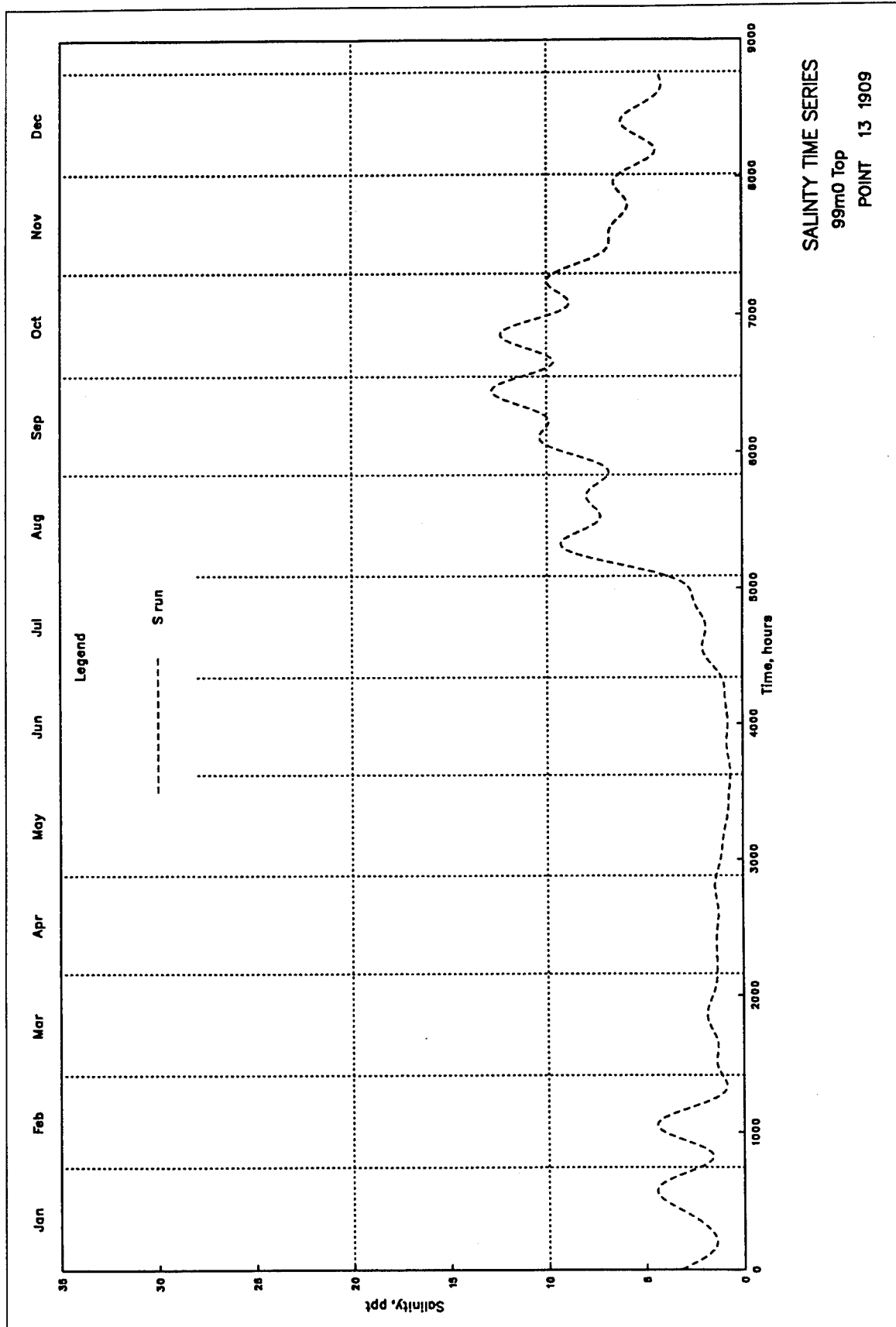


Plate 78



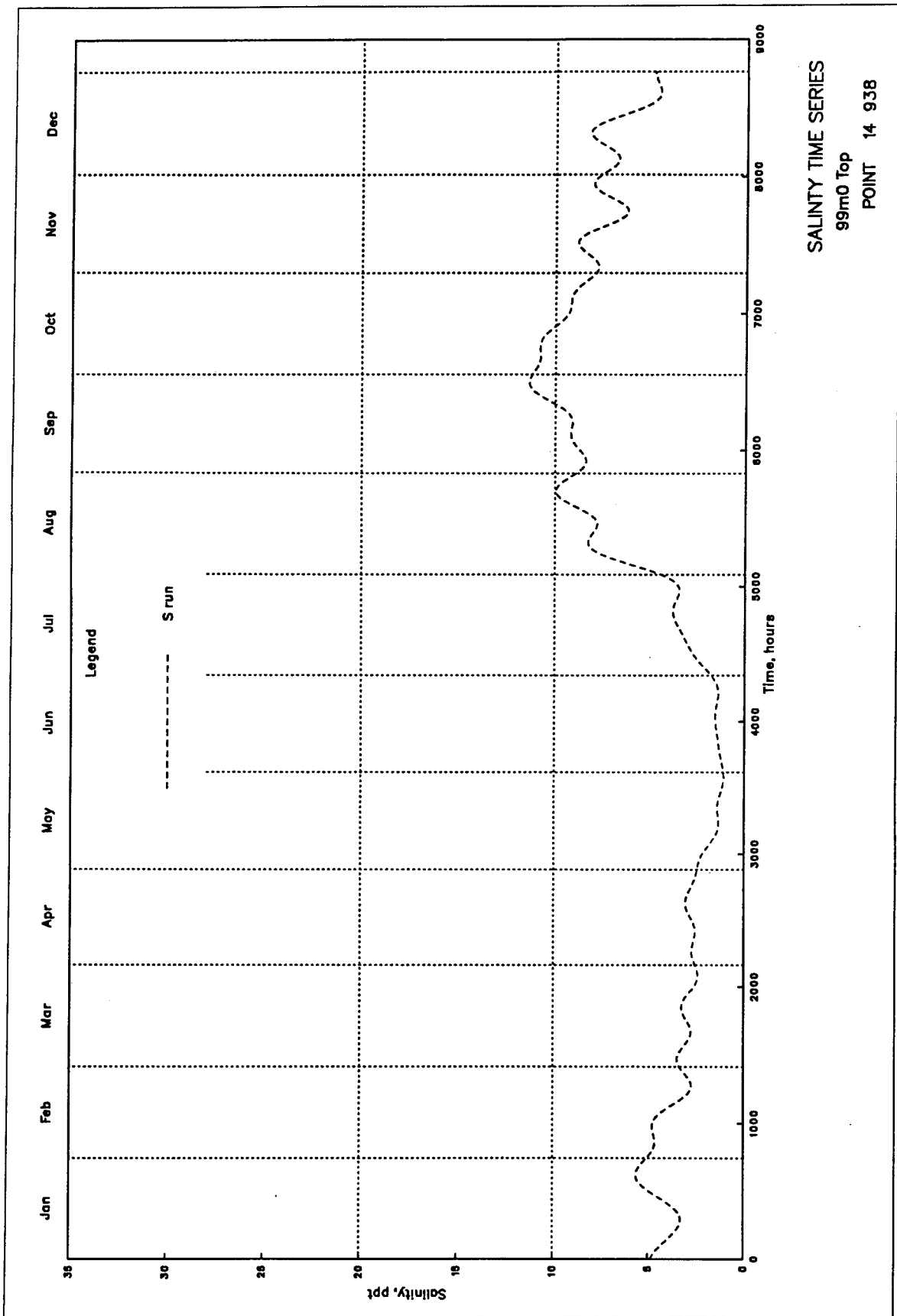
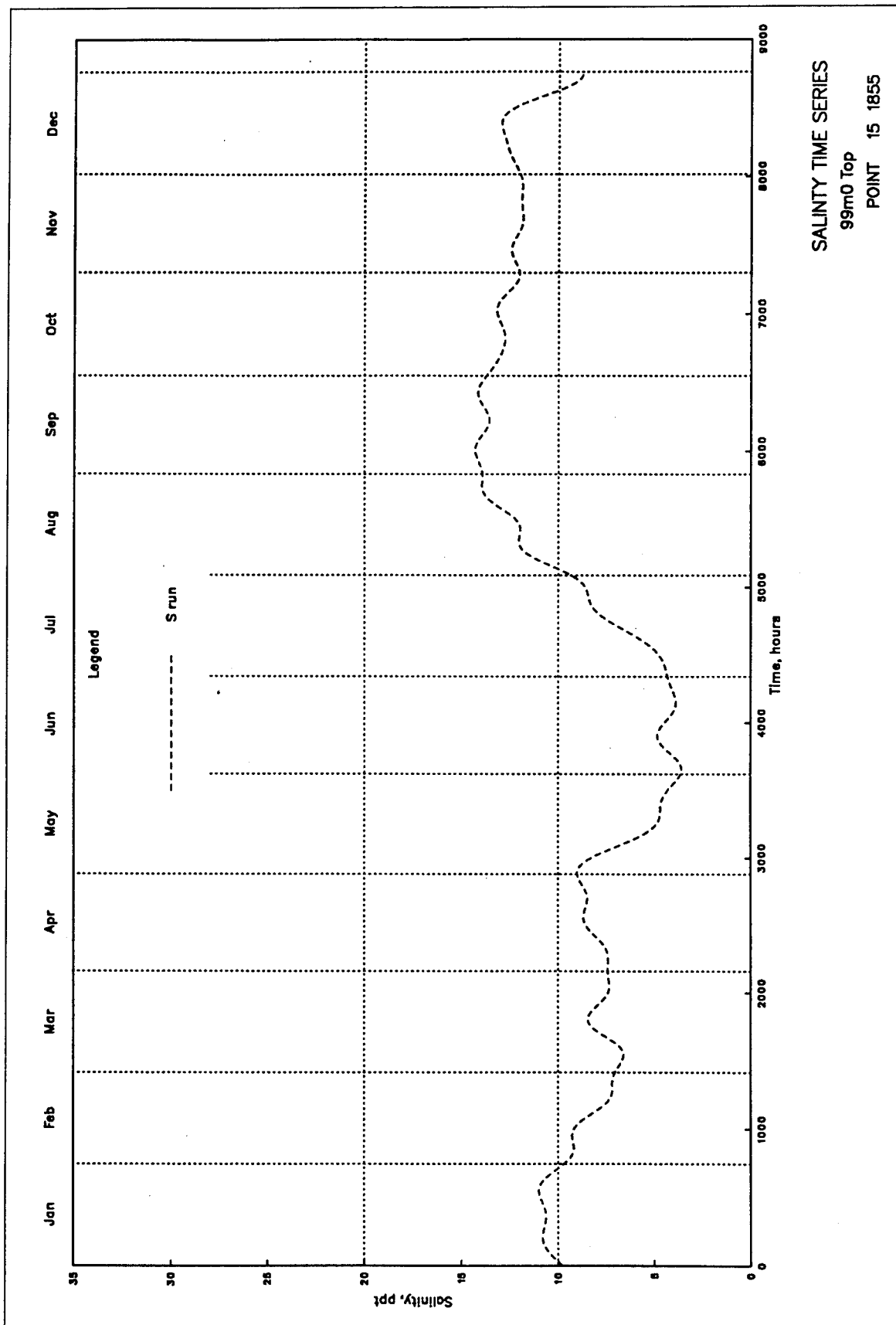


Plate 80



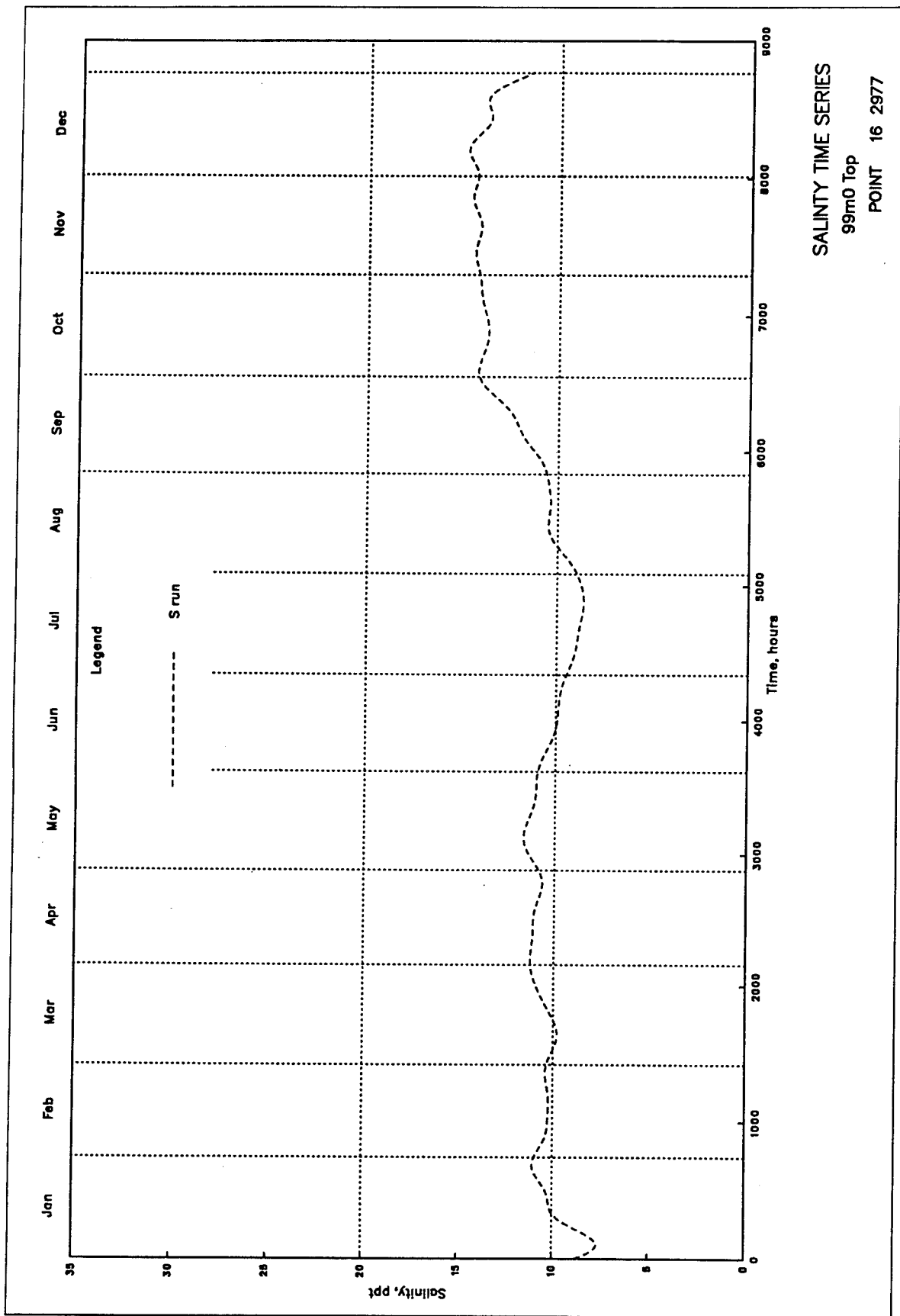
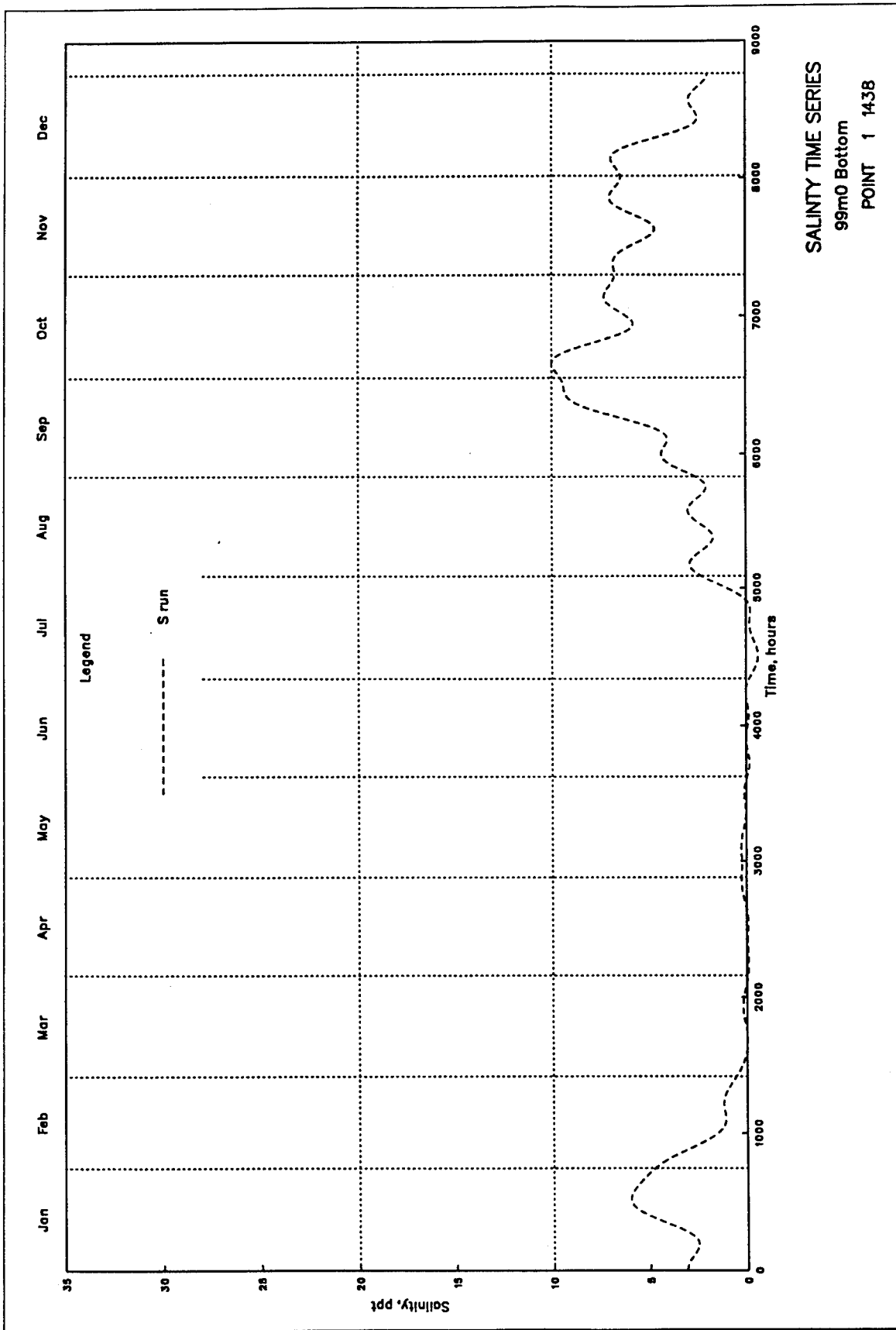


Plate 82



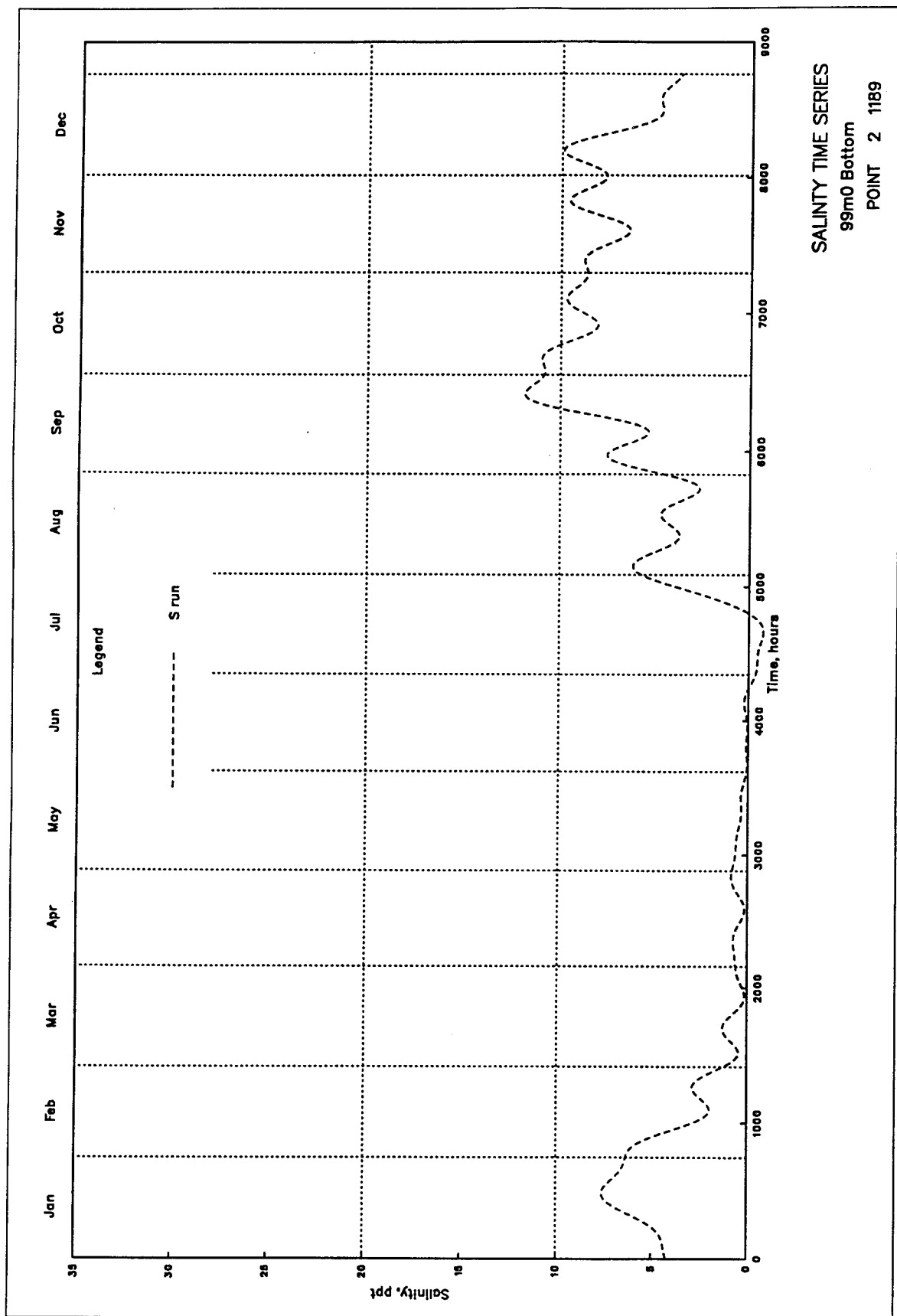
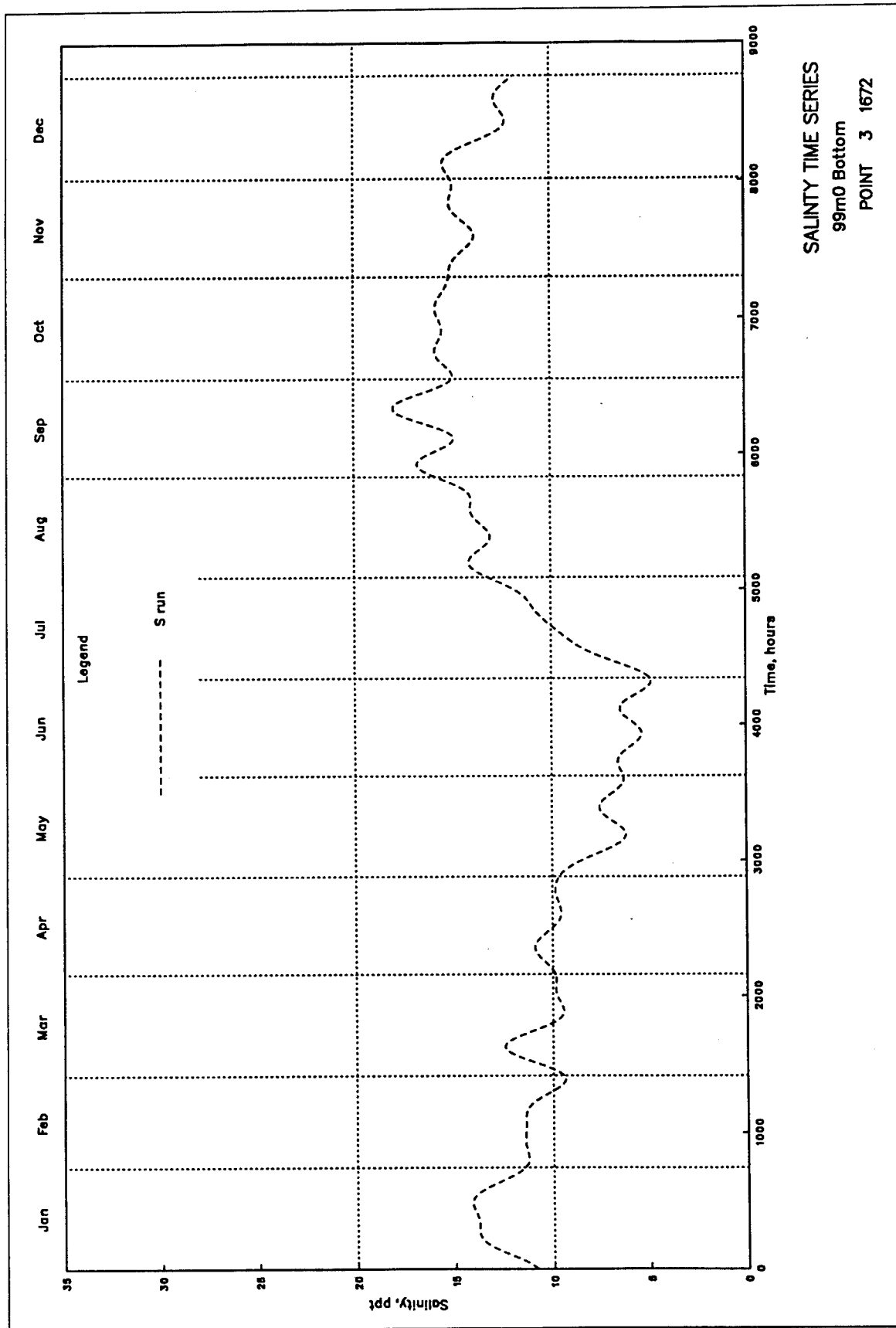
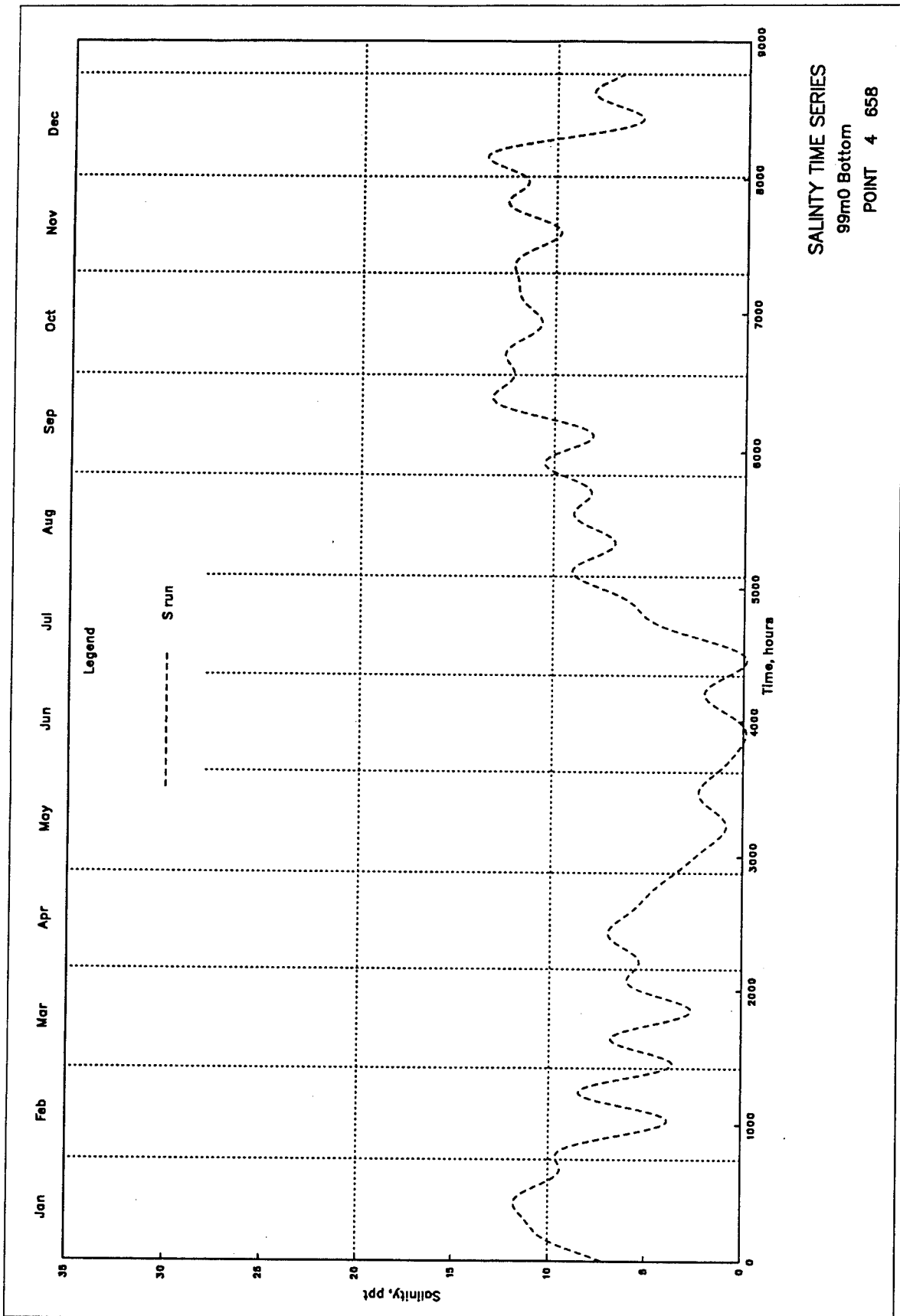
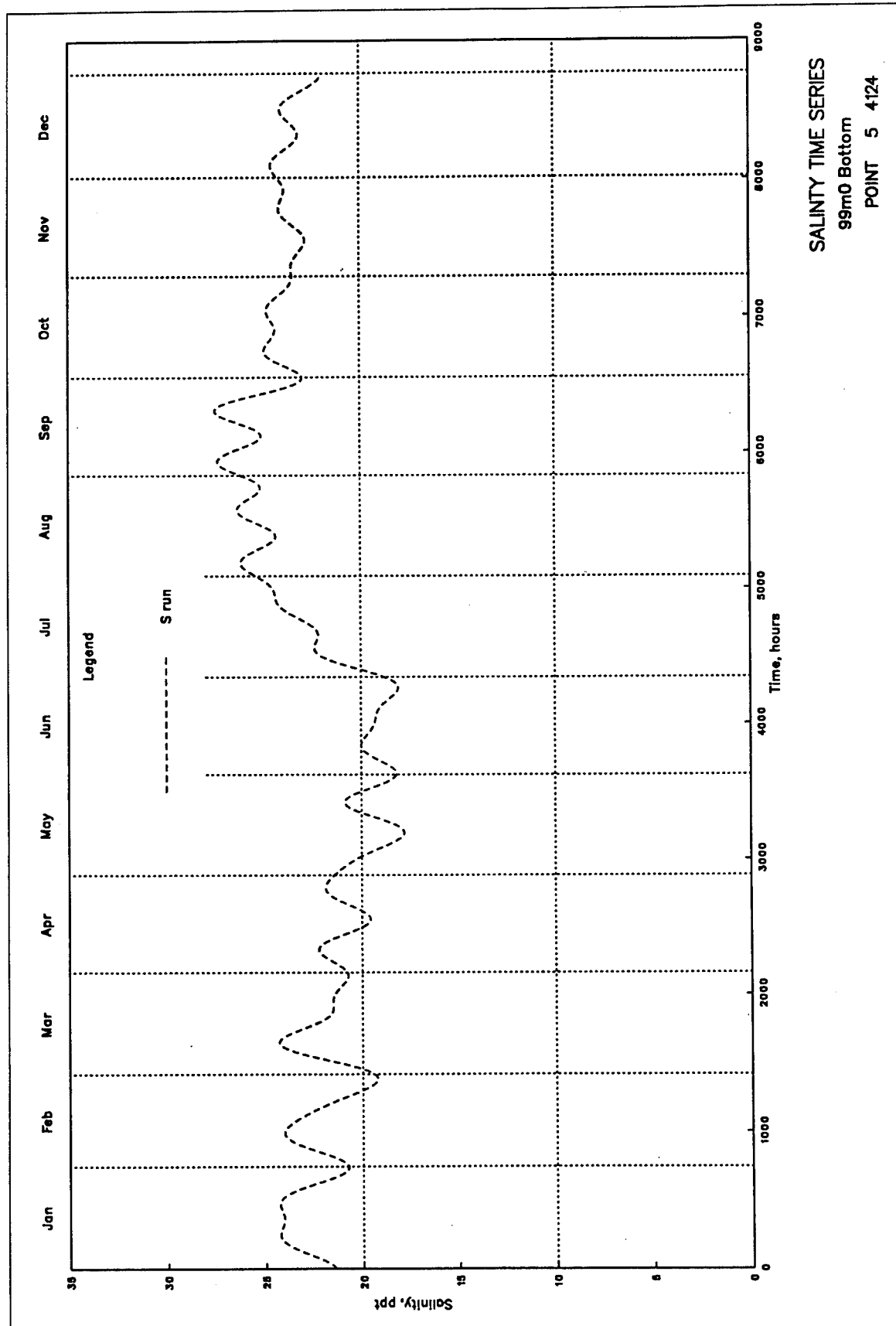


Plate 84







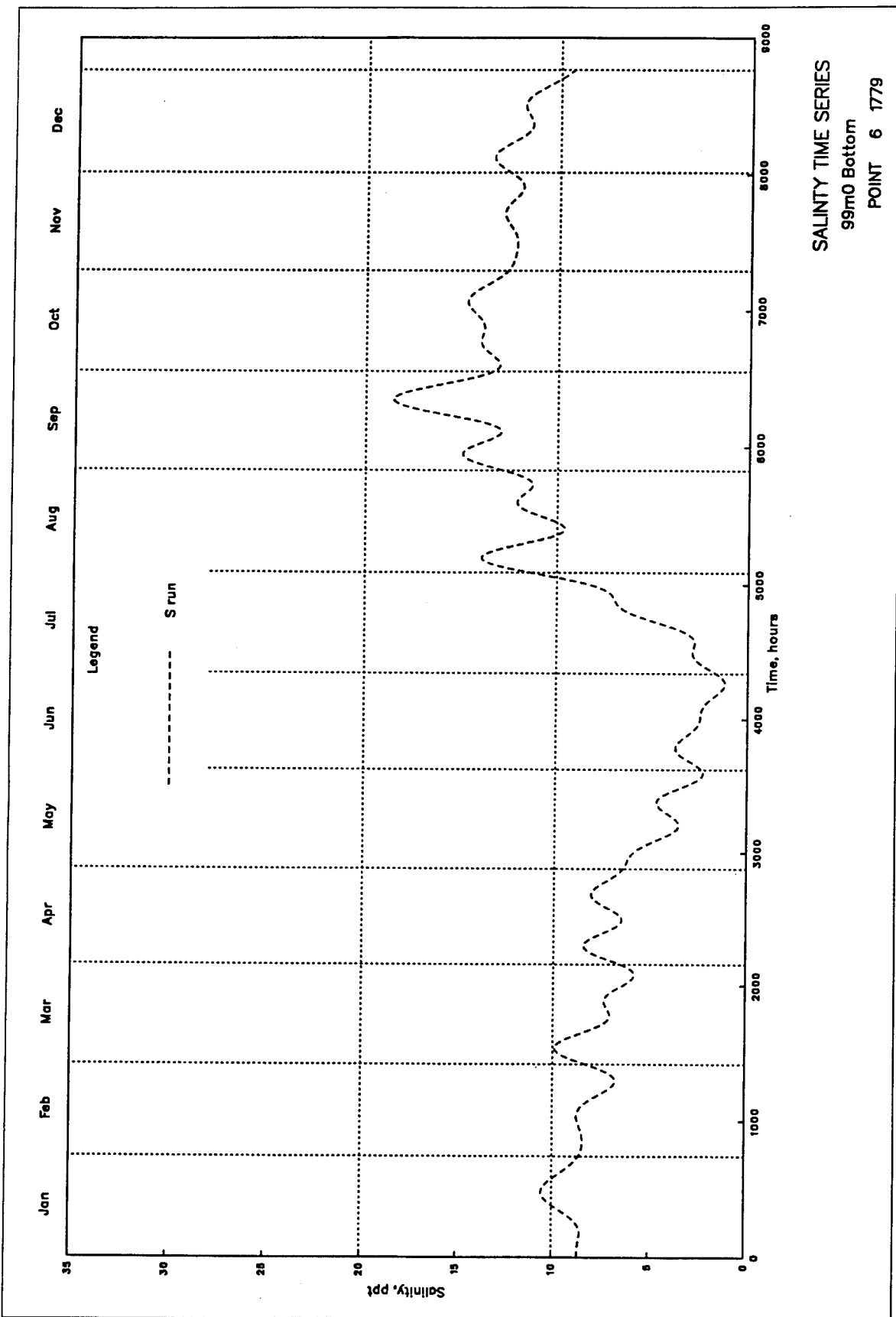
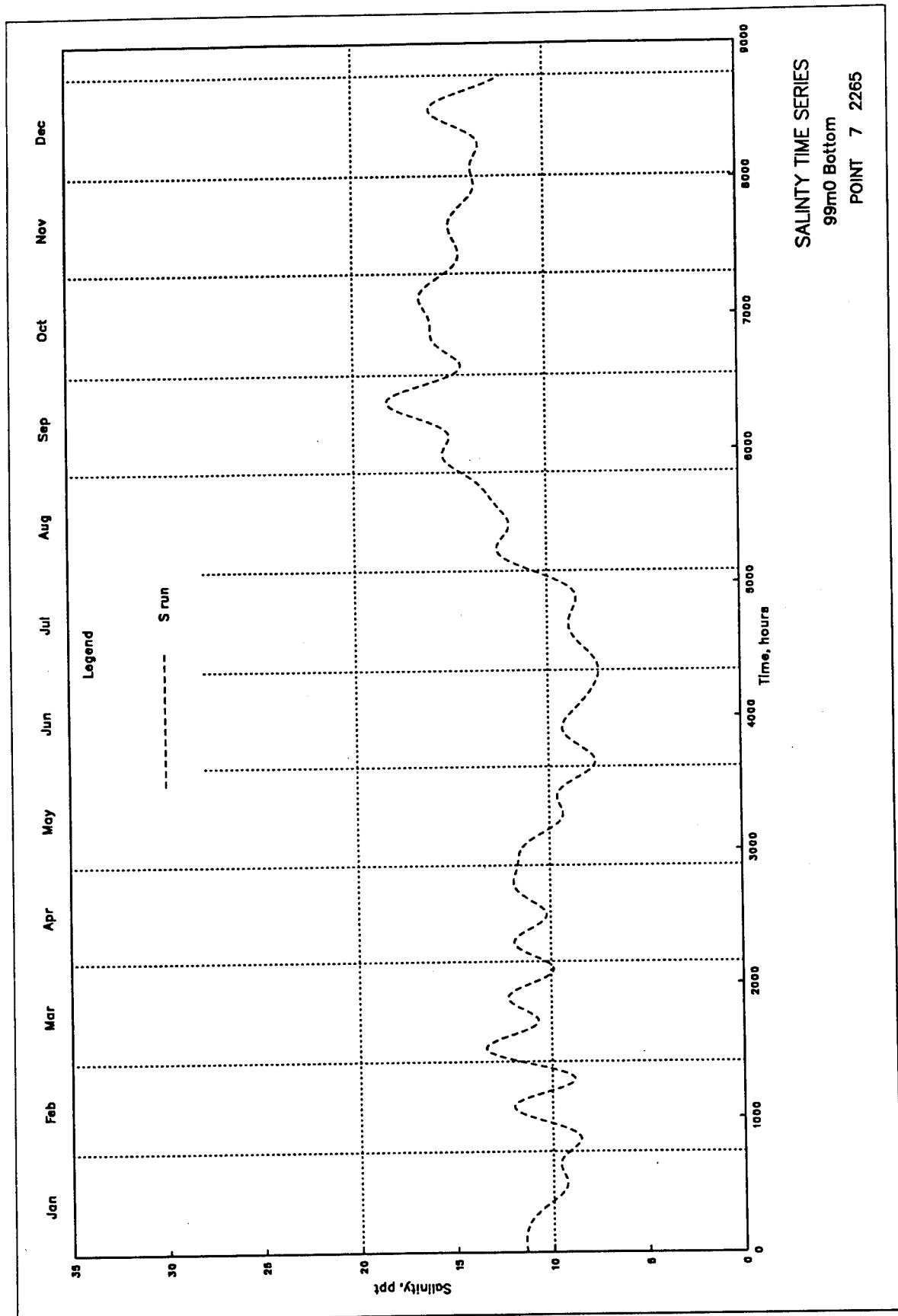


Plate 88



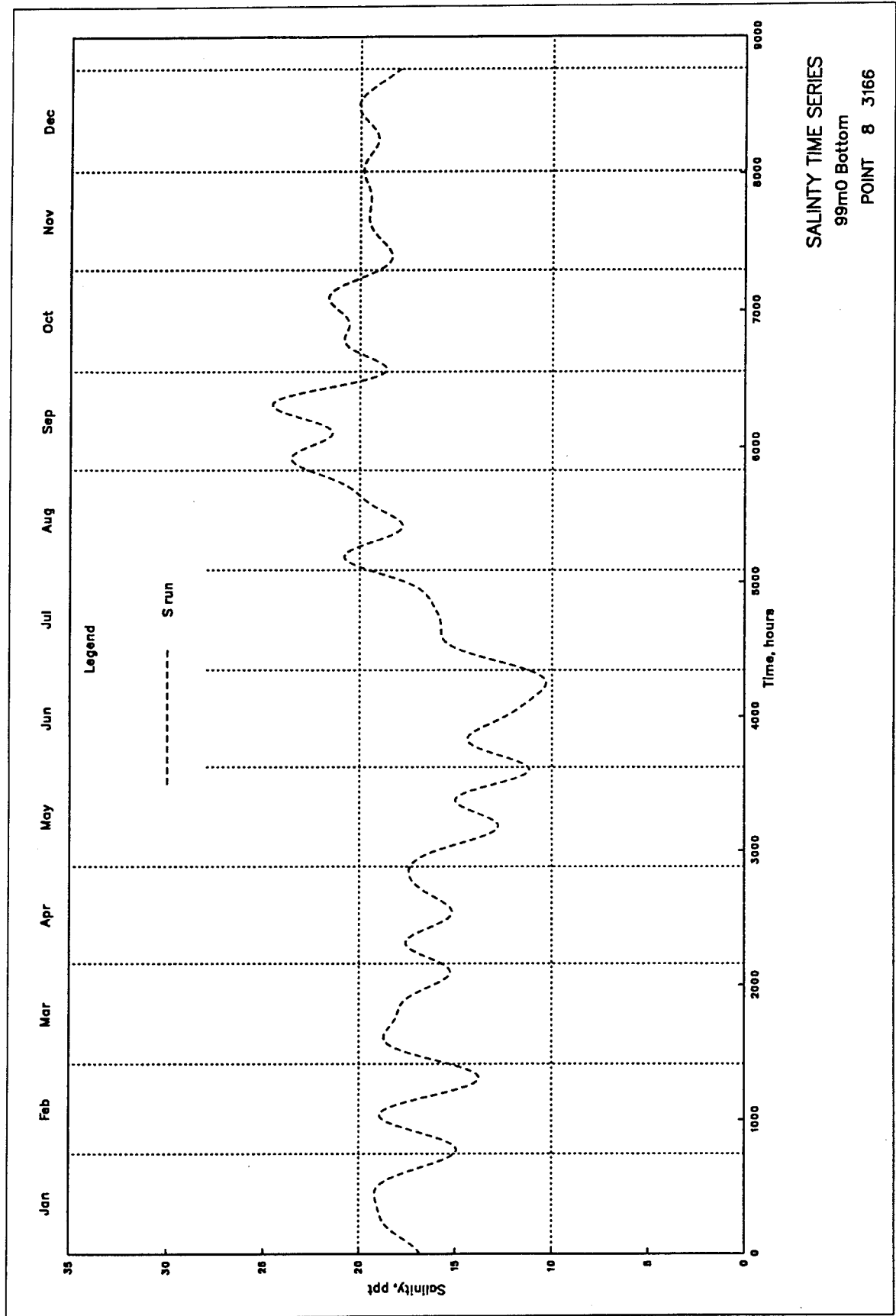
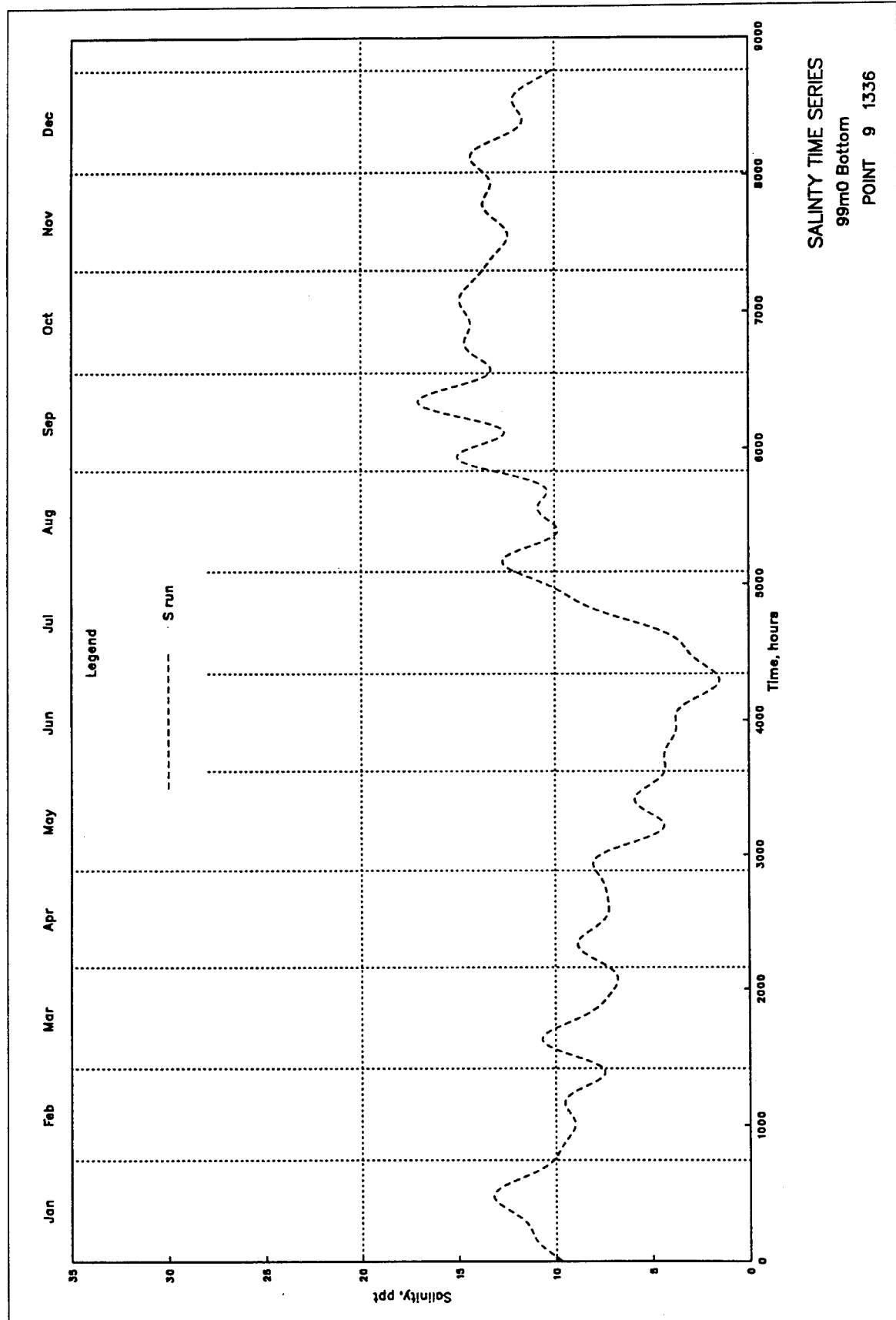


Plate 90



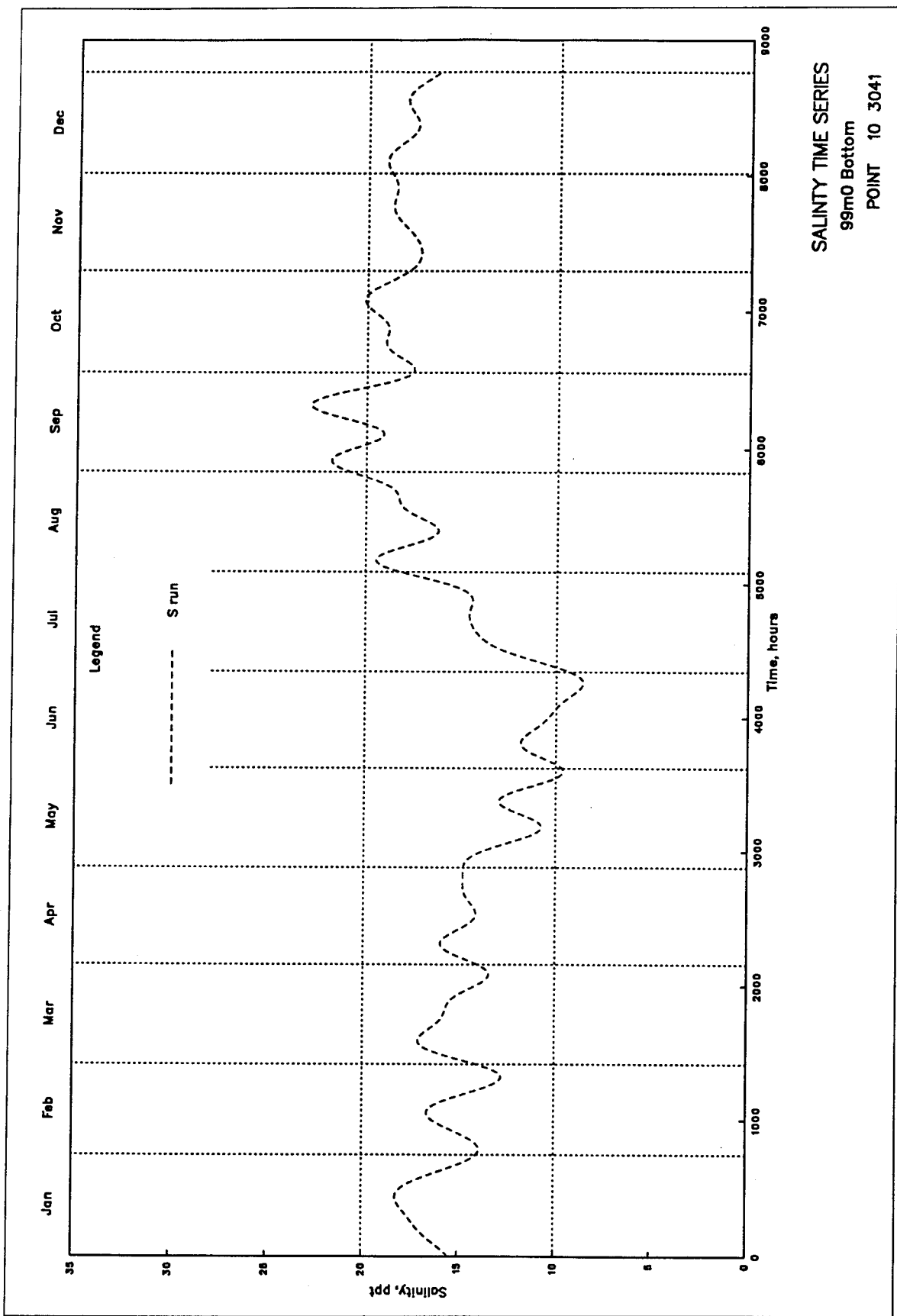
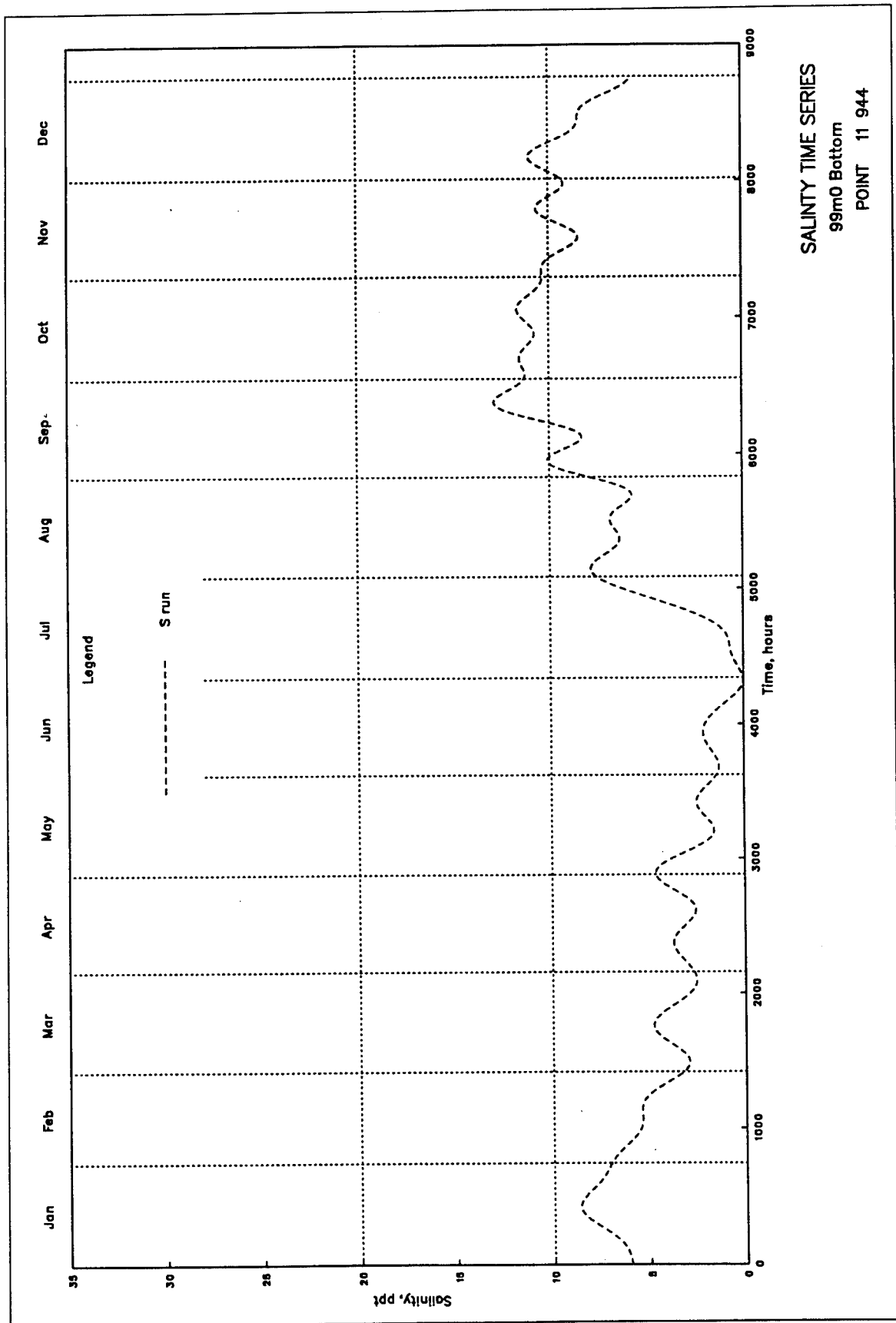


Plate 92



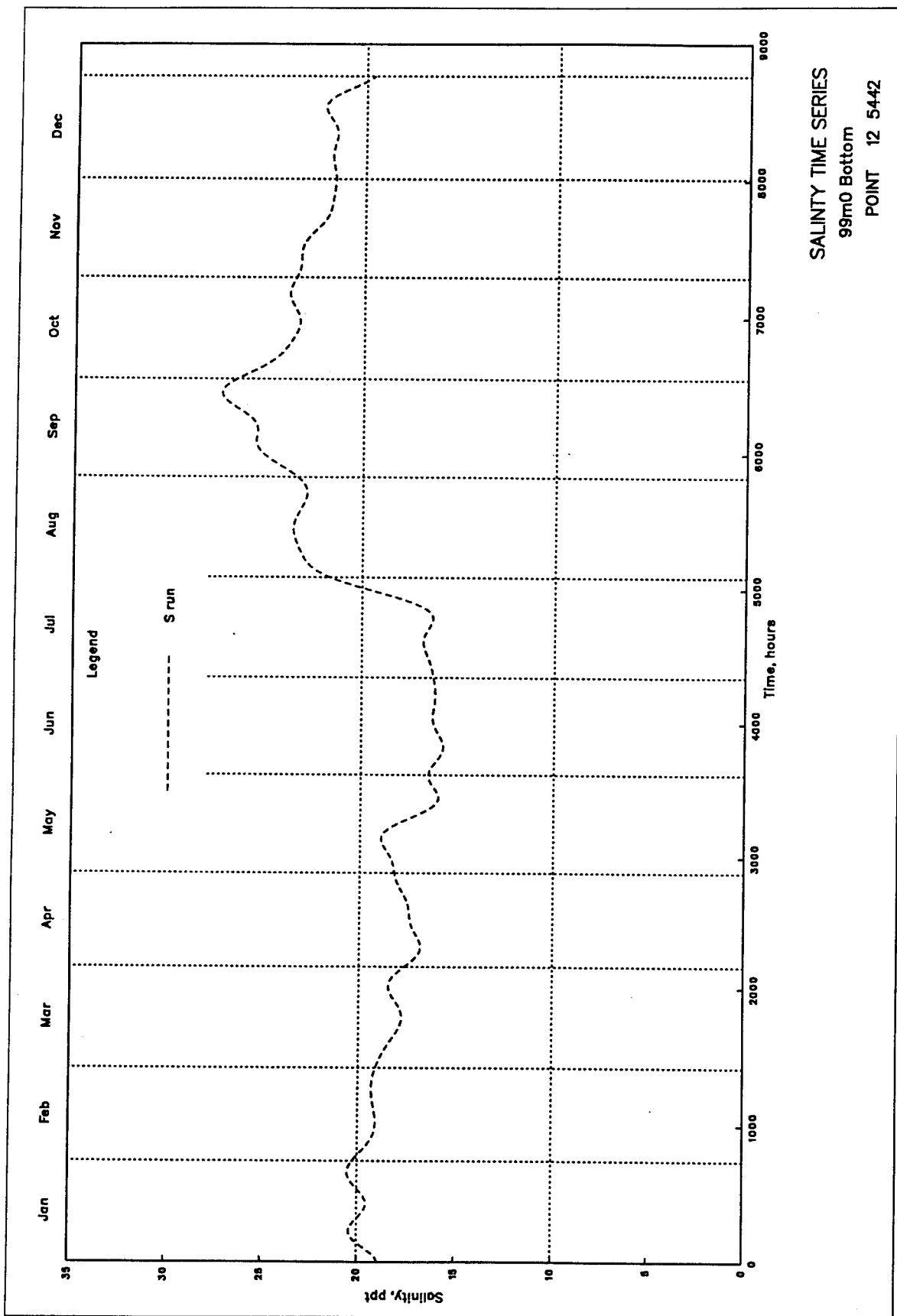
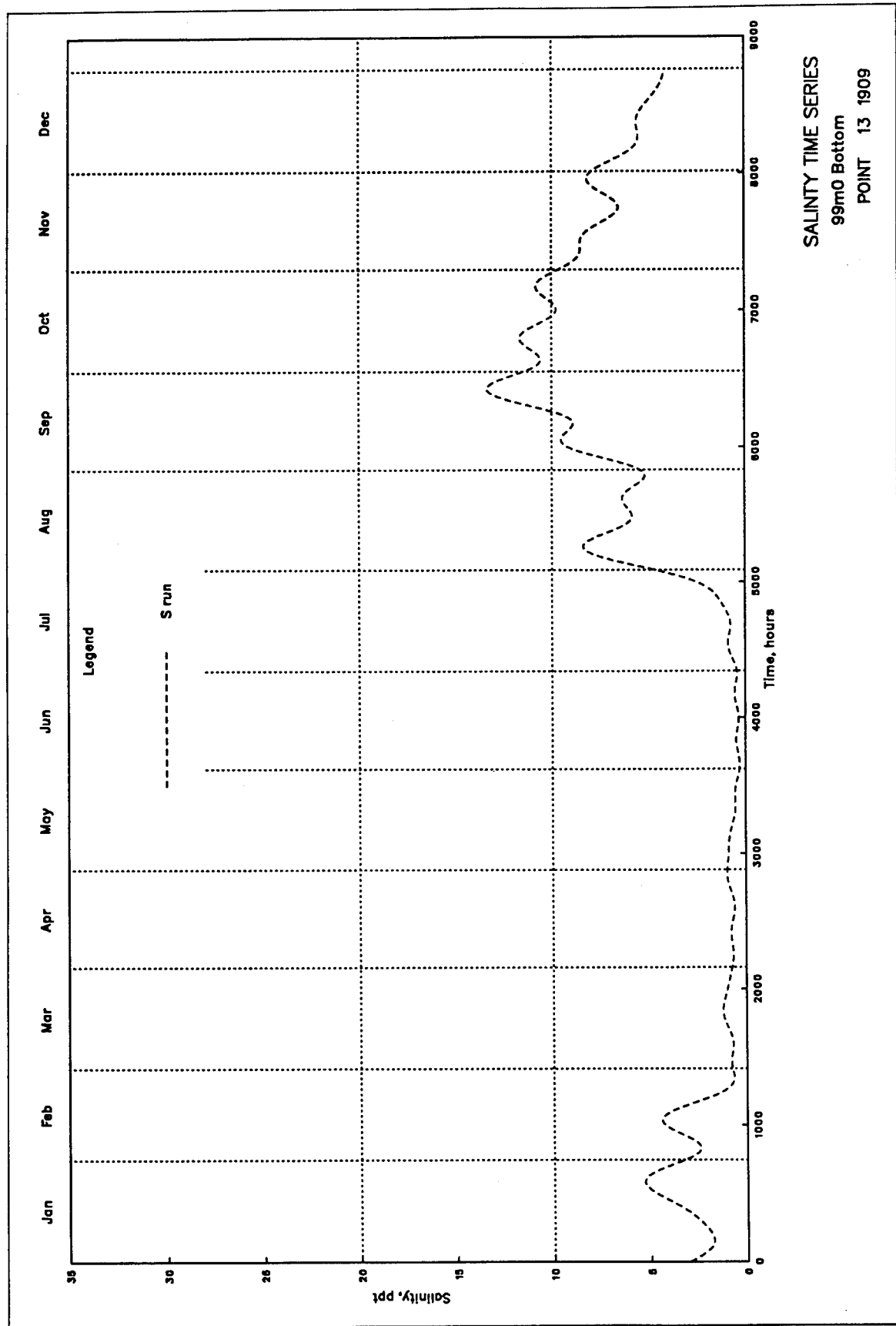
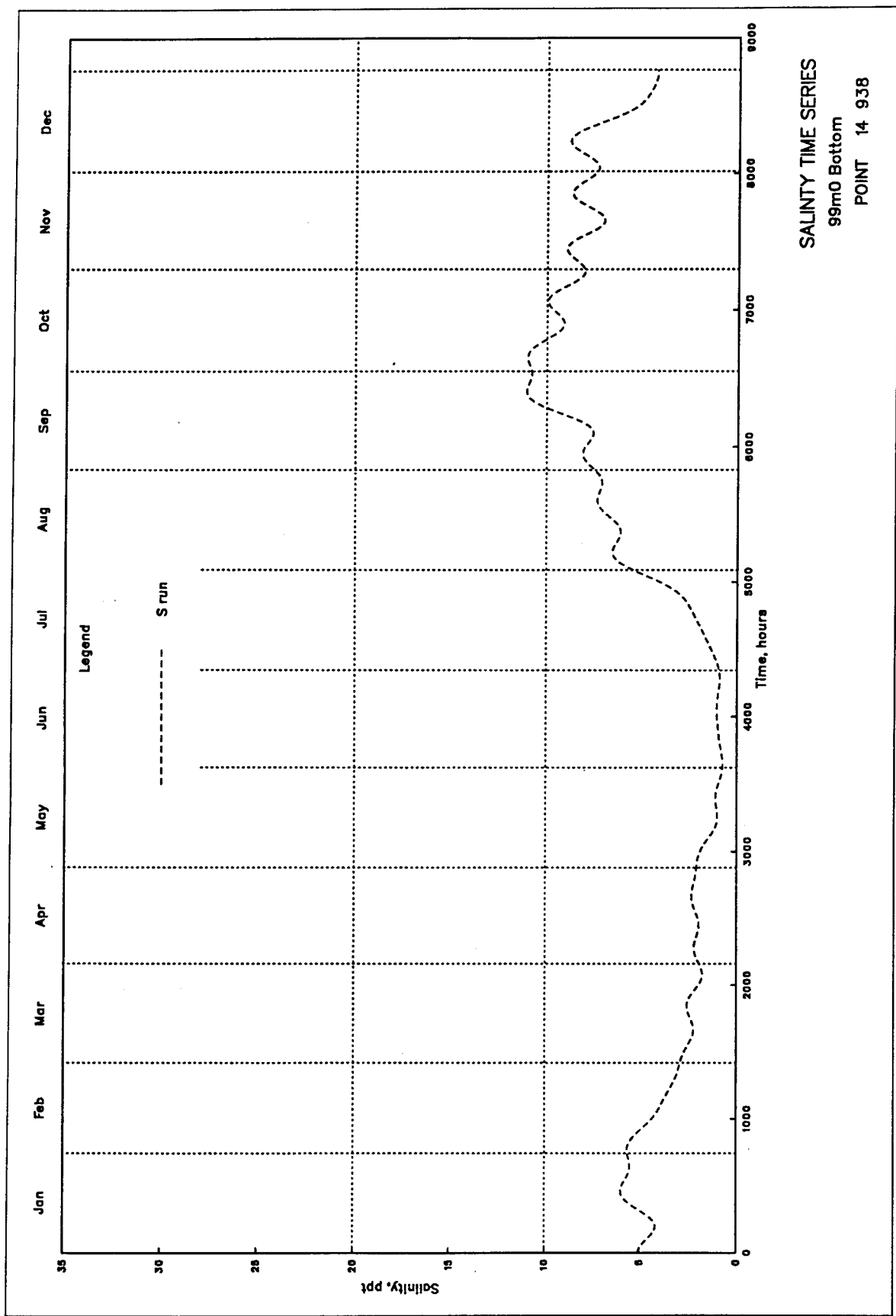
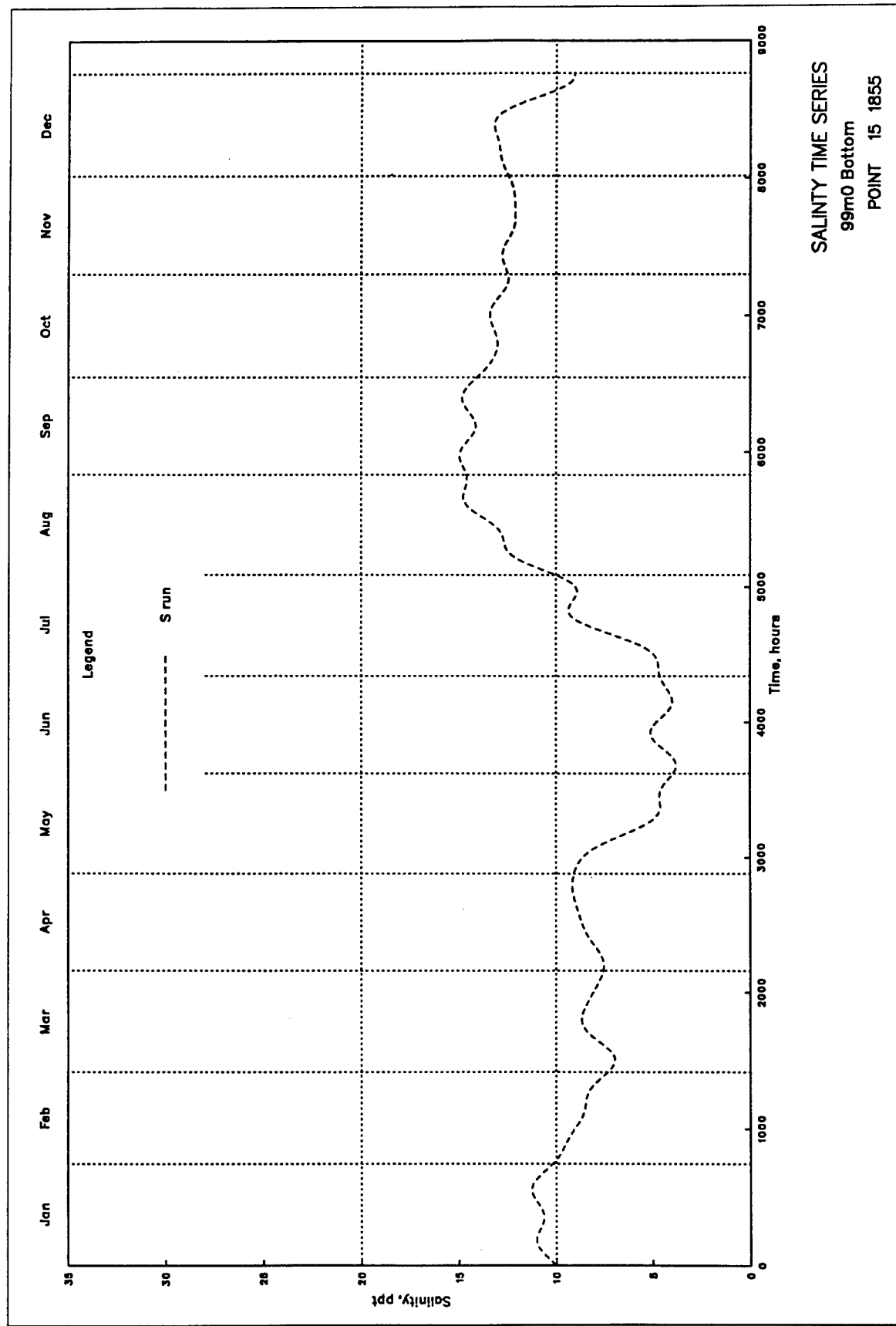


Plate 94







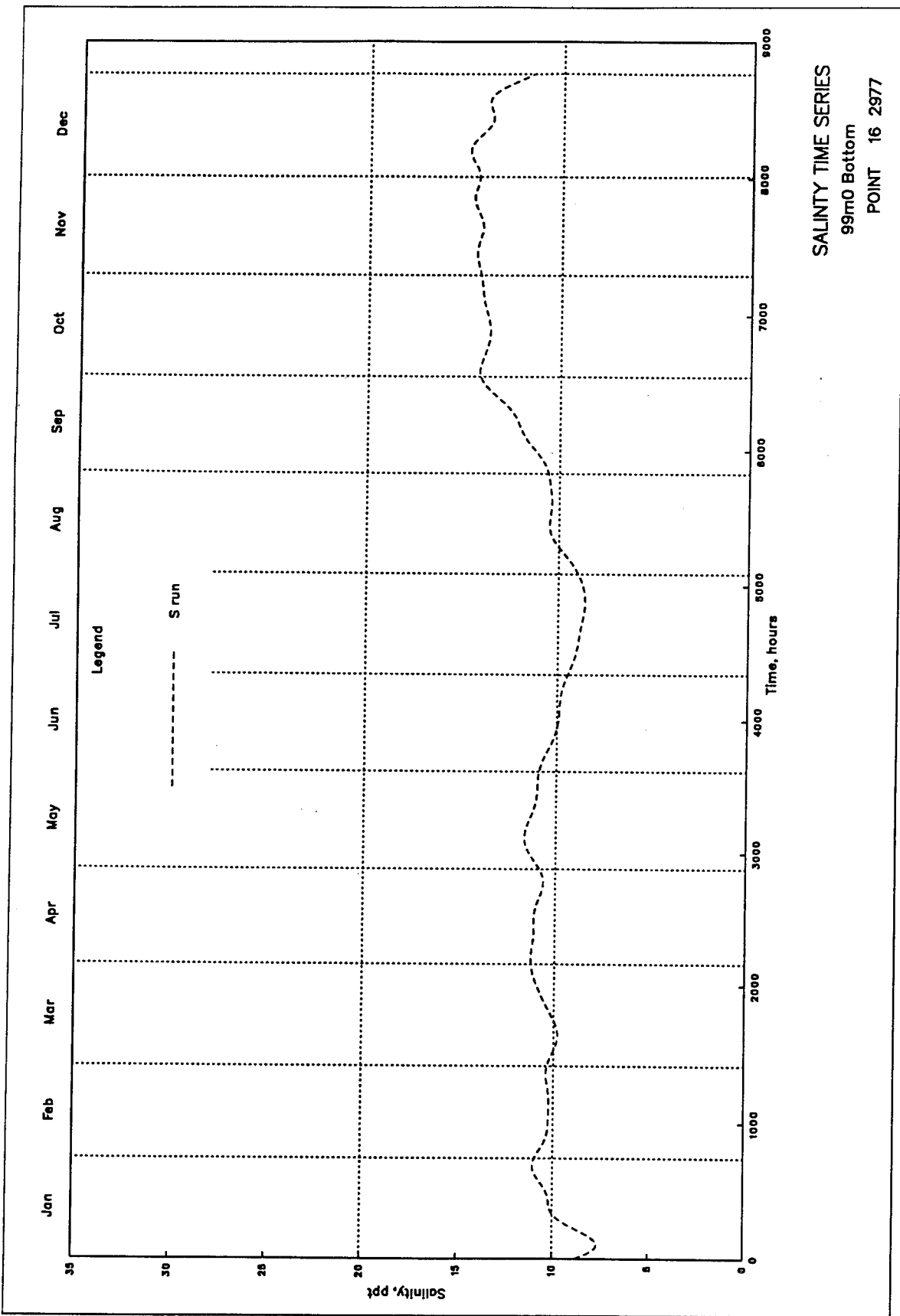
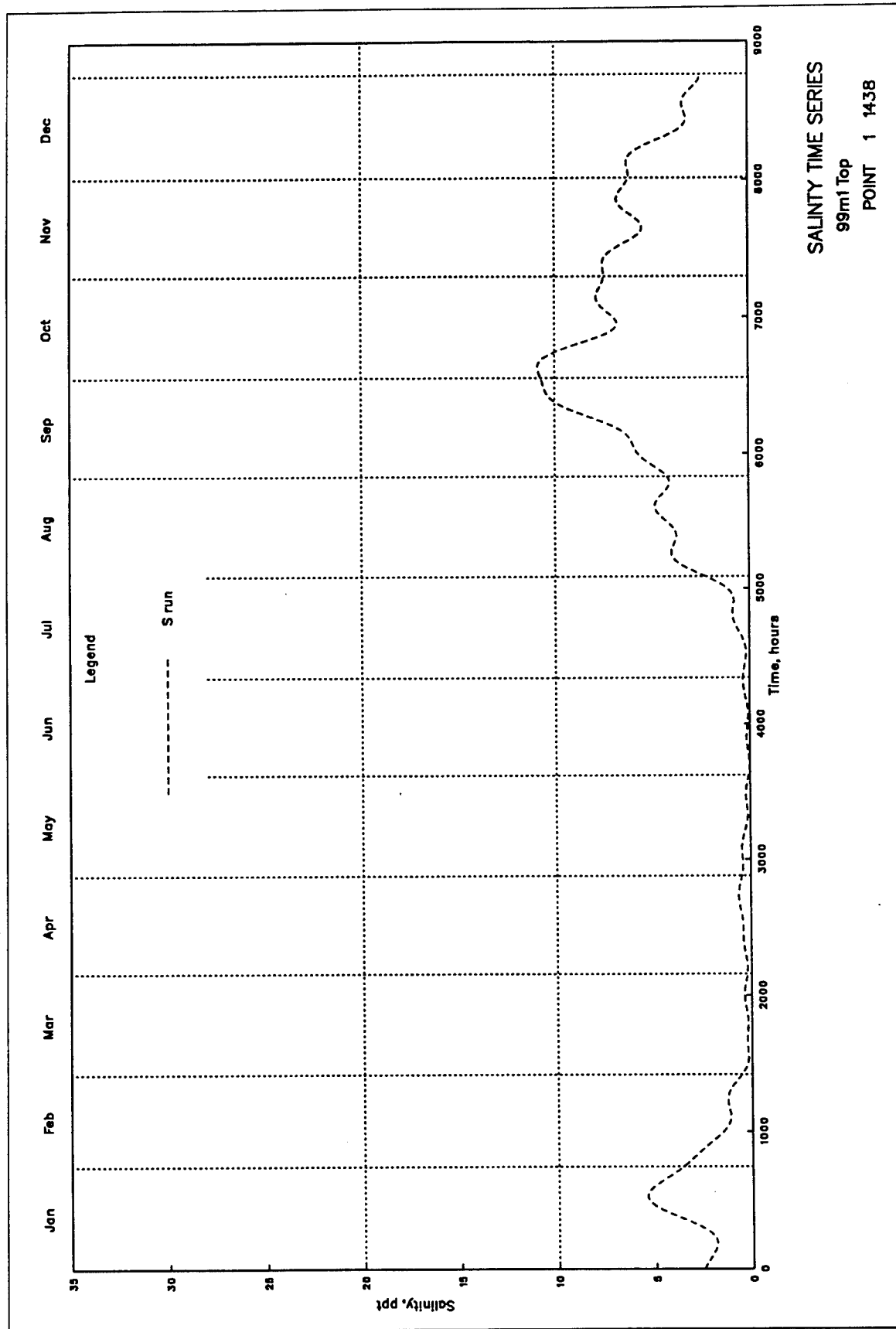


Plate 98



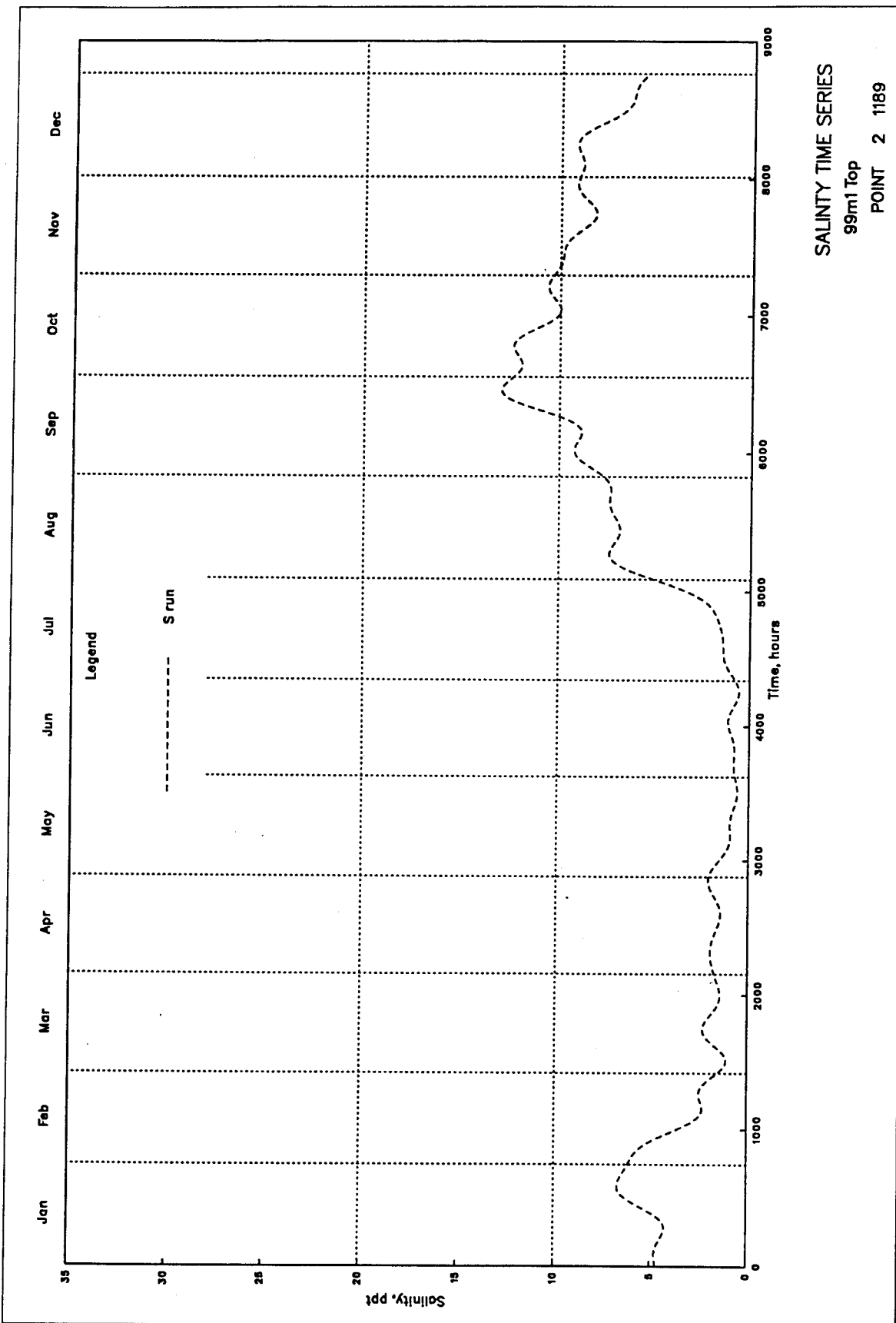


Plate 100

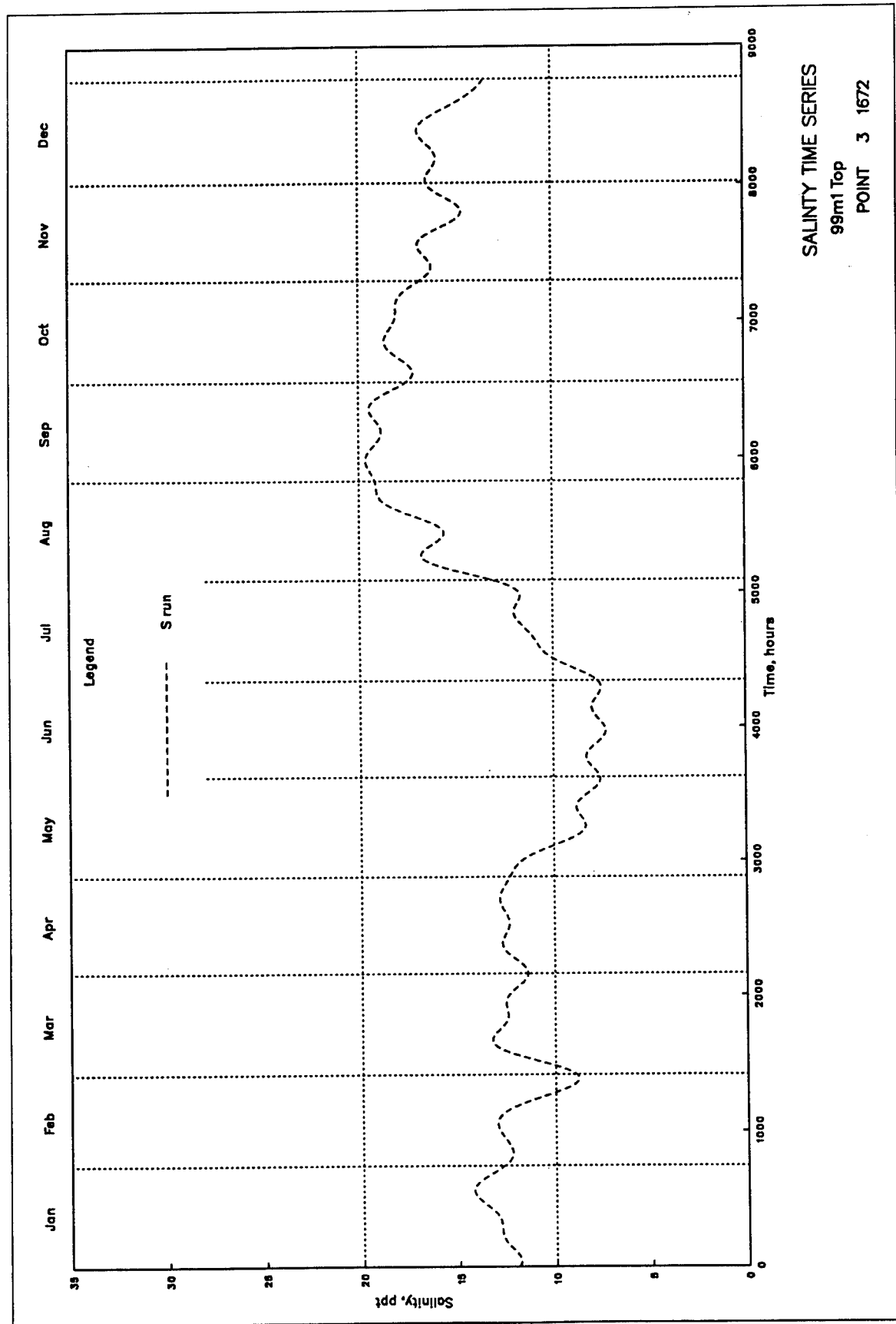


Plate 101

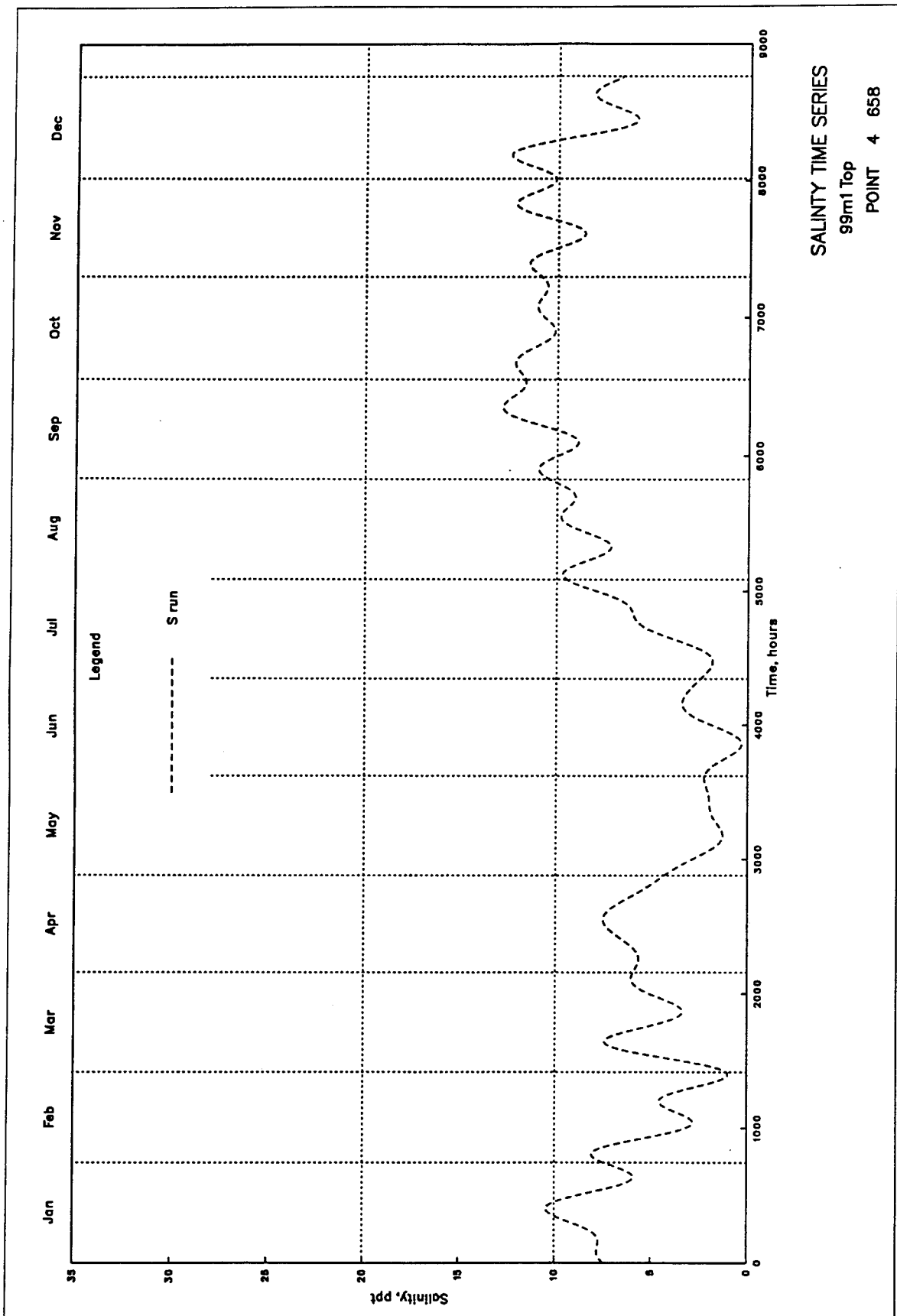
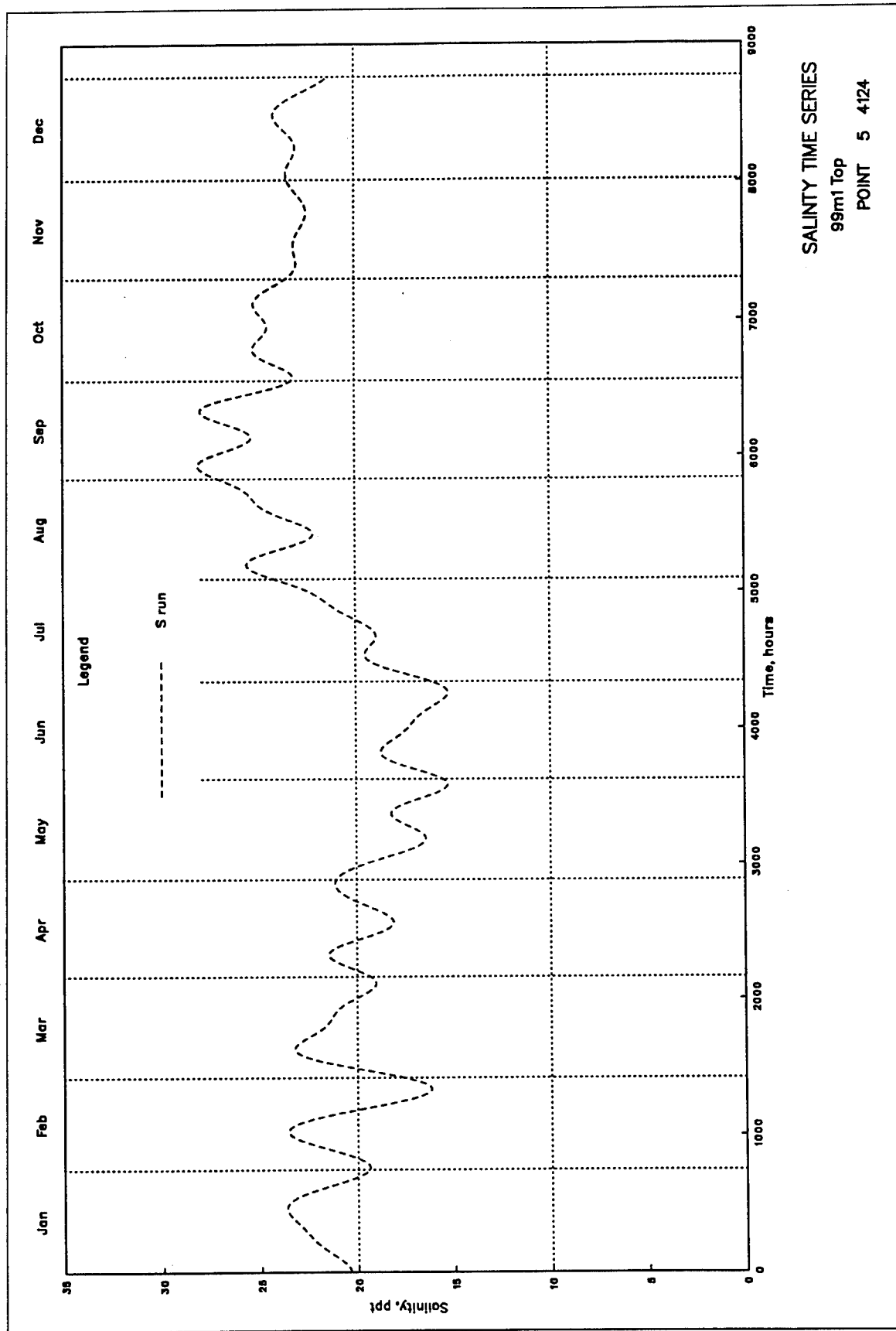


Plate 102



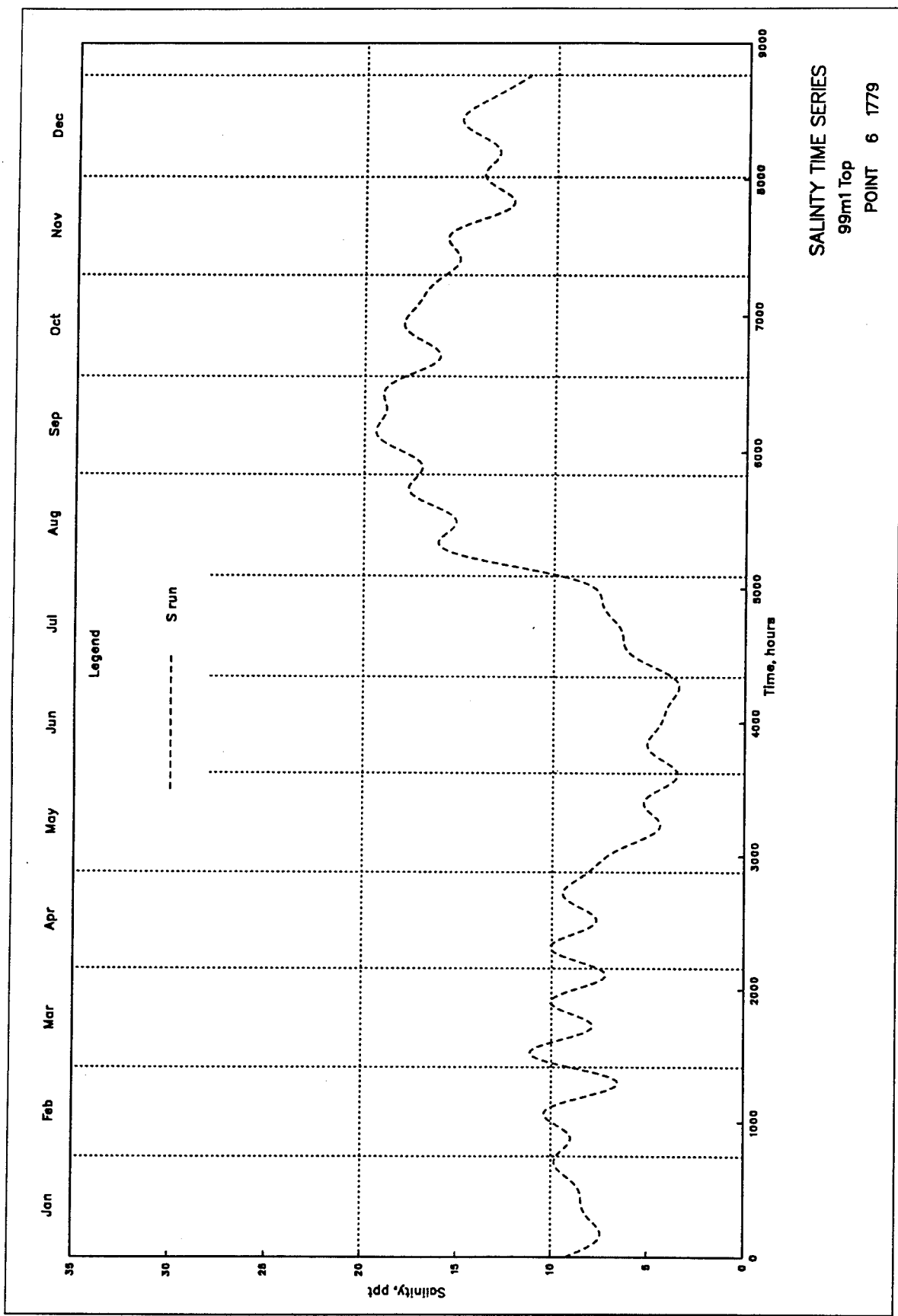
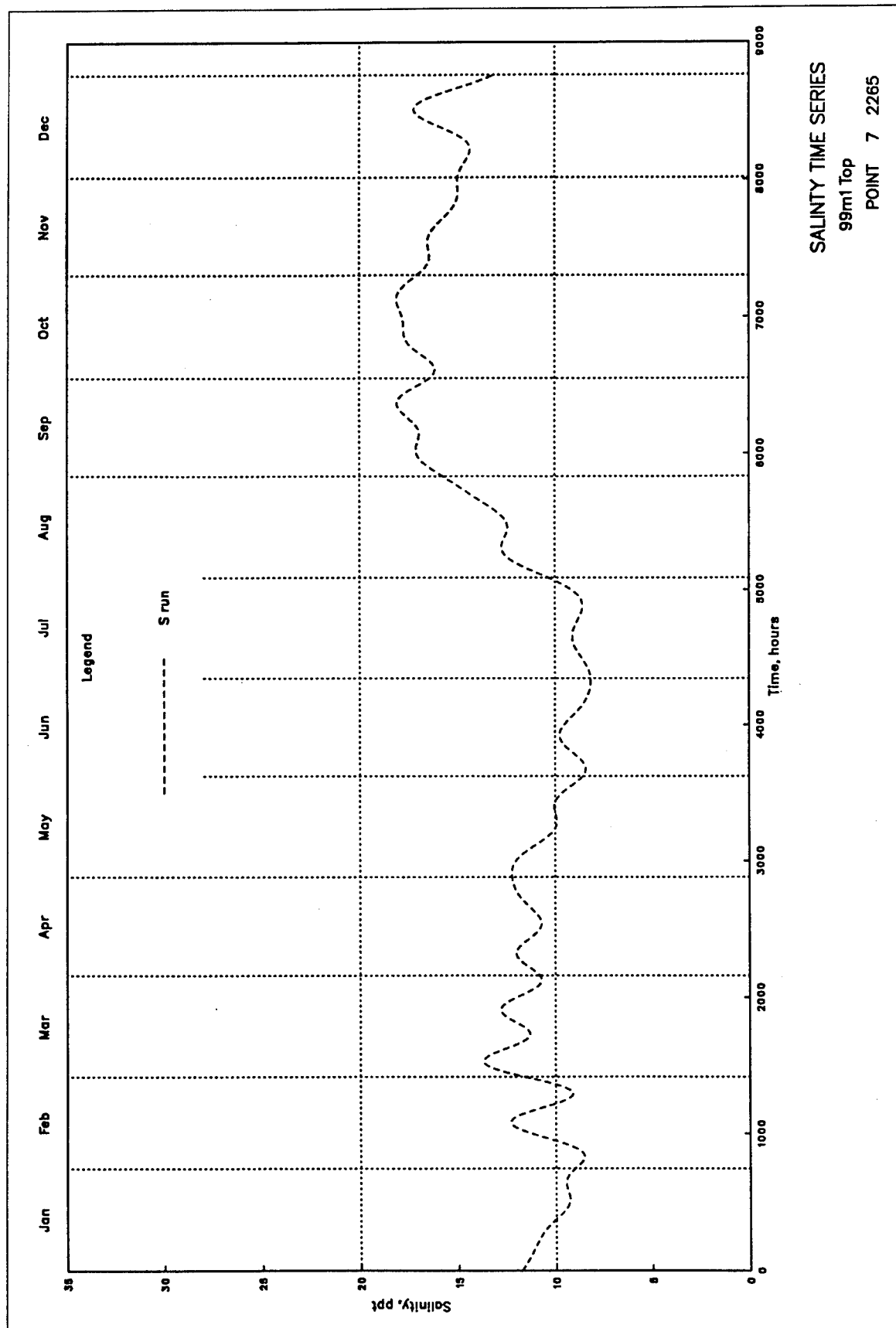


Plate 104



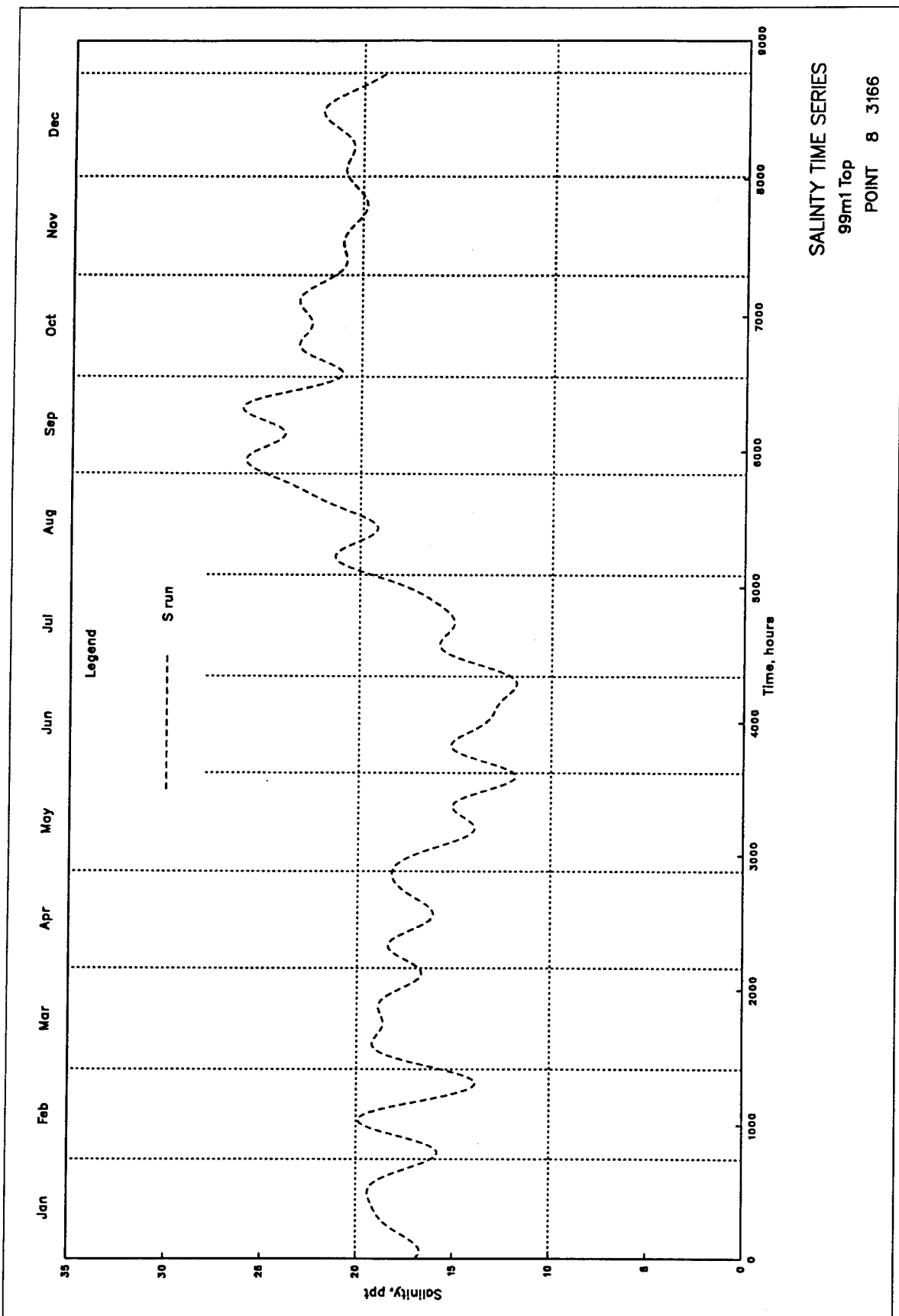
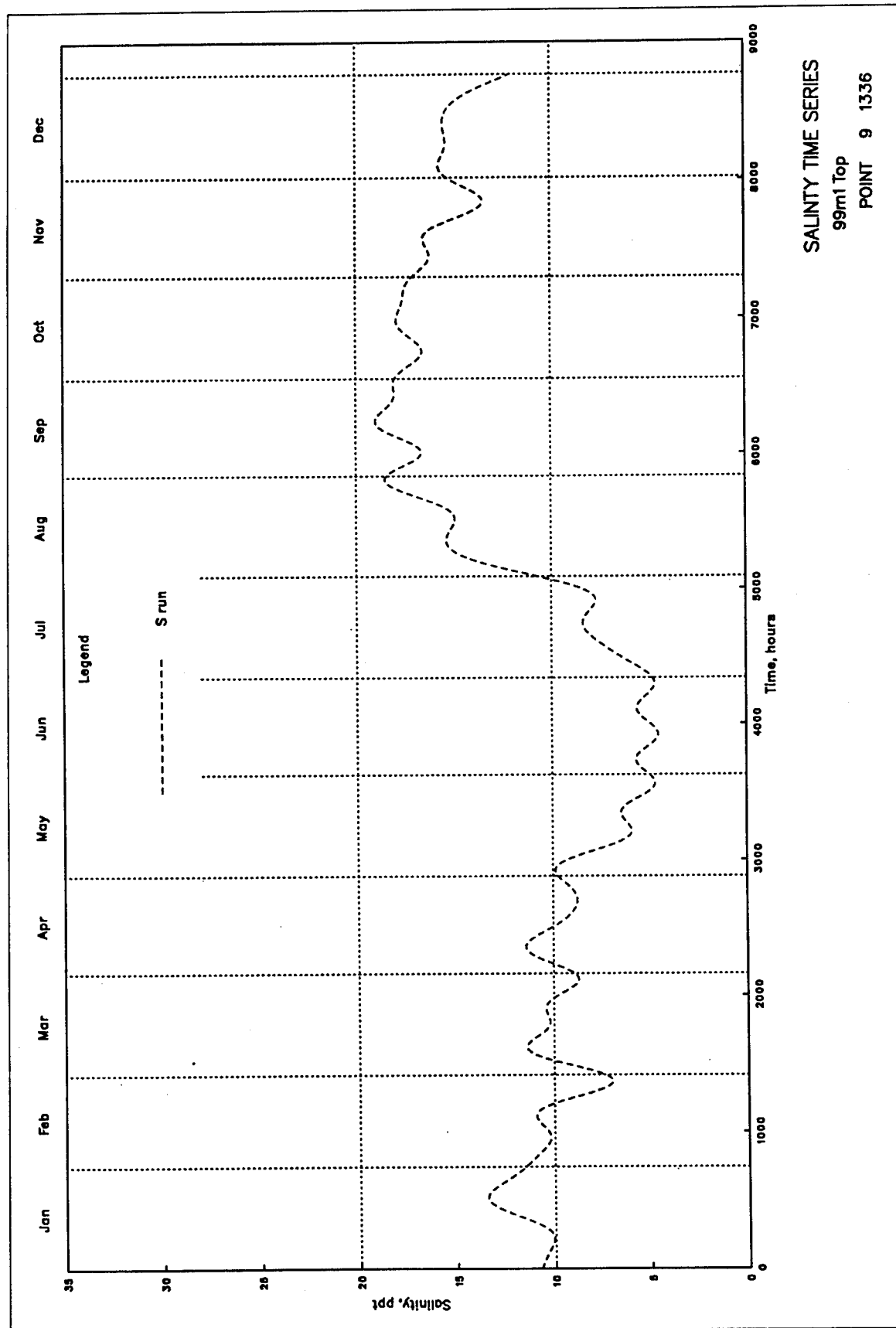


Plate 106



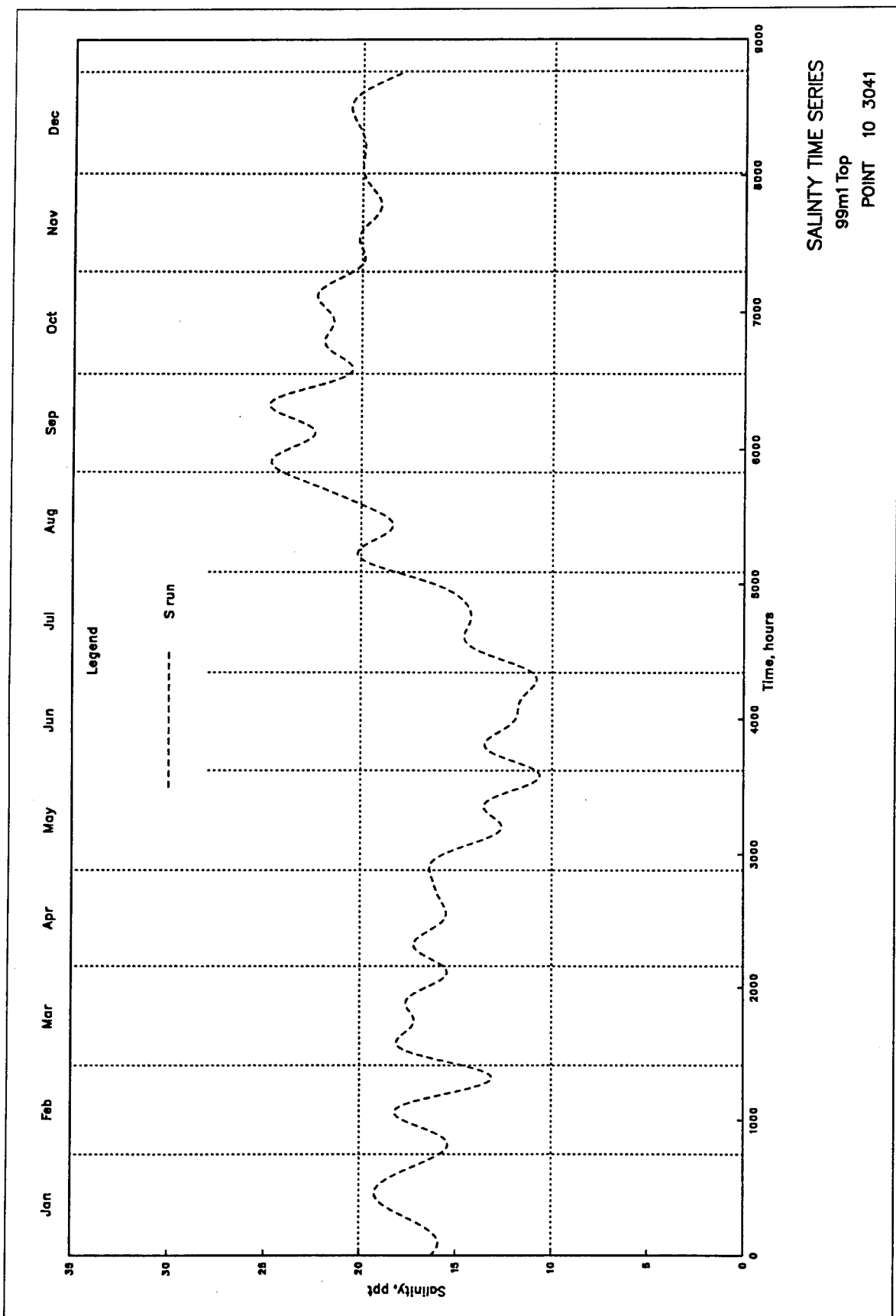
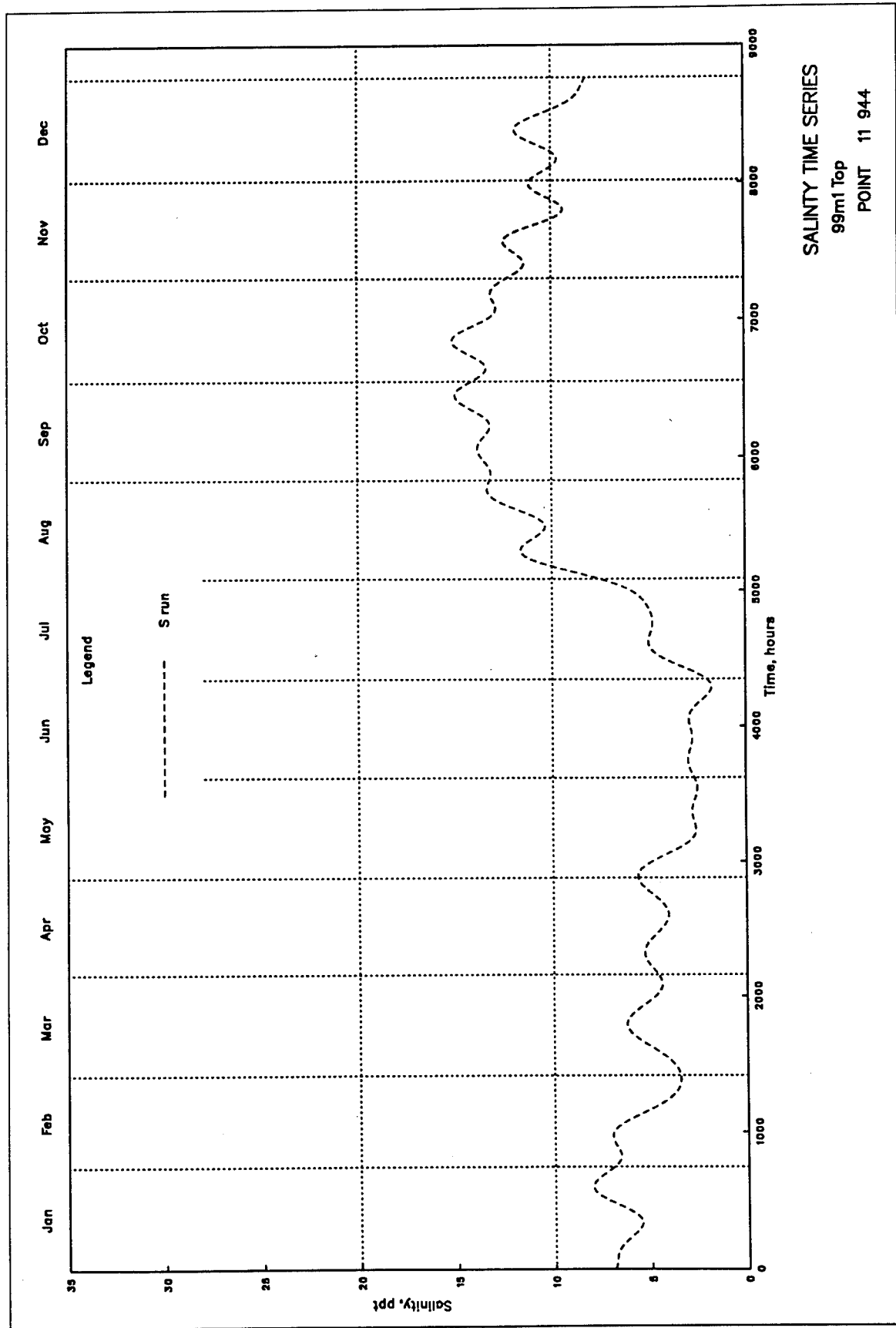


Plate 108



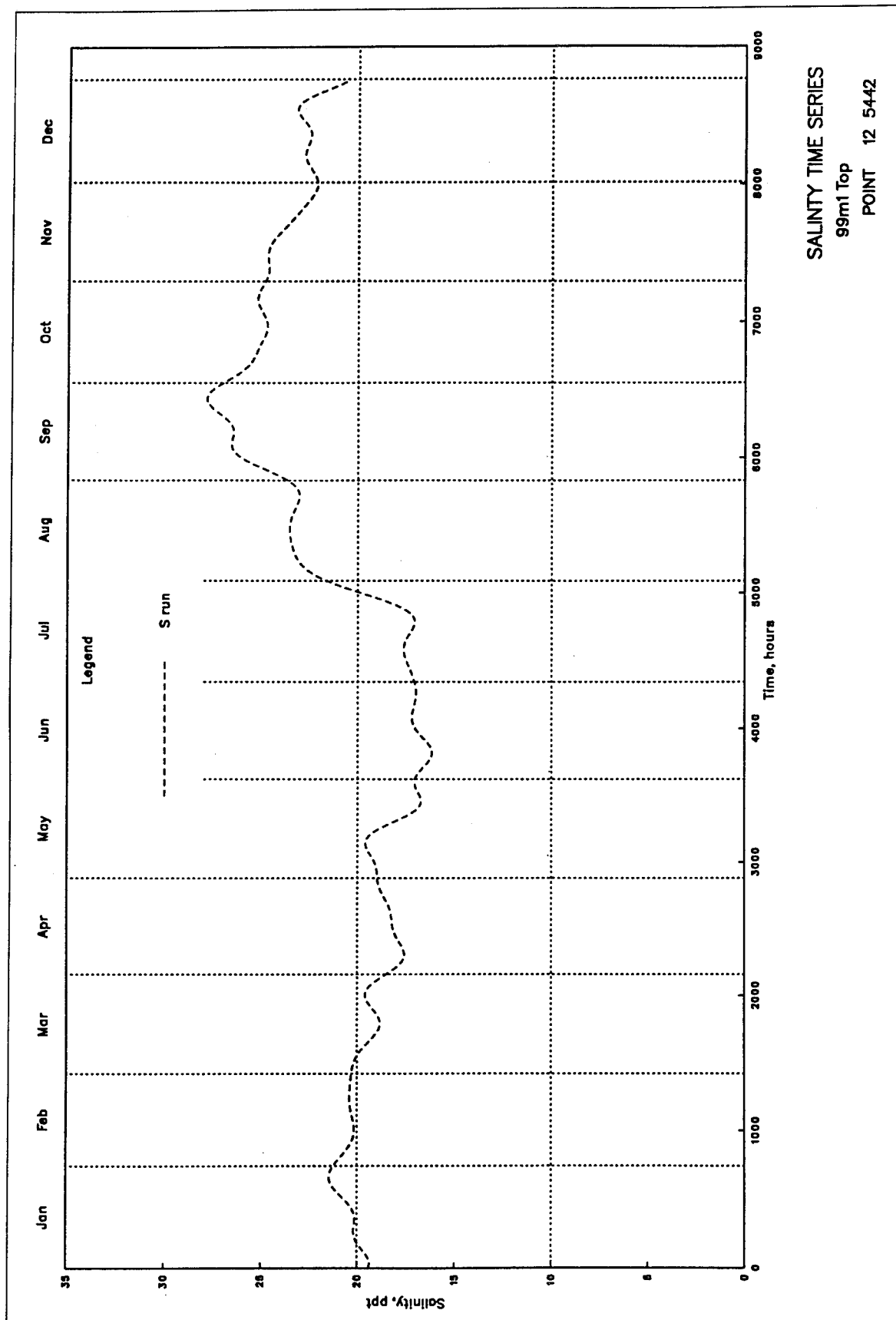
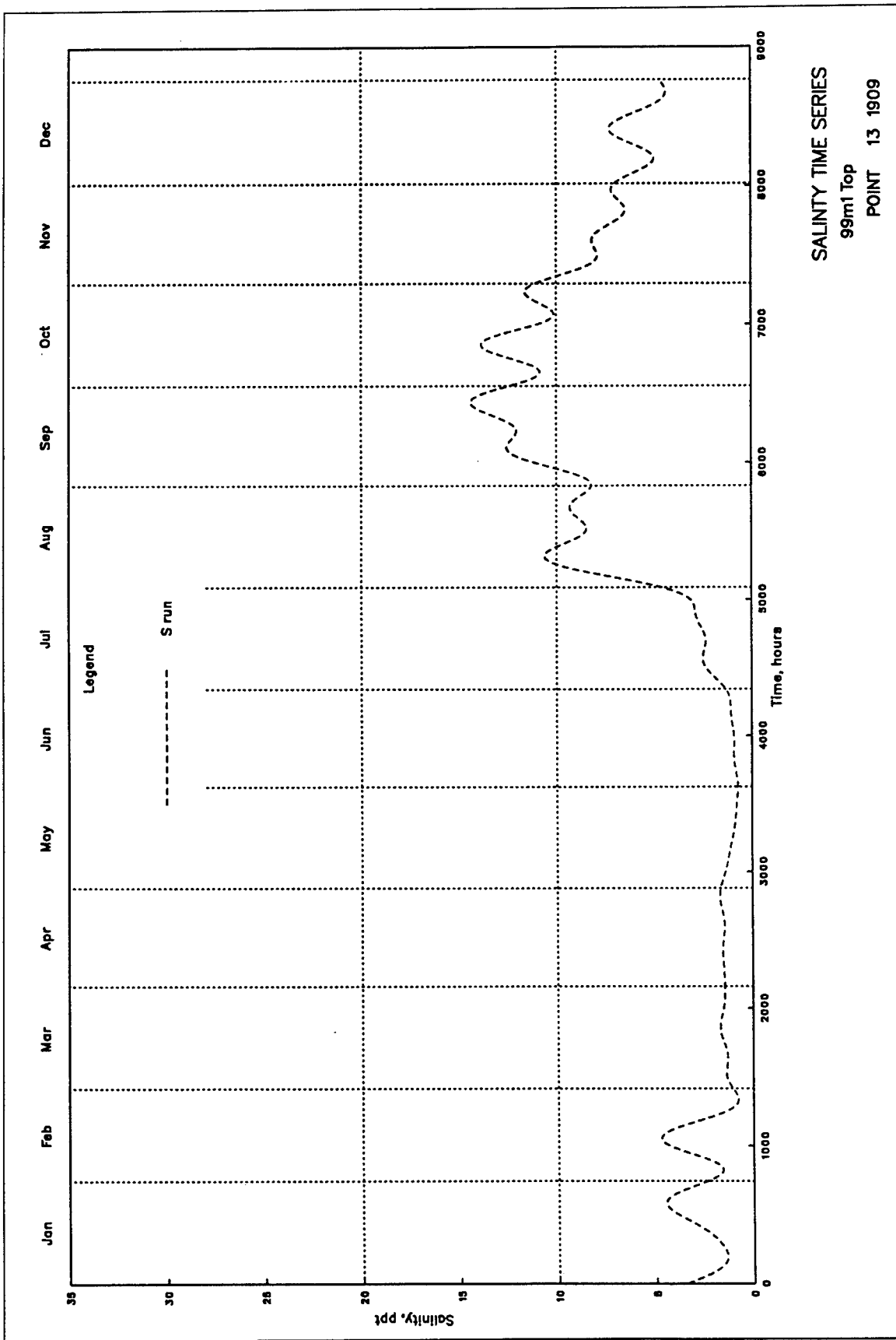


Plate 110



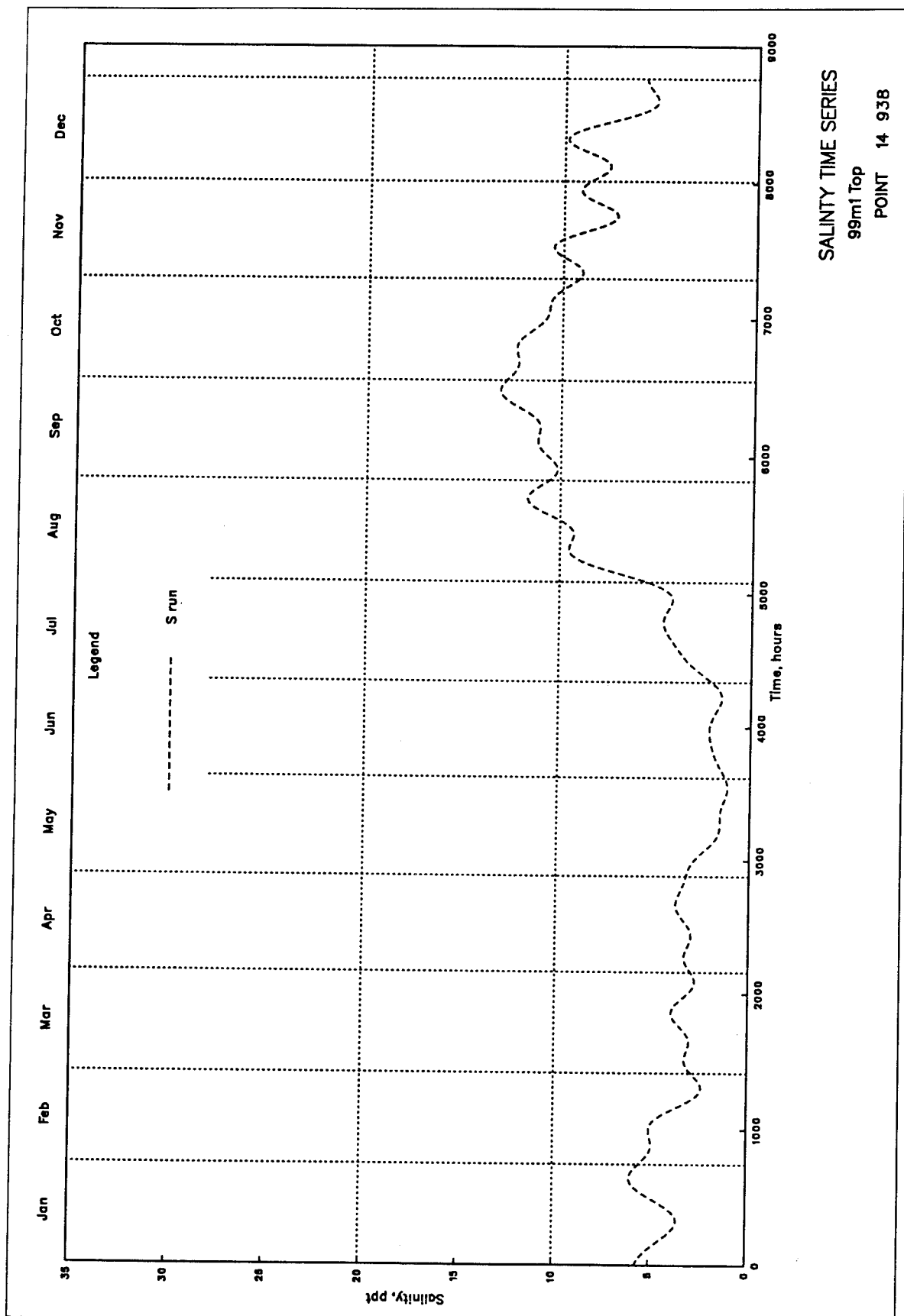
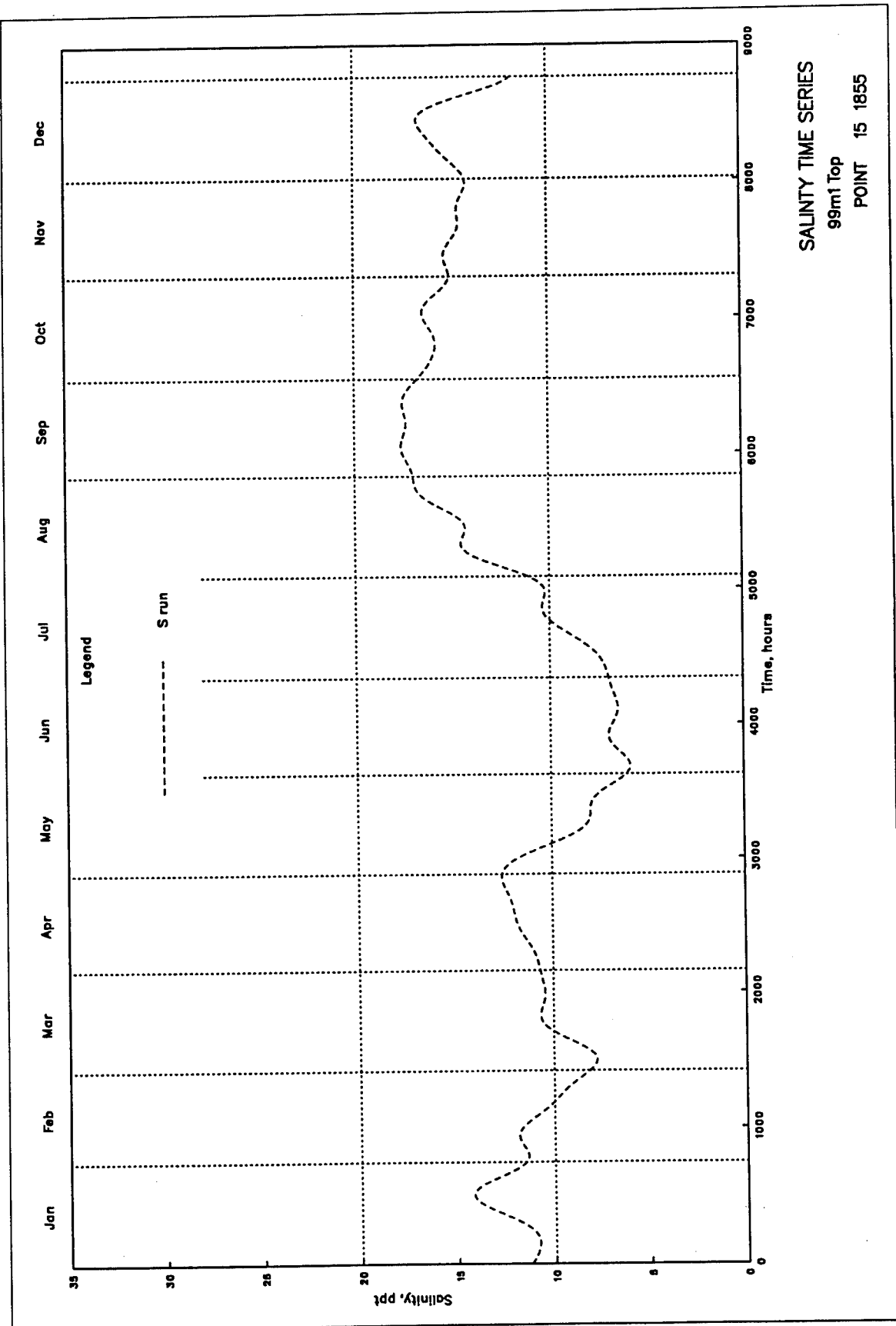


Plate 112



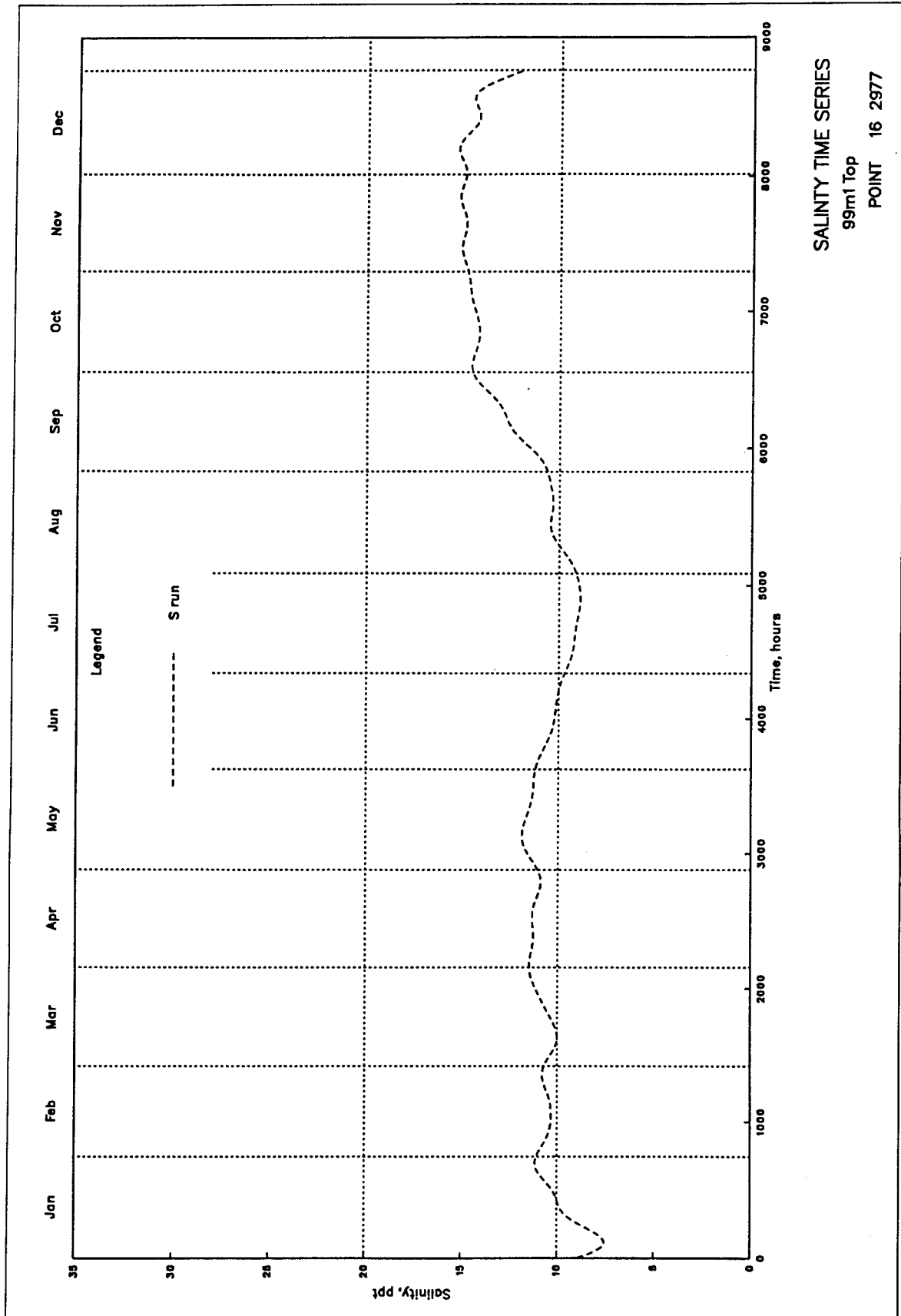
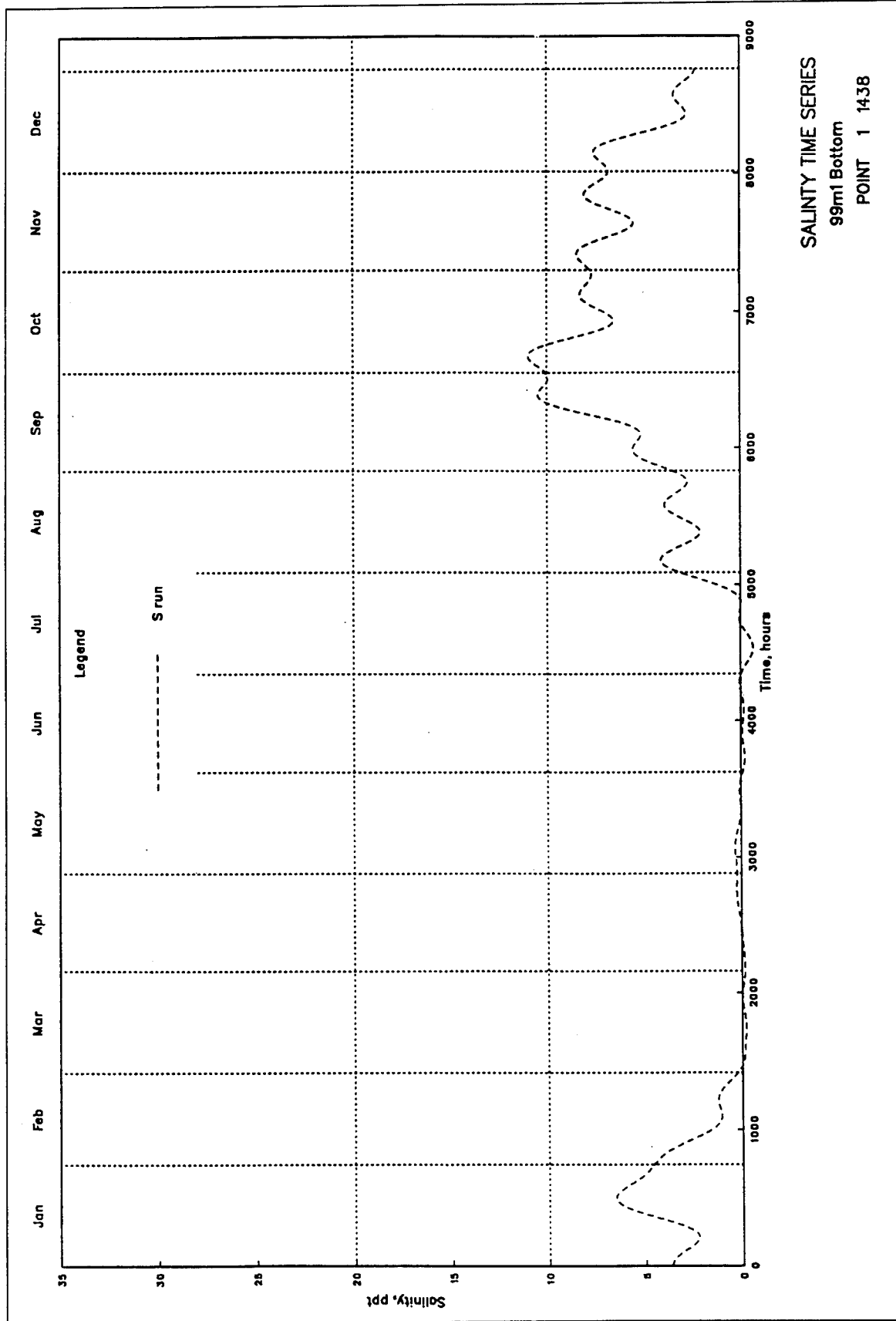


Plate 114



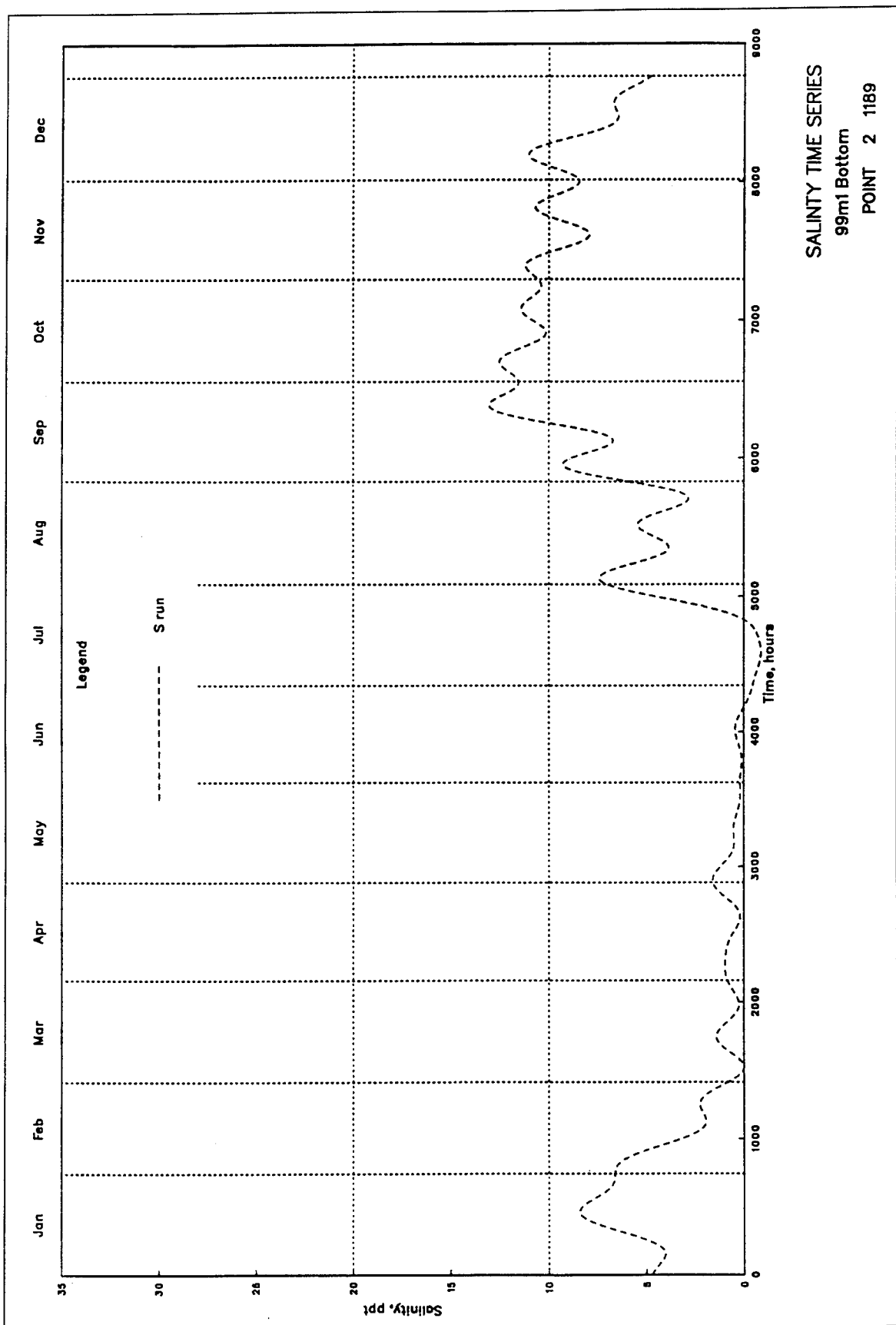
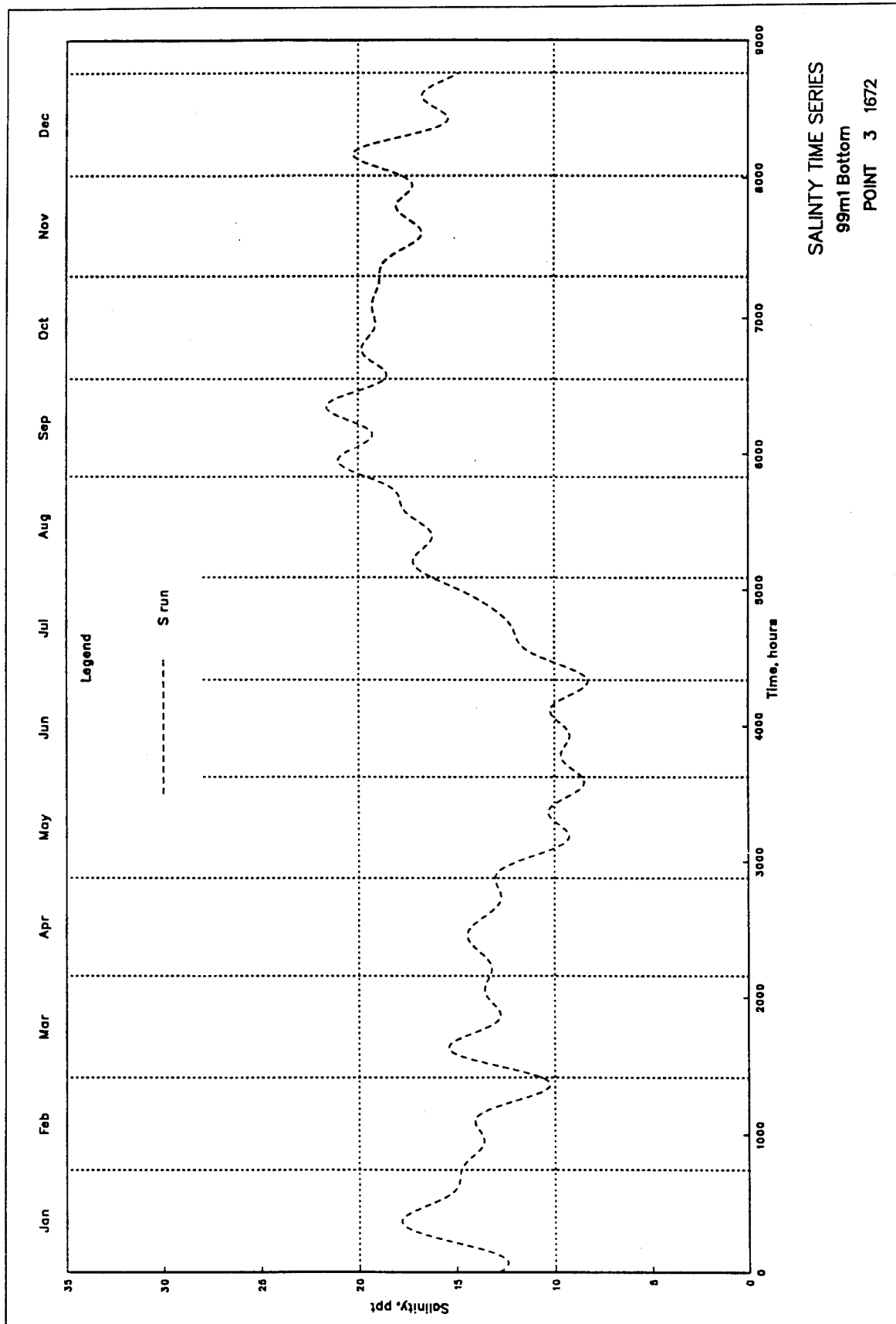


Plate 116



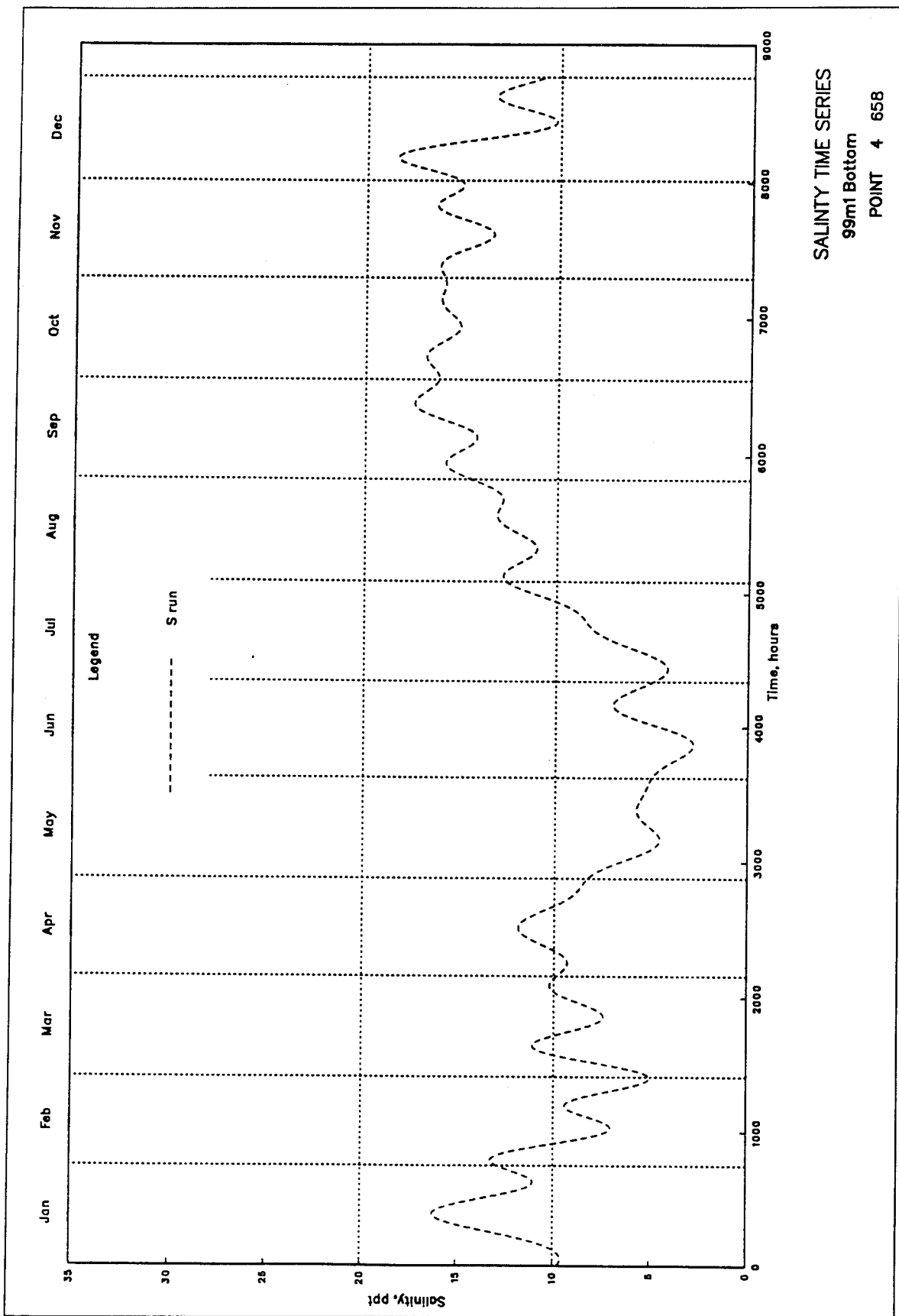
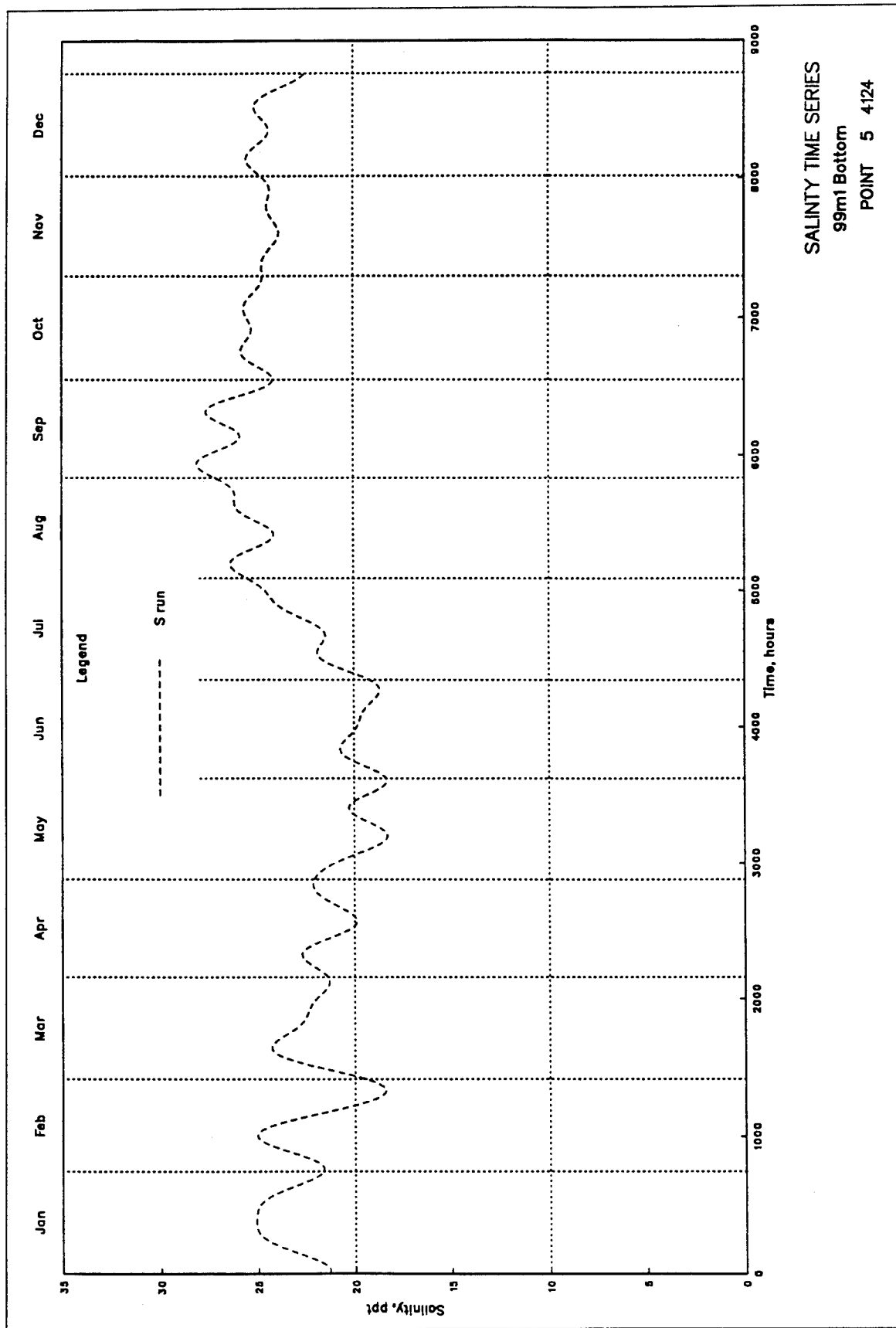


Plate 118



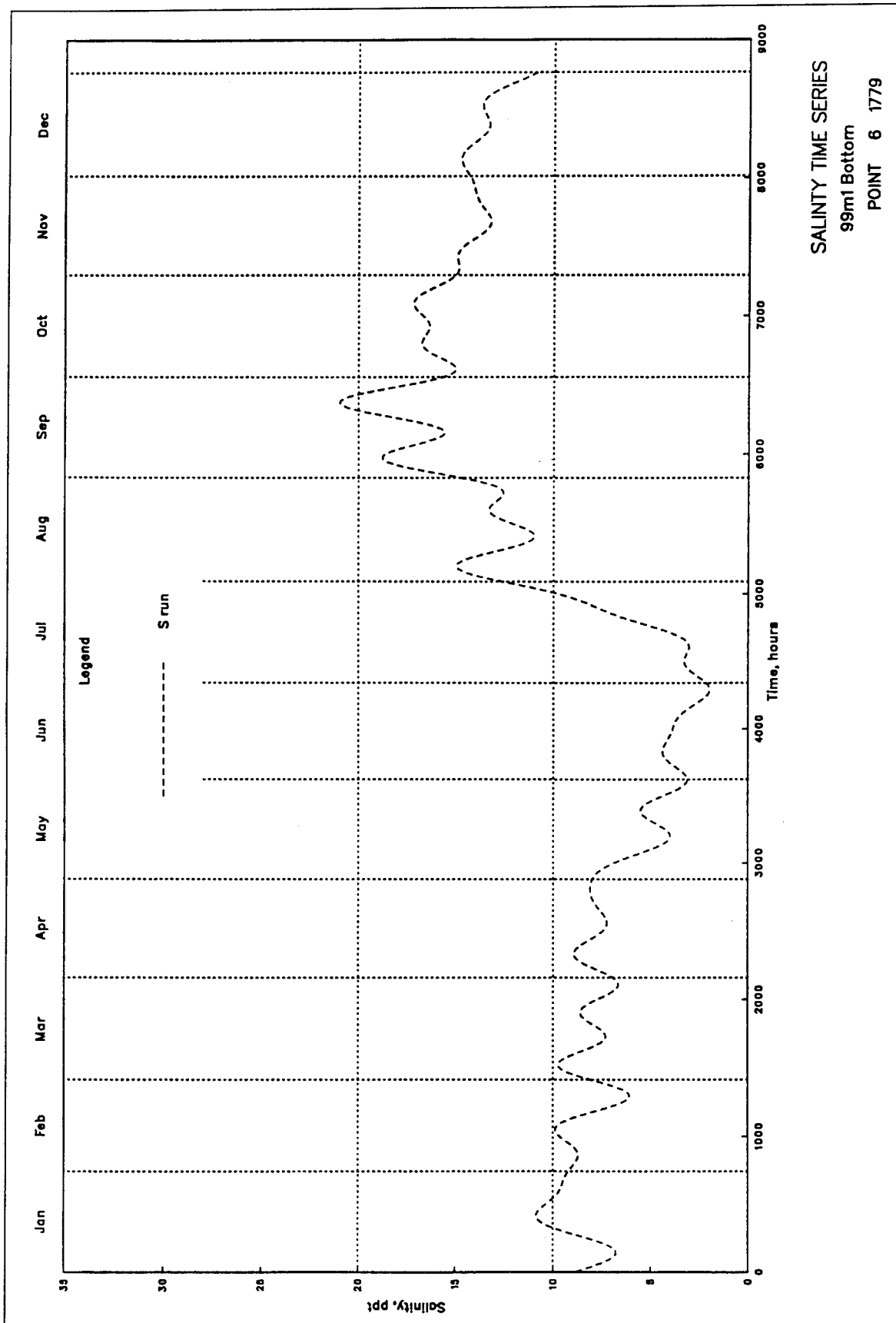
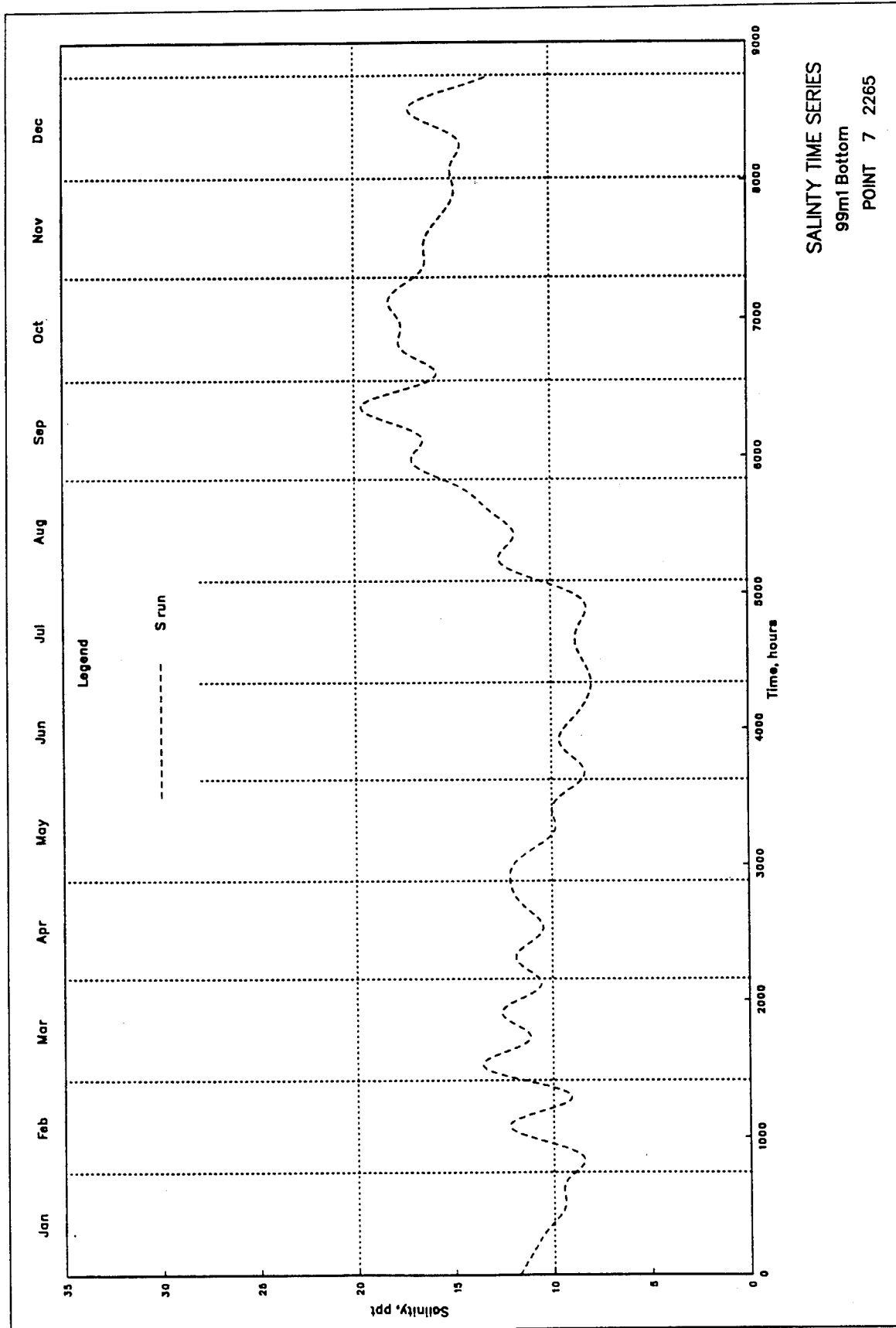


Plate 120



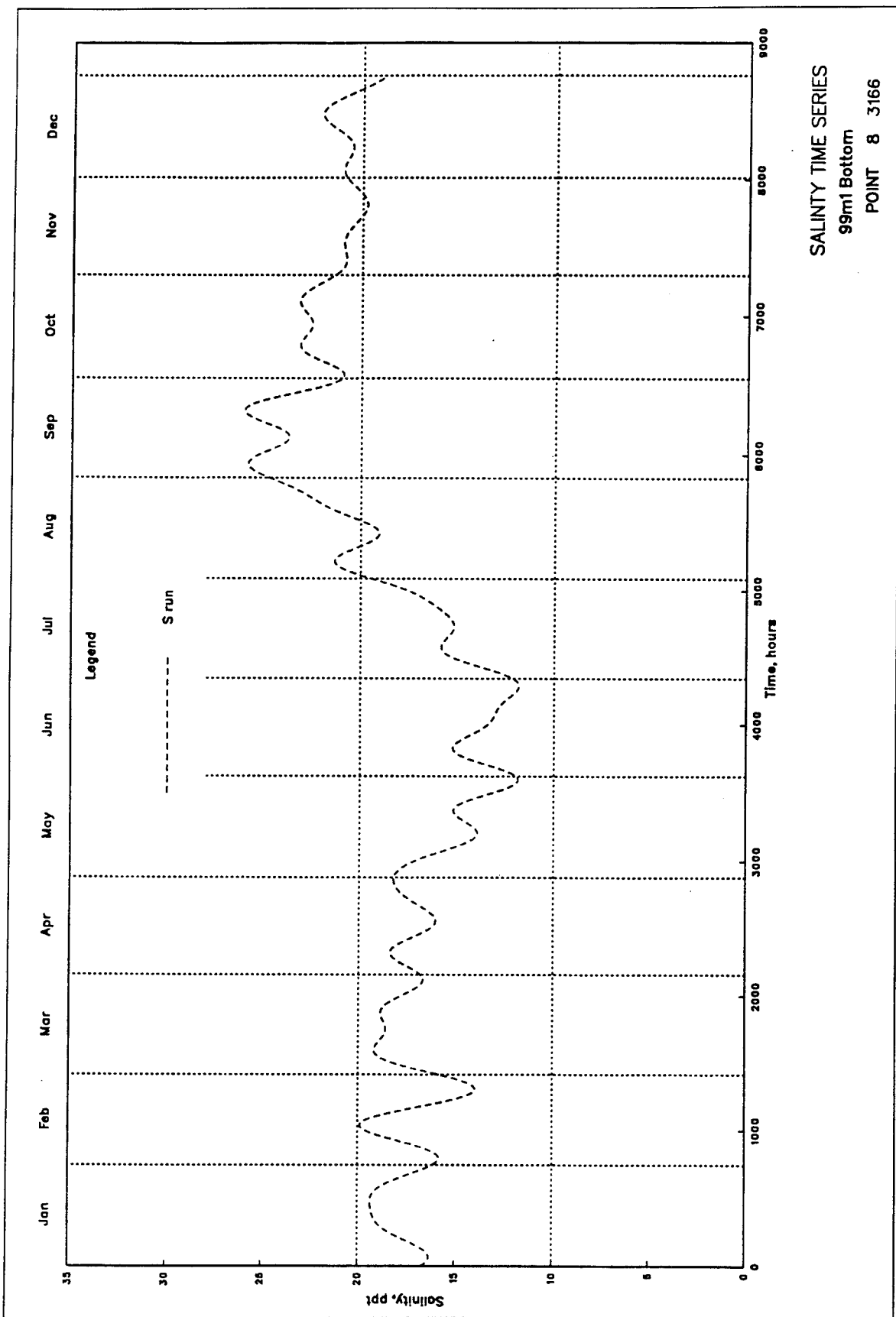
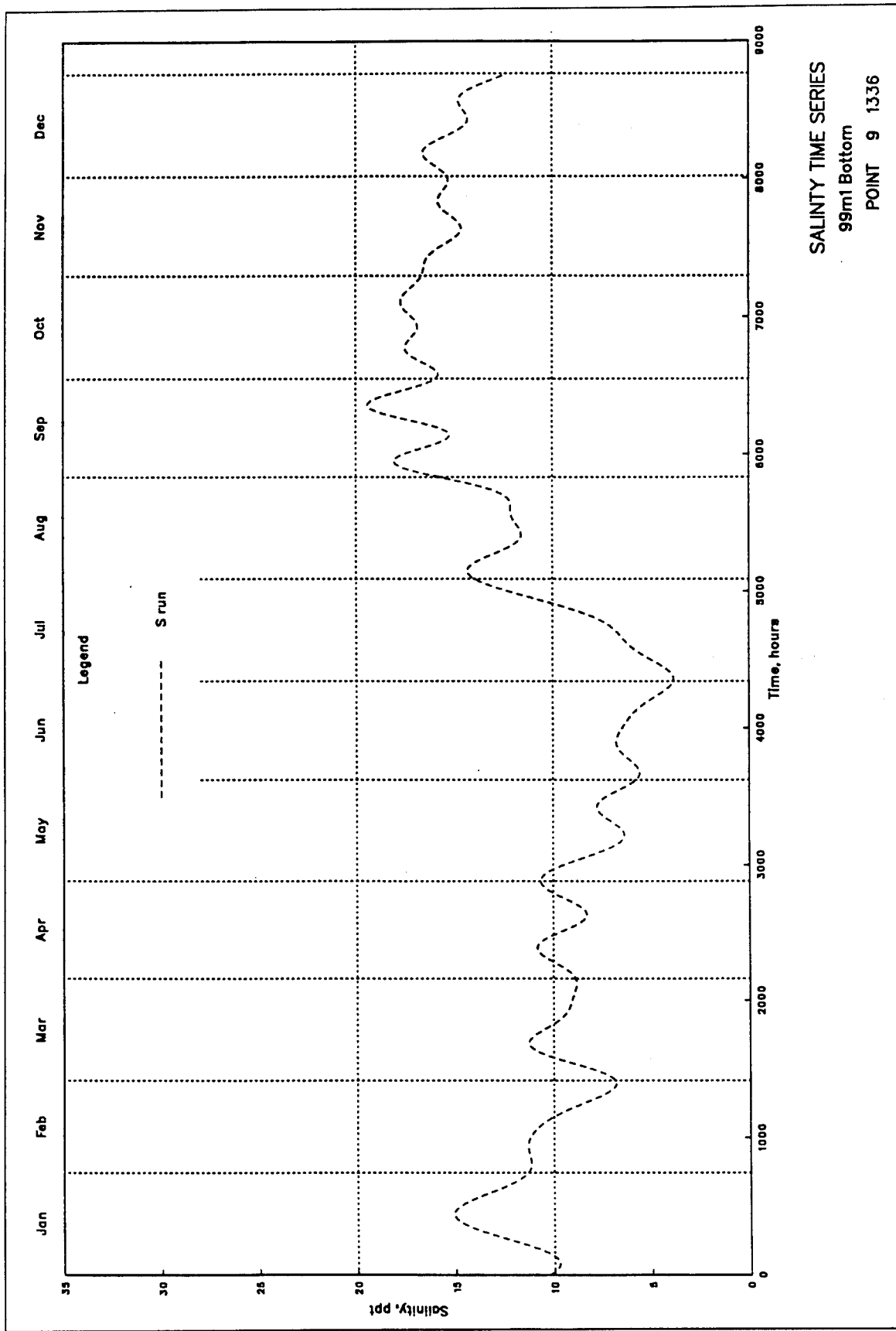


Plate 122



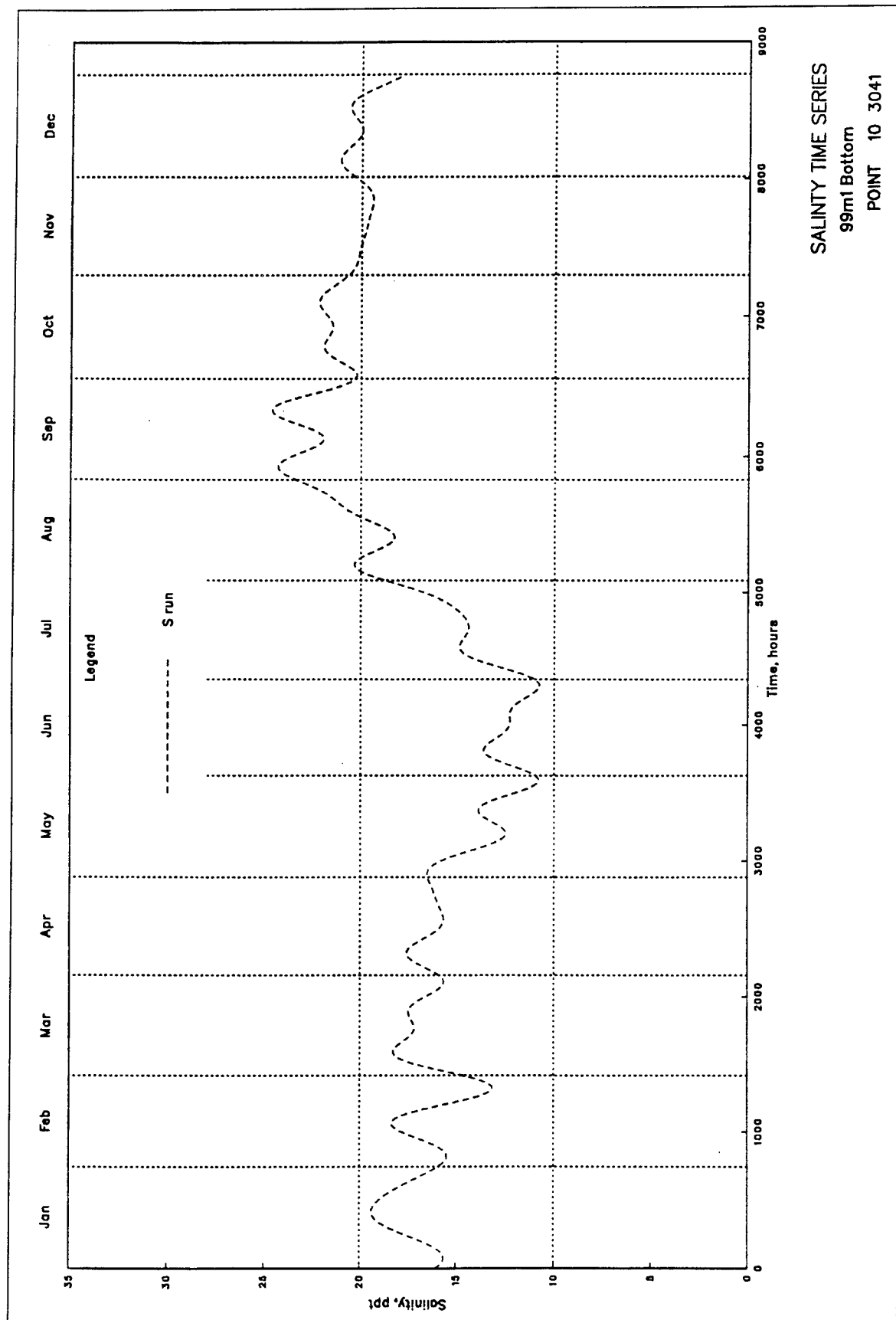
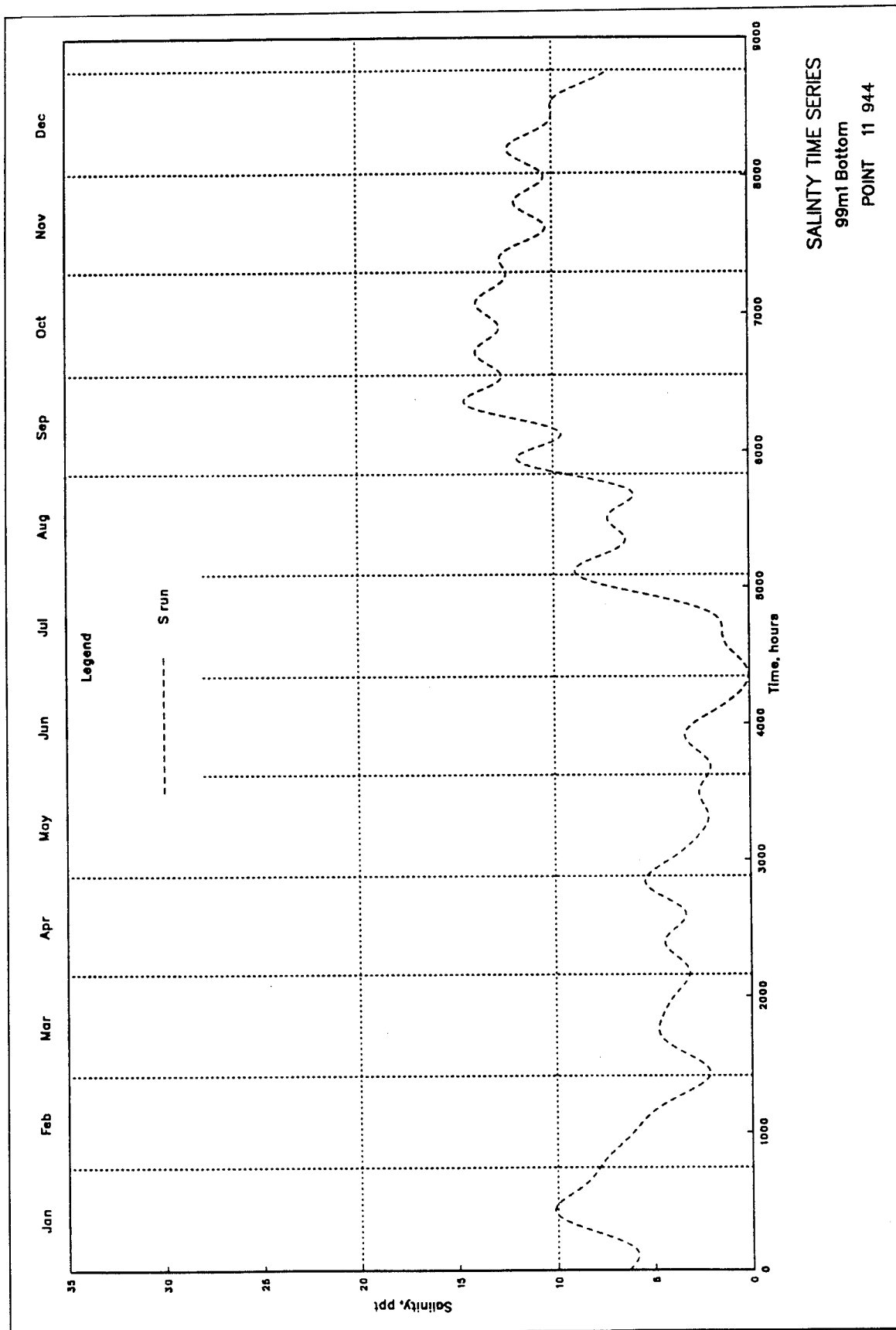


Plate 124



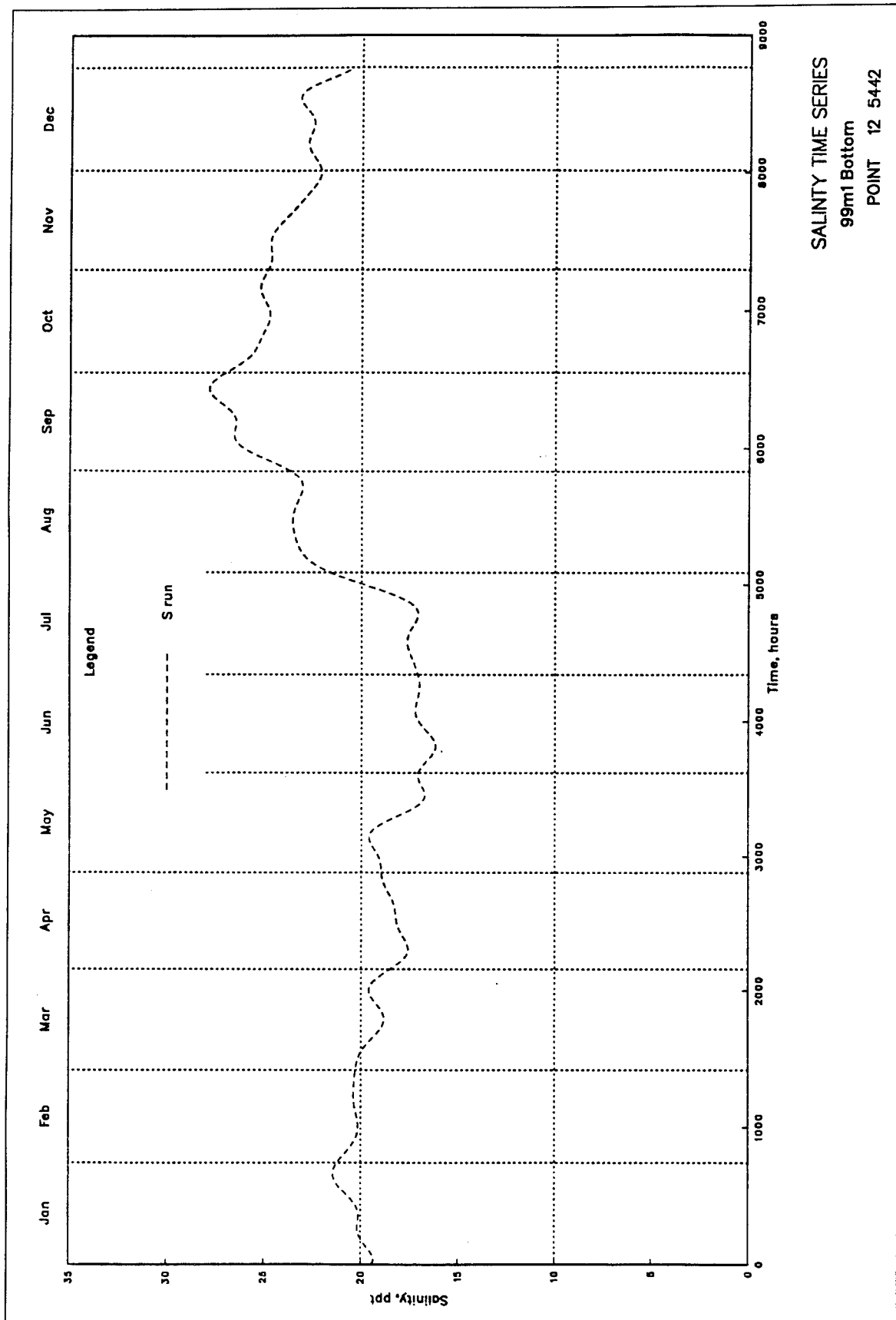
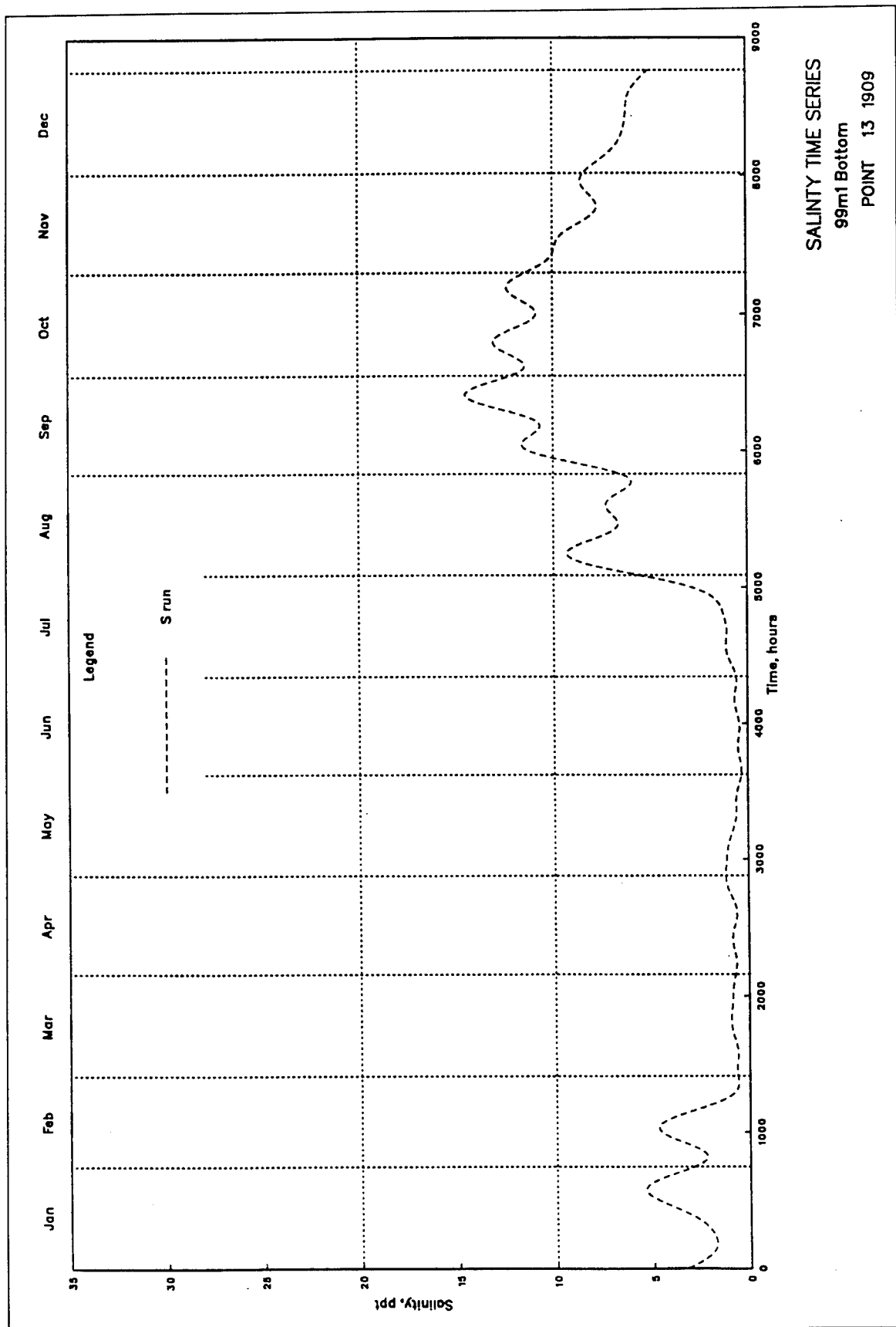


Plate 126



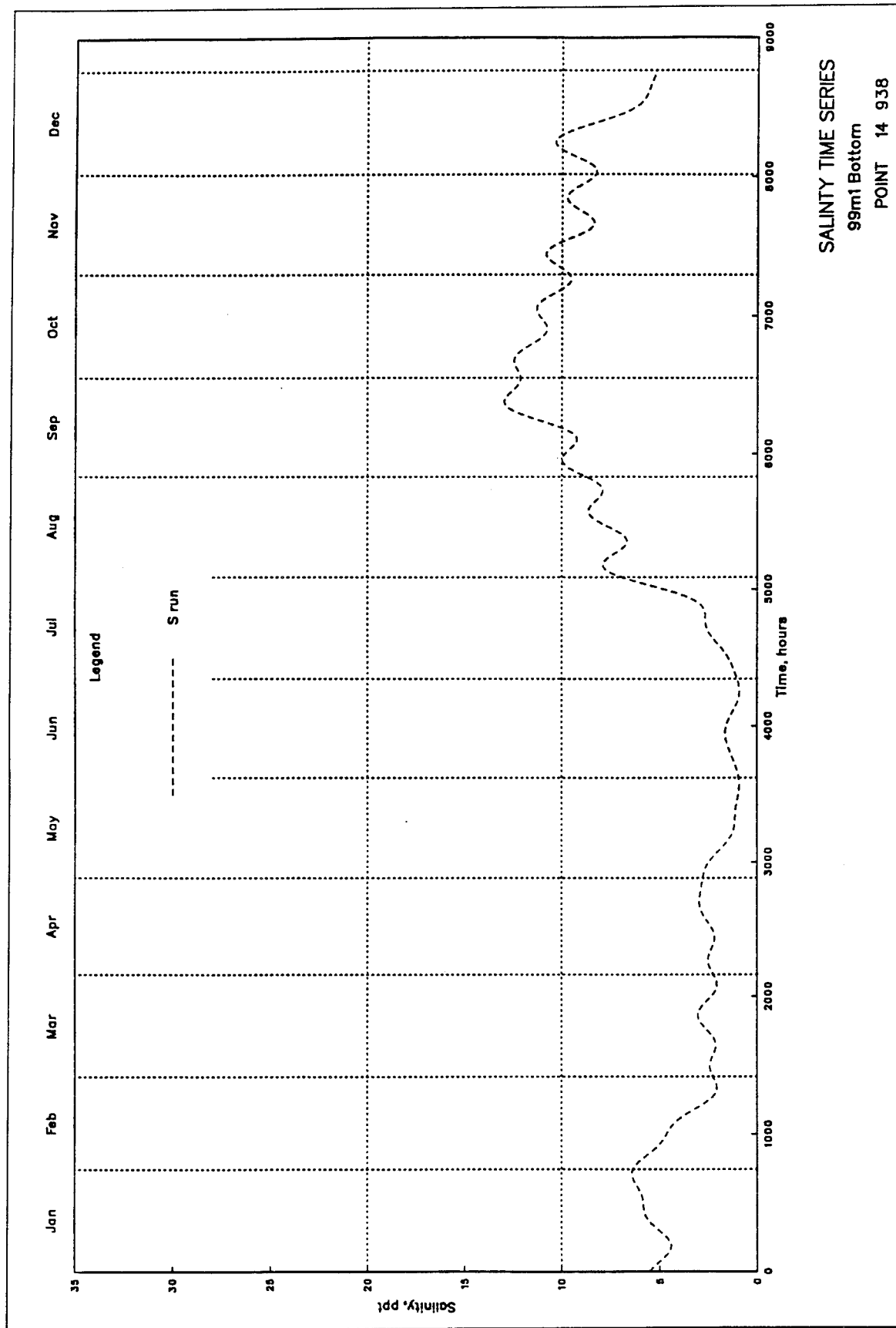
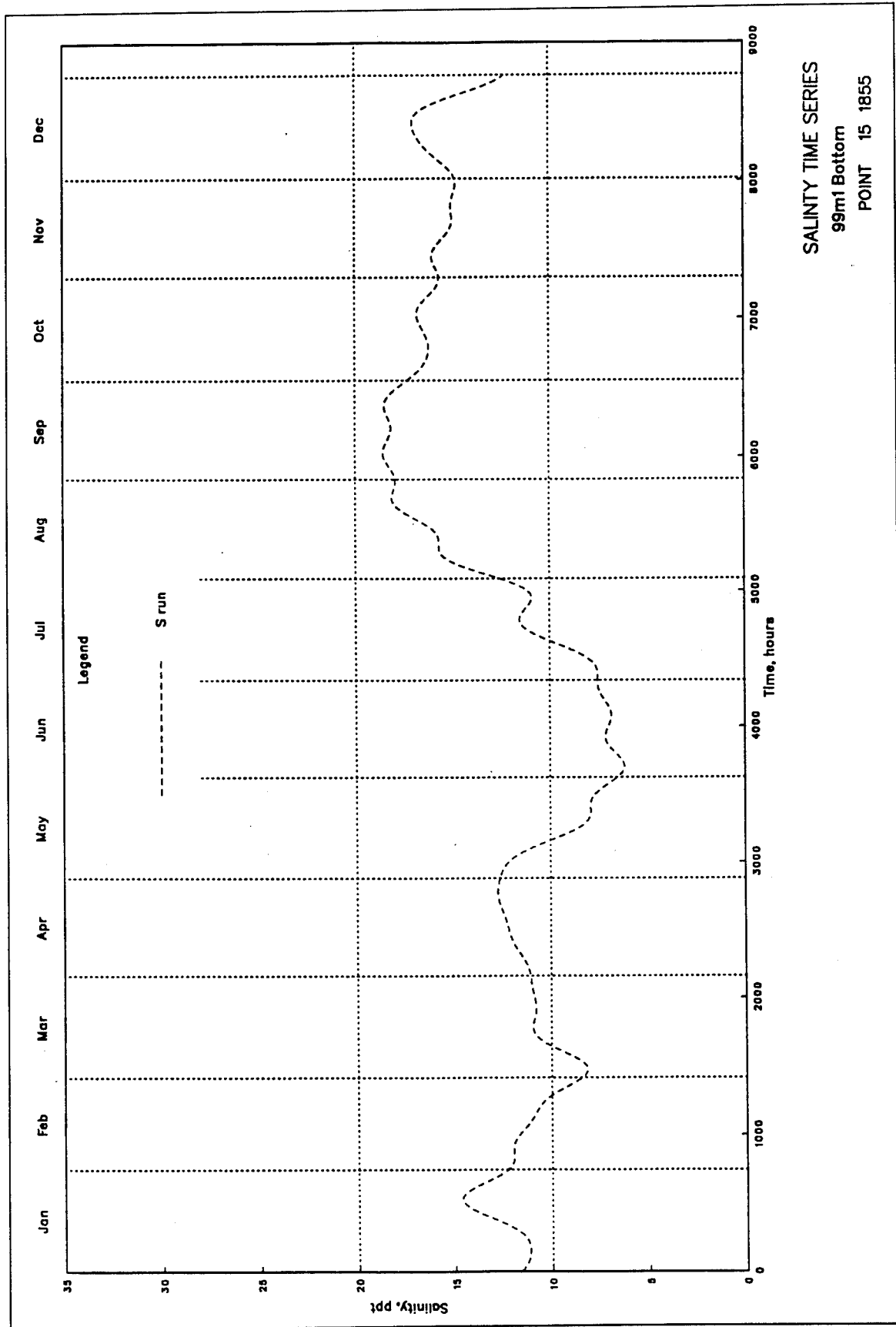


Plate 128



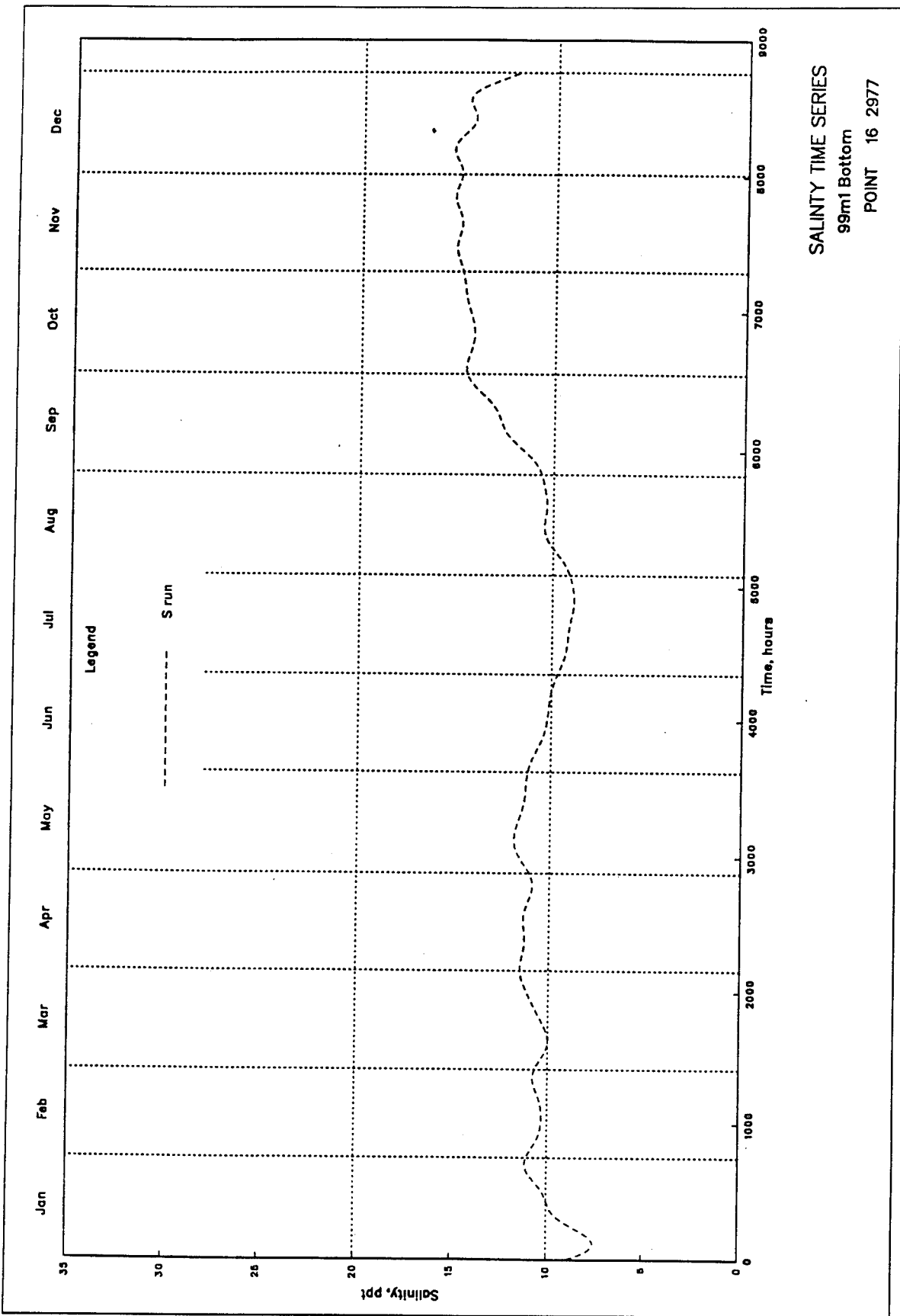


Plate 130

REPORT DOCUMENTATION PAGE

*Form Approved
OMB No. 0704-0188*

Public reporting burden for this collection of information is estimated to average 1 hour per response, including the time for reviewing instructions, searching existing data sources, gathering and maintaining the data needed, and completing and reviewing the collection of information. Send comments regarding this burden estimate or any other aspect of this collection of information, including suggestions for reducing this burden, to Washington Headquarters Services, Directorate for Information Operations and Reports, 1215 Jefferson Davis Highway, Suite 1204, Arlington, VA22202-4302, and to the Office of Management and Budget, Paperwork Reduction Project (0704-0188), Washington, DC20503.

1. AGENCY USE ONLY (Leave blank)			2. REPORT DATE February 1996		3. REPORT TYPE AND DATES COVERED Final report	
4. TITLE AND SUBTITLE System Simulation of Tidal Hydrodynamic Phenomena in Galveston Bay, Texas			5. FUNDING NUMBERS			
6. AUTHOR(S) Bernard B. Hsieh						
7. PERFORMING ORGANIZATION NAME(S) AND ADDRESS(ES) U.S. Army Engineer Waterways Experiment Station 3909 Halls Ferry Road, Vicksburg, MS 39180-6199			8. PERFORMING ORGANIZATION REPORT NUMBER Technical Report HL-96-1			
9. SPONSORING/MONITORING AGENCY NAME(S) AND ADDRESS(ES) U.S. Army Engineer District, Galveston P.O. Box 129 Galveston, TX 77553			10. SPONSORING/MONITORING AGENCY REPORT NUMBER			
11. SUPPLEMENTARY NOTES Available from National Technical Information Service, 5285 Port Royal Road, Springfield, VA 22161.						
12a. DISTRIBUTION/AVAILABILITY STATEMENT Approved for public release; distribution is unlimited.				12b. DISTRIBUTION CODE		
13. ABSTRACT (Maximum 200 words) <p>An alternative method, capable of analyzing changes at individual points in an estuary system, as opposed to the global solutions generated by the numerical model, was developed. A system response approach using input/output relationships via nonlinear frequency domain analysis of Fourier Transform from a numerical model to describe the dynamic behavior of tidal hydrodynamic phenomena was used to play this role. Under this design, the system response functions from a verified numerical model for a particular location can be used to simulate the resulting output function, such as change in salinity, when input forcing functions, such as tidal variation and freshwater inflow, change. This approach was applied to address the salinity response due to freshwater inflow changes for 16 selected locations in Galveston Bay, TX. The system model base was constructed by selecting node points from 3-D numerical hydrodynamic model results. The annual numerical simulation of both base geometry (12-m-deep channel) and project conditions (13.7-m-deep channel) for 1990 medium-flow conditions was used to construct the system response function. Three major tributaries (Trinity River, San Jacinto River, and Buffalo bayou) were considered as primary freshwater inflow sources for conducting these simulations.</p>						
14. SUBJECT TERMS Fourier Transform Frequency domain analysis			15. NUMBER OF PAGES 158			
16. PRICE CODE						
17. SECURITY CLASSIFICATION OF REPORT UNCLASSIFIED	18. SECURITY CLASSIFICATION OF THIS PAGE UNCLASSIFIED	19. SECURITY CLASSIFICATION OF ABSTRACT		20. LIMITATION OF ABSTRACT		